TELOMERE FOLDING IN *S. CEREVISIAE* DEPENDS ON CHROMATIN MODIFIERS AND RECOMBINATION FACTORS AND IS LOST DURING REPLICATIVE SENESCENCE

Dissertation

zur Erlangung des Grades

Doktor der Naturwissenschaften

am Fachbereich Biologie

der Johannes Gutenberg-Universität Mainz

Tina Wagner

Mainz, Juni 2020

Dekan:

1. Berichterstatter:

2. Berichterstatter:

Tag der mündlichen Prüfung: 09. Juli 2020

Table of contents

Abstract

The fact that eukaryotic chromosomes are linear requires the implementation of a protection mechanism that prevents their ends from being recognized as double strand breaks. Telomeres, the repetitive DNA elements at chromosome ends, fulfill this protective function by counteracting inappropriate checkpoint activation and repair. The protective capacity of telomeres has been largely attributed to specific telomere-associated protein complexes. In addition, telomere loop structures have been proposed to contribute to end protection by sequestering the chromosome end and thereby preventing telomere fusions and degradation. Human telomeres form a lariat structure within the telomeric repeat tract, referred to as a t-loop. *Saccharomyces cerevisiae* telomeres were proposed to fold back into subtelomeric regions, however, a robust method to study these structures has been lacking. In this thesis, a chromosome conformation capture-based approach, dubbed Telo-3C, was optimized to quantify telomere-subtelomere interactions at a single unmodified yeast telomere. This methodology allowed for the identification of key regulatory factors that establish telomere folding. Studying the regulation of telomere folding in a genetically versatile system such as budding yeast offers the opportunity to draw parallels to the human system and to reveal regulatory mechanisms of the human telomere folding behavior.

Using Telo-3C, I have determined the homologous recombination machinery, comprising the factors Rad51 and Rad52, as well as the checkpoint kinase Rad53 as key folding regulators of budding yeast telomeres. My results show that the histone modifiers Sir2, Sin3 and Set2 are major regulatory factors of telomere folding indicating that the distinct telomeric chromatin environment might be a critical requirement for its establishment. Interestingly, the structural maintenance of chromosomes (SMC) complexes cohesin, condensin and SMC5/6 are not required for efficient folding of *S. cerevisiae* telomeres. Therefore, the mechanism by which telomere folding is established might be different from canonical internal chromatin loops. The Telo-3C analysis demonstrated that wild type length telomeres fold back efficiently, however, as telomeres shorten and cells enter replicative senescence, telomere folding is compromised. I show that the unfolding of chromosome ends during senescence is independent from telomere shortening *per se*, but seems to be linked to the senescence program. Indeed, telomeres also unfold upon treatment with the DNA damaging agent MMS (methyl methanesulfonate), which induces a similar stress response and global gene expression changes as replicative senescence in budding yeast. A quantitative mass spectrometry approach revealed that the telomere folding regulators Sir2, Sin3 and Set2 are less abundant during replicative senescence. Therefore, their downregulation might contribute to the opening of the telomere fold-back structure during this process.

The data presented in this thesis point towards the homologous recombination machinery and certain chromatin modifiers being major requirements for the folding of yeast telomeres. Additionally, this thesis contributes to our understanding of the topological reorganization that telomeres undergo during senescence, a potent tumor suppressor mechanism in human cells.

Zusammenfassung

Durch die Tatsache, dass eukaryotische Chromosomen linear sind, müssen deren Enden geschützt werden und dürfen nicht von der Zelle als DNA Doppelstrangbrüche interpretiert werden. Telomere sind die repetitiven DNA Sequenzen an Chromosomenenden und übernehmen diese Schutzfunktion, indem sie einer unangemessenen „Checkpoint"-Aktivierung und DNA Reparaturvorgängen entgegenwirken. Telomere üben ihre Schutzfunktion vor allem durch die Proteinkomplexe aus, die spezifisch an sie gebunden sind. Darüber hinaus wurden dreidimensionale, gefaltete Telomerstrukturen damit in Verbindung gebracht, dass sie zum Schutz der Chromosomenenden beitragen. Dabei verbergen sie diese Endstücke und verhindern somit die irrtümliche Verknüpfung von Telomeren oder deren Abbau. Humane Telomere bilden eine lassoähnliche Struktur innerhalb der repetitiven Telomersequenzen, die als „t-loop" bezeichnet wird. Vorangegangene Studien legen nahe, dass sich die Telomere der Bäckerhefe *S. cerevisiae* in die Chromosomenregionen zurückfalten, die an Telomere grenzen und als Subtelomere bezeichnet werden. Allerdings fehlte bis jetzt eine Methode, mit der diese Strukturen robust nachgewiesen werden können. In dieser Doktorarbeit wurde eine Methode namens Telo-3C optimiert, um Interaktionen zwischen Telomer und Subtelomer an einem einzelnen, unmodifizierten Telomer zu quantifizieren. Diese Telo-3C Methode ermöglichte es, regulatorische Schlüsselfaktoren der Telomerfaltung zu identifizieren. Da Bäckerhefe ein genetisch vielseitiger Modellorganismus ist, wurde die Regulation der Telomerfaltung in diesem Organismus untersucht. Dies bietet die Möglichkeit, Parallelen zu humanen Telomeren zu ziehen und unbekannte Regulationsmechanismen der menschlichen Telomerstruktur aufzudecken.

Mit der Telo-3C Methode habe ich die Maschinerie der homologen Rekombination, einschließlich Rad51 und Rad52, sowie die „Checkpoint"-Kinase Rad53 als bisher unbekannte Schlüsselfaktoren der Telomerfaltung in der Bäckerhefe ermittelt. Meine Ergebnisse zeigen außerdem, dass die Histonmodifikatoren Sir2, Sin3 und Set2 wichtige regulatorische Faktoren für die Telomerfaltung sind. Diese Ergebnisse deuten darauf hin, dass eine spezifische Chromatinumgebung am Telomer unabdingbar für die Telomerfaltung sein könnte. Interessanterweise sind die SMC („structural maintenance of chromosomes") Komplexe Cohesin, Condensin und der SMC5/6 Komplex für die effiziente Faltung von Hefetelomeren nicht erforderlich. Daher liegt es nahe, dass sich der Mechanismus der Telomerfaltung von dem interner Chromatinschleifen („chromatin loops") unterscheidet. Die Telo-3C Analysen zeigten, dass sich Wildtyp-Telomere effizient zurückfalten. Im Gegensatz dazu ist die Telomerfaltung beeinträchtigt, wenn Zellen in die replikative Seneszenz eintreten. Ich konnte zeigen, dass sich Telomere in der Seneszenz jedoch unabhängig von ihrer verkürzten Telomerlänge entfalten. Vielmehr scheint diese Entfaltung der Telomere mit einem

bestimmten Seneszenzprogramm der Zelle in Verbindung zu stehen. Tatsächlich entfalten sich Telomere auch bei Behandlung mit dem DNA-schädigenden Mittel MMS (Methylmethansulfonat), das in der Bäckerhefe eine ähnliche Stressreaktion und globale Genexpressionsveränderungen auslöst wie die replikative Seneszenz. Eine quantitative massenspektrometrische Analyse ergab, dass bestimmte Regulatoren der Telomerfaltung (Sir2, Sin3 und Set2) während der Seneszenz in geringerer Menge vorhanden sind. Deren reduzierte Verfügbarkeit könnte dazu beitragen, dass sich die Telomerfaltung während der Seneszenz verringert.

Die hier vorgestellten Daten deuten darauf hin, dass die homologe Rekombinationsmaschinerie und bestimmte Chromatinmodifikatoren wichtige Voraussetzungen für die Faltung von Hefetelomeren sind. Darüber hinaus trägt diese Arbeit zu unserem Verständnis bei, wie sich die Telomerstruktur während der replikativen Seneszenz verändert, die einen wichtigen Mechanismus zur Unterdrückung von Tumoren im Menschen darstellt.

Abbreviations

3D	Three dimensional
5-FOA	5-Fluoroorotic acid
ABC	ATP-binding cassette
ac	Acetylation
AID	Auxin-inducible degron
alt-NHEJ	Alternative non-homologous end joining
APB	ALT-associated promyelocytic leukaemia body
ARS	Autonomously replicating sequence
BIR	Break-induced replication
bp	Base pairs
ChIP	Chromatin immunoprecipitation
CID	Chromosomal interaction domain
c-NHEJ	Classical non-homologous end joining
DDR	DNA damage response
d-loop	Displacement-loop
DNA	Deoxyribonucleic acid
ds	Double-stranded
DSB	Double-strand break
EV	Empty vector
Exp	Exponential
FACS	Fluorescence-activated cell sorting
FISH	Fluorescence *in situ* hybridization
G4	Guanine-quadruplex
gDNA	Genomic DNA
GO	Gene ontology
HDR	Homology directed repair
IAA	Indole-3-acetic acid; auxin
kb	Kilo-bases
kDa	Kilodalton
KO	Knockout
LAD	Lamina-associated domain
lncRNA	Long non-coding RNA
Mb	Mega-bases
me	Methylation
me1	Mono-methylation
me2	Di-methylation
me3	Tri-methylation
min	Minutes
MMEJ	Microhomology mediated end joining
MMS	Methyl methanesulfonate

NHEJ	Non-homologous end joining
nt	Nucleotides
OB	Oligonucleotide/oligosaccharide binding
PCR	Polymerase chain reaction
PD	Population doubling
PTM	Posttranslational modification
qPCR	Quantitative polymerase chain reaction
qRT-PCR	Quantitative reverse transcription PCR
rcf	Relative centrifugal force
RT	Room temperature
SAHF	Senescence associated heterochromatin foci
SC	Synthetic complete
sec	Seconds
SGD	*Saccharomyces* genome database
ss	Single-stranded
STR	Subtelomeric repeats
TAD	Topologically associated domain
TAP	Tandem affinity purification
TERRA	Telomeric repeat-containing RNA
TIF	Telomere dysfunction induced foci
t-loop	Telomere-loop
TPE	Telomere position effect
TPE-OLD	Telomere position effect over long distances
TSA	Trichostatin A
T-TF	Telomere-telomere fusion
UAS	Upstream activating sequence
wt	Wild type
YPD	Yeast peptone dextrose

1 Introduction

1.1 Telomeres

In the 1930s, two decades before the structure of DNA was elucidated, the chromosome researchers Hermann Muller and Barbara McClintock realized that the “free ends” of linear chromosomes behave differently than “broken ends” within the genome (Müller 1938; McClintock 1939). They claimed that the protective capping function of chromosome ends prevents them from fusing and called these ends “telomeres”, derived from the Greek words “telos” (end) and “meros” (part). In 1941, Barbara McClintock visualized the ends of individual chromosomes of maize (corn) cells as knobs of heterochromatin (McClintock 1941). At the same time, she observed, that chromosome breaks could also “heal” in a way that they would become stable free ends (McClintock 1939). Today we know that this finding was the first indication that the enzymatic activity of telomerase is involved in chromosome healing by elongating chromosome ends.

In 1961, Hayflick observed that cells can only undergo a limited amount of divisions in culture before they stop dividing (Hayflick & Moorhead 1961). Thereby, he introduced the concept of senescence and aging not knowing about the connection to telomeres. The link between telomeres and senescence was then made by Olovnikov (Olovnikov 1971; Olovnikov 1973) who proposed that the replication machinery could not copy telomeres completely thereby leading to their gradual shortening with each cell division. The molecular nature of telomeres was first described by Elizabeth Blackburn in the ciliate *Tetrahymena thermophila* as repetitive elements at the ends of chromosomes (Blackburn & Gall 1978). Together with Jack Szostak, she showed that the telomeric sequences from *Tetrahymena* have protective capacities, when introduced into yeast cells (Szostak & Blackburn 1982), supporting the idea that the capping function of telomeres is evolutionarily conserved. The next milestone for telomere research was the discovery of the enzyme adding *de novo* telomere repeats to chromosome ends (Greider & Blackburn 1985; Greider & Blackburn 1987). Carol Greider and Elizabeth Blackburn called this new enzyme telomerase, a specialized reverse transcriptase for telomere replication. Soon after, a genetic screen in the budding yeast *Saccharomyces cerevisiae* identified mutations in the telomere maintenance pathway, including components of the telomerase complex (Lundblad & Szostak 1989). Since then, the employment of budding yeast as a model to understand telomere biology, has greatly contributed to the understanding of telomere maintenance and the mechanism of telomerase action.

In 2009, Blackburn, Greider, and Szostak received the Nobel Prize "for the discovery of how chromosomes are protected by telomeres and the enzyme telomerase" and created the basis for the research on telomeres and telomerase to follow.

1.1.1 Human and yeast telomeres

The ends of eukaryotic chromosomes are protected by telomeres which consist of non-coding, double-stranded (ds) repeat sequences and a specific set of telomere-associated proteins. Although their sequence and exact protein composition differ between organisms, their protective function is highly conserved between all species with linear chromosomes (Giraud-Panis et al. 2010; Linger & Price 2009; Palm & de Lange 2008). Generally, their sequence is G-rich and extends into a 3' single-stranded (ss) overhang, a conserved feature among eukaryotes (McElligott 1997; Makarov et al. 1997). The overhang gets processed by several nucleases and its length is regulated on many layers (reviewed in de Lange 2018). Due to its guanine rich sequence and repetitive nature, the telomeric tract is prone to the formation of guanine-quadruplex (G4) structures, secondary structures that form when guanine quartets arrange in a helical shape (Sen & Gilbert 1988). Even though the ends of chromosomes are heterochromatic, a long non-coding RNA (lncRNA) is transcribed at telomeres (Luke et al. 2008; Azzalin et al. 2007a; Schoeftner & Blasco 2008). This RNA, dubbed TERRA (telomeric repeat-containing RNA), was described to form a three-stranded RNA:DNA hybrid structure at telomeres by base-pairing with its complementary DNA strand (Balk et al. 2013; Arora et al. 2014; Nanavaty et al. 2017).

The human telomeric sequence consists of TTAGGG repeats (Moyzis et al. 1988) with a length of 10-15 kb and an overhang of 50-400 nt (de Lange et al. 1990). In mammalian cells, it is well established that the 3' overhang assists in the formation of a lariat-like structure at telomeres, called t-loop (section 1.1.2.2).

Budding yeast telomeric sequences consist of $(TG)_{1\text{-}3}$ repeats and their sequence is heterogeneous in contrast to many other species. Yeast telomeres are 300 ± 75 bp long and the G-rich strand protrudes into a 12-14 nt overhang during most of the cell cycle (Larrivée et al. 2004). In late S/G2 phase, the overhang was detected to be much longer (≥30-100 nt), which coincides with the time when telomeres are replicated and elongated by telomerase (Wellinger et al. 1993; Dionne & Wellinger 1996; Dionne & Wellinger 1998). The regions adjacent to the telomeric repeats are called subtelomeres and they bear two classes of telomere-associated sequences, X elements and Y' elements (**Figure 1**). All budding yeast telomeres carry an X element and half of the chromosome ends additionally contain between one to four Y' elements (**Figure 1**) (Horowitz et al. 1984; Zakian et al. 1986). The X elements are more heterogeneous in sequence than the Y' elements and consist

of the so-called "core X" and subtelomeric repeats (STR) including binding sites for the essential transcription factor Tbf1 (**Figure 1**) (Brigati et al. 1993; Louis 1995). Additionally, the core X contains an ARS (autonomously replicating sequences) consensus sequence and an Abf1-binding site, the multifunctional regulator ARS-binding factor 1 (Louis 1995). Short stretches of telomeric sequences can connect the junctions between X-Y' and between Y'-Y' elements (**Figure 1**) (Walmsley et al. 1984). Also on Y' elements, potential origins of replication (ARS) were identified (**Figure 1**). The notion that the subtelomeric regions of budding yeast telomeres and the recruited proteins are variable often leads to differences in the behavior of individual telomeres.

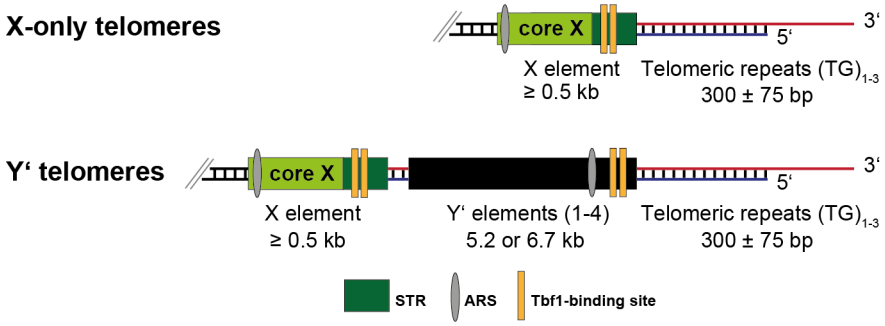

Figure 1. Composition of telomeres and subtelomeric elements in *S. cerevisiae*. Budding yeast telomeres consist of telomeric repeats and can have two classes of subtelomeric elements, X elements shown in green and Y' elements shown in black. Telomeres either only contain the X element (X-only telomeres) or additionally harbor one to four Y' elements. Y' elements exist in two sizes, 5.2 and 6.7 kb long. The X element consists of the core X and subtelomeric repeats (STR; dark green box) containing Tbf1-binding sites (yellow squares). Telomeric repeat sequences are depicted in blue and red, the blue strand being the C-rich strand with the 5' end. The red strand is the G-rich strand forming the 3' overhang. Potential replication origins (ARS) are shown as grey ovals. Adapted from Wellinger & Zakian 2012.

1.1.2 Solving the end protection problem

1.1.2.1 Telomere binding proteins

When left unprotected, the ends of chromosomes resemble DNA double-strand breaks (DSBs) and elicit a DNA damage response (DDR) leading to unscheduled repair activities. This phenomenon is referred to as the "end protection problem" (reviewed in de Lange 2018). The protein complexes binding to chromosome ends share the conserved function of solving the end protection problem. The telomere binding proteins not only distinguish telomeres from DNA breaks and prevent DNA repair activities at chromosome ends but also regulate telomere maintenance by telomerase, telomere replication and the telomeric chromatin state (reviewed in de Lange 2018).

In mammalian cells, the telomere binding protein complex is composed of six subunits and was called shelterin. It consists of Telomeric Repeat binding Factor 1 and 2 (TRF1 and TRF2), Protection Of Telomeres 1 (POT1), TRF2- and TRF1-Interacting Nuclear protein 2 (TIN2), RAP1 (the human ortholog of the yeast Repressor/Activator Protein 1) and TPP1 (reviewed in Palm & de Lange 2008). Both TRF1 and TRF2 bind the ds telomeric region as homodimers and recruit the other members

of the shelterin complex in a sequence-specific manner (**Figure 2A**) (Bianchi 1997; Nishikawa et al. 2001; Broccoli et al. 1997). POT1 is the only member of the shelterin complex that binds to the single-stranded telomeric overhang with its oligonucleotide/oligosaccharide binding (OB) folds (**Figure 2A**) (Lei et al. 2004; Baumann 2001). The bridge between the single- and double-stranded portions of the complex is provided by TIN2 and TPP1 which bind to TRF1/TRF2 and POT1 respectively (**Figure 2A**) (reviewed in Palm & de Lange 2008). The mammalian RAP1 protein is devoid of a DNA binding ability and associates with telomeres via TRF2 (**Figure 2A**). All shelterin members were described to be sufficiently abundant to cover the entire telomeric DNA throughout the cell cycle (Palm & de Lange 2008).

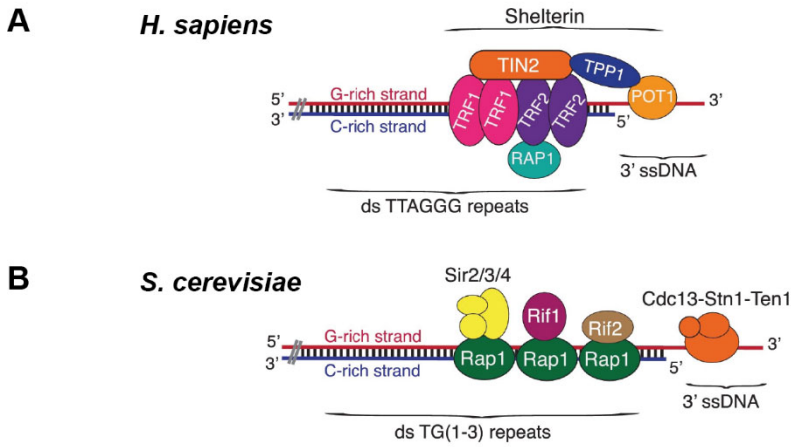

Figure 2: Telomere binding proteins in budding yeast and human cells. (A) Human telomeres (*H. sapiens*) are covered by the shelterin complex, comprising six different proteins. TRF1 and TRF2 form homodimers and are direct binders of the ds telomeric repeat DNA. POT1 associates with the 3' overhang of the telomere and is connected to TRF1 and TRF2 via TIN2 and TPP1. RAP1 associates with TRF2. **(B)** The double-stranded telomeric repeats in budding yeast (*S. cerevisiae*) are covered by Rap1 which recruits the Sir2/3/4 complex, Rif1 and Rif2. The CST complex (Cdc13-Stn1-Ten1) specifically binds to the single-stranded 3' overhang. Figure and legend adapted from Geronimo & Zakian 2016.

In budding yeast, the telomeric repeats are associated with Rap1, Rif1 and Rif2 (RAP1-Interacting Factor 1 and 2), the SIR (Silent Information Regulator) complex (Sir2/3/4) and the CST complex (Cdc13-Stn1-Ten1). In contrast to the mammalian shelterin complex, in *S. cerevisiae* the Rap1 protein takes the role of the direct telomere DNA binder via its tandem Myb-like domains and recruits other telomere-associated proteins (**Figure 2B**) (König et al. 1996; Gao et al. 2007). On the one hand, Rap1 recruits Rif1 and Rif2, key factors for telomere length regulation and end protection (Wotton & Shore 1997; Hardy et al. 1992; Bonetti et al. 2010; Anbalagan et al. 2011). On the other hand, Rap1 recruits the SIR histone deacetylase complex (HDAC) which is responsible to establish transcriptional silencing at subtelomeres (**Figure 2B**) (Moretti et al. 1994; Rusche et al. 2003) (section 1.1.4). The CST complex, comprising the proteins Cdc13, Stn1 and Ten1, covers the single-stranded portion of budding yeast telomeres (**Figure 2B**). Although Cdc13 binds the 3' overhang through a single OB-fold, it was suggested not to be a POT1 ortholog (Palm & de Lange 2008). The

CST complex rather resembles the trimeric replication protein A (RPA) complex from which it might have evolved (Gao et al. 2007). The most prominent role of RPA is covering the single-stranded template DNA during lagging strand replication. The CST complex is essential for telomere capping and their protection by preventing nucleolytic degradation of telomeres and their recombination (Garvik et al. 1995; Polotnianka et al. 1998). Additionally, the CST complex promotes the elongation of the telomeric repeats by telomerase through the interaction of its subunit Cdc13 with telomerase (Bianchi et al. 2004). The interaction of the CST complex with DNA polymerase alpha/primase supports the synthesis of the telomeric C-rich strand (Grandin 2001; Giraud-Panis et al. 2010; Nugent et al. 1996; Diede & Gottschling 1999; Qi & Zakian 2000).

The core telomeric protein complex performs many of its tasks through the recruitment of accessory factors, in both human and yeast cells. These associated factors mostly only interact transiently with telomeres or the telomere binding proteins. Additionally, they are less abundant at telomeres in contrast to the main complex, which binds throughout the cell cycle. The major role of these accessory factors is not at telomeres, but they are mostly involved in other nuclear processes, such as DNA repair, DNA damage signaling, DNA replication or chromatin structure. Prominent examples in human cells are the Mre11 complex (Zhu et al. 2000), the Apollo nuclease (Lenain et al. 2006; van Overbeek & de Lange 2006), the structure-specific endonuclease SLX4 (Sarkar et al. 2015) and RAD51 (Tarsounas et al. 2004), all best known for DNA repair activities. Other human shelterin-associated factors are HP1 (heterochromatin protein 1) proteins important for providing heterochromatin structure (García-Cao et al. 2004), the replicative RecQ helicases (Opresko et al. 2002) and Tankyrase 1 which is important for telomere length regulation and the cohesion of telomeres (Dynek & Smith 2004; Smith & De Lange 2000; Smith et al. 1998). In many organisms, including yeast and humans, the Ku70/80 complex is key for telomere function (Hsu et al. 1999; Hsu 2000; Gravel et al. 1998; Porter et al. 1996; Boulton & Jackson 1996). Budding yeast cells, lacking components of the Ku complex show altered telomeric phenotypes such as drastically short telomeres, longer G-strand overhangs and deregulated subtelomeric chromatin (Gravel et al. 1998; Porter et al. 1996).

1.1.2.2 Telomeric structures – the t-loop and telomere folding

Besides the specific protein complexes at telomeres, architectural features were also implicated in end protection. Mammalian telomeres share a lariat-like structure, dubbed the telomere-loop (t-loop) (**Figure 3**). The t-loop forms by strand invasion of the 3' ss overhang into the telomeric repeats thereby base pairing with the C-strand. This results in the displacement of the G-strand into a d-loop (displacement-loop) (**Figure 3**). The first evidence for the existence of t-loop structures was

obtained from electron microscopy images of isolated protein-free DNA from human and mouse telomeres, where the t-loop structure was stabilized by psoralen-crosslinking (Griffith et al. 1999). Later, t-loops were also detected on non-crosslinked telomeric chromatin where nucleosomes covered the loop (Nikitina & Woodcock 2004) and via super-resolution microscopy approaches (Doksani et al. 2013; Van Ly et al. 2018). The size of the t-loop is variable and so far, there is no evidence that the size is important for its function. How frequently t-loops form at chromosome termini and how many telomeres of one cell are packed into loops is still under debate.

T-loops or similar structures were observed in trypanosomes, ciliates, plants and in over-elongated telomeres of the yeast *Kluyveromyces lactis* (Cesare et al. 2003; Cesare et al. 2008; Murti & Prescott 1999; Muñoz-Jordán et al. 2001). Interestingly, t-loops were also detected in the mitochondrial DNA of the yeast *C. parapsilosis* (Tomaska et al. 2002).

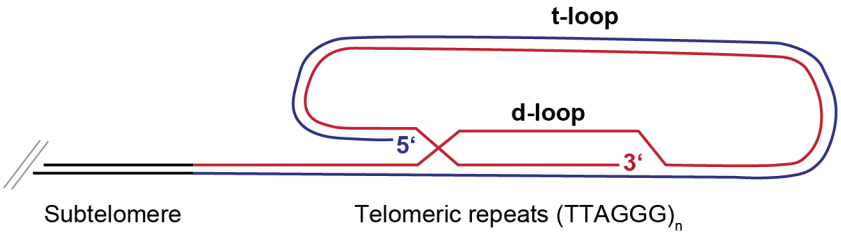

Figure 3: Schematic illustration of the t-loop at mammalian telomeres. The telomere loop (t-loop) is established by strand invasion of the 3’ overhang of the G-rich strand (red) into the C-strand (blue). Thereby the G-strand gets displaced into a d-loop. The size of the t-loop is variable. Adapted from Palm & de Lange 2008.

Functionally, the t-loop was suggested to provide an additional layer of protection to the described telomere binding protein complex. By sequestering the 3’ overhang within the d-loop, t-loops are implicated in limiting the accessibility of nucleases and DNA repair activities to chromosome ends (Griffith et al. 1999). Further, it was proposed that the t-loop protects telomeres from fusions and might repress exchanges between sister telomeres, however, it became evident that the t-loop is not the only mechanism in place (Celli et al. 2006; Wang et al. 2009). Recent studies provided evidence that the t-loop contributes to preventing a DNA damage response at telomeres (Van Ly et al. 2018; Cesare et al. 2013). These studies showed that telomeres aberrantly activate the DNA damage checkpoint kinase ATM (Ataxia telangiectasia mutated) when they cannot fold into a t-loop. However, these telomeres are still resistant to fusions.

At human and mouse telomeres, TRF2 is the main player for the establishment of the t-loop (Doksani et al. 2013). TRF2 has the capacity to change the topology of DNA as well as to promote DNA unwinding and thus supports strand invasion (Amiard et al. 2007; Poulet et al. 2009). With its basic domain, TRF2 can bind to branched DNA structures and Holliday junctions *in vitro* (Fouché et al. 2006; Poulet et al. 2009). The activity to mediate t-loop formation was assigned to its TRF-

homology (TRFH) domain which can wrap 90 bp of DNA around this domain itself (Benarroch-Popivker et al. 2016). As a result, a mutant of the TRFH domain – Top-less TRF2 – has a reduced capacity to establish t-loops *in vivo* (Benarroch-Popivker et al. 2016). Super-resolution microscopy experiments provided evidence that POT1 is not required for the t-loop formation, although it was speculated that it might bind the three-way junction at the d-loop and thereby stabilize the t-loop (Doksani et al. 2013). Although TRF2 was shown to be both necessary and sufficient for the formation of t-loops (Doksani et al. 2013), other factors were suggested to assist TRF2 *in vivo.* Recombination and repair proteins might help in the strand invasion process after replication, including the MRN (MRE11, RAD50, NBS1) complex, RAD51 and RAD52 (Radiation sensitive 51 and 52) (Verdun & Karlseder 2006; Verdun et al. 2005). Recent studies suggested that t-loops can also form between the telomeric repeats and interstitial telomeric sequences, arrays of intra-chromosomal telomeric repeats (Wood et al. 2014; Meyne et al. 1990; Azzalin et al. 1997; Weber et al. 1990). The authors referred to these loop structures as interstitial t-loops and found that they form in a TRF2-dependent manner and additionally require lamin A/C, a nuclear intermediate filament protein (Wood et al. 2014). It was proposed that interstitial t-loops provide an additional layer of chromosome end protection and contribute to telomere stability (Wood et al. 2014).

T-loops are an obstacle for the progression of the replication fork and to this end, t-loops have to be resolved for the unimpeded passage of the replication machinery. Additionally, it has been speculated that it might be necessary to dismantle t-loop for telomerase access in late S phase. The RTEL1 (regulator of telomere elongation helicase 1) helicase was shown to be an important player in this process (Ding et al. 2004; Uringa et al. 2012). RTEL1 is capable of unwinding telomeric G-quadruplex (G4) structures but is also involved in t-loop opening during S phase and therefore serves a dual function at telomeres (Vannier et al. 2012; Uringa et al. 2012). Through the interaction with TRF2, RTEL1 is recruited to telomeres specifically in S phase and unwinds the t-loop for the passage of the replication fork (Sarek et al. 2019; Sarek et al. 2015). The importance of t-loop unwinding becomes clear when RTEL1 is absent. In this scenario, t-loops are cleaved off by the SLX1/4 nuclease complex leading to the excision of telomeric circles (t-circles) and drastic telomere shortening (Vannier et al. 2012). The telomeric G4 unwinding function of RTEL1 is based on its interaction with PCNA (Proliferating cell nuclear antigen). When RTEL1 cannot execute its G4 unwinding function telomere replication problems and subsequent telomere fragility occur (Vannier et al. 2012). Interestingly, the interaction of RTEL1 with PCNA, traveling with the replication fork, is required for preventing telomere fragility but it is not necessary for t-loop unwinding (Vannier et al. 2013). Other players for the dissolution of the human t-loop were proposed to be the WRN (Werner syndrome ATP-dependent helicase) and BLM (Bloom syndrome

protein) helicases and other members of the RecQ helicase family (Opresko et al. 2002; Lillard-Wetherell et al. 2004; Opresko et al. 2004; Ghosh et al. 2012).

To date, it has not be unraveled if budding yeast telomeres engage in a structure similar to the t-loop. Yeast telomeres are shorter than mammalian telomeres and their shorter length has been proposed to put physical constraints on the formation of folded telomere structures (de Lange 2009). Additionally, the heterogeneous nature of telomeric repeats might limit the strand invasion potential for a t-loop (de Lange 2009). Nevertheless, yeast telomeres are thought to fold back into the subtelomere although the mechanisms for the maintenance and regulation of the so-called "fold-back" structure are largely unknown (de Bruin et al. 2000; Poschke et al. 2012; Strahl-Bolsinger et al. 1997). Due to the shorter telomere length in yeast compared to mammalian telomeres, imaging methods such as electron microscopy or super-resolution microscopy could not be applied efficiently so far. Additionally, the base composition of *S. cerevisiae* telomeres does not fulfill the sequence requirements for stabilizing three-dimensional (3D) structures with psoralen for electron microscopy (reviewed in De Lange 2004). The first evidence for the existence of a folded telomere structure was based on a reporter construct, integrated near the telomeric repeats of telomere 7L (de Bruin et al. 2001). In this study, the Gal4 upstream activating sequence (UAS*) was inserted downstream of a *URA3* reporter gene and acts as an enhancer element for its transcription (Figure 4) (de Bruin et al. 2001). In the presence of Galactose, *URA3* transcription would only be activated when this telomere folds back bringing the UAS* into close proximity of the gene promoter (Figure 4). The readout for the magnitude of telomere folding was based on cell growth on Uracil-containing media and reduced cell viability on media that contains 5-FOA (5-fluoroorotic acid), which is toxic for cells expressing *URA3* (Figure 4). Importantly, *URA3* transcription only gets activated when the reporter construct is placed into the vicinity of telomeres and not at an internal chromosomal locus (de Bruin et al. 2001). In the same study, the authors identified the SIR complex as a regulator of telomere folding, as *URA3* transcription was not efficiently activated in *sir3* mutants (de Bruin et al. 2001).

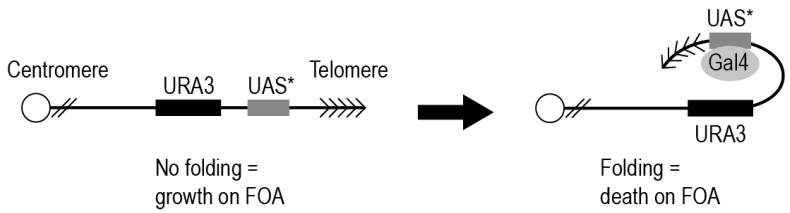

Figure 4. Genetic reporter for telomere folding in budding yeast. The genetic reporter construct for telomere folding was introduced at telomere 7L. It contains a *URA3* gene followed by a Gal4 UAS* (upstream activating sequence). A telomere fold-back structure brings the UAS* into the proximity of the *URA3* promoter and supports *URA3* transcription in the presence of Galactose. Adapted from Poschke et al. 2012.

A genome-wide screen on the yeast knockout (KO) collection with the described telomere folding reporter construct revealed, that several biological processes seem to be involved in the regulation of telomere folding (Poschke et al. 2012). The screen showed that histone deacetylation and chromatin remodeling were enriched biological processes among the potential regulators of telomere folding (Poschke et al. 2012). The authors specifically implicate the histone deacetylase complexes Rpd3L, Rpd3S and Hda1 in promoting a fold-back structure at yeast telomeres (Poschke et al. 2012). The Rpd3L and Rpd3S complexes are multisubunit histone deacetylase complexes that have Sin3 as a common member (Carrozza et al. 2005; Keogh et al. 2005). Based on data from the genetic reporter, telomere folding was shown to be compromised in *sin3* mutants, as well as in mutants of the Rpd3L (*rxt2, sap30*) and Rpd3S (*eaf3, rco1*) complexes (Poschke et al. 2012). The authors propose that telomere folding through histone deacetylation might specifically prevent excessive resection at uncapped telomeres and therefore implicate telomere folding in end protection (Poschke et al. 2012). Additionally, Poschke et al. identified the telomere binding proteins Rif1 and Rif2 as regulators of telomere folding. As detected by the *URA3* telomere folding reporter, they showed that the establishment of the telomere fold-back structure is compromised in *rif1* and *rif2* mutants (Poschke et al. 2012).

In addition, chromatin immunoprecipitation (ChIP) experiments of telomeric proteins suggest that budding yeast telomeres fold back. Several studies showed, that the telomeric proteins Rap1 and Cdc13 are not only detected at the telomeric repeats themselves, but also immunoprecipitate at more distant regions along the subtelomere (Poschke et al. 2012; Strahl-Bolsinger et al. 1997). This points towards a mechanism by which Rap1 and Cdc13 might bind to subtelomeric regions mediated by a folded telomere structure. Using the ChIP approach, Poschke et al. confirmed that the presence of the fold-back structure depends on Rif1 and Rif1 as well as on several chromatin modifiers, including the SIR and Rpd3 complexes (Poschke et al. 2012).

1.1.3 Solving the end replication problem

The classical definition of the “end replication problem” was based on the observation that the eukaryotic replication machinery cannot completely duplicate chromosome ends and therefore telomeres shorten which each replication cycle (Olovnikov 1971; Olovnikov 1973; Watson 1972). Eukaryotic DNA polymerases cannot start DNA synthesis *de novo* but need an RNA primer to start (reviewed in Hug & Lingner 2006). DNA synthesis is unidirectional and can only proceed in 5’-3’ directionality resulting in only one DNA strand, the leading strand, being synthesized continuously. On the leading strand, the replication machinery starts from a replication origin, and DNA can be synthesized until the chromosome end, creating a blunt end. The DNA synthesis on the lagging

strand is discontinuous as it has to be synthesized as Okazaki fragments, each fragment being primed with its own RNA primer. When the most distal primer is removed, the 5' telomeric end is left with a gap that corresponds to the size of the RNA primer and cannot be replicated. This would result in a shorter replication product than the template DNA and was originally proposed to explain the end replication problem leading to the gradual telomere shortening with each replication round (Olovnikov 1971; Olovnikov 1973; Watson 1972).

Since then, researchers have realized that there is another layer of complexity in the end replication problem. First hints arose from the observation that the telomere shortening rate is only half of the expected 10 nt per replication round, which is the average size of the RNA primer (Lundblad & Szostak 1989; Singer & Gottschling 1994). Therefore, according to a more recent model, the end replication problem is mostly a leading strand problem (Lingner et al. 1995). The G-strand, which is the lagging strand template, carries the 3' overhang and is, therefore, longer than the C-strand, the leading strand template (Figure 5). After replication, the leading strand creates a blunt end product which needs to be processed via resection to create a 3' overhang (Figure 5) (Soudet et al. 2014). The resection generates a long G-tail and the C-rich strand needs to be filled in by an RNA primed C-strand synthesis. After removal of the RNA primer for C-strand fill-in, the replication product from the leading strand is shorter than from the lagging strand (Figure 5) (Lingner et al. 1995; Soudet et al. 2014). In conclusion, it was suggested that the complex interplay between the end replication problem, the 3' overhang processing and C-strand fill-in defines the actual shortening rate of telomeres (reviewed in Wellinger & Zakian 2012; Mieczkowski et al. 2003).

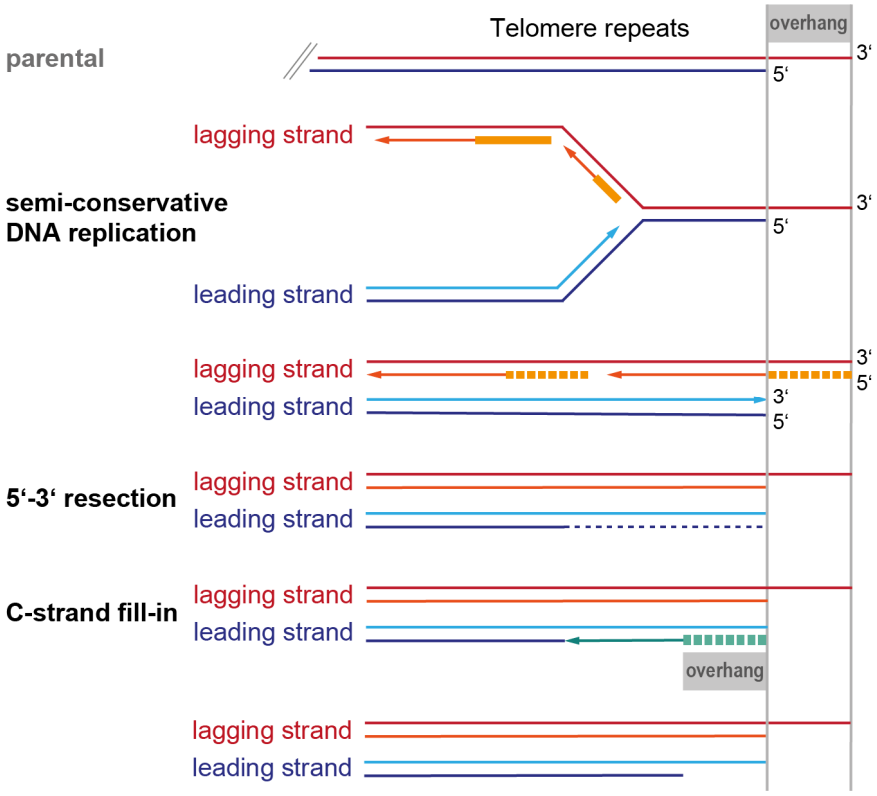

Figure 5. Model for the end replication problem in budding yeast. Telomeres get replicated in a unidirectional way, with the G-rich strand being the lagging strand template (red) and the C-rich strand being the leading strand template (blue) for semi-conservative DNA replication. When telomere replication is completed, the leading strand may end in a blunt end, while the lagging strand contains a 3’ overhang after the removal of the RNA primer. The blunt-ended leading strand gets processes by 5’-3’ resection and subsequently, the C-strand is filled in again leaving a 5-10 nt telomeric overhang. This schematic shows that telomere shortening due to the end replication problem is mostly attributed to the leading strand. Okazaki fragments are depicted in orange and the RNA primer in yellow. Adapted from Soudet et al. 2014.

1.1.3.1 Telomerase

Most organisms counteract the telomere shortening that results from the end replication problem with the expression of a specialized enzyme, telomerase, which can add new telomeric repeats to chromosome ends. This enzyme contains a reverse transcriptase activity, composed of a catalytic protein component and an RNA moiety serving as a template for DNA synthesis (Greider & Blackburn 1987; Greider & Blackburn 1989). Telomerase is not capable of adding telomeric repeats to blunt ends but only elongates 3’ G-rich overhangs (reviewed in Wellinger & Zakian 2012). Subsequently, conventional DNA polymerases fill in the C-strand using an RNA primer (reviewed in Hug & Lingner 2006). Interestingly, the shortest telomeres in budding yeast and human cells get preferentially elongated by telomerase (Teixeira et al. 2004; Britt-Compton et al. 2009; Hemann et al. 2001).

Human telomerase is composed of the protein component, hTERT, and the telomerase RNA hTR (reviewed in Schmidt & Cech 2015). Active telomerase is only expressed in the germline and certain stem cell compartments but transcriptionally silenced in most human somatic cells (reviewed in

Schmidt & Cech 2015). Additionally, telomerase is upregulated in 73 % of human cancers to counteract telomere shortening (Barthel et al. 2017). This allows the transformed cells to divide indefinitely, which is a hallmark of cancer (Hanahan & Weinberg 2011).

In budding yeast, telomerase is constitutively expressed and consists of the catalytic component Est2 and the Tlc1 template RNA (Singer & Gottschling 1994; Lundblad & Szostak 1989). A 17 nt stretch in Tlc1 serves as a template for telomere synthesis (reviewed in Wellinger & Zakian 2012). The associated factors Est1 and Est3 are required for the effective function and recruitment of telomerase (Chan et al. 2008; Lendvay et al. 1996). Yeast telomerase is not active throughout the cell cycle but specifically adds telomeric repeats to chromosome ends in late S and G2 phase of the cell cycle (Diede & Gottschling 1999; Marcand et al. 2000).

1.1.3.2 Telomere shortening and senescence

In the absence of telomerase, telomeres gradually shorten and during this process they progressively lose their protective capacities. As a result, these eroded telomeres activate a DNA damage checkpoint which results in a permanent cell cycle arrest, referred to as replicative senescence (reviewed in Teixeira 2013). Replicative senescence is considered a potent tumor suppressor mechanism for human somatic cells as telomere shortening limits the growth potential of transformed cells (reviewed in Maciejowski & De Lange 2017). The role of telomere shortening in aging is still discussed controversially. However, it is clear that with increasing age, the mean telomere length of individuals decreases and the proportion of senescent cells rises (Lansdorp 2008).

In mammalian cells, telomere erosion leads to the recognition of chromosome ends as sites of DNA damage and activates ATM and ATR (ataxia telangiectasia and Rad3-related protein) signaling. This results in the formation of so-called telomere dysfunction induced foci (TIFs), defined by the colocalization of DNA damage markers such as γH2AX or 53BP1 with telomeres (Takai et al. 2003). As a result, the activation of p53 and the induction of the cyclin-dependent kinase inhibitors p21 and p16 lead to a G1 arrest in mammalian cells (Takai et al. 2003; Jacobs & De Lange 2004; Maciejowski & De Lange 2017). Thereby, the activation of the p53 and p16/pRB (retinoblastoma) pathways act as potent tumor suppressor pathways to inhibit additional cell divisions. During the process of replicative senescence, cells go through drastic phenotypic changes including an enlarged cell morphology, specific alterations of the transcriptional and metabolic profile, the secretory program, as well as changes in chromatin state (Campisi & D'Adda Di Fagagna 2007). The chromosomes of senescent mammalian cells become more condensed, forming senescence-associated heterochromatin foci (SAHFs) (Campisi & D'Adda Di Fagagna 2007). Interestingly,

telomeres are excluded from SAHFs, pointing towards a mechanism where heterochromatin might be lost at telomeres during senescence (Ye et al. 2007).

Mammalian cells can divide beyond the cell cycle arrest imposed by senescence through the inactivation of the p53 and pRB tumor suppressor pathways and enter the state of telomere crisis (Mieczkowski et al. 2003; Campisi & D'Adda Di Fagagna 2007). Telomere crisis is characterized by many dysfunctional telomeres, telomere-telomere fusions, high levels of genome instability and frequent cell death (Artandl et al. 2000; Artandi & DePinho 2009). The activation of telomere elongation mechanisms, e.g. telomerase, provides a way out of telomere crisis and restores cell viability which are early steps in tumorigenesis (Mieczkowski et al. 2003).

The response of budding yeast cells to telomere shortening is similar to what has been described for human fibroblasts and other mammalian cells (reviewed in Teixeira 2013). Thus, the model organism *S. cerevisiae* is widely used to study the senescence process. In the absence of catalytically active telomerase, e.g. by knockout of the catalytic subunit *EST2* or the telomerase RNA *TLC1*, the growth potential of yeast cells progressively decreases (Lundblad & Szostak 1989). After 60-80 population doublings (PDs), telomerase negative yeast cells exhibit a cell cycle arrest at the G2/M border and increase their cell volume over time (Lundblad & Szostak 1989; Singer & Gottschling 1994; Lendvay et al. 1996). Despite the permanent cell cycle arrest, these cells remain in a metabolically viable state (IJpma & Greider 2003; Enomoto et al. 2002). In budding yeast, one critically short telomere is enough to anticipate the onset of senescence and elicit a checkpoint response (Khadaroo et al. 2009; Abdallah et al. 2009). Even though both major checkpoint kinases Mec1 and Tel1 are localized to this telomere, the critically short telomere is recognized by Mec1 which activates the DNA damage checkpoint and the growth arrest (Abdallah et al. 2009). This checkpoint response leads to the phosphorylation of the effector kinase Rad53 which depends on the Mec1 kinase, and on the adaptor proteins Rad9 and Rad24 (Grandin et al. 2005; IJpma & Greider 2003). Interestingly, Rad53 phosphorylation also requires Mrc1, an S phase checkpoint protein needed for replication (Alcasabas et al. 2001). This points towards a mechanism in which eroded telomeres are recognized both as DSBs and replication stress (Grandin et al. 2005). Recombination between telomeres can compensate for telomere shortening upon telomerase knockout, exemplified by a synthetic growth defect of cells lacking the key recombination protein Rad52 from the time when telomerase is deleted (Lundblad & Blackburn 1993; Lendvay et al. 1996). Accordingly, telomeric recombination centers, visualized as Rad52 foci, can be observed very early after the loss of telomerase (Khadaroo et al. 2009).

1.1.3.3 Telomere maintenance without telomerase

In the absence of telomerase from *S. cerevisiae* cells, some cells overcome the cell cycle arrest of senescence and elongate their telomeres in a telomerase independent mechanism (Lundblad and Blackburn 1993). These cells, referred to as post-senescence survivors, have acquired a telomere elongation mechanism that relies on homologous recombination (Lundblad & Blackburn 1993; Le et al. 1999; Teng & Zakian 1999). Key players in this process are proteins encoded by the *RAD52* epistasis group of genes and the Pol32 subunit of DNA polymerase δ required for a homologous recombination repair pathway for one-ended DSBs, called break-induced replication (Lundblad & Blackburn 1993; Teng & Zakian 1999; Chen et al. 2001; Le et al. 1999). Survivors were categorized into type I and type II survivors depending on the amplification pattern of telomeres and subtelomeric elements in combination with their additional genetic requirements. Type I survivors amplify the subtelomeric Y' repeats while their telomeric tract remains very short (50-150 bp) (see also **Figure 1**) (Lundblad & Blackburn 1993; Larrivée & Wellinger 2006). The Rad51 recombinase has a major function during Y' recombination and is assisted by Rad54, Rad57 and supposedly Rad55 (Le et al. 1999; Chen et al. 2001). Type I survivors arise at high frequency but grow slowly due to constitutive activation of the DNA damage checkpoint (Teng & Zakian 1999; Churikov et al. 2016). Therefore, they are often overgrown by yeast type II survivors in liquid culture. The *RAD51*-independent type II survivors are defined by a drastic increase of the $(TG)_{1\text{-}3}$ telomeric repeats resulting in heterogeneous telomere length. For the dramatic lengthening of short telomeres arising in type II survivors, the MRX complex (Mre11, Rad50 and Xrs2), Rad59 and the yeast RecQ helicase Sgs1 are required (Teng et al. 2000; Le et al. 1999; Johnson et al. 2001). Additionally, it was suggested that a relocalization of eroded telomeres to the nuclear pore complex during senescence promotes type II recombination between telomeres (Churikov et al. 2016; Khadaroo et al. 2009).

Between 5 to 15 % of human cancers maintain their telomeres using a telomerase independent mechanism, called Alternative Lengthening of Telomeres (ALT) (Barthel et al. 2017; Bryan et al. 1997). The activation of the ALT pathway happens during tumorigenesis when cells have inactivated the p53 and pRB tumor suppressor pathways and experience telomere crisis (reviewed in Maciejowski & De Lange 2017). Many parallels were described between ALT cancer cells and yeast survivors concerning the proteins involved and the employed mechanisms of telomere recombination but also the phenotypes by which they are identified. One shared characteristic between yeast survivors and ALT cells is the drastic heterogeneity in telomere length (Henson et al. 2002; Bryan et al. 1995; Teng & Zakian 1999; Chen et al. 2001). The telomere length in these cells is highly dynamic, due to rapid lengthening and shortening events (Murnane et al. 1994). Additionally, increased amounts of extra-chromosomal telomeric DNA have been observed in ALT

cells and yeast survivors, both in linear and circular forms (Tokutake et al. 1998; Ogino et al. 1998; Cesare & Griffith 2004; Wang et al. 2004; Larrivée & Wellinger 2006). A hallmark of ALT cells, which is often used as a marker for ALT tumors, is a specific nuclear body, the ALT-associated promyelocytic leukemia body (APB), containing telomere-binding proteins and several different DNA repair and replication factors (Yeager et al. 1999). Similarly, the regulation of the long non-coding RNA TERRA transcribed from telomeres shares parallels in ALT cells and yeast survivors, as both of them exhibit increased TERRA levels (Misino et al. 2018; Episkopou et al. 2014; Ng et al. 2009).

1.1.4 Telomeric chromatin

Nucleosomes are the fundamental organizational units of chromatin. Within one nucleosome, 145 to 147 bp of DNA is wrapped around an octamer of the four core histone proteins, H2A, H2B, H3 and H4 (Luger et al. 1997; McGinty & Tan 2015). The individual nucleosomes are connected via a segment of linker DNA which is associated with the linker histone H1 (Zhou et al. 1998; McGinty & Tan 2015). The chromatin structure is regulated by posttranslational modifications (PTMs) mostly on lysine residues at the N-terminal histone tails changing the histone-DNA interaction, its recognition by chromatin-modifying enzymes or chromatin remodelers. The modification of histone tails also affects the regulation of gene expression through transcription factor binding and establishes euchromatin and heterochromatin environments (Rusche et al. 2003; Grunstein & Gasser 2013; Ichikawa et al. 2015; Wood et al. 2005; Bannister & Kouzarides 2011). Heterochromatin is a tightly packed and condensed form of DNA and was described to be less accessible for the transcription machinery (Solovei et al. 2016; Monneron & Bernhard 1969). The less condensed euchromatin is generally more accessible and associated with active transcription (Solovei et al. 2016; Monneron & Bernhard 1969). The combination of different histone modifications, the histone code, forms the basis for the chromatin state of a locus, creating either an active or a repressed chromatin environment. Generally, the acetylation of histone tails is considered a main regulator of chromatin accessibility in eukaryotic cells by reducing the positive charge of lysine residues, where the acetylation is attached. This results in reduced histone-DNA interactions and loosely packed euchromatin. On the contrary, loci where acetyl modifications get removed from histone tails tend to be more heterochromatic and less accessible (reviewed in Kurdistani & Grunstein 2003). However, the chromatin environment also depends on the combination with other histone marks.

An intact chromatin environment of telomeres and subtelomeres is fundamental for their regulation and function. When the telomeric chromatin environment is disrupted, they become

dysfunctional and unstable (Brunet & Berger 2014; Tardat & Déjardin 2018; Bitterman et al. 2003; Lombard et al. 2008). The telomeric repeats in budding yeast were reported to be free of nucleosomes. In contrast, nucleosomes are associated with subtelomeric sequences, which are of a heterochromatic nature (Wellinger & Zakian 2012). Currently, it is controversial whether also the yeast telomeric repeats themselves are truly heterochromatic or only the subtelomeric regions (Cubiles et al. 2018). The boundary between the subtelomeric heterochromatin and the more centromere proximal euchromatin is tightly regulated and there are several mechanisms in place on both sides (Rusche et al. 2003).

The heterochromatin at budding yeast subtelomeres is established via histone deacetylation by the SIR complex, composed of Sir2, Sir3 and Sir4 (Grunstein 1997). The SIR complex is recruited to telomeres in a sequence-specific manner via the direct telomeric repeat binder Rap1 (see **Figure 2**) (Moretti et al. 1994; Rusche et al. 2003). More specifically, Sir3 and Sir4 can bind to Rap1 either independently or in cooperation (Wright et al. 1992; Moretti & Shore 2001; Luo et al. 2002; Liaw & Lustig 2006; Feeser & Wolberger 2008). Additionally, Sir4 can also be recruited to chromosome ends via the Ku complex (Tsukamoto et al. 1997), allowing for Rap1-independent recruitment of the SIR complex to telomeres (Martin et al. 1999; Luo et al. 2002). Sir4 in turn recruits the catalytic subunit Sir2, an NAD^+-dependent deacetylase, to the telomeric repeats which deacetylates histone 4 on lysine 16 (H4K16) (Liou et al. 2005). The nucleosomes with deacetylated H4 provide a binding site for Sir3 and therefore recruit additional SIR complexes to chromosome ends (Onishi et al. 2007). This observation led to the model of the SIR complex "spreading" from the telomeric repeats, where is has the highest association, a few kilo-base pairs towards the subtelomeric regions (Strahl-Bolsinger et al. 1997; Imai et al. 2000; Hecht et al. 1995; Luo et al. 2002; Carmen et al. 2002; Hoppe et al. 2002). This heterochromatin spreading leads to transcriptional silencing of many genes near telomeres, a phenomenon that was dubbed telomere position effect (TPE) (Gottschling et al. 1990). TPE was discovered by reporter genes (*URA3* or *ADE2*) which were introduced adjacent to a synthetic telomere on the right arm of Chr V or the left arm of Chr VII (Gottschling et al. 1990). It was originally proposed that the silencing effect of telomeres on these genes was independent from the gene and its promoter placed into proximity of the telomere (Gottschling et al. 1990; Renauld et al. 1993; Fourel et al. 1999). Importantly, telomere length affects the telomere position effect, and also the nuclear localization of telomeres can affect the degree of TPE (Anderson et al. 2014). Later studies showed however, that TPE depends on the telomere-associated sequences and differs between X-only telomeres and Y' telomeres and the combination of both elements (Power et al. 2011). Interestingly, it was shown that some telomeres (*TEL03L, TEL04L* or *TEL10L*) do not at all exert any silencing effect on a reporter gene placed into

their proximity (Pryde & Louis 1999). At certain telomeres, even a discontinuous SIR complex binding has been reported (Zill et al. 2010; Thurtle & Rine 2014). More recently, the concept of SIR complex spreading was additionally challenged by a report stating that Sir2 binding is not continuous but rather increased at specific subtelomeric positions (Ellahi et al. 2015; Pryde & Louis 1999). By Sir2 chromatin immunoprecipitation experiments the authors did not detect a gradient of Sir2 binding towards subtelomeres and therefore suggest that also subtelomeric silencing might be discontinuous. This goes in line with their finding, that only 6 % of all subtelomeric genes are silenced in a SIR-dependent manner (Ellahi et al. 2015). Nevertheless, subtelomeric genes are expressed at a lower level than other genes in the rest of the genome (Ellahi et al. 2015; Wyrick et al. 1999). Thus, the Sir2 mediated histone deacetylation cannot be the only mechanism for transcriptional repression at subtelomeric regions.

The histone acetyltransferase Sas2 counteracts the action of the SIR complex and was proposed to be an essential boundary element for the establishment of subtelomeric heterochromatin. Sas2 acetylates H4K16 and thereby might block the binding site for Sir3 and prevent the propagation of heterochromatin (Kimura et al. 2002; Suka et al. 2002; Shia et al. 2006; Altaf et al. 2007). Additionally, the histone methyltransferase Dot1 (disruptor of telomeric silencing) was identified through its role in promoting telomeric silencing. Dot1 catalyzes the methylation of histone 3 lysine 79 (H3K79) residues and was suggested to cooperate with Sas2 to establish the boundary between heterochromatin and euchromatin at subtelomeres in yeast (Hocher et al. 2018; Verzijlbergen et al. 2009). However, the role of Dot1 and H3K79 methylation on telomeric silencing is controversial since only little transcriptional changes were observed in *dot1* mutants using microarray analysis (Takahashi et al. 2011).

Telomeric and subtelomeric chromatin in mammalian cells share many parallels with the chromatin state of telomeres in budding yeast but are also characterized by some additional features. At mammalian telomeres, the heterochromatic state is also maintained by PTMs of histones, and a telomere position effect was described (Baur et al. 2001; Koering et al. 2002; Pedram et al. 2006). Additionally, DNA methylation, which is generally absent in budding yeast, plays a role in the establishment of telomeric and subtelomeric chromatin (García-Cao et al. 2004; Gonzalo et al. 2006). The Sir2 equivalent in mammals is the histone deacetylase SIRT6, an H3K9ac-, H3K18ac- and H3K56ac-specific deacetylase (Michishita et al. 2008; Mostoslavsky et al. 2006; Tasselli et al. 2016). SIRT6 was shown to associate with telomeres and participate in the silencing of telomere-proximal genes (Tennen et al. 2011). Similar to the SIR complex in yeast, it is also required for telomere function and counteracts premature senescence (Michishita et al. 2008; Mostoslavsky et al. 2006).

1.1.4.1 Telomere position effect over long distances (TPE-OLD)

In human cells, the telomeric heterochromatin was proposed to affect the expression of genes with several mega-bases of distance from telomeres, in addition to the telomere position effect. This phenomenon was dubbed “telomere position effect over long distances” (TPE-OLD) (Robin et al. 2014). Fluorescence *in situ* hybridization (FISH) and chromosome conformation capture approaches point towards the presence of a chromatin loop between the telomeric repeats and several gene promoters (Robin et al. 2014). In this way, TPE-OLD was shown to influence the expression of several genes, including the telomerase catalytic component TERT itself (Robin et al. 2015; Kim et al. 2016). Interestingly, the silencing function that telomeric heterochromatin might impose on the genes affected by TPE-OLD is dependent on telomere length (Robin et al. 2014; Robin et al. 2015). Thus, telomere shortening might lead to a desilencing of those genes and their telomere length-dependent expression. Interestingly, the establishment of long-range chromatin loops for TPE-OLD might have parallels to interstitial t-loops, which were proposed to contribute to telomere end protection (section 1.1.2.2) (Wood et al. 2014; Wood et al. 2015).

1.1.4.2 Additional regulators of telomeric chromatin in yeast – Sin3 and Set2

Many different histone-modifying enzymes are involved in the regulation of telomeric chromatin. In this paragraph I focus on the histone modifiers that will be important in this work: the Sin3 (switch independent 3) protein as part of the Rpd3 histone deacetylase complex and the histone methyltransferase Set2 (SET domain-containing 2).

Originally identified as a transcriptional repressor in *S. cerevisiae,* the Sin3 protein is part of the Rpd3L (Rpd3 large) and the Rpd3S (Rpd3 small) complex, both multi-subunit HDACs (Carrozza et al. 2005; Keogh et al. 2005; Sternberg et al. 1987; Nasmyth et al. 1987). Both complexes share the core subunits Sin3, Ume1 and the catalytic histone deacetylase component Rpd3 (Carrozza et al. 2005; Keogh et al. 2005). However, Rpd3L and Rpd3S were shown to fulfill distinct functions. The Rpd3L complex was suggested to act as a co-repressor for transcription by associating with promoter regions and promoting their deacetylation (Carrozza et al. 2005; Sharma et al. 2007; Lee & Shilatifard 2007; Kadosh & Struhl 1998b; David & Kevin 1997). Since Sin3 and the other core components of the Rpd3L complex have no DNA binding activity, they are recruited to chromatin by different transcription factors (Grzenda et al. 2009). The Rpd3S complex fulfills its role during active transcription (Keogh et al. 2005; Carrozza et al. 2005). Rpd3S recognizes histones that were methylated by the Set2 histone methyltransferase during transcription elongation. As a result Rpd3S deacetylates histones within transcribed genes which was suggested to prevent unscheduled (cryptic) transcription initiation (Carrozza et al. 2005).

Studies with the Rpd3 complex in yeast showed that is has a general deacetylation activity on lysine residues on histone H3 and histone H4, with a slight preference for H4K5 and H4K12 (Rundlett et al. 1996; Kadosh & Struhl 1998b; Kadosh & Struhl 1998a). In yeast mutants lacking *RPD3* or *SIN3,* histone acetylation globally increases (Vogelauer et al. 2000; Robyr et al. 2003; Reid et al. 2004; Rundlett et al. 1996). However, the consequence of this genome-wide hyper-acetylation is a combination of up- and downregulated genes, suggesting roles for the Rpd3 complex in transcriptional repression but also activation (Bernstein et al. 2000). Interestingly, *RPD3* or *SIN3* deletion results in enhanced silencing of mating loci, ribosomal genes and telomeres, leading to the downregulation of many telomere-proximal genes (Bernstein et al. 2000; Sun & Hampsey 1999; Keogh et al. 2005; Rundlett et al. 1996; Vannier et al. 1996). The lack of Rpd3, Sin3 or other Rpd3L complex members was shown to results in the unscheduled spreading of silencing mediated by the SIR complex (Keogh et al. 2005; Zhou et al. 2009; Ehrentraut et al. 2010; Verzijlbergen et al. 2009). However, the enhanced spreading of the SIR complex does not result in the dissociation of SIR proteins from telomeres (Ehrentraut et al. 2010). Therefore, the Rpd3 complex was suggested to contribute to the formation of the heterochromatin boundary at subtelomeres (Zhou et al. 2009; Ehrentraut et al. 2010).

As previously mentioned, Set2 mediates co-transcriptional methylation, specifically placing mono-, di- and tri-methylation marks on H3K36 residues (Strahl et al. 2002). Set2 associates with elongating RNA polymerase II and subsequently places histone marks at the gene bodies of active genes (Krogan et al. 2003; Huang & Zhu 2018; Li et al. 2003; Xiao et al. 2003). H3K36 methylation (H3K36me) attracts and activates the Rpd3S complex via its Eaf3 subunit (Joshi & Struhl 2005; Keogh et al. 2005; Carrozza et al. 2005; Ruan et al. 2015). Histone deacetylation by Rpd3S then establishes repressive chromatin behind RNA polymerase II, which prevents re-initiation of transcription within gene bodies (Carrozza et al. 2005). Besides recruiting the Rpd3 complex, H3K36me also promotes proper nucleosome spacing within coding regions and ensures that nucleosomes remain assembled after the passage of the transcription machinery (Venkatesh et al. 2012).

Studies in budding yeast suggest that also histone methylation by Set2 plays a role at telomeric chromatin (Tompa & Madhani 2007; Ryu et al. 2014). In particular, the deletion of either Set2 or mutations in H3K36 cause increased silencing of heterochromatin-adjacent regions, such as subtelomeres (Tompa & Madhani 2007). The hyper-silencing in these regions is a result of enhanced SIR association, supposedly due to spreading from subtelomeres, and leads to decreased expression of telomere-proximal genes (Tompa & Madhani 2007; Ryu et al. 2014). In summary, H3K36me at subtelomere-adjacent regions is important for boundary formation to prevent ectopic

SIR complex spreading. Interestingly, this function is independent from the role of H3K36me in recruiting the Rpd3S complex, as the lack of Rpd3S subunits does not show the same effect.

1.1.4.3 Transcription at telomeres into the long non-coding RNA TERRA

Even though telomeres are heterochromatic, they are transcribed into a long non-coding RNA (lncRNA), dubbed TERRA (telomeric repeat-containing RNA). Telomere transcription is evolutionary conserved and has been described in many eukaryotes, including yeast, plants and mammals (Azzalin et al. 2007a; Luke et al. 2008; Schoeftner & Blasco 2008). TERRA gets transcribed primarily by RNA polymerase II from subtelomeric sequences into the telomeric repeats (Schoeftner & Blasco 2008; Azzalin et al. 2007b; Luke et al. 2008; Nergadze et al. 2009; Pfeiffer & Lingner 2012). The length of TERRA was shown to be heterogeneous, even within the same organism (Luke et al. 2008; Azzalin et al. 2007b; Schoeftner & Blasco 2008).

TERRA transcription is regulated by the subtelomeric chromatin environment. In human cells this regulation is mostly executed by DNA methylation and HP1 whereas in budding yeast the SIR histone deacetylase complex is key for TERRA regulation (Arnoult et al. 2012; Iglesias et al. 2011). The deletion of SIR complex members results in a reduced heterochromatic environment at telomeres and leads to a drastic accumulation of TERRA molecules (Iglesias et al. 2011). In addition to its regulation on chromatin level, TERRA levels are also controlled by the RNA exonuclease Rat1 (Luke et al. 2008). In senescent *S. cerevisiae* cells, when telomeres shorten in the absence of telomerase, TERRA transcripts accumulate due to the lack of Rat1 at short telomeres (Graf et al. 2017). Elevated TERRA levels were also observed in post-senescence yeast survivors as well as in several ALT cancers (Episkopou et al. 2014; Ng et al. 2009; Misino et al. 2018).

Many different studies described relevant functions of TERRA at telomeres. This becomes evident in the observation that both the decreased abundance of TERRA but also an uncontrolled TERRA accumulation can lead to dysfunctional telomeres (De Silanes et al. 2014; Deng et al. 2009; Deng et al. 2012; De Silanes et al. 2010). Among the proposed roles of TERRA, it was suggested to act as a regulator of the chromatin state at telomeres and promote heterochromatin formation (Arnoult et al. 2012; Montero et al. 2018). This suggests, that TERRA might be part of a feedback mechanism for the epigenetic state of the telomere. Additionally, TERRA could act as a recruitment platform for auxiliary factors at telomeres which are critical for telomere function (Rippe & Luke 2015). In budding yeast, TERRA was implicated in telomere length maintenance. Since TERRA accumulates at short telomeres, it was suggested to promote telomerase recruitment to these telomeres and thereby support their elongation (Cusanelli et al. 2013; Moravec et al. 2016).

By annealing to its template DNA, TERRA can form three-stranded RNA:DNA hybrid structures, called R-loops (Balk et al. 2013; Arora et al. 2014; Nanavaty et al. 2017). The formation of TERRA R-loops was proposed to primarily occur in a co-transcriptional manner (Arora & Azzalin 2015). R-loops generally impose barriers for the replication fork and can be a source for replication stress, chromosome instability and telomere loss (Aguilera & García-Muse 2012; Gan et al. 2011; Rippe & Luke 2015). To prevent the detrimental outcomes of R-loop accumulation, their levels are tightly controlled by several mechanisms. The RNase H family of enzymes are major regulators of telomeric R-loops due to their ability to degrade the RNA moiety of the R-loop (Balk et al. 2013; Arora et al. 2014; Arudchandran et al. 2000). Additionally, the helicase FANCM (Fanconi anemia protein M) and its yeast homolog Mph1 as well as the chromatin remodeler ATRX (Alpha thalassemia/mental retardation syndrome X-linked) contribute to the removal of R-loops at telomeres (Nguyen et al. 2017; Pan et al. 2017; Silva et al. 2019; Lafuente-Barquero et al. 2017). In contrast to the unscheduled R-loop accumulation, R-loops at telomeres have been shown to become particularly important at critically short telomeres in pre-senescent yeast cells. Here, they contribute to homology-directed repair (HDR)-mediated telomere elongation and can thereby compensate for telomere shortening (Balk et al. 2013; Fallet et al. 2014). Due to their dual roles at telomeres, the formation and accumulation of TERRA R-loops are tightly regulated depending on telomere length and the cell cycle phase (Graf et al. 2017).

1.1.5 Telomere clustering and localization

The telomeres of human cells are attached to the nuclear matrix via the shelterin complex and its interaction with the lamins (Ludérus et al. 1996; Kaminker et al. 2009). However, human telomeres do not preferentially localize to the nuclear envelope but rather are distributed throughout the nuclear space.

Yeast chromosomes engage in a “Rabl” configuration where centromeres cluster on one side of the nucleus and telomeres localize to the opposite side at the nuclear envelope (Rabl 1885; Palladino et al. 1993; Nagai et al. 2010). In *S. cerevisiae,* telomeres form 5-8 telomere clusters at the nuclear periphery which can be visualized as Rap1 foci. The number of clusters suggests that one cluster contains several of the 16 telomeres of a haploid yeast cell. These clusters also include additional telomeric proteins such as the SIR complex and the Ku complex (Palladino et al. 1993; Gotta et al. 1996; Laroche et al. 1998). Within the SIR complex, particularly Sir3 was proposed to be an important player for regulating telomere clustering (Ruault et al. 2011). It was shown that telomere clusters do not specifically form between certain telomeres (Therizols et al. 2010). However, the

telomeres of chromosomes with similar size arms are more likely to cluster together (Schober et al. 2008).

The tethering of budding yeast telomeres to the nuclear envelope involves several redundant pathways and the nuclear envelope proteins Esc1 (establishes silent chromatin 1) and Mps3 (monopolar spindle 3) (Bupp et al. 2007; Andrulis et al. 2002). Esc1 contributes to telomere tethering through its interaction with Sir4 (Andrulis et al. 2002). The Mps3 protein spans the inner nuclear envelope and interacts with Sir4 or the Ku complex via its N-terminus protruding into the nucleoplasm (Bupp et al. 2007). Additionally, the SUMO (small ubiquitin-related modifier) E3 ligase Siz2 plays a key role in anchoring telomeres to the nuclear periphery (Zhao & Blobel 2005; Ferreira et al. 2011; Hang et al. 2011). Both Sir4 and yKu80 are targeted by Siz2 and their modification with SUMO is important for the tethering behavior of telomeres (Zhao & Blobel 2005; Ferreira et al. 2011; Hang et al. 2011). Surprisingly, TPE and the formation of telomeric clusters are not affected in cells lacking *SIZ2,* even though many studies in different organisms described a connection between heterochromatin formation, gene silencing, and the localization to the nuclear envelope (Hiraga et al. 2008; Ferreira et al. 2011). This and several other observations, therefore, suggest that telomere anchoring at the nuclear periphery and TPE are independent processes (Tham et al. 2001; Mondoux & Zakian 2007).

1.1.6 Telomere replication

Accurate and unimpeded telomere replication is crucial for telomere homeostasis and telomere length control. The replication of telomeres is initiated from more centromere-proximal replication origins and is therefore unidirectional (Maestroni et al. 2017). Telomeres were described as one of the regions in the genome which are the most difficult to replicate (Maestroni et al. 2017). When replication forks approach the telomere, they tend to slow down and may also stall (Miller et al. 2006; Ivessa et al. 2002; Makovets et al. 2004). Telomeres are therefore considered fragile sites and trigger replication stress (Sfeir et al. 2009).

The observation that telomeres are difficult to replicate is based on several telomere specific characteristics. These features include their heterochromatic nature and the formation of secondary structures such as G4s and t-loops (Maestroni et al. 2017). Additionally, the presence of TERRA R-loops can be a barrier for the replication machinery and contributes to telomeric replication stress (reviewed in Rippe & Luke 2015; Maestroni et al. 2017). The attachment of telomeres at the nuclear periphery or the nuclear matrix might also constrain the progression of the replication fork (Maestroni et al. 2017). The tight association of large protein complexes to telomeres was proposed to additionally interfere with DNA replication (Ivessa et al. 2002; Makovets

et al. 2004). Indeed, *in vitro* and *in vivo* experiments indicate that DNA-bound Rap1 is sufficient to cause replication stalling even when its interactions with the SIR complex and the Rif proteins are prevented by deleting the Rap1 C-terminus (Makovets et al. 2004; Koc et al. 2016).

The outcome of unsuccessful telomere replication is detrimental. Persistent fork stalling at telomeric repeats eventually leads to a scenario where replication forks cannot be stabilized and collapse. A fork collapse might include the dissociation of replication factors from the fork and the formation of a double-strand break (Zeman & Cimprich 2014; Carr et al. 2011). In case replication forks at telomeres cannot restart successfully, telomeres would break, or become resected, resulting in abrupt telomere loss and telomere aberrations (Maestroni et al. 2017). Therefore, many different mechanisms are in place to ensure efficient replication of telomeres. By collaborating with the replisome, the telomere binding proteins themselves have been implicated in ensuring efficient replication through the telomeric tract and therefore avoid fork stalling (Miller et al. 2006; Sfeir et al. 2009; Martínez et al. 2009; Ye et al. 2010). The most prominent example is the shelterin component TRF1 which is indispensable for telomere replication. In its absence, replication forks become more prone to stalling, and telomere fragility increases (Martínez et al. 2009; Sfeir et al. 2009).

G4 structures are kept in check by the action of several helicases, such as BLM, WRN and RTEL1 in mammalian cells, and Pif1 in budding yeast (Paeschke et al. 2011; H. Sun et al. 1998; Mohaghegh 2001; Huber 2002; Vannier et al. 2012; Sfeir et al. 2009). In addition to helicases, single-stranded DNA binding proteins might contribute to resolving G4 structures or may prevent their formation. They were suggested to act by either recruiting or stimulating helicase activities or bind to a displaced single DNA strand and prevent its folding into a G4 (Masuda-Sasa et al. 2008; Brosh et al. 1999; Wang et al. 2011). Accordingly, several mechanisms control the resolution of telomere folding or t-loops for the passage of the replication machinery (section 1.1.2.2) and the unscheduled accumulation of TERRA R-loops (section 1.1.4.3).

1.1.6.1 Telomere replication timing

The firing of replication origins is tightly controlled during the synthesis phase of the cell cycle. This results in a subset of origins that fire early in S phase and others late in S phase. Many studies in different organisms showed that the replication timing of origins does not only correlate with their chromatin environment but also their nuclear positioning (Arnoult et al. 2010; Heun et al. 2001; Ferguson & Fangman 1992; Newlon & Theis 1993; Friedman et al. 1997; Yamashita et al. 1997; Poloumienko et al. 2001; Raghuraman 2001; Yabuki et al. 2002). Synchronized replication origins often associate with each other in the nuclear space (Duan et al. 2010; Hand 1975; Hiratani et al.

2008). This results in specific chromosome domains replicating at the same time. Generally speaking, early-replicating domains are more likely to be euchromatic with active chromatin marks (reviewed in Méchali 2010). Late replicating domains, in contrast, usually lie within inactive heterochromatin (reviewed in Méchali 2010). It was hypothesized that heterochromatic regions might generally fire later in S phase as a result of a passive process (reviewed in Boos & Ferreira 2019). Replication proteins might have limited access to heterochromatin and additionally, a competition for a limited amount of replication initiation factors was described (reviewed in Boos & Ferreira 2019).

Whereas human telomeres are replicated throughout S phase (Verdun & Karlseder 2006; Arnoult et al. 2010), budding yeast telomeres replicate late in S phase (Raghuraman 2001). Interestingly, telomere replication timing in budding yeast depends on telomere length. Short telomeres are replicated earlier in S phase than wild type (wt) telomeres (Bianchi & Shore 2007a) which is a Tel1-dependent mechanism (Sridhar et al. 2014). The SIR complex, the Ku complex and the telomeric protein Rif1 were identified as important regulators of replication timing in budding yeast (Mattarocci et al. 2016; Lian et al. 2011; Cosgrove et al. 2002; Stevenson & Gottschling 1999). The SIR complex was proposed to delay replication initiation by its histone deacetylase function introducing a heterochromatin environment (Stevenson & Gottschling 1999). However, the understanding of how histone deacetylation affects the replication timing program in *S. cerevisiae* is limited. The Ku complex was suggested to regulate telomere replication timing due to its function of tethering telomeres to the nuclear periphery (Aparicio 2013; Cosgrove et al. 2002). In *yku70* mutants, telomeres lose their clustering behavior, detach from the nuclear envelope, and might therefore lose their association with late-replicating domains (Aparicio 2013; Cosgrove et al. 2002; Bystricky et al. 2005).

Rif1 has a general role in replication timing control which seems to be conserved from yeast to mammals (reviewed in Mattarocci et al. 2016). Rif1 was shown to suppress replication initiation and acts as a negative regulator of replication origin activation (Lian et al. 2011; Peace et al. 2014). Mechanistically, recent studies demonstrated that Rif1 recruits the PP1 phosphatase (Glc7 in budding yeast) and thereby antagonizes Dbf4-dependent kinase (DDK) activity, which is required for origin activation (Hiraga et al. 2014; Mattarocci et al. 2014; Hiraga et al. 2017). In mouse and human cells, the absence of Rif1 was shown to interfere with the replication timing domains (Cornacchia et al. 2012; Yamazaki et al. 2012; Foti et al. 2016). This might point towards a mechanism where Rif1 is involved in establishing these domains. In budding yeast, Rif1 most specifically affects the replication timing of telomere proximal origins in a way that telomere replication in *rif1* mutants is advanced (Lian et al. 2011). However, in the absence of Rif1 several

internal late replicating origins also display premature firing (Peace et al. 2014). Through a genome-wide binding analysis of Rif1 in budding yeast, Hafner et al. showed that Rif1 binds directly to the replication origins that it regulates (Hafner et al. 2018). The authors propose that Rif1 is sequestered to telomeres which limits its localization to origins that are located more internally on the chromosome. This sequestration also contributes to the repression of origin firing at loci in close proximity to telomeres, within ~50-60 kb from chromosome ends (Hafner et al. 2018). However, Rif1 was shown to localize to both early- and late initiating origins genome-wide, suggesting that the mechanism by which Rif1 is recruited to the respective origins needs further investigation (Hiraga et al. 2018).

1.1.7 DNA damage repair and telomeres

Even though telomeres prevent the recognition of chromosome ends as double-strand breaks (DSBs), the DNA damage response proteins that recognize and repair DSBs within the genome, are important regulators of telomere function. In the following, the cellular response to DSBs will be introduced briefly.

1.1.7.1 Double-strand break repair and the DNA damage checkpoint

Double-strand breaks can either arise from exogenous sources, such as ionizing radiation or from endogenous sources, e.g. replication stress. The DNA damage response (DDR) to DSBs shares many conserved features between eukaryotic cells. The favored repair pathway for DSBs depends on the cell cycle stage when they get processed. The non-homologous end joining (NHEJ) repair pathway, by which the broken DNA ends get fused via DNA ligase activities, is the preferred mechanism during G1 phase even though it is error-prone (**Figure 6**) (Daley et al. 2005). In the S and G2 phases of the cell cycle, when the sister chromatid is available as a repair template, an error-free homology directed repair (HDR) pathway is employed preferentially for DSB repair (**Figure 6**).

The recruitment of the budding yeast Mre11-Rad50-Xrs2 (MRX) complex or the human MRE11-RAD50-NBS1 (MRN) complex to the lesion is the first step for the repair of a DSB. Subsequently, the checkpoint kinase Tel1 (ATM in human) localizes to the break, triggered by MRX complex (MRN complex in human) (**Figure 6**). Additionally, the heterodimeric yKu70-yKu80 complex (KU70-KU80 in human) associates to the DNA ends with its ring-like structure (**Figure 6**) (Walker et al. 2001; Clerici et al. 2008). The Ku complex can then act as a recruitment platform for the NHEJ machinery and the DNA ends get ligated by the ligase Dnl4 and its cofactor Lif1 (DNA ligase IV and XRCC4 in human) (Daley et al. 2005; Herrmann et al. 1998; Y. Zhang et al. 2007; Wu et al. 2008). In the S/G2 phases of the cell cycle, rapid end resection of the 5' strand is favored which leads to the eviction of Ku and initiates homology directed repair (**Figure 6**) (Pâques & Haber 1999; Garcia et al. 2011;

Chanut et al. 2016). The MRX complex itself is involved in this first resection step together with Sae2 (CtIP in human) (Cannavo & Cejka 2014; Garcia et al. 2011). A long-range 5'-3' end-resection is then performed by the exonuclease Exo1 (EXO1 in human) and the helicase/nuclease complex Sgs1 (BLM in human) and Dna2 (DNA2 in human) (**Figure 6**) (Pâques & Haber 1999; Zhu et al. 2008; Mimitou & Symington 2008). The long single-stranded 3' overhangs get covered by RPA, the main ssDNA binding protein in eukaryotes. Subsequently, the major yeast recombination protein Rad52 (BRCA2 in human, breast cancer gene 2) assists in the exchange of RPA for the central recombinase Rad51 (RAD51 in human) (**Figure 6**) (New et al. 1998; Sung 1997; Shinohara & Ogawa 1998; Jensen et al. 2010). The Rad51-coated nucleoprotein filament is crucial for homology search and strand invasion into the homologous template for repair. Even though the role of the human RAD52 protein is less well characterized, recent studies showed that it is important for HDR, especially in the absence of e.g. BRCA2 (Lok et al. 2013; Lok & Powell 2012; Feng et al. 2011).

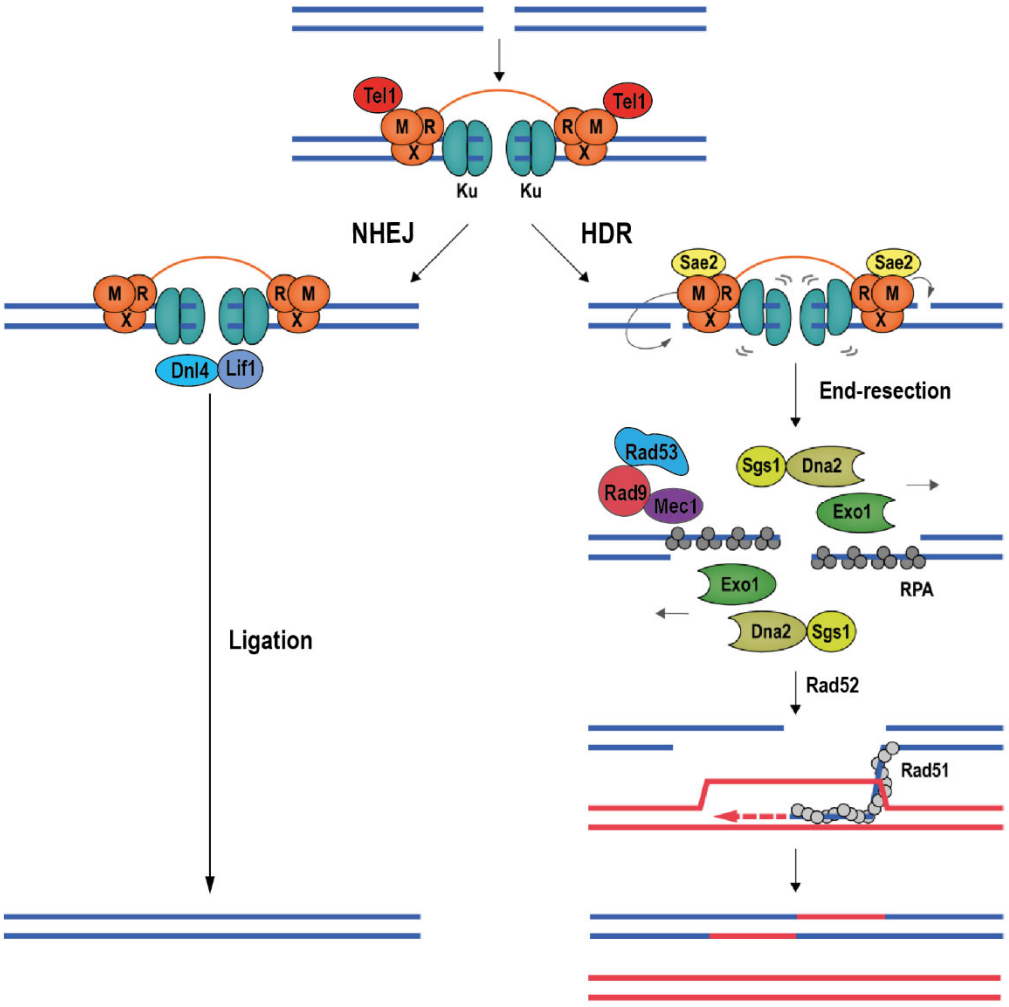

Figure 6: Double-strand break repair by NHEJ and HDR. The conserved mechanism of DSB repair is initiated by the recruitment of the MRX complex to the lesion, followed by the checkpoint kinase Tel1 and the Ku complex (top). Repair by NHEJ is mediated by the Ku complex and DNA ligation via Dnl4 and Lif1 (left). The initial end resection of the 5' strand

is mediated by MRX and Sae2 (right), which destabilizes Ku. Exo1 together with Sgs1 and Dna1 performs further resection resulting in long 3' overhangs which get covered with RPA. RPA loading stimulates the recruitment of the checkpoint kinase Mec1. Mec1 subsequently phosphorylates Rad9 which supports the phosphorylation and activation of Rad53. Rad52 mediates the exchange of RPA for the recombinase Rad51 which is required for homology search and strand invasion for HDR. The budding yeast proteins are depicted. Figure and legend adapted from Fontana et al. 2018.

In parallel to the repair processes at DSBs, cells also activate a signaling cascade to trigger the DNA damage checkpoint as they recognize the presence of a DSB. The activation of the DNA damage checkpoint leads to a multitude of cellular responses, including cell cycle arrest, the inhibition of origin firing and a transcriptional response. Checkpoint activation elicits a cascade of rapid phosphorylations and other post-translational modifications at the site of damage, mediated by evolutionarily conserved protein kinases. Initially, the checkpoint kinase Tel1 (ATM in human) phosphorylates histone H2A at the lesion. This leads to the spreading of γH2A (γH2AX in human) over several kb along the chromosome and the recruitment of further checkpoint factors such as Rad9 (53BP1 in human, P53-Binding Protein 1) (Downs et al. 2000; Shroff et al. 2004). Further downstream, the RPA coated ssDNA attracts the other major checkpoint kinase Mec1 (ATR in human), which phosphorylates and activates Rad9 (53BP1 in human) (Lydall & Weinert 1995; Zou & Elledge 2003) (Figure 6). Rad9 functions as molecular adaptor and supports the phosphorylation of the main checkpoint effector kinase Rad53 (CHK2 in human, checkpoint kinase 2) by Mec1, and to a lesser extent also Chk1 (CHK1 in human, checkpoint kinase 1) (Schwartz et al. 2002; Sanchez et al. 1996; Gilbert et al. 2001; Z. Sun et al. 1998). Phosphorylated Rad53 then dissociates from the lesion and phosphorylates its downstream targets to allow cell cycle arrest. Importantly, the Mec1 pathway can also be activated upon replication stress, when RPA coated ssDNA accumulates at stalled replication forks. In this case, the replisome component and checkpoint adapter Mrc1 (Claspin in human) mediates Rad53 activation by Mec1 (Alcasabas et al. 2001; Osborn & Elledge 2003). In contrast to human cells, Rad53 performs almost all checkpoint effector functions in budding yeast, and Chk1 was shown to be less important for checkpoint activation (Sanchez et al. 1999). In human cells, the effector kinases CHK1 and CHK2 play equally important roles.

1.1.7.2 DNA damage repair proteins at telomeres

Crucial players of the NHEJ pathway were discovered to have important roles at telomeres, in parallel to their role in DNA damage repair. The most prominent example is the Ku complex which was shown to localizes to human and yeast telomeres (Gravel et al. 1998; Hsu et al. 1999; Hsu 2000). Several lines of evidence support the view that the yeast Ku complex contributes to telomere stability and executes various functions at telomeres and the human the Ku70-Ku80 complex was shown to interact with shelterin (Hsu et al. 1999; Hsu 2000; Gravel et al. 1998; Porter et al. 1996; Boulton & Jackson 1996; Song et al. 2000; Chai et al. 2002). In budding yeast mutants lacking Ku, telomere length is drastically decreased and telomeres are additionally characterized by long

3’ overhangs throughout the cell cycle (Porter et al. 1996; Gravel et al. 1998; Polotnianka et al. 1998; Boulton & Jackson 1996). Additionally, the Ku complex is also critical for telomere tethering to the nuclear envelope (section 1.1.5), promotes the telomere position effect (section 1.1.4) and plays a role in telomere replication (section 1.1.6.1) (Cosgrove et al. 2002; Gravel & Wellinger 2002).

Due to the processing of telomeres by nucleases and possibly due to structural changes, telomeres were reported to elicit a transient DNA damage response, mainly by Tel1. In budding yeast, Tel1 has a fundamental role in telomere length control in addition to its function in DNA damage repair (Shima et al. 2005; Nakada et al. 2003). During S phase, by the time that telomeres are replicated, Tel1 localizes to telomeres and this localization depends on MRX (Hector et al. 2007; Sabourin et al. 2007; Ritchie & Petes 2000; Tsukamoto et al. 2001; Sabourin & Zakian 2008). Comparable to what happens at DSBs, MRX and Tel1 recruitment leads to a 5’-3’ resection resulting in a longer 3’ telomeric overhang detectable after telomere replication (Dionne & Wellinger 1996; Larrivée et al. 2004; Bonetti et al. 2009). The long overhang does, however, not lead to the activation of Mec1 or the downstream DDR factors (McGee et al. 2010). Interestingly, Tel1 preferentially associates with short telomeres which results in the recruitment of telomerase to the shortest telomeres and promotes their elongation (Teixeira et al. 2004; Goudsouzian et al. 2006; Arnerić & Lingner 2007; Bianchi & Shore 2007b). In mutants lacking *TEL1* or *MRE11,* telomere length is drastically decreased because telomerase is less frequently recruited to telomeres in these cells (Goudsouzian et al. 2006). Thus, the early steps during the recognition and processing of short telomeres in S phase are similar to the mechanisms at DSBs. However, short telomeres subsequently get elongated by telomerase which is not the case during canonical DNA damage repair.

The checkpoint kinase Mec1 was only attributed to a minor role for telomere length in budding yeast (Ritchie et al. 1999; Longhese et al. 2000). At normal length telomeres, the telomeric ssDNA binder Cdc13 hinders binding of RPA to telomeric overhangs and therefore restricts a Mec1-mediated checkpoint activation (Gao et al. 2007; McGee et al. 2010; Gelinas et al. 2009). Mec1 localizes, however, to critically short telomeres which were suggested to have already lost their functionality (Abdallah et al. 2009; McGee et al. 2010; Hector et al. 2012). This is, for example, the case in a later stage during replicative senescence, when Mec1 becomes essential for the G2/M arrest of senescent cells (Enomoto et al. 2002; Abdallah et al. 2009).

The transient checkpoint activation at telomeres during S phase follows a similar pattern in human cells. DNA damage response proteins transiently localize to telomeres in a cell cycle dependent manner (Verdun et al. 2005; Verdun & Karlseder 2006). During the process of telomere replication an ATR-dependent DNA damage response was described in primary human fibroblasts suggesting

a replication fork stalling event (Verdun et al. 2005; Verdun & Karlseder 2006). Interestingly, when replication is completed, telomeres additionally elicit an ATM-mediated DDR (Verdun et al. 2005; Verdun & Karlseder 2006). The MRN complex also localizes to telomeres during S phase and this localization seems to precede the recruitment of both ATR and ATM (Verdun et al. 2005; Verdun & Karlseder 2006; Sabourin & Zakian 2008). Subsequently, the HDR factors RAD51, RAD52 and the RAD51 paralog XRCC3 get recruited to telomeres and were suggested to assist in the processing of telomeres after replication is completed (Verdun & Karlseder 2006). However, this transient localization to telomeres does not lead to unscheduled recombination and sister chromatid exchanges between telomeres. Instead, it might induce the formation of t-loops after replication possibly with RAD51 and RAD52 assisting in strand invasion (Verdun & Karlseder 2006). These findings suggest that telomeres might be recognized as DNA damage triggered in two ways – first as replication stress during the fork passage and second as a DSB soon after. Since both inhibition of ATM and the depletion of MRE11 lead to an increase of dysfunctional telomeres, it was suggested that the localization of the DDR factors to telomeres is essential for telomere structure and function (Verdun et al. 2005). Additionally, a previous study found that mutations in a RAD51 paralog cause telomere protection defects in mammals, supporting a relevant role of HR proteins for telomere maintenance (Tarsounas et al. 2004).

1.1.7.3 Telomere-telomere fusions

Telomere-telomere fusions (T-TFs) occur, when telomeres are subject to the NHEJ repair pathway. These fusion events have detrimental effects for genome stability as they give rise to dicentric chromosomes and DNA breaks during the following mitosis. Thus, functional telomeres have to be protected from T-TFs, a role which was mainly attributed to the telomere-associated protein complexes.

T-TFs can arise from either classical NHEJ (c-NHEJ) or alternative-NHEJ (alt-NHEJ). C-NHEJ is dependent on the KU70-KU80 and DNA ligase IV in human cells (Smogorzewska et al. 2002; Celli & de Lange 2005; Celli et al. 2006) or yKu70-yKu80 and Dnl4 in budding yeast (Figure 6) (Daley et al. 2005; Y. Zhang et al. 2007; Wu et al. 2008). One branch of alt-NHEJ, which is of particular importance for repetitive regions, requires the presence of microhomology between the two DNA ends and it is therefore referred to as microhomology-mediated end joining (MMEJ) (Lee & Sang 2007; Ma et al. 2003). Important factors for this mechanism in human cells are PARP1 (Poly (ADP-ribose) polymerase 1) and Ligase III (Audebert et al. 2004; Audebert et al. 2008; Robert et al. 2009; Mansour et al. 2010; Bennardo et al. 2008; Wang et al. 2005; Sallmyr et al. 2008; Simsek et al. 2011). In budding yeast, alt-NHEJ might not be a separate repair pathway but depends on the

activity of the MRX complex (Lee & Sang 2007; Ma et al. 2003; Chiruvella et al. 2013; Paull & Gellert 2000).

In human cells, TRF2 is the major shelterin component that prevents T-TFs which was partially attributed to its role in t-loop formation (Doksani et al. 2013; Benarroch-Popivker et al. 2016; Stansel et al. 2001). In the original model of the t-loop, the 3' overhang would not be accessible for loading of the Ku complex for c-NHEJ because it is tucked away (**Figure 3**) (Griffith et al. 1999; Doksani et al. 2013). However, recent studies showed that additional mechanisms are in place that prevent T-TFs of telomeres in an open configuration (Benarroch-Popivker et al. 2016; Van Ly et al. 2018; Cesare et al. 2013). The fusion of human telomeres by c-NHEJ depends on the activation of the checkpoint kinase ATM and its adapter 53BP1 (Denchi & De Lange 2007; Dimitrova et al. 2008). The alt-NHEJ pathway for telomere fusion is mainly in place when classical NHEJ is not functional, for example in the absence of the Ku complex (Sfeir & De Lange 2012). In the context of shelterin removal from telomeres in Ku deficient cells, 2 bp of microhomology between the G-tails of different telomeres is enough to initiate their fusion (Sfeir & De Lange 2012).

Budding yeast *tel1* mutants exhibit a short telomere phenotype (Ritchie et al. 1999). Strikingly, when *MEC1* is deleted in addition to *TEL1*, telomeres progressively shorten similar to what is observed in telomerase negative cells (Ritchie et al. 1999; Chan et al. 2001). Budding yeast *mec1 tel1* mutants are characterized by high levels of chromosome aberrations, such as dicentric chromosomes, and unstable genomes (Myung et al. 2001; Craven et al. 2002). Additionally, T-TFs significantly increase in cells lacking *MEC1* and *TEL1* as compared to wt cells (Mieczkowski et al. 2003). The accumulation of T-TFs in *mec1 tel1* mutants as well as their genome instability can be rescued by restoring the telomere length to wt levels, and thereby restoring their protective capacity (Mieczkowski et al. 2003). This finding suggests that the telomere defect of *mec1 tel1* cells strongly promotes genome instability. The telomeres in *mec1 tel1* mutants are still proficient in recruiting Rap1 and the Ku complex (Mieczkowski et al. 2003). Therefore, the authors concluded that the release of telomere-associated proteins might not be the reason why these telomeres are more prone to fusions. The functions of Mec1 and Tel1 in protecting telomeres from fusions might be conserved from yeast to human, as T-TFs also accumulate in mammalian cells lacking ATM and ATR (Chan & Blackburn 2003; Naito et al. 1998; Pandita et al. 1995; Metcalfe et al. 1996).

The main inhibitor of T-TFs in budding yeast is the telomere binding protein Rap1 (Pardo & Marcand 2005; Marcand et al. 2008). Interestingly, in telomerase negative budding yeast cells, T-TFs increase modestly (Chan & Blackburn 2003; Mieczkowski et al. 2003). This observation was attributed to reduced Rap1 binding at telomeres during senescence (Platt et al. 2013; Teixeira 2013). However,

the accumulation of T-TFs in pre-senescent *mec1 tel1* mutants was shown to be much higher than in pre-senescent telomerase negative cells, suggesting that telomerase negative cells can repress telomeric NHEJ (Murnane 2012; Cesare & Karlseder 2012; Barrientos-Moreno et al. 2018). Telomere shortening in pre-senescent telomerase negative cells is accompanied by a global reduction in histone levels in human and mammalian cells (O'Sullivan et al. 2010; Platt et al. 2013). Barrientos-Moreno et al. showed that histone depletion prevents the increase of T-TFs in *mec1 tel1* mutants by a mechanism that favors Rad52-dependent HDR over NHEJ at telomeres (Barrientos-Moreno et al. 2018). This suggests, that the reduced histone pool in telomerase-negative pre-senescent cells protects telomeres from undergoing unscheduled fusions.

1.2 Nuclear organization and chromosome folding

The DNA of the eukaryotic genome is tightly packed within the nuclear space, but still needs to be accessible for fundamental biological processes such as gene expression and DNA replication. During the recent years, the development of important techniques has contributed significantly to our understanding about how the interplay between genome organization and these biological processes is achieved.

In the finest scale of chromosome folding, DNA is wrapped around nucleosomes, leaving a linker DNA between the individual nucleosomes. On electron micrographs, a nucleosome array appears as a "beads on a string" and forms an ~11 nm fiber, as further supported by recent EM data showing these fibers in intact cells (**Figure 7**) (Ou et al. 2017). The association of nucleosomes with DNA is dynamic and regulated by chromatin remodeling complexes, which can reposition, evict or restructure nucleosomes on the DNA double helix (Nagano et al. 2017; Zhang et al. 2011). Beyond the level of nucleosomes and chromatin, many layers of genome topology have been characterized. These comprise loop structures such as enhancer-promoter loops (Sanyal et al. 2012) and gene loops (Ansari & Hampsey 2005; O'Sullivan et al. 2004). Higher-order domains include topologically associated domains (TADs)/ chromosomal interaction domains (CIDs) (Dixon et al. 2012; Le et al. 2013; Mizuguchi et al. 2014; Nora et al. 2012; Sexton et al. 2012) and lamina-associated domains (LADs) (**Figure 7**) (Pickersgill et al. 2006). On a larger scale, eukaryotic genomes are organized in chromatin compartments (Lieberman-Aiden et al. 2009) and chromosome territories (**Figure 7**).

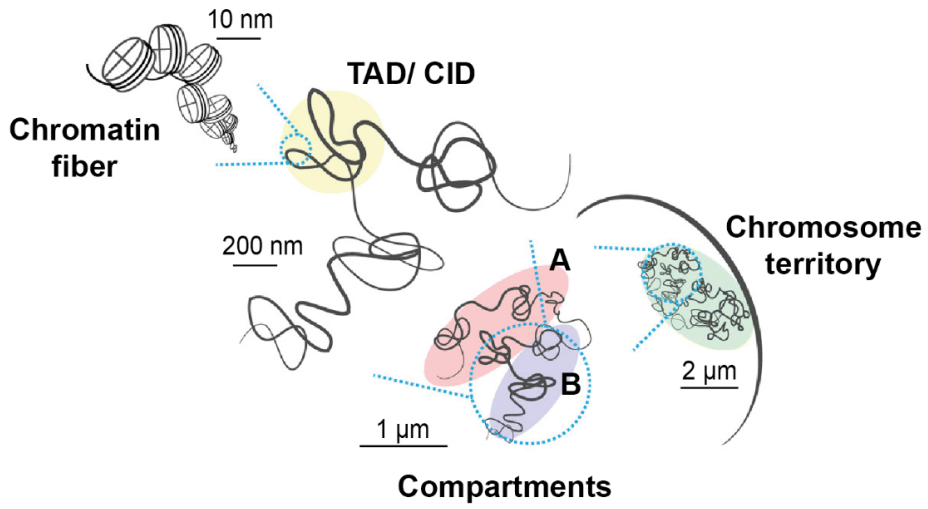

Figure 7. Hierarchical organization of the genome in eukaryotes. The smallest level of chromatin organization is the association of histones with DNA, giving rise to an ~11-nm chromatin fiber. In the next layer of organization, chromatin is structured into higher-order domains, dubbed TADs or CIDs, which are characterized by preferential internal interactions. Additionally, chromatin segregates into active A compartments and repressed B compartments. On the chromosomal scale, chromosomes occupy individual spaces within the nucleus, their chromosome territories. TAD = topologically associated domain. CID = chromosomal interaction domain. Figure and legend adapted from Szabo et al. 2019.

Chromatin loops are generally described as chromosome segments on the same chromosome that localize in closer proximity to each other than the sequences between them (reviewed in Kadauke & Blobel 2009). The juxtaposing of important genetic elements has been observed at various loci in the form of promoter-enhancer loops or gene loops. First described in budding yeast, gene loops were reported to bring the promoter and terminator elements of certain genes into close proximity during transcription (O'Sullivan et al. 2004; Ansari & Hampsey 2005). Gene loops were proposed to support promoter directionality (Tan-Wong et al. 2012) and transcriptional memory in yeast (Lainé et al. 2009; Tan-Wong et al. 2009). Also in higher eukaryotes, gene loops have been reported to occur during the transcription of certain genes (Goel et al. 2012; Wang et al. 2010; Henriques et al. 2012; Tan-Wong et al. 2008).

The establishment of chromosome conformation capture (3C) techniques (section 1.2.3) provided intra-chromosomal contact maps that give information about contact frequencies between different loci on the same chromosome (Dekker et al. 2002). The further development of Hi-C then allowed for genome-wide interaction maps (Lieberman-Aiden et al. 2009). With 3C-based techniques, TADs and CIDs were characterized as self-interacting domains, in which DNA segments physically interact more frequently than outside the TAD/CID (Dixon et al. 2012; Le et al. 2013). In mammalian cells, the SMC (structural maintenance of chromosomes) complex cohesin and the transcription insulator and boundary factor CTCF (CCCTC-binding factor) specifically associate with the boundaries of TADs (Rao et al. 2014). Interestingly, TADs are highly conserved between cell types and species (Dixon et al. 2012; Rao et al. 2014). TADs are generally regarded as functional units, since the genes within one TAD tend to be co-regulated (Zhan et al. 2017). The alteration of TAD structures or the removal of boundaries can lead to changes in gene expression (Lupiáñez et al. 2015; Flavahan et al. 2016). However, it is not clear how TADs contribute to transcriptional regulation, as both the depletion of CTCF and cohesin which eliminates both chromatin loops and TADs, only result in minimal gene expression changes in mammalian cells (Rao et al. 2017; Nora et al. 2017; Schwarzer et al. 2017).

A general principle of nuclear organization is the localization of more compact heterochromatic regions to the nuclear periphery, while the less dense euchromatin is found in the center of the nucleus (reviewed in Solovei et al. 2016; van Steensel & Belmont 2017). This observation is in line with the principle of chromatin compartments, discovered by Hi-C for the first time (Lieberman-Aiden et al. 2009). Lieberman-Aiden et al. proposed that the whole genome is partitioned into alternating compartments, namely the transcriptionally active euchromatic A compartments, and the repressed heterochromatic B compartments (Lieberman-Aiden et al. 2009). These compartments are characterized by more frequent contacts within the same compartment,

compared to the respective other chromatin compartment. Interestingly, replication timing strongly correlates with the compartment identity such that early-replicating regions overlap with A compartments and late-replicating regions overlap with heterochromatic B compartments (McCord et al. 2020; Dixon et al. 2012; Ryba et al. 2010; Pope et al. 2014).

From microscopy data of mammalian cells it became evident that chromosomes occupy territories during the interphase (reviewed in Cremer & Cremer 2010). In terms of nuclear positioning, gene-poor chromosomes tend to localize more toward the nuclear periphery, while chromosomes that have a higher density of genes are located in the center of the nucleus more frequently (Bolzer et al. 2005; Croft et al. 1999). Interestingly, chromosome territories were not observed in the yeast nucleus, where chromosomes tend to intermingle (Therizols et al. 2010; Berger et al. 2008) and adopt a "Rabl" conformation (section 1.2.3.2) (Rabl 1885).

1.2.1 SMC complexes

The SMC complexes cohesin, condensin and SMC5/6, belong to a highly conserved family of protein complexes from bacteria to higher eukaryotes. Through the formation of chromatin loops, the SMC complexes convey important functions during interphase and mitosis. They are essential for nuclear organization and chromosome structure contributing to chromosome segregation, compaction, DNA repair and gene regulation (reviewed in Uhlmann 2016).

All SMC complexes are characterized by a ring shape which is formed by two SMC proteins and a kleisin subunit (Figure 8A). Eukaryotic SMC complexes are comprised of heterodimers of the SMC subunits that associate with several cofactors to form functional complexes. The dimerization of the SMC subunits is conveyed by their hinge domains (reviewed in Losada & Hirano 2005; Hirano 2006; Nasmyth & Haering 2005). The SMC proteins fold into intra-molecular coiled-coil domains which bring the two parts of their ATPase domains together into a functional globular head domain (Figure 8A). Both ATP-binding cassette (ABC) ATPase heads of the SMC proteins dimerize in the presence of ATP, which gets sandwiched between them and are additionally held together by the kleisin subunit (Lammens et al. 2004; Hu et al. 2011; Haering et al. 2002).

With their ring shape structure, the SMC complexes can topologically entrap DNA and tether more than one DNA strand together. Powered by ATP hydrolysis, the SMC complexes were shown to undergo cycles of association and release from chromatin repeatedly (Gerlich et al. 2006; Badrinarayanan et al. 2012; Lopez-Serra et al. 2013). Like this, all SMC complexes are able to move laterally along chromosomes. Thereby they perform essential functions for chromosome organization but do not interfere with other activities on the same chromosome (Uhlmann 2016).

Cohesin, condensin and the SMC5/6 complex are essential for eukaryotic organisms and have specific but also partially redundant functions.

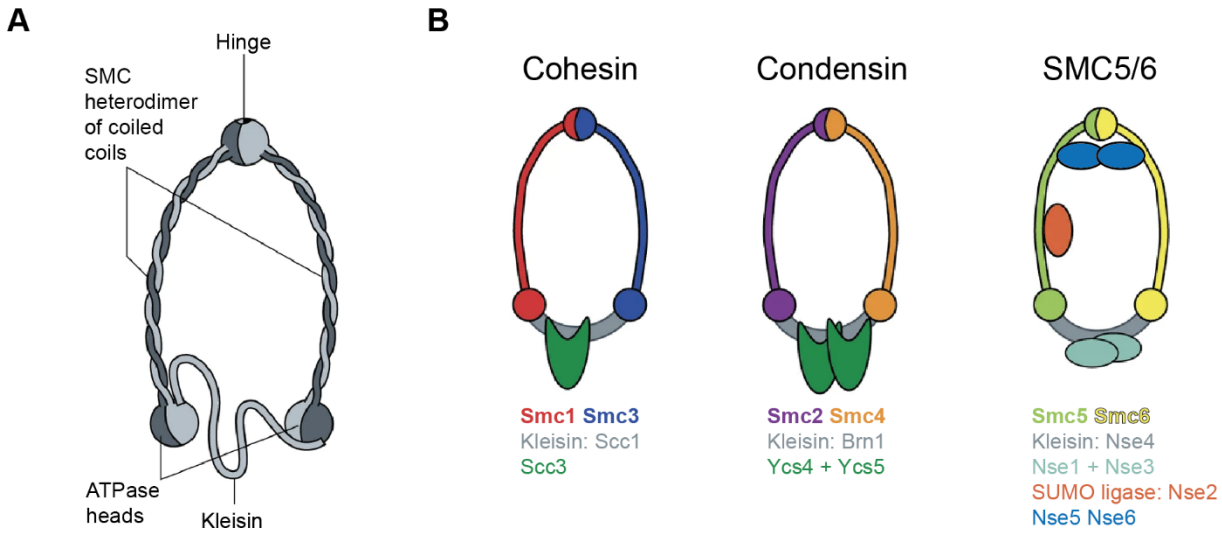

Figure 8: Architecture of eukaryotic SMC complexes. (A) Eukaryotic SMC complexes are composed of two SMC proteins that form a heterodimer of coiled-coils and are connected at the hinge. The ATPase activity of the SMC proteins is located at the heads which are connected by the kleisin subunit. **(B)** Overview of the SMC complexes cohesin, condensin and SMC5/6. The SMC ring associates with several cofactors to form functional complexes. The *S. cerevisiae* proteins are displayed. Adapted from Eeftens & Dekker 2017.

The *S. cerevisiae* **cohesin** complex consists of Smc1, Smc3, Scc3 and the kleisin Scc1 (**Figure 8B**). The first described role of cohesin was its function in sister chromatid cohesion (Uhlmann & Nasmyth 1998; Guacci et al. 1997; Michaelis et al. 1997). In this role, cohesin mediates a stable connection of DNA replication product pairs from S phase throughout G2 phase until mitosis. This cohesion is alleviated when the cohesin ring is opened through the cleavage of Scc1 in anaphase (Uhlmann et al. 2000; Oliveira et al. 2010). Sister chromatid cohesion is the basis for chromatid pairs to be recognized and oriented and is therefore essential for proper chromosome segregation. Additionally, it became evident that the formation of chromatin loops in interphase and the establishment of TADs depend on cohesin (Gassler et al. 2017; Rao et al. 2017; Wutz et al. 2017). Experiments, where cohesin was depleted from mammalian cells, showed that all loop and TAD structures disappear under these conditions (Schwarzer et al. 2017; Wutz et al. 2017; Rao et al. 2017; Haarhuis et al. 2017).

Condensin is composed of Smc2 and Smc4 which form a complex together with Ycs4, Ycs5 and the kleisin Brn1 in budding yeast (**Figure 8B**). Condensin is the main player for mitotic chromosome assembly and mediates proper chromosome compaction and segregation in mitosis (Hirano et al. 1997; Hirano & Mitchison 1994; Strunnikov et al. 1995; Cuylen et al. 2011). The action of condensin is essential for separating individual chromosomes for the preparation of cell division. When condensin is inactivated in cells, chromosomes fail to get compacted and remain in an interphase-

like structure with many local interactions between each other (Gibcus et al. 2018; Kakui et al. 2017). As a result, sister chromatids cannot be resolved in anaphase leading to chromosome bridges (Strunnikov et al. 1995; Hudson et al. 2003).

The SMC5/6 complex shares the ring-shaped structure with cohesin and condensin which consists of a Smc5-Smc6 heterodimer and the kleisin Nse4 (Figure 8B). Additional subunits are Nse1 and Nse3, which associate with the kleisin subunit, as well as Nse5 and Nse6. A unique characteristic of the SMC5/6 complex is its SUMO-ligase subunit Nse2 (Mms21) that associates with the coiled-coil domain of Smc5 (Duan et al. 2009). SMC5/6 plays its major role in DNA damage repair by facilitating the resolution of recombination intermediates (Wu & Yu 2012; Fousteri & Lehmann 2000; De Piccoli et al. 2006; Bermudez-Lopez et al. 2010). For its function in response to exogenous DNA damage, the SUMO ligase activity is required (Pebernard et al. 2008; Zhao & Blobel 2005; Branzei et al. 2006; Bermúdez-López et al. 2015). SMC5/6 localizes to replication origins during S phase (Bustard et al. 2012). In the G2 phase of the cell cycle, the SMC5/6 complex is found at centromeres and regions with topological intermediates, such as sister chromatid intertwinings (Jeppsson et al. 2014; Kegel et al. 2011). The essential function of the SMC5/6 complex was assigned to the late G2/M phase, where it was proposed to contribute to the repair of recombination structures caused by replication stress and to stabilize fragile structures (Menolfi et al. 2015).

The SMC5/6 complex has also been attributed several roles at telomeres in yeast and human cells, including the mechanism of alternative lengthening of telomeres (ALT) (section 1.1.3.3) (Chavez et al. 2010; Noël & Wellinger 2011; Wan et al. 2013). In human ALT cells, the SMC5/6 complex is essential for telomere maintenance via recombination (Potts & Yu 2007). This function is conveyed by SUMOylation of several telomere binding proteins thereby promoting their recruitment to APBs, where telomeres are elongated in ALT cells (Potts & Yu 2007). Similarly, in telomerase negative budding yeast, mutants of SMC5/6 complex members are characterized by accelerated senescence due to the accumulation of recombination intermediates (Chavez et al. 2010; Noël & Wellinger 2011). In addition, the SMC5/6 complex is involved in chromatin maintenance at telomeres and their organization within the nucleus (Moradi-Fard et al. 2016). In budding yeast, the SMC5/6 complex localizes to telomeres throughout the cell cycle which is crucial for the binding of the silencing factor Sir4 to telomeres (Moradi-Fard et al. 2016). Consequently, when the SMC5/6 complex is compromised in telomere binding, the telomere position effect and telomere clustering are disrupted, as well as TERRA levels are increased (Moradi-Fard et al. 2016). Moreover, the SMC5/6 complex is required for the chromosome segregation of repetitive regions, such as telomeres and the rDNA locus (Torres-Rosell, Mahín, et al. 2005). Consistent with this role, the

absence of SMC5/6 results in X-shaped DNA recombination intermediates in mitosis (Torres-Rosell, Mahín, et al. 2005).

Similar to the SMC5/6 complex, both condensin and cohesin take part in the response to DNA damage. Cohesin, together with SMC5/6, localizes to double-strand breaks where it mediates chromatid cohesion for the repair of the lesions by homologous recombination (Ünal et al. 2004; Ström et al. 2004; Betts Lindroos et al. 2006). Condensin was shown to accumulate at stalled replication forks, also in conjunction with the SMC5/6 complex (D'Ambrosio et al. 2008; Betts Lindroos et al. 2006). There, condensin stabilizes the stalled replication forks by preventing the separation of the broken strands and supports replication restart.

1.2.2 Mechanisms of chromosome folding and chromatin organization: Loop extrusion and compartmentalization

The folding of chromosomes can be explained by two different mechanistic models: The compartmentalization of the genome via affinity interactions of heterochromatin (Falk et al. 2019) and an active loop extrusion mechanism by the SMC complexes (Mirny et al. 2019).

As DNA has all characteristics of a classical polymer, many insights on the structure and dynamics of DNA within the nucleus are derived from polymer theory (Pethrick 1988; Cho 2016), in particular the loop extrusion model for chromosome folding. This model for the formation of chromatin loops favors a mechanism by which SMC complexes are loaded onto chromatin and then extrude the DNA through their ring shape. Thereby the chromatin loops get progressively enlarged over time until they either encounter a boundary element or are removed from the DNA (reviewed in Mirny et al. 2019). Many studies suggest that the mechanic energy for loop extrusion is provided by the ATP-driven movement of the SMC complexes on DNA (Vian et al. 2018; Ganji et al. 2018; Hansen et al. 2017). In addition to *in silico* modeling, the loop extrusion mechanism is increasingly supported by many lines of experimental evidence from Hi-C and microscopy data (Dekker & Mirny 2016; Sanborn et al. 2015; Britton et al. 1998; Bintu et al. 2018; Schwarzer et al. 2017; Rao et al. 2017; Gassler et al. 2017; Haarhuis et al. 2017).

Loop extrusion was shown to play a major role in TAD formation by cohesin in interphase but it is also employed by condensin for the compaction of DNA into mitotic chromosomes (**Figure 9**) (reviewed in Mirny et al. 2019). The loop extrusion model proposes that TADs are formed via an active extrusion of multiple chromatin loops by the cohesin complex (**Figure 9**) (Fudenberg et al. 2016). The loop extrusion would stop at obstacles, such as DNA-bound CTCF, thereby defining the borders of the TAD (Fudenberg et al. 2016). The gradual compaction of chromosomes in metaphase

can also be attributed to a loop extrusion mechanism (**Figure 9**). Here, condensin was proposed to form consecutive and nested loops in mitotic chromosomes, resulting in an array of loops extruding from a central scaffold (Gibcus et al. 2018).

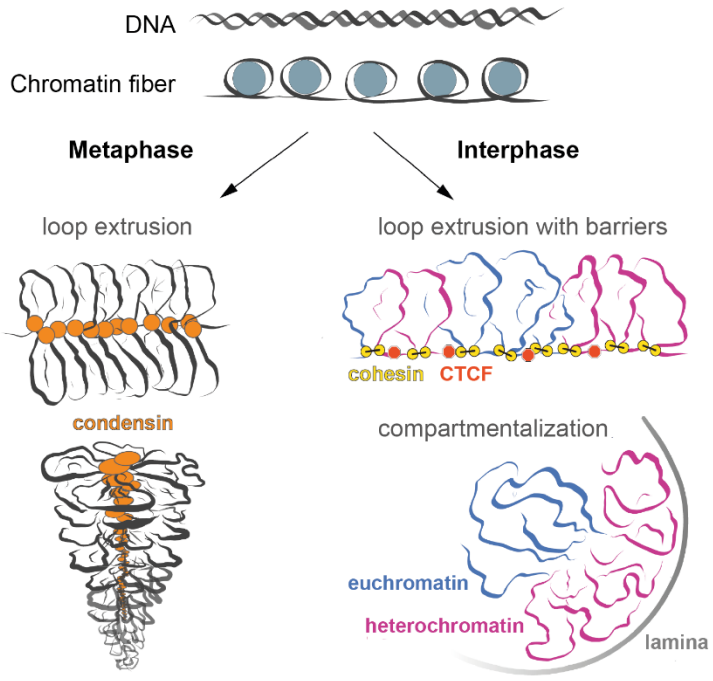

Figure 9: Chromosome organization is driven by loop extrusion and compartmentalization. DNA is wrapped around nucleosomes, making up a chromatin fiber. A loop extrusion mechanism by the condensin complex conveys the chromatin condensation into mitotic chromosomes (left). During interphase, chromosome architecture is dominated by two major pathways (right). The cohesin complex is responsible for loop extrusion resulting in a dynamic array of loops, which are contained by CTCF as boundary elements. The compartmentalization of the genome into euchromatic A compartments and heterochromatin B compartments is driven by the attraction of heterochromatin to each other. Figure and legend adapted from Mirny et al. 2019.

Compartmentalization generally refers to the observation that active and inactive chromatin spatially separate in the nucleus, giving rise to A and B compartments (Lieberman-Aiden et al. 2009). Many attempts to explain the mechanisms behind the formation of chromatin compartments are based on the observation that they highly correlate with specific post-translational histone modifications (Lieberman-Aiden et al. 2009). The modified histones might act as a platform for potential scaffold proteins with a high level of self-interaction or properties that promote phase separation (Erdel & Rippe 2018). Using modeling approaches, recent studies suggested a compartmentalization mechanism which is directed by attractive interactions of heterochromatin regions, rather than the attraction between euchromatic regions or the attachment to nuclear structures (Falk et al. 2019; Nuebler et al. 2018; Pereira et al. 2018). Therefore, the formation of membrane-less heterochromatin compartments is reminiscent of the phase separation of the included proteins and nucleic acids from the surrounding environment (reviewed in Mirny et al. 2019).

Recent findings support the idea that the mechanisms by which TADs and compartments are formed are uncoupled from each other (Rao et al. 2017; Ricci et al. 2015; Schwarzer et al. 2017). Interestingly, compartment formation increases, when cohesin or its loader is absent (Schwarzer et al. 2017). This suggests that the two processes might rely on different mechanisms that counteract each other. A major difference between chromatin compartments and loop extrusion domains is that the interactions within a compartment are global and can be observed both within the same chromosome but also between chromosomes (Figure 9). On the contrary, cohesin-dependent TADs are rather local and do not interact with other TADs (Mirny et al. 2019).

1.2.3 Methods to study nuclear organization and chromosome interactions

Our knowledge about the 3D architecture of the genome is based on two sets of techniques: microscopy approaches and chromosome conformation capture (3C) methods. A combination of different microscopy techniques revealed the basic principles of nuclear architecture. Early light and electron microscopy studies provided evidence for the presence of nuclear bodies, such as Cajal bodies (Cajal 1903; Nizami et al. 2010), the nucleolus (Valentin 1836; Wagner 1835; Pederson 2011) and PML bodies (The et al. 1960; Lallemand-Breitenbach & de The 2010). Our knowledge about euchromatin and heterochromatin and their positions in the nucleus also started off with conventional microscopy studies (Heitz 1928). With fluorescence RNA and DNA *in situ* hybridization (FISH) approaches it was possible to analyze the positioning of genes and chromosome within the nuclear space leading to the discovery of chromosome territories (Cremer & Cremer 2001; Cremer et al. 1982; Gall & Pardue 1969; Speicher et al. 1996; Haaf & Schmid 1991; Stack et al. 1977; Bolzer et al. 2005). Live-cell fluorescence microscopy then gave insight into the dynamics of chromosome arrangements (Chubb et al. 2002; Heun et al. 2001; Janicki et al. 2004; Marshall et al. 1997; Masui et al. 2011; Robinett et al. 1996). Using this technique, it was possible to follow endogenous loci in living cells and relate chromosome organization and localization to transcription (Alexander et al. 2019; Chen et al. 2013; Germier et al. 2017; Gu et al. 2018; Saad et al. 2014). Recent advances in electron and super-resolution microscopy have largely contributed to our understanding of chromatin topology and the fine-scale structure of the chromatin fiber on a single-cell level (Lakadamyali & Cosma 2015; Ou et al. 2017; Belmont 2014).

In addition to these key findings from microscopy techniques, the development of 3C approaches has significantly contributed to our understanding of the nuclear 3D architecture. The 3C technologies can provide genome-wide contact maps and additionally give spatial information about the different genomic regions and thus have overcome many limitations of previously available methods.

1.2.3.1 Chromosome conformation capture (3C) approaches

The original 3C protocol was developed as a novel method to detect the *in vivo* contact frequency of two genomic loci of interest (Dekker et al. 2002). The principle of detecting chromatin contacts by 3C is based on chromatin crosslinking and proximity ligation. Chromatin contacts, which are mediated by protein-DNA, RNA-DNA or DNA-DNA interactions, are fixed with formaldehyde. After digesting the chromatin with a restriction enzyme, the cross-linked chromatin fragments are ligated resulting in preferential ligations between fragments contacting each other (Dekker et al. 2002). The result of this ligation reaction is referred to as a "3C library" and contains all genome-wide ligation products. All 3C-based techniques use this 3C library as an input, but they differ in their approach to detect the ligation junctions (Denker & De Laat 2016). It is important to note that all 3C technologies, except for a recently developed single-cell approach, provide contact frequencies from population averages.

The original 3C protocol quantifies the interaction frequency between two loci of interest ("one-to-one") by PCR using suitable primer pairs across the ligation junction (Dekker et al. 2002). The initial findings with 3C include the detection of long-range gene regulation mechanisms, such as promoter-enhancer loops at the murine β-globin locus (Tolhuis et al. 2002). These loops were studied during differentiation and shown to be tissue-specific (Palstra et al. 2003). Further, the indispensable roles of CTCF and specific transcription factors were described for looping interactions between promoters and enhancers (Drissen et al. 2004; Vakoc et al. 2005; Splinter et al. 2006). Additional 3C studies involved CTCF in the formation of chromatin loops for chromosome architecture (Handoko et al. 2011; Li et al. 2012).

3C was further developed into 4C (circular chromosome conformation capture) which allowed for the detection of the ligation junctions in higher throughput (Van De Werken et al. 2012; Zhao et al. 2006). The 4C method made it possible to detect all genome-wide contacts of a locus of interest, the "viewpoint" or anchor point ("one-to-all"). Involving a second digestion and ligation step, all ligation partners of the anchor point get amplified and deep sequenced.

5C (chromosome conformation capture carbon copy) was developed to study the contacts between multiple selected sequences ("many-to-many") (Dostie et al. 2006). With 5C, large regions (up to several mega-bases) can be amplified from 3C libraries using a complex primer mix complementary to the region of interest. In several steps, a "carbon copy" of all ligation junctions is created which can be analyzed by high-throughput sequencing (or microarrays) at high resolution (Ferraiuolo et al. 2012). As an alternative to the 5C approach, capture-based 3C technologies were developed (e.g. Capture-C, Capture-Hi-C and CAPTURE) (Hughes et al. 2014; Mifsud et al. 2015; Liu

et al. 2017). In different variations of the protocol, capture probes to selected “viewpoints” are used to pull-down specific ligation products from the 3C library. With capture-based methods, detailed genome-wide interactions maps can be determined of larger genomic regions or many loci in parallel (Franke et al. 2016; Andrey et al. 2017; Schoenfelder et al. 2018).

The most widely used 3C technique is Hi-C (chromosome capture followed by high-throughput sequencing) allowing for the detection of whole-genome contact maps (“all-to-all”) (Lieberman-Aiden et al. 2009). After restriction digest of the crosslinked chromatin, biotin-labeled nucleotides are incorporated at the ends of the crosslinked restriction fragments and they are subsequently ligated. With a streptavidin pulldown on the sheared Hi-C library, the biotin-containing ligation products are enriched. The Hi-C library gets sequenced by high-throughput sequencing obtaining a matrix of pair-wise interactions. The resolution of this interaction matrix depends on the sequencing depth and on how dense the restriction sites are present in the genome (Denker & De Laat 2016).

Additionally, the recent development of single-cell Hi-C protocols provided insight into the heterogeneity of genome organization between cells, also during the cell cycle, and thereby overcame the population analysis of 3C methods (Nagano et al. 2013; Nagano et al. 2015; Nagano et al. 2017).

Alternative ligation-free approaches, e.g. GAM (genome architecture mapping), SPRITE (split-pool recognition of interactions by tag extension), ChIA-PET (chromatin interaction analysis by paired-end tag sequencing) and ChIA-Drop (chromatin interaction analysis via droplet-based and barcode-linked sequencing), have been developed to map chromatin contacts genome-wide (Beagrie et al. 2017; Kempfer & Pombo 2020; Quinodoz et al. 2018; Zheng et al. 2019; Fullwood et al. 2009). These methods reproduce Hi-C data but additionally give insight into more complex interactions involving three or more contact partners (Kempfer & Pombo 2020). DamID (DNA adenine methyltransferase identification) is another ligation-free technique that allows to define chromatin positions with respect to nuclear landmarks, such as the nuclear lamina (Van Steensel & Henikoff 2000; Vogel et al. 2007; Marshall et al. 2016).

In summary, all 3C-based methods gave remarkable insights into genome topology and are powerful methods to investigate the folding of the genome, providing both sequence and special information.

1.2.3.2 Looking at Hi-C maps in *S. cerevisiae*

The 3C methodology was originally developed in *S. cerevisiae* (Dekker et al. 2002). Since then the method was further refined and genome-wide interaction studies were performed with greatly improved resolution. A recent modification of Hi-C, dubbed Micro-C, defined genome-wide interactions at nucleosome resolution in budding yeast by using Micrococcal Nuclease (MNase) for chromatin fragmentation (Hsieh et al. 2016; Hsieh et al. 2015). For the first time in budding yeast, the authors identified self-associating domains, chromosomal interaction domains (CIDs), which are similar to topologically associated domains described in mammals (Nora et al. 2017; Dixon et al. 2012). Interestingly, even though the size of TADs in mammalian cells (~100 kb – 1 Mb) is one to two orders of magnitude bigger than the self-interacting domains in yeast (~2 – 10 kb), their size seems to be conserved in terms of gene number. CIDs in budding yeast typically range over one to five genes, and TADs in mammalian cells cover roughly the same number of genes. Budding yeast has no CTCF insulator protein and therefore CID boundaries must be defined by a different mechanism from TAD boundaries in mammalian cells. The aforementioned Micro-C study specifically localized the boundaries of the CIDs to active promoters, which are enriched for the RSC chromatin remodeling complex and the cohesin loading factor Scc2 and are devoid of nucleosomes (Hsieh et al. 2015). These findings are in agreement with previous observations that active genes play a role as boundaries between domain structures (Dixon et al. 2012; Le et al. 2013; Nora et al. 2012; Gheldof et al. 2006). According to genome-wide Micro-C maps of *S. cerevisiae* nuclei, gene loops, the described specific interaction of promoter and terminator factors, are rather manifested as strong interaction frequencies throughout the entire gene body (Hsieh et al. 2015; Hsieh et al. 2016).

The “Rabl” conformation of yeast interphase nuclei was discovered in cytological studies (Rabl 1885) and can also be observed in 3C experiments and Hi-C maps (Dekker et al. 2002; Duan et al. 2010; Hsieh et al. 2016). It is characterized by robust centromere-centromere contacts at the spindle pole body, the yeast microtubule organization center, and telomere tethering and clustering at the nuclear envelope (Taddei & Gasser 2012).

1.3 Scope of this thesis

Telomeres are the protective caps of chromosome ends and prevent the activation of a local DNA damage response. They can adopt a lariat like conformation and engage in long- and short-range chromosome interactions. In many organisms, these telomere structures provide an additional layer of protection. Two decades ago, budding yeast telomeres were proposed to fold back into subtelomeric regions (de Bruin et al. 2001). However, a robust method to study these structures has been lacking. To date, only indirect methods were available to characterize telomere folding in *S. cerevisiae.* Additionally, the visualization of folded telomere structures by microscopy has been challenging. Therefore, it is not well understood how telomere-subtelomere interactions are established and regulated in budding yeast.

Telo-3C is a chromosome conformation capture-based method to detect telomere-subtelomere interactions in budding yeast and was established as part of the doctoral dissertation of René Schellhaas (Schellhass 2016). In my thesis, I aim to optimize the Telo-3C technology for the quantification of telomere folding interactions to study the genetic requirements for its establishment. I am interested in elucidating the mechanisms of telomere folding and integrating them into the context of genome architecture. I focus on identifying critical telomere folding regulators and interrogate how chromatin modifiers contribute to its regulation. I am particularly interested in characterizing telomere folding during replicative senescence, which can be easily modelled in budding yeast through the deletion of the telomerase genes. I aim to understand the changes of telomere folding during senescence and characterize the underlying mechanisms by additionally employing a mass spectrometry approach. As the functional consequences of telomere unfolding remain to be elucidated in budding yeast, I address whether telomere folding might provide an additional layer of protection to chromosome ends.

Studying the regulation of telomere folding in the genetically versatile budding yeast system offers the opportunity to elucidate parallels to human telomeres. We might gain insight into novel regulatory mechanisms and interesting features of the human telomere folding behavior. Understanding telomere structure during replicative senescence is of particular interest, as most telomerase-negative human somatic cells eventually undergo this process. During senescence, telomeres gradually shorten and erode until cells stop dividing which is a potent tumor suppressor mechanism and prevents unscheduled growth of potential cancer cells.

2 Results

2.1 Characterizing telomere folding in budding yeast

2.1.1 Telo-3C detects telomere folding in *S. cerevisiae*

To gain insight into the dynamic regulation of the folding of *S. cerevisiae* telomeres, we employed a chromosome conformation capture approach (3C) (Dekker et al. 2002), dubbed Telo-3C. The Telo-3C methodology was initially developed in the Luke lab by René Schellhaas (Schellhass 2016) and further optimized as part of this doctoral dissertation. Telo-3C is a direct approach to quantitatively assess the interaction of one telomere (left telomere of chromosome 1) with its adjacent subtelomeric region. As illustrated in Figure 10A, chromosome contacts, such as a folded telomere structure, are crosslinked in intact cells using formaldehyde. Subsequently, the extracted chromatin gets digested with an appropriate restriction enzyme for telomere 1L (NcoI) and the compatible sticky DNA ends are ligated with DNA ligase under diluted conditions. This way, chromatin segments that localize in close proximity to each other within the intact nucleus get ligated more frequently than others that localize further apart. After reversing the crosslink, a specific Telo-3C PCR product can be amplified with primers that were co-directionally oriented on genomic DNA (no PCR product) but get converted during the Telo-3C reaction (PCR product from convergent primers; blue arrows Figure 10A). The abundance of this specific PCR product can be quantified by quantitative PCR (qPCR). To account for the amount of input DNA that is used for the qPCR reaction, the Telo-3C-specific qPCR signal is normalized to the intensity of a control qPCR product, which is robustly amplified from genomic DNA (gDNA). The relative interaction frequencies of telomere 1L with its corresponding subtelomere in the investigated conditions are then determined relative to the respective wild type (wt) or untreated sample.

To test the specificity of the Telo-3C methodology, the Telo-3C protocol was performed without ligating or digesting the crosslinked chromatin. Even though a Telo-3C qPCR product was amplified under conditions without ligation or digestion, its abundance was at the detection limit of the qPCR supporting the specificity of the method (Figure 10B). Therefore, the detected interaction frequency without ligating or digesting the chromatin was considered background (Figure 10B). When establishing any 3C technique, it is critical to determine the level of random collisions between two loci (Dekker 2006). Therefore, we assessed the frequency of random collisions by performing the Telo-3C protocol with chromatin, which was not crosslinked with formaldehyde. Even with increasing amounts of non-crosslinked chromatin input, the Telo-3C product intensity was barely detected by qPCR or drastically lower than the one obtained with crosslinked chromatin (Figure 10C). This suggests that a specific Telo-3C PCR product could only be amplified when the

loci of interest were located in close proximity within the intact nucleus. We were interested in measuring the interaction of the telomeric repeats with several loci along the subtelomere and designed primers according to the NcoI restriction sites present on subtelomere 1L (Figure 10D). The primer P5 served as the anchor primer as it was designed in close proximity to the telomeric repeats. Due to the proximity of P5 to the telomere, we have made the assumption that the interaction frequency of this locus will give us an indication of how the telomeric repeats themselves interact with other loci. We used this anchor primer in combination with P6 or P7, thereby comparing the interaction of the telomeric repeats to a subtelomeric region with a distance of ~2 kb (P6) or ~9 kb (P7). The interaction frequency was reduced to half when moving from ~2 kb (P5+P6) to ~ 9 kb (P5+P7) distance from the telomeric repeats (Figure 10E). The P9 primer binds outside of the subtelomere with a distance of ~47 kb to the telomeric repeats. We also detected a Telo-3C product between primers P5 and P9 (~47 kb) (Figure 10E). This suggests that the telomere might as well interact with loci of greater distance to the telomeric repeats, although with lower frequency (Figure 10E). Importantly, the sequences of all depicted Telo-3C PCR products were confirmed by Sanger sequencing (data not shown, performed by René Schellhaas (Schellhass 2016)). Exclusively sequences from subtelomere 1L were detected, which excludes the possibility that our approach amplifies interactions between different telomeres. Therefore, Telo-3C is a reliable and specific method to detect intra-telomere interactions of telomere 1L in *S. cerevisiae*. In the following, I will refer to these intra-telomere contacts as telomere folding or telomere fold-back structure.

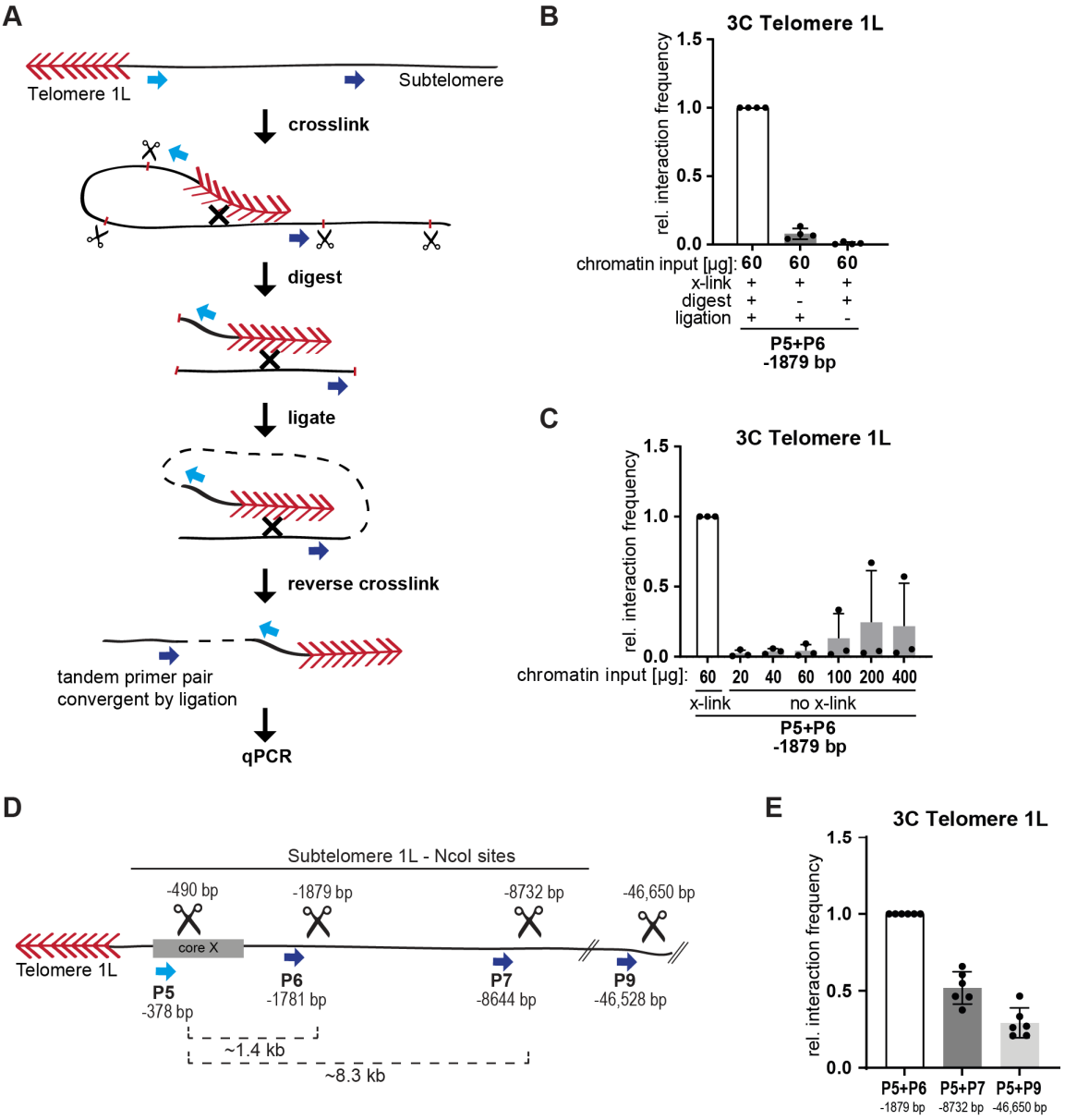

Figure 10. Telo-3C detects telomere folding in *S. cerevisiae*. **(A)** Schematic representation of the Telo-3C method. Formaldehyde was used to crosslink chromosome interactions such as telomere folding. DNA was digested with the restriction enzyme NcoI. DNA ends were ligated under diluted DNA conditions to prevent ligation artifacts. The tandem primer pairs on linear DNA (blue arrows) got converted to convergent primer pairs upon ligation, and telomere contacts were detected by qPCR. Red arrowheads = telomere repeats; Scissors = NcoI restriction sites. **(B)** The Telo-3C protocol was performed without digesting or ligating the chromatin as indicated. The positions of the primers P5 and P6 are shown in **Figure 10D**. All interaction frequencies were normalized to a control qPCR product. Relative interaction frequencies were calculated by setting the normalized interaction frequency of the sample which was performed with the complete Telo-3C protocol to 1. Mean +/- SD of 4 independent experiments. **(C)** The Telo-3C protocol was performed on increasing amounts of chromatin without formaldehyde crosslinking (no x-link). All interaction frequencies were normalized to a control qPCR product. Relative interaction frequencies were calculated by setting the normalized interaction frequency of the sample which was performed with the complete Telo-3C protocol to 1. Mean +/- SD of 3 independent experiments. **(D)** Illustration of NcoI cut sites along the subtelomere 1L and the binding sites of the primers (blue arrows) used to detect interaction frequencies between the respective sites. P5 was used as anchor primer in close proximity to the telomeric repeats. Genomic location of primers and cut sites (scissors) were calculated from the end of telomere 1L (depicted in bp) as annotated in the SGD (Saccharomyces genome database). **(E)** Relative interaction frequencies of telomere 1L with loci of increasing distance from the telomeric repeats (primers P6, P7 and P9). All interaction frequencies were normalized to a control qPCR product. Relative interaction frequencies were calculated by setting the normalized interaction frequency of P5 + P6 to 1. Mean +/- SD of 6 independent experiments.

2.1.2 Telomere folding occurs more frequently than intra-chromosomal non-telomeric contacts

I wanted to understand if the folding of the telomeric repeats onto the subtelomere occurs more frequently than random interactions of two loci located internally on the same chromosome. Internal NcoI restriction sites on chromosome 1 (**Figure 11A**) and the respective 3C primers (P10, P11 and P12) were chosen, which had similar distances as the ones on subtelomere 1L (P5, P6 and P7). Even though a weak 3C product was detected using the non-telomeric primer sets (green bars in **Figure 11B**), the telomeric fold-back structure formed more robustly than the interaction between internal loci (non-telomeric 3C). These results show that the interaction at the end of the chromosome occurs more frequently than a random encounter of two internal loci on the same chromosome (**Figure 11B**).

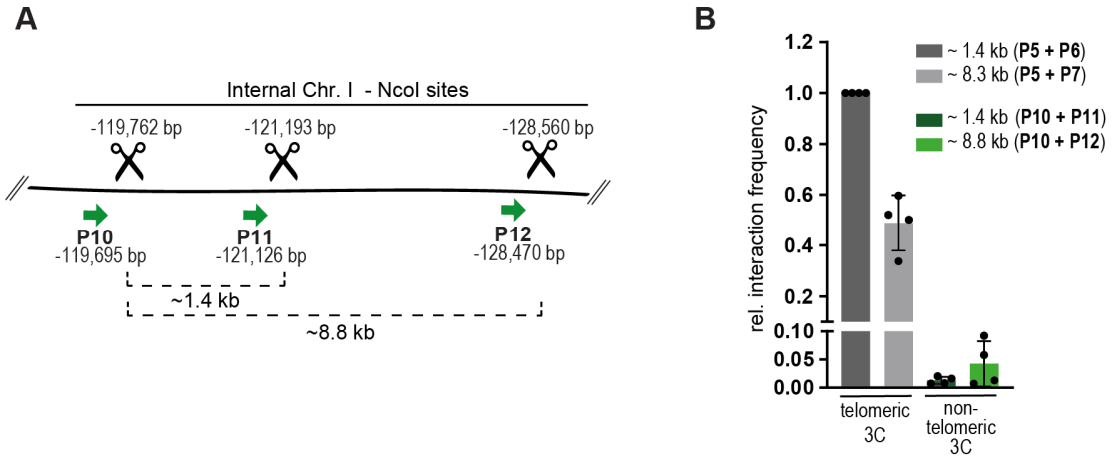

Figure 11. Telomere folding occurs more frequently than intra-chromosomal non-telomeric contacts. (A) Illustration of NcoI cut sites at a non-telomeric, internal locus on chromosome 1 (non-telomeric) and the primers (green arrows) used to detect the interaction frequencies between the respective sites. Genomic location of primers and cut sites were calculated from the end of telomere 1L as annotated in the SGD. **(B)** 3C results comparing the relative interaction frequencies of telomeric with non-telomeric loci on chromosome 1 using the indicated primer pairs. The interaction frequencies of telomeric and non-telomeric 3C were normalized to a control qPCR product. The relative interaction frequencies were calculated by setting the normalized interaction frequency of P5 + P6 to 1. Mean +/- SD of 4 independent experiments.

2.1.3 Telomere 1L folding is unaffected by the cell cycle

Having optimized the Telo-3C method, I was interested in studying the dynamic regulation of telomere folding during the cell cycle. I arrested cells in the G1 phase of the cell cycle with the mating pheromone α-factor. After washing the pheromone out, the culture was released into the S phase at 25 °C to ensure a synchronous and slow cell cycle progression (**Figure 12A**). This experiment was performed in cells lacking the *BAR1* gene, which encodes for a protease that cleaves α-factor (Ballenstefen & Schmitt 1997; Chan & Otte 1982). *BAR1* deletion therefore prevents the rapid inactivation of α-factor. The analysis of the DNA content by flow cytometry

showed that a synchronous population of yeast cells was obtained (Figure 12B). The increased protein levels of the G1-specific CDK inhibitor Sic1 confirmed that cells were in the G1 phase for 30 min after release (Figure 12C). After 45 min, the cells entered the S phase coinciding with the decrease of Sic1 and a right shift in the flow cytometry profile (Figure 12B). Starting from 60 min after release the population entered the G2/M phase as the expression of the G2/M cyclin Clb2 increased and the 2N peak in the flow cytometry profile appeared (Figure 12B, C). Telo-3C results during the release of the culture from G1 arrest did not display significant changes compared to the exponential culture grown at the same temperature. However, the standard deviations between the replicates were exceptionally high in this experiment (Figure 12D). Nevertheless, it is interesting to note, that the relative Telo-3C interaction frequency did not drop below the signal of the exponential culture at any cell cycle phase (Figure 12D). These data suggest that the telomere folding status of a synchronous cell population does not undergo drastic changes during the cell cycle in the manner that the experiments was performed.

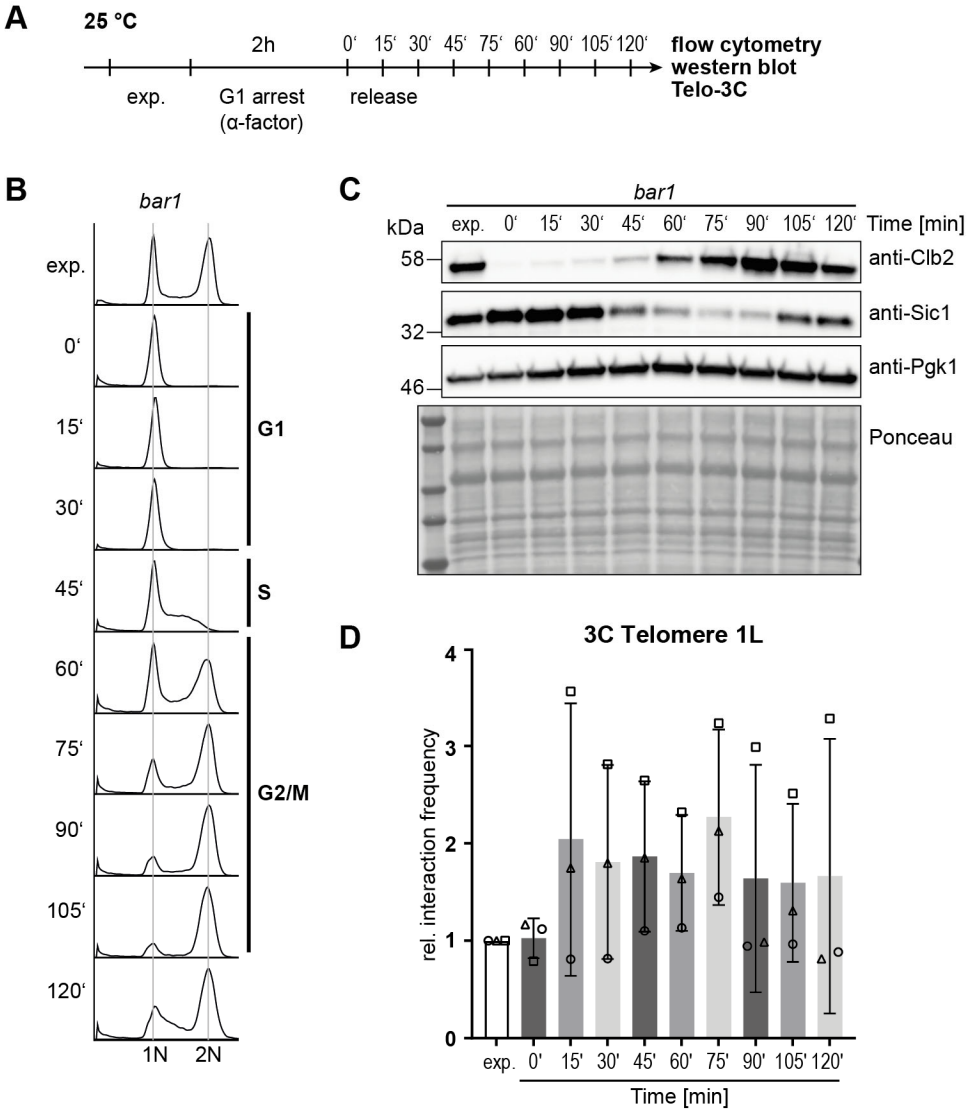

Figure 12. Telomere 1L folding is unaffected by the cell cycle. (A) Experimental setup to detect telomere folding during the cell cycle in *bar1* cells. Cells were arrested in the G1 phase with 1 µM α-factor for 2 h at 25 °C. The α-factor was washed out with water and the cells were released into S phase. Samples for flow cytometry, western blot and Telo-3C were collected every 15 min. **(B)** Flow cytometry histograms of the DNA content in exponential cells (exp.) and after release into the cell cycle from the G1 arrest. The respective cell cycle phases are indicated as G1, S and G2/M. G1 cells have a DNA content of 1N, while G2/M cells have a duplicated genome (2N). **(C)** Western blots using anti-Clb1 and anti-Sic1 antibodies. The anti-Pgk1 antibody and Ponceau staining served as loading controls. **(D)** Telo-3C analysis of *bar1* cells using the primers P5 and P6. The relative interaction frequency in exponential cells (exp.) and after release from the G1 arrest is shown. All interaction frequencies were normalized to a control qPCR product. Relative interaction frequencies were calculated by setting the normalized interaction frequency of exponential cells to 1. Mean +/- SD of 3 independent experiments, which are depicted as different symbols.

2.2 Identifying regulators of telomere folding

In order to identify regulators of telomere folding, I took a candidate approach of factors involved in different processes that could potentially be implicated in the formation or maintenance of telomere folding. The candidates comprised factors that are implicated in chromosome architecture, telomere function, homologous recombination and the DNA damage response.

2.2.1 SMC complexes are not involved in the establishment of telomere folding

The structural maintenance of chromosomes (SMC) complexes comprise cohesin, condensin and the SMC5/6 complex. The C-termini of one subunit of each SMC complex were endogenously tagged with an improved auxin-inducible degron (AID*) and a 9MYC-tag (9MYC) (Morawska and Ulrich 2013) (Figure 13A). As all of these complexes are essential in yeast, this system allowed me to investigate their impact on telomere folding by transiently degrading these tagged proteins through the addition of the plant hormone auxin (indole-3 acetic acid = IAA) to the culture media. I treated the cultures with auxin for 1 h, resulting in complete protein depletion (Figure 13B). Importantly, Telo-3C results showed that the addition of auxin to a wt culture without an AID*-fusion protein did not influence the folding of telomere 1L (Figure 13C). Therefore, the auxin-inducible system is compatible with the Telo-3C method. My data demonstrate that telomere folding was not affected by the lack of Smc6 or the cohesin complex member Smc1 under these conditions (Figure 13C). The depletion of the condensin subunit Smc4 slightly enhanced the interaction frequency of the fold-back structure at telomere 1L (Figure 13C). Importantly, flow cytometry analysis showed that cell viability was not affected after depletion of any of the SMC complexes (Figure 13D). Accordingly, I conclude that the SMC complexes do not contribute to the establishment of a closed fold-back structure at yeast telomeres.

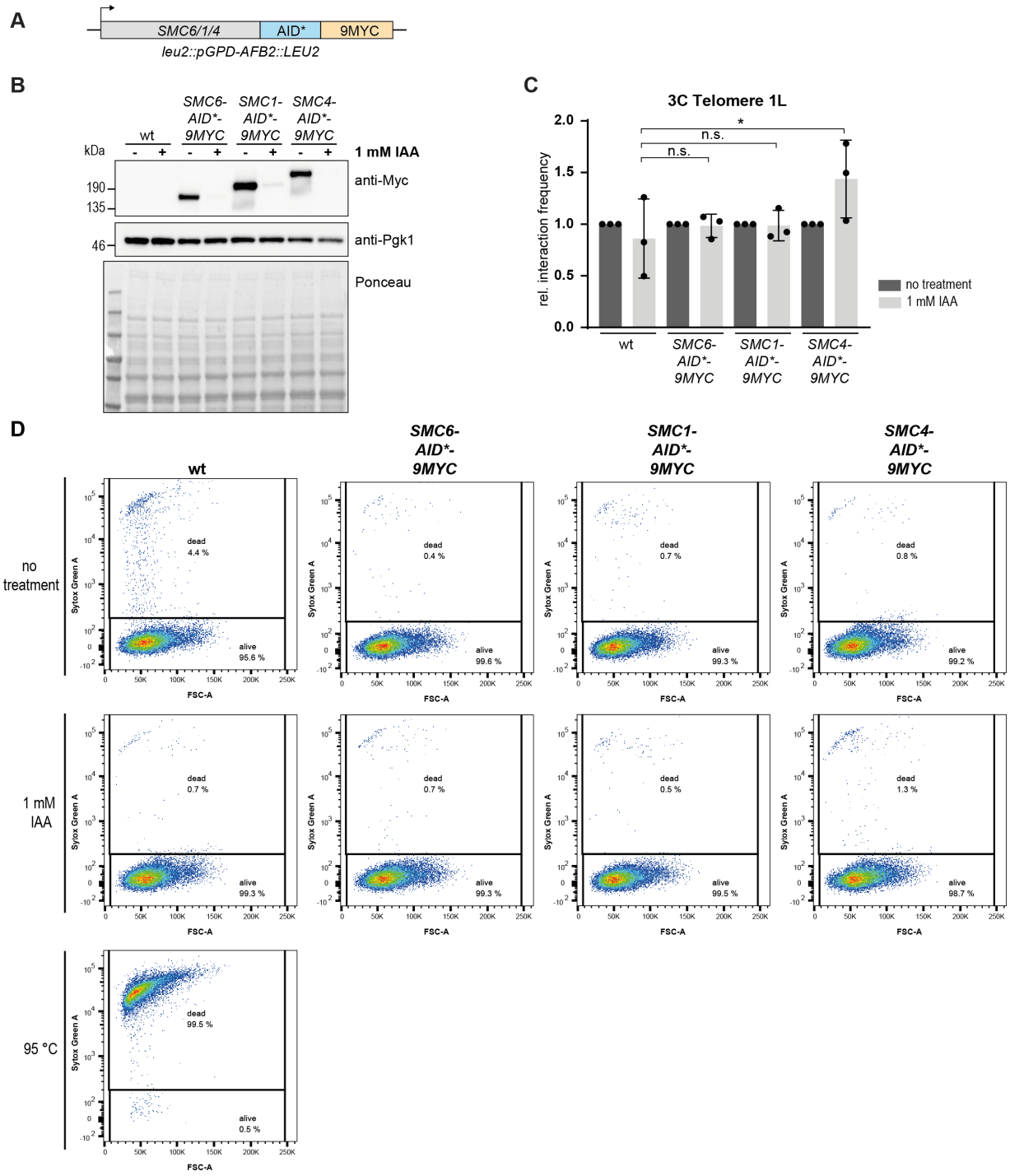

Figure 13. SMC complexes are not involved in the establishment of telomere folding. **(A)** Schematic representation of tagging *SMC6*, *SMC1* and *SMC4* with an auxin-inducible degron (AID*) and a 9MYC-tag. **(B)** Western blots were performed to detect protein levels after treatment with 1 mM auxin (IAA) for 1 h. The anti-Pgk1 antibody and Ponceau staining served as loading controls. **(C)** Telo-3C analysis after depletion of SMC complex members for 1 h with 1 mM IAA. The interaction frequencies between the primers P5 and P6 are shown. All interaction frequencies were normalized to a control qPCR product. Relative interaction frequencies were calculated by setting the normalized interaction frequency of the untreated samples to 1. Mean +/- SD of 3 independent experiments. Adjusted p-values were obtained from two-way ANOVA with Tukey's multiple comparison test (*p ≤ 0.05, n.s. not significant). **(D)** Flow cytometry histograms depict the cell viability. Cells were stained with SYTOX green after the depletion of the SMC complex members for 1 h with 1 mM IAA. As a control for dead cells, wt cells were boiled at 95 °C for 15 min.

2.2.2 The telomeric proteins Rif1 and Rif2 are dispensable for telomere folding

The two telomeric proteins, Rif1 and Rif2, were previously reported to regulate the telomere fold-back structure (Poschke et al. 2012). Using a genetic telomere folding reporter, the authors showed that telomere folding is compromised in *rif1* and *rif2* mutants (Poschke et al. 2012), which are characterized by overelongated telomeres and an altered chromatin environment (Hardy et al. 1992; Wotton & Shore 1997). Poschke et al. proposed that specifically Rif2 might promote telomere folding through the recruitment of the histone deacetylase complex Rpd3L, which was suggested to be a critical regulator of telomere folding (Poschke et al. 2012). By Telo-3C I did not observe a telomere folding defect in *rif1* or *rif2* deletion mutants arguing that these two telomeric proteins might not contribute to the establishment of a folded structure at the natural telomere 1L (**Figure 14**).

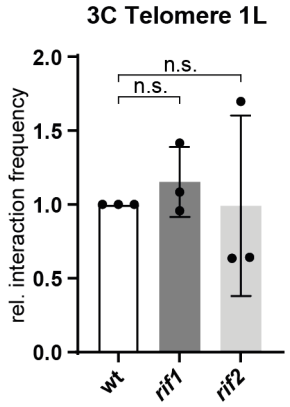

Figure 14. The telomeric proteins Rif1 and Rif2 are dispensable for telomere folding. Telo-3C analysis of *rif1* and *rif2* mutants. The interaction frequencies between the primers P5 and P6 are shown. All interaction frequencies were normalized to a control qPCR product. Relative interaction frequencies were calculated by setting the normalized interaction frequency of the wt to 1. Mean +/- SD of 3 independent experiments. Adjusted p-values were obtained from one-way ANOVA with Dunnett's multiple comparison test (n.s. not significant).

2.2.3 The homologous recombination factors Rad51 and Rad52 are required for telomere folding

I was interested to study if the recombination machinery might play a role in the folding of yeast telomeres and performed Telo-3C experiments in cells lacking the main yeast homology directed repair (HDR) factors *RAD51* and *RAD52*. The Telo-3C analysis showed that telomere folding was significantly decreased in *rad51* and *rad52* mutants (**Figure 15**). Due to the high mutation rate and increased chromosome instability in these mutants (McDonald et al. 2016; Ang et al. 2016; Hwang et al. 2008; Yi et al. 2016), I confirmed this result in three independent clones of each genotype in several experiments. Consistently, the *rad51* and *rad52* mutants failed to establish a folded telomere structure. This suggests that a strand invasion mechanism might play a role in the folding mechanism of yeast telomeres, like at mammalian chromosome ends.

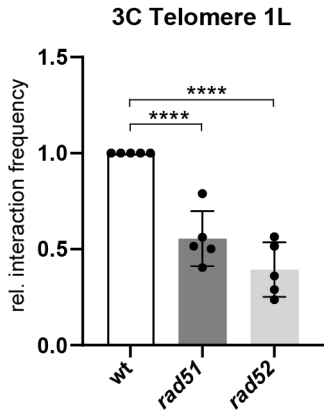

Figure 15. The homologous recombination factors Rad51 and Rad52 are required for telomere folding. Telo-3C analysis of *rad51* and *rad52* mutants. The interaction frequencies between the primers P5 and P6 are shown. All interaction frequencies were normalized to a control qPCR product. Relative interaction frequencies were calculated by setting the normalized interaction frequency of the wt to 1. Mean +/- SD of 5 independent experiments. Adjusted p-values were obtained from one-way ANOVA with Dunnett's multiple comparison test (****p ≤ 0.0001).

2.2.4 The checkpoint kinase Rad53 is involved in telomere folding

Rad51 and Rad52 are part of the repair machinery after the activation of a DNA damage response (DDR). Having discovered that these HDR factors contribute to telomere folding, I aimed to investigate if the upstream factors of the DDR, the checkpoint kinase Mec1 (ATR in human), Tel1 (ATM in human) and Rad53 (CHK2 in human), are also involved in telomere folding. In order to analyze telomere folding in cells lacking the *MEC1* gene, I performed Telo-3C in *sml1 mec1* double mutants, since the *SML1* deletion suppresses the lethality of *mec1* cells (Zhao et al. 1998). Even though I observed high variability within the samples of the same genotype, the mean relative Telo-3C interaction frequency was comparable in *sml1* and *sml1 mec1* cells (Figure 16A). Accordingly, the deletion of the other major DNA damage checkpoint kinase *TEL1* did also not affect the folding of telomere 1L (Figure 18C). Next, I tested whether Rad53, which acts downstream of Mec1 and Tel1 (reviewed in Lanz et al. 2019), contributes to a closed telomere fold-back structure. Using an endogenous C-terminal auxin-inducible degron tag on Rad53 (Figure 16B), I depleted cells of this protein by treatment with 1 mM IAA for 2 h (Figure 16C). When Rad53 was lacking, I observed a significant reduction of telomere folding suggesting that a compromised DNA damage checkpoint may affect the structure of the telomere (Figure 16D). Importantly, the depletion of the essential protein Rad53 did not drastically affect cell viability for the time frame of this experiment, as measured by flow cytometry after SYTOX green nucleic acid staining (Figure 16E). According to these data, I propose that Mec1 and Tel1 might have overlapping functions in terms of telomere folding which could potentially compensate for each other. Another possibility is, that Rad53's contribution to telomere folding might be independent from Mec1 and Tel1.

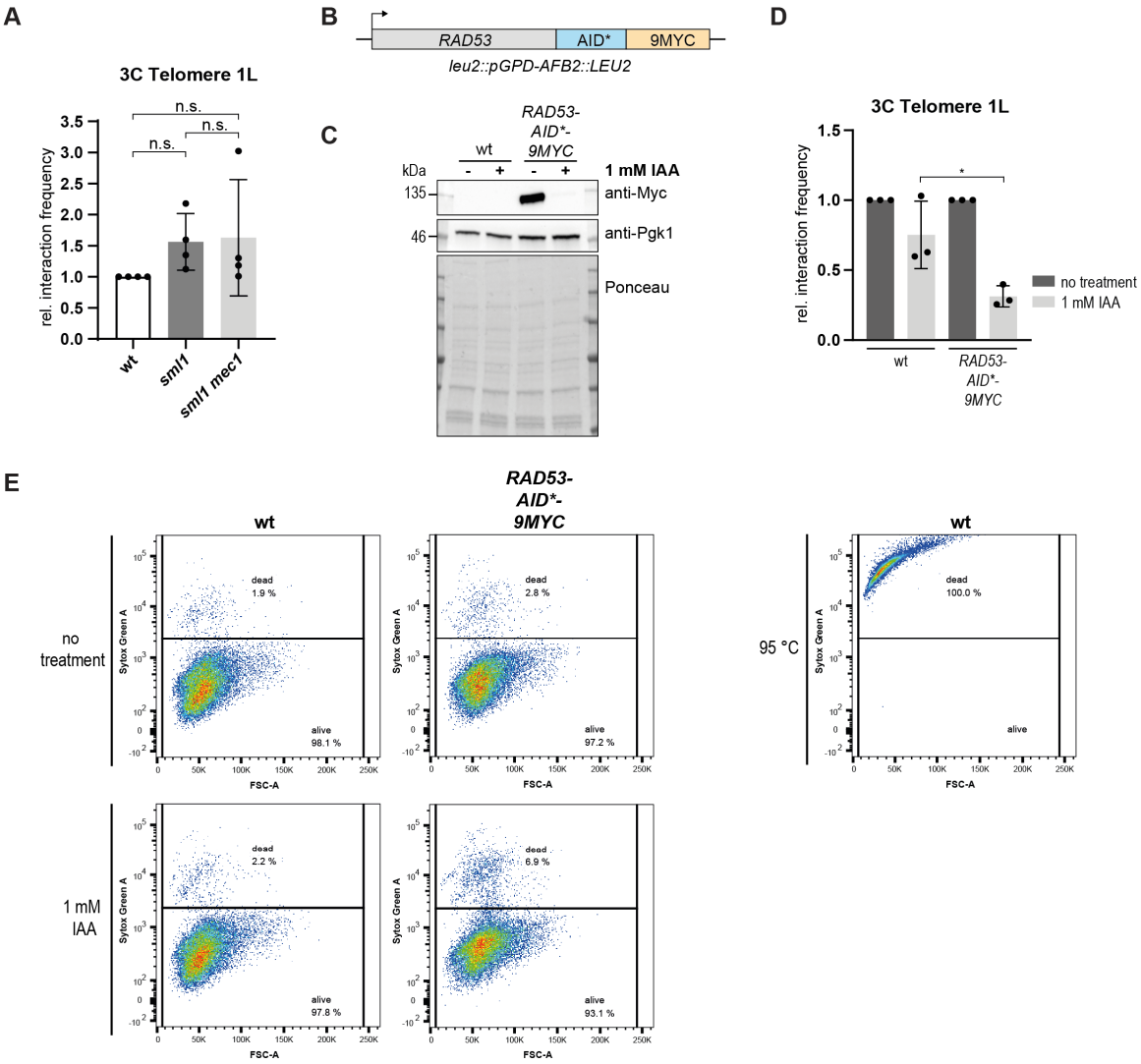

Figure 16. The checkpoint kinase Rad53 is involved in telomere folding. **(A)** Telo-3C analysis of *sml1* and *sml1 mec1* mutants. The interaction frequencies between the primers P5 and P6 are shown. All interaction frequencies were normalized to a control qPCR product. Relative interaction frequencies were calculated by setting the normalized interaction frequency of the wt to 1. Mean +/- SD of 4 independent experiments. Adjusted p-values were obtained from one-way ANOVA with Tukey's multiple comparison test (n.s. not significant). **(B)** Schematic representation of tagging *RAD53* with an auxin-inducible degron (AID*) and a 9MYC-tag. **(C)** Western blot to detect protein levels after treatment with 1 mM auxin (IAA) for 2 h using an anti-Myc antibody. The anti-Pgk1 antibody and Ponceau staining served as loading controls. **(D)** Telo-3C analysis after depletion of Rad53 for 2 h with 1 mM IAA. The interaction frequencies between the primers P5 and P6 are shown. All interaction frequencies were normalized to a control qPCR product. Relative interaction frequencies were calculated by setting the normalized interaction frequency of the untreated samples to 1. Mean +/- SD of 4 independent experiments. Adjusted p-values were obtained from two-way ANOVA with Tukey's multiple comparison test (*p ≤ 0.05). **(E)** Cell viability analysis by flow cytometry using SYTOX green stain after the depletion of Rad53 for 2 h with 1 mM IAA. As a control for dead cells, wt cells were boiled at 95 °C for 15 min.

In summary, I identified several novel regulators of telomere structure in *S. cerevisiae*. The finding that the HDR factors Rad51 and Rad52 contribute to a folded telomere structure points towards a potential strand invasion mechanism of the 3' telomeric overhang into homologous sequences within the subtelomere. Through the temporary depletion of Rad53, I additionally found that the DNA damage checkpoint might play a role in the establishment of a fold-back structure at telomere 1L.

2.3 Exploring telomere structure during senescence and in the presence of DNA damage

2.3.1 Telomere 1L unfolds during replicative senescence

In budding yeast, replicative senescence can be easily modeled by passaging cells lacking the RNA component of telomerase (*TLC1*) over several population doublings (PDs). For this purpose, I derived telomerase negative (*tlc1*) and wt haploid spores from a heterozygous diploid knockout strain. In a senescence assay, wt and *tlc1* cells were propagated over ~100 PDs in liquid media by diluting the cultures daily. As expected, the viability of *tlc1* cells gradually decreased while wt cells maintained their growth potential (Figure 17A). The loss of viability was caused by progressive telomere shortening due to the lack telomerase activity. The decreasing telomere length of a representative *tlc1* clone becomes apparent on a Southern blot for telomeric DNA (telomere restriction fragment analysis) where bulk telomere length can be estimated by the size of all Y' telomeres between 1 and 1.5 kb (Figure 17B). When cells progress through replicative senescence they eventually reach a point of telomeric crisis, the point of lowest viability. At this point, some yeast cells can overcome the permanent cells cycle arrest and have acquired the capacity to elongate their telomeres based on a recombination-mediated pathway (Lundblad & Blackburn 1993). These type II survivors showed the amplification of TG repeats by the appearance of multiple additional bands on the telomere restriction fragment analysis (Teng & Zakian 1999) (Figure 17B). I was interested in interrogating the regulation of telomere folding throughout replicative senescence and employed Telo-3C during this time course (time points are indicated as + in Figure 17A). Telo-3C analysis in pre-senescent cells, at PD 9, revealed that telomere folding of *tlc1* mutants was comparable to wt cells (Figure 17C), although their telomeres were much shorter than wt telomeres (Figure 17B). At the point of crisis, *tlc1* cells had critically short telomeres (PD 47, 56 and 64 in Figure 17B) and telomere folding decreased significantly (Figure 17C). In established survivors, however, telomeres again acquired the ability to establish a fold-back structure (PD 101 in Figure 17C). By Southern blot with a telomere 1L specific probe, I additionally assessed the length of the telomere at which telomere folding was tested by Telo-3C. Importantly, telomere 1L followed the same shortening and recombination pattern as bulk telomeres (Figure 17D). Flow cytometry analysis for DNA content showed expected changes in cell cycle distribution due to a G2/M arrest during senescence (Figure 17E) (IJpma & Greider 2003; Enomoto et al. 2002). The enlarged cell morphology during senescence contributed to an altered flow cytometry histogram at PD 47 (Figure 17E) (Enomoto et al. 2002). However, the DNA content analysis also confirmed that the analyzed cells contained only a minor population of dead cells (Figure 17E).

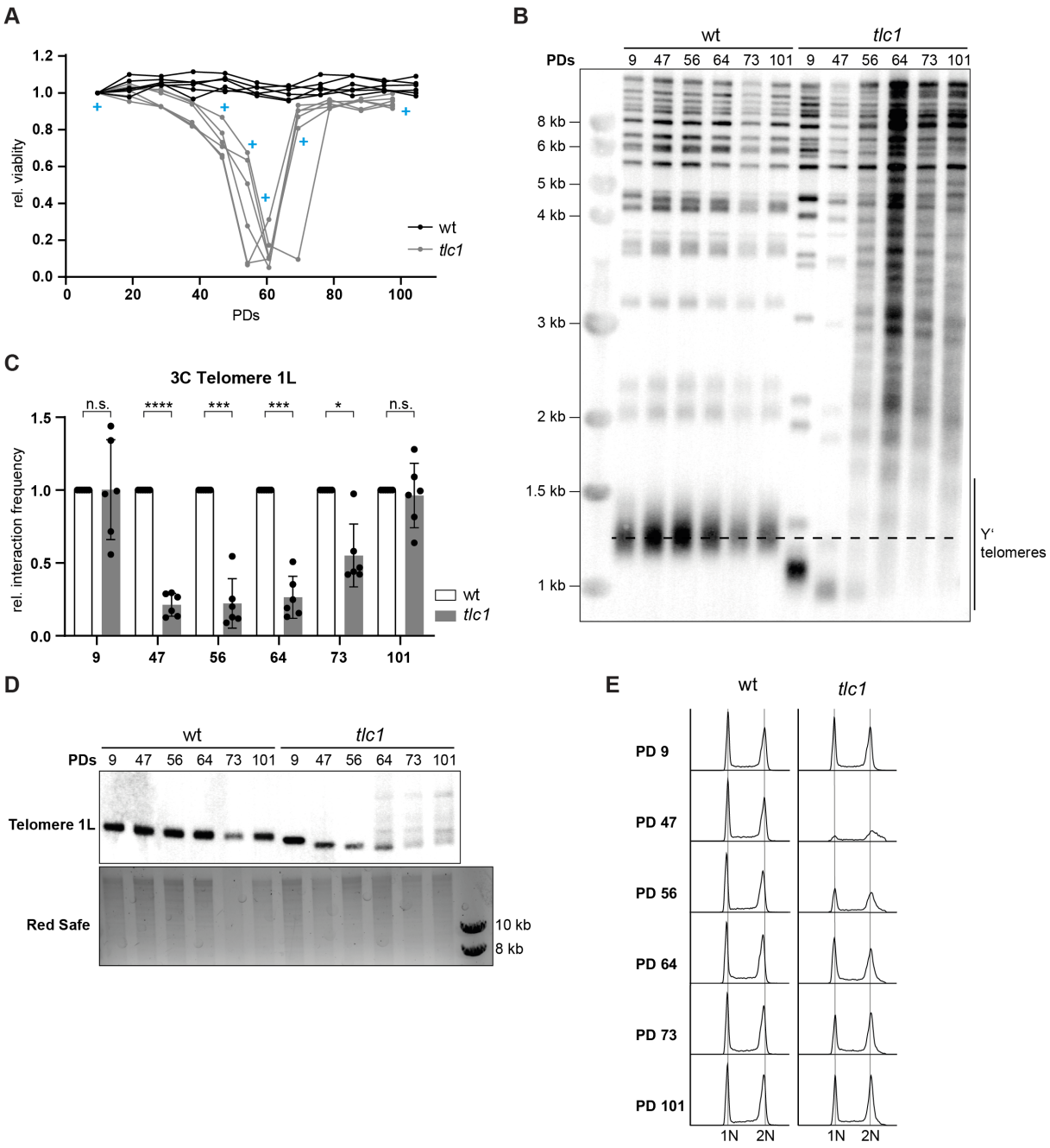

Figure 17. Telomere 1L unfolds during replicative senescence. (A) The relative viability of 6 independent wt and *tlc1* cultures was followed over ~100 PDs. Samples for Telo-3C were collected at the indicated time points (blue +). PD 0 was defined as the time point when the senescence curve was started in liquid culture from the spore colony. **(B)** Southern blot for all telomeres with XhoI digested genomic DNA using a radio-labeled (TG)n-repeat containing vector fragment as a probe. One representative sample for each genotype is shown. The dotted line indicates wt telomere length of Y' telomeres. **(C)** Telo-3C analysis during the time course shown in **Figure 17A**. The interaction frequencies between the primers P5 and P6 are shown. All interaction frequencies were normalized to a control qPCR product. Relative interaction frequencies were calculated by setting the normalized interaction frequency of the wt of the respective day to 1. Mean +/- SD of 6 different clones in 3 independent experiments. Adjusted p-values were obtained from two-way ANOVA with Sidak's multiple comparison test (*p ≤ 0.05, ***p ≤ 0.001, ****p ≤ 0.0001, n.s. not significant). **(D)** Southern blot for telomere 1L on genomic DNA digested with SalI using a specific PCR product labeled with ^{32}P as a probe. The agarose gel was stained with Red Safe to visualize DNA loading. One representative sample per genotype is shown. **(E)** Flow cytometry histograms for the DNA content of wt and *tlc1* cells during the time course shown in **Figure 17A**. One representative sample per genotype is shown. PDs = population doublings.

2.3.2 Short telomeres are proficient for engaging in a fold-back structure

The observation that short telomeres of pre-senescent cells (PD 9 in Fig **Figure 17B, C**) retain a folded conformation led me to the hypothesis that telomere shortening during senescence might not be the reason why telomeres unfold in crisis. To test this hypothesis, I investigated telomere folding of several yeast mutants harboring very short telomeres, which were stable in length and did not progressively shorten (Ritchie & Petes 2000; Lustig & Petes 1986; Greenwell et al. 1995; Morrow et al. 1995). These mutants were not characterized by a senescence phenotype, even though their telomeres were comparably short to the telomeres of telomerase negative *tlc1* cells, as detected by Southern blot for bulk telomere length and 1L specific telomere PCR (**Figure 18A, B**). As shown before, telomere folding was not maintained in *tlc1* cells analyzed at ~PD 40 (**Figure 18C**). I found that the telomeres of the analyzed mutants showed variability in their relative interaction frequency with their subtelomeric region. In contrast to the *tlc1* mutant, however, *upf1, ku70, mre11, tel1* and *rad50* mutants established telomere folding as efficiently as wt telomeres (**Figure 18C**). In conclusion, short telomeres *per se* are still able to fold back onto the subtelomere. Since the accumulation of the long non-coding RNA TERRA is repressed by silenced telomeric chromatin, I estimated the telomere silencing state in these mutants by measuring TERRA levels from telomere 1L. The relative TERRA expression in *ku70, mre11, tel1* and *rad50* mutants was comparable to wt (**Figure 18D**). As previously observed in our lab, TERRA levels significantly increased in telomerase negative cells (Graf et al. 2017) and this increase correlated with an open telomere structure (**Figure 18C**). On the contrary, I noticed that the increased TERRA expression in the *upf1* mutant did not coincide with decreased telomere folding in this case (**Figure 18C, D**).

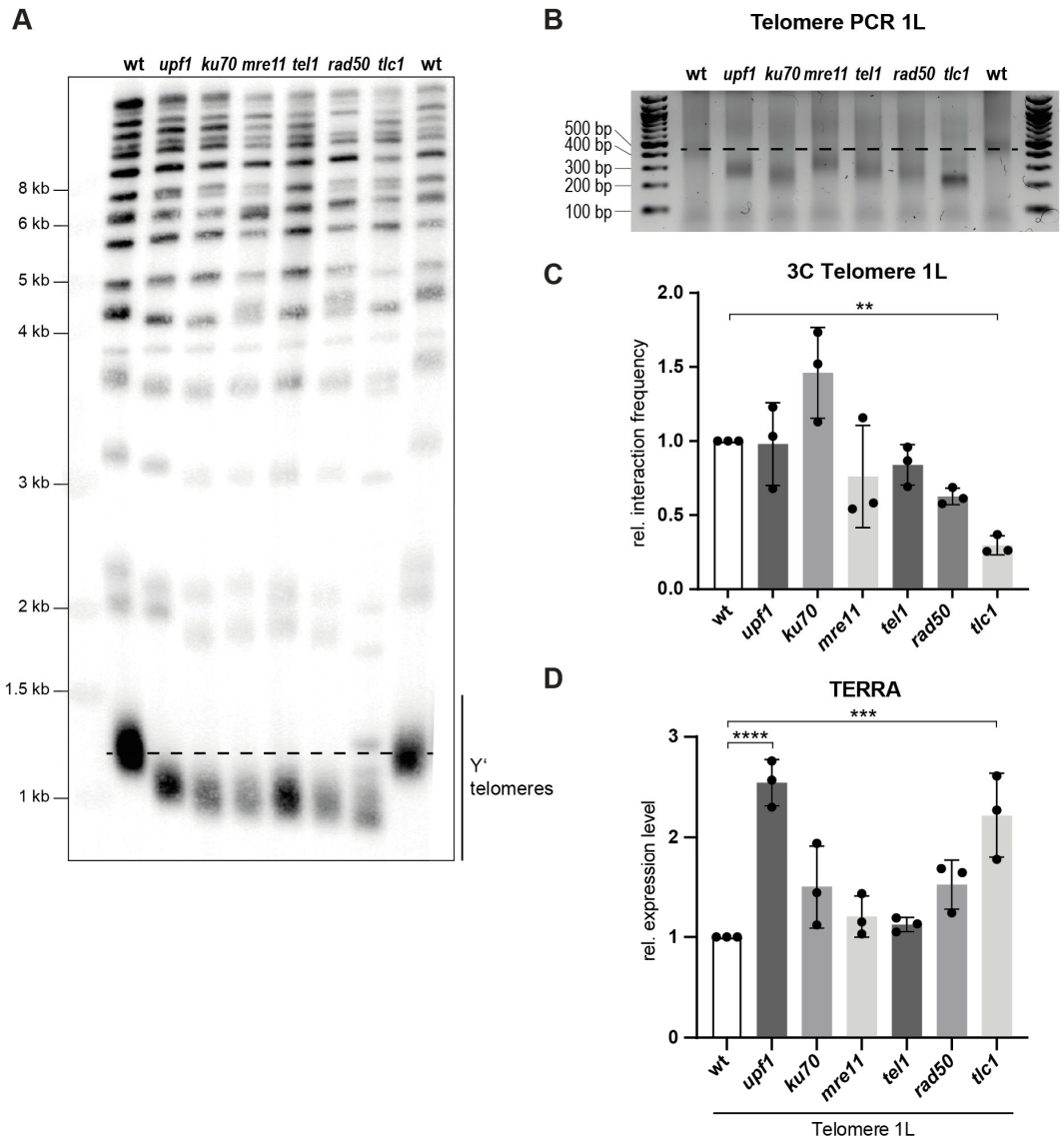

Figure 18. Short telomeres are proficient for engaging in a fold-back structure. (A) Southern blot for all telomeres of XhoI digested genomic DNA from the indicated deletion mutants using a radio-labeled (TG)n-repeat containing vector fragment as a probe. The *tlc1* mutant was analyzed at PD 40. One representative sample for each genotype is shown. The dashed line indicates wt telomere length of Y' telomeres. **(B)** Telomere PCR for the length of telomere 1L in the depicted mutants. The *tlc1* mutant was analyzed at ~PD 40. Dashed line indicates the wt telomere length. **(C)** Telo-3C analysis of the displayed mutants. The *tlc1* mutant was analyzed at ~PD 40. The interaction frequencies between the primers P5 and P6 are shown. All interaction frequencies were normalized to a control qPCR product. Relative interaction frequencies were calculated by setting the normalized interaction frequency of the wt to 1. Mean +/- SD of 3 independent experiments. Adjusted p-values were obtained from one-way ANOVA with Dunnett's multiple comparison test (**p ≤ 0.01). **(D)** TERRA levels from telomere 1L in the displayed mutants. TERRA levels were normalized to Actin RNA levels. Relative TERRA expression levels were calculated by setting the normalized TERRA expression of wt cells to 1. The *tlc1* mutant was analyzed at ~PD 40. Mean +/- SD of 3 experiments. Adjusted p-values were obtained from one-way ANOVA with Dunnetts multiple comparison test (***p ≤ 0.001, ****p ≤ 0.0001).

Taken together, I observed that critically short telomeres cannot maintain a folded structure during replicative senescence and adopt an open conformation. In contrast, telomere folding is re-established in post-senescence survivors. By analyzing telomere folding in a set of mutants with stable short telomeres, I demonstrated that short telomeres are proficient in adopting a folded conformation.

2.3.3 Histone deacetylases are potential regulators of telomere folding during replicative senescence

As previously shown in this thesis, telomere folding is compromised in senescent cells (Figure 17C) and the unfolding of telomeres during crisis does not depend on telomere length (Figure 18). In order to understand the mechanisms underlying these structural changes, we analyzed the whole proteome of *tlc1* cells at telomeric crisis and compared it to wt cells. Lara Perez Martinez (Butter lab, IMB Mainz) performed label-free quantitative proteomics analysis which revealed 751 significantly downregulated and 678 upregulated proteins during senescence (Figure 19A). Merve Öztürk (Butter lab, IMB Mainz) processed the data and performed the bioinformatics analysis providing a comprehensive list of all identified proteins whose levels significantly changed during senescence as a function of their log2 fold change (Figure 25, Appendix). The significantly enriched gene ontology (GO) terms for biological processes for both up- and downregulated proteins were analyzed and are displayed in Figure 26 (Appendix). Enriched GO terms of the downregulated proteins include RNA processing (primarily ribosomal RNAs), ribosome localization, chromatin and nucleosome disassembly. The GO terms enriched in the upregulated proteins include metabolic energy producing processes, ATP synthesis and metabolism supporting the notion that senescent cells change their metabolic program (Nautiyal et al. 2002). As previously reported by Nautiyal et al., the DNA repair protein Rad51 was upregulated during senescence and the subunits of the ribonucleotide-diphosphate reductase (Rnr2, Rnr3 and Rnr4) are among the upregulated proteins, that show the highest fold-change (Nautiyal et al. 2002).

To identify candidates that potentially regulate telomere folding during senescence, we took advantage of a screen for regulators of telomere folding in *S. cerevisiae* (Poschke et al. 2012). We compared the telomere folding defective candidates from this screen to all significantly downregulated proteins from our newly generated proteomics data set. The published screen, using a telomere folding reporter gene (Poschke et al. 2012), identified 113 genes and *sir2* was manually added to this list. The *sir2* knockout cannot be included in genetic screens due to its mating deficiency, however, it is well established, that the SIR complex promotes telomere folding (de Bruin et al. 2001; de Bruin et al. 2000; Zaman et al. 2002). We found 21 overlapping candidates between the fold-back defective mutants and the downregulated proteins during senescence (Figure 19B, C). This suggests that a reduced availability of any of these candidates might contribute to the fact that telomeres cannot maintain a folded state during senescence. From all 751 downregulated proteins during senescence, the 21 overlapping candidates were significantly enriched for the GO terms of protein and histone deacetylation (Figure 19D). As highlighted in the

heat map four out of 21 potential regulators are histone deacetylases (bold in **Figure 19C**), suggesting an epigenetic mechanism underlying telomere folding regulation during senescence.

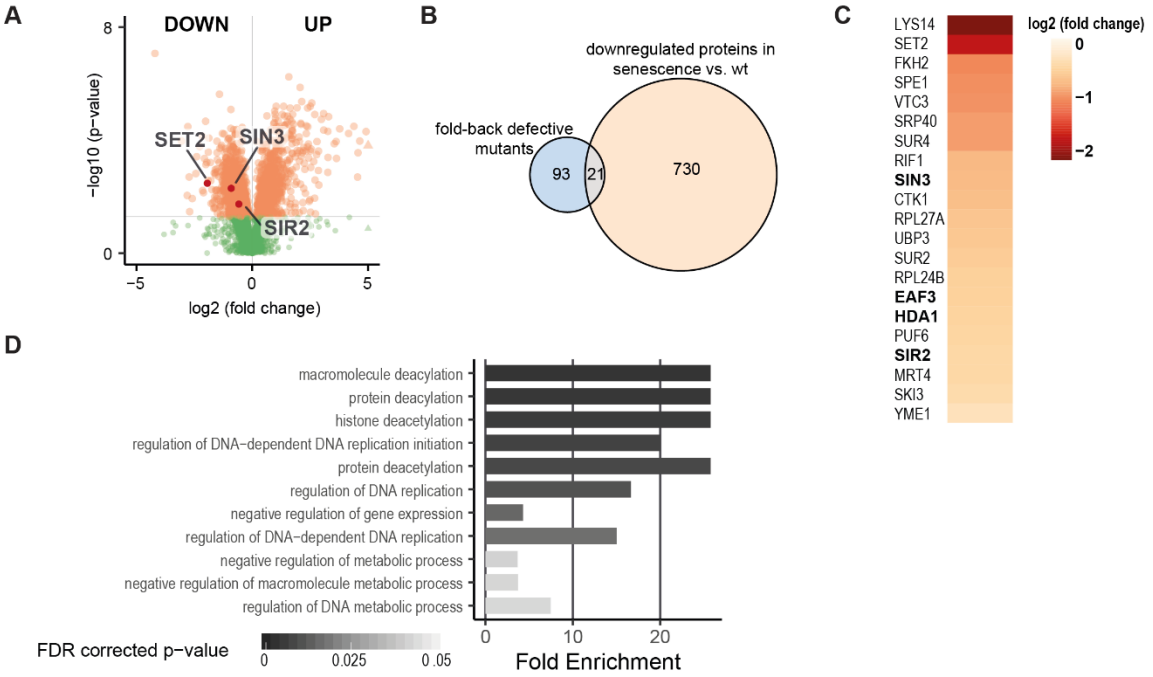

Figure 19. Histone deacetylases are potential regulators of telomere folding during replicative senescence. (A) Volcano plot for up- and downregulated proteins when comparing whole protein extracts from senescent cells (*tlc1*) and extracts from wt cells using label-free quantitative proteomics. Significantly changed proteins are shown in orange (p-value ≤ 0.05). **(B)** Venn diagram of genes/proteins overlapping between downregulated proteins in senescent cells (*tlc1*) and mutants defective for telomere folding as described in Poschke et al. 2012. *sir2* was manually included in the list of fold-back defective mutants. **(C)** Heatmap of the 21 overlapping candidates from **Figure 19B** and the log2 of their fold change during senescence as compared to wt. Histone deacetylases are shown in bold letters. **(D)** Results from gene ontology analysis for molecular function of the 21 overlapping candidate genes from **Figure 19B**. Shown are GO terms with p-values below 0.05. *sir2* was included in the list of fold-back defective mutants. The mass spectrometry analysis was performed by Lara Perez Martinez (Butter lab, IMB Mainz) and the data was processed and analyzed by Merve Öztürk (Butter lab, IMB Mainz).

2.3.4 The Loss of Sir2, Sin3 and Set2 contribute to telomere opening in senescence

From the 21 overlapping candidates (**Figure 19B, C**), the proteins Sir2, Sin3 and Set2 were of special interest as they antagonize histone acetylation and were reported to be involved in telomere silencing or the regulation of the telomeric chromatin state (Cockell et al. 1995; Gottschling et al. 1990; Imai et al. 2000; Rundlett et al. 1996; Sun & Hampsey 1999; Vannier et al. 1996; Rubertis et al. 1996; Keogh et al. 2005). Telo-3C analysis of these histone modifiers revealed that cells lacking either *SIR2, SIN3* or *SET2* show decreased telomere folding (**Figure 20A**). I confirmed our mass spectrometry results by western blot using epitope-tagged *SIN3-TAP* (tandem affinity purification) and *SET2-TAP* alleles and observed the downregulation of Sin3 and Set2 as well as Sir2 during senescence (*tlc1*) (**Figure 20B, C**). In contrast, their protein levels were comparable to wt in pre-senescent cells and post-senescent survivors (**Figure 20B, C**). Of note, I observed a strong increase in a modified Sir2 species in senescent cells. This suggests a specific regulation of Sir2's activity,

localization or stability within the senescence program (Figure 20B). The telomere length of mutants lacking *SIR2* or *SET2* was similar to wt and slightly shorter in the *sin3* mutant as shown in the telomere restriction fragment analysis (Figure 20D, uncropped blot in Figure 27, Appendix). This observation further supports my previous conclusion that the telomere folding state is not coupled to telomere length and *vice versa*. I was interested to analyze TERRA levels from telomere 1L in these mutants and thereby gain insight into their telomere silencing state. Subtelomeres of cells lacking *SIR2* were desilenced and TERRA levels were ~10 times higher than wt (Figure 20E). Even though I did not observe this increase to be statistically significant, this finding is in line with a previous report by Iglesias et al. (Iglesias et al. 2011). As expected, TERRA levels were increased in telomerase negative cells (*tlc1*) in comparison to wt cells (Graf et al. 2017) (Figure 20E). However, this increase was not homogenous due to the fact that critically short telomeres, which are the source of high TERRA levels, arise stochastically during senescence (Graf et al. 2017). In *sin3* and *set2* mutants TERRA levels were only slightly elevated (Figure 20E). Thus, at this point there is not enough evidence to correlate the decreased telomere folding in *sir2, sin3* and *set2* mutants with a desilencing of their telomeres. Nonetheless, telomere folding might affect TERRA levels.

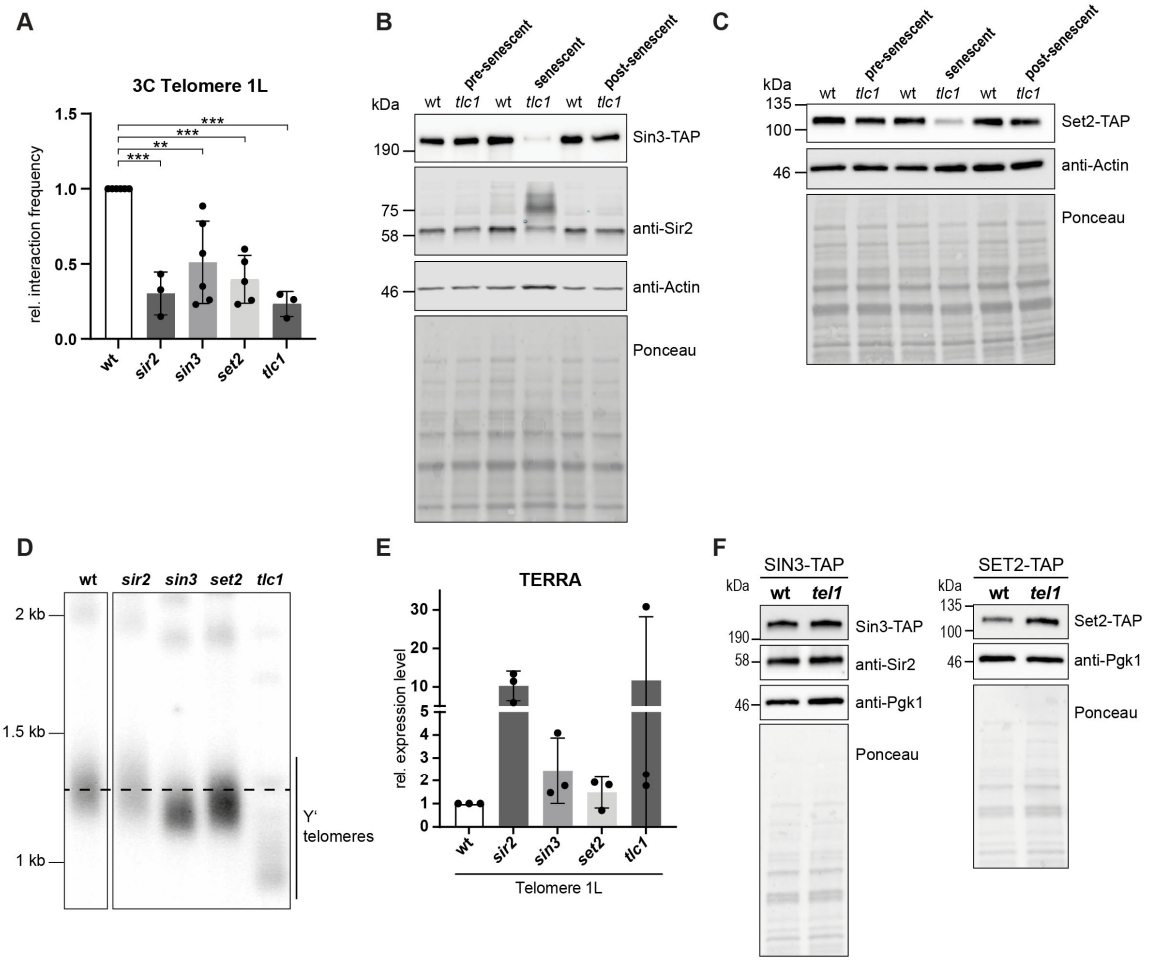

Figure 20. Loss of Sir2, Sin3 and Set2 contribute to telomere opening in senescence. (A) Telo-3C analysis in *sir2, sin3*, *set2* and *tlc1* mutants using the primers P5 and P6. All interaction frequencies were normalized to a control qPCR product. Relative interaction frequencies were calculated by setting the normalized interaction frequency of the wt to 1. Mean +/- SD of 3-6 independent experiments. For *sir2* and *tlc1* mutants adjusted p-values were obtained from one-way ANOVA with Dunnetts multiple comparison test. For *sin3* and *set2* mutants adjusted p-values were obtained from unpaired t-tests (**p ≤ 0.01, ***p ≤ 0.001). **(B)** Western blot for TAP-tagged Sin3, as well as Sir2 levels in pre-senescent (~PD 28), senescent (~PD 46) and post-senescent (~PD 62) cells. Endogenously tagged Sin3-TAP was detected using the PAP antibody. Sir2 levels were visualized using an anti-Sir2 antibody. Sir2 and the respective Actin loading control were visualized with fluorescent secondary antibodies. The Sin3-TAP western blot was developed using an HRP-coupled primary antibody. **(C)** Western blot for TAP-tagged Set2 levels in pre-senescent (~PD 28), senescent (~PD 46) and post-senescent (~PD 62) cells. The anti-Actin antibody and Ponceau staining served as loading controls. The western blots were developed using HRP-coupled antibodies. **(D)** Cropped Southern blot for all telomeres using a (TG)n-repeat containing vector fragment labeled with ^{32}P as a probe. Dashed line indicates the wt telomere length. The complete blot is shown in **Figure 27**. **(E)** TERRA levels from telomere 1L in in *sir2, sin3*, *set2* and *tlc1* mutants. TERRA levels were normalized to Actin RNA levels. Relative TERRA expression levels were calculated by setting the normalized TERRA expression of wt cells to 1. TERRA levels of the depicted mutants are not significantly different from wt. Mean +/- SD of 3 experiments. Adjusted p-values were obtained from one-way ANOVA with Dunnetts multiple comparison test. No significant changes in TERRA levels were observed. **(F)** Western blot of TAP-tagged Sin3 and Set2, as well as Sir2 levels in *tel1* mutants. Endogenously tagged Sin3-TAP and Set2-TAP were detected using the PAP antibody. Sir2 levels were visualized using an anti-Sir2 antibody. The anti-Pgk1 antibody and Ponceau staining served as loading controls.

I showed here, that Sir2, Sin3 and Set2 are involved in the regulation of telomere folding. The levels of these histone modifiers were downregulated during senescence, which correlates with the unfolding of telomeres. Interestingly, Sir2, Sin3 and Set2 protein levels were not downregulated in a *tel1* mutant with very short telomeres which was able to establish a telomere fold-back

comparable to wt cells (Figure 20F, Figure 18C). This observation supports my hypothesis, that telomere folding is reduced during senescence due to components of the senescence program, but it is not caused by telomere shortening *per se.* Telomere folding might require a specific heterochromatic environment of the subtelomere. Perturbations of histone modification may be the reason for the structural changes that occur at telomeres throughout senescence.

2.3.5 Overexpression of Sin3 during senescence does not prevent telomeres from opening during senescence

Having identified three potential regulators of telomere folding during senescence, Sir2, Sin3 and Set2, I wanted to test if they are directly involved in the opening of telomere folding during senescence. In order to do this, I chose to overexpress the candidate Sin3 during senescence. According to my hypothesis, overexpressing Sin3 at the point during senescence when Sin3 levels are low would prevent telomere folding from opening at the point of crisis. For this experiment I used a high copy number 2µ plasmid bearing the *SIN3-TAP* construct under the control of a galactose-inducible promoter (pGAL). I noticed that the Sin3 protein load produced by the constitutive overexpression in galactose-containing media was toxic to cells. When Sin3 overexpressing cells were propagated for more than 24 h, their viability drastically decreased, and the analysis of these cells was not possible (data not shown). For this reason, I propagated telomerase negative *tlc1* cells carrying empty vector (EV) or a plasmid for Sin3 overexpression (pGal-SIN3-TAP) in glucose-containing media, which suppressed the Sin3 expression. As expected, the presence of these plasmids under non-inducing conditions did not affect the senescence rate (Figure 21A). The senescence associated loss of viability of one culture (blue in Figure 21A; *tlc1* + EV) was premature compared to the other *tlc1* samples. This is not unusual as senescence is a stochastic process and its progression can be slightly different between clones. For the analysis of telomere folding upon Sin3 overexpression, I chose both pre-senescent and senescent cells during the time course (grey boxes in Figure 21A). Starting from a saturated culture in glucose-containing media, the glucose was washed out from the media and cells were brought into exponential phase in raffinose-containing media (Figure 21B). As soon as the cells had undergone two division cycles, Sin3 overexpression was induced for 2 h by adding galactose to the media (Figure 21B). Western blotting for Sin3-TAP confirmed that the degree of overexpression was comparable in the pre-senescent and senescent *tlc1* cells as well as in wt cultures (Figure 21C). As previously shown, pre-senescent *tlc1* cells were proficient for telomere folding (Figure 17C). In line with this, the relative Telo-3C interaction frequency of *tlc1* cells carrying either EV or pGAL-SIN3-TAP did not differ from wt cells with either of the plasmids in pre-senescence (Figure 21D). Telo-3C analysis in senescent *tlc1* cells revealed that telomere folding was equally reduced in both EV and pGal-SIN3-TAP samples

(Figure 21D). These data demonstrate that the overexpression of Sin3 for 2 h was neither sufficient to prevent the opening of the telomere fold-back structure nor to re-establish telomere folding during senescence. Therefore, I suggest that either the duration of Sin3 overexpression was not long enough or that the presence of Sin3 alone might not be sufficient for the establishment of a folded structure. These results led me to the conclusion that Sin3 acts in conjunction with other telomere folding regulators, possibly Sir2 and Set2, and likely acts in a complex network of the senescence program including other factors.

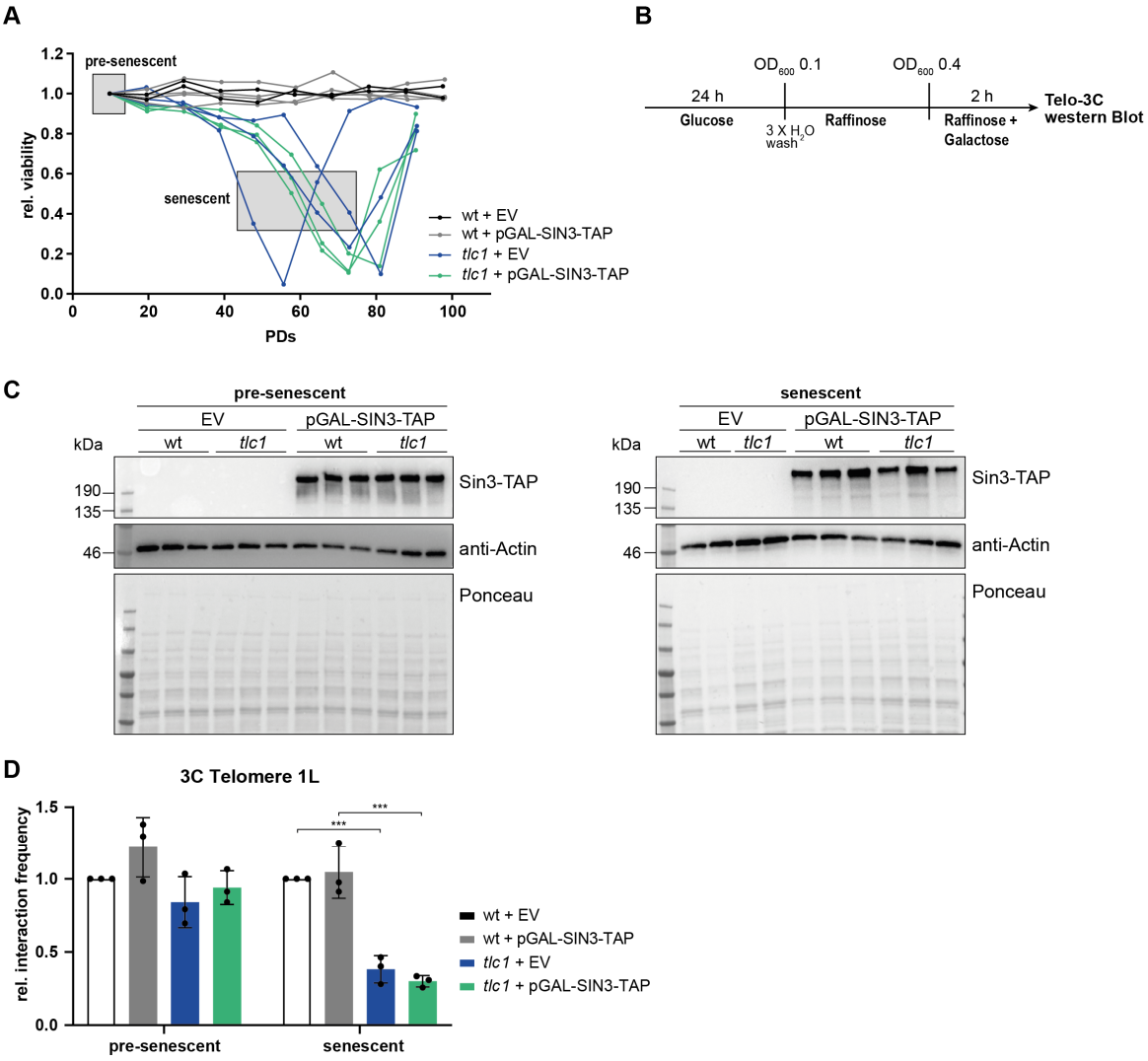

Figure 21. Overexpression of Sin3 during senescence does not prevent telomeres from opening during senescence. (A) wt and *tlc1* cells were transformed with empty vector (EV) or a plasmid containing the *SIN3* gene fused to a TAP-tag under the control of a galactose inducible promoter (pGAL-SIN3-TAP). The relative viability of 3 independent cultures for each genotype was followed over time. Samples of pre-senescent and senescent cells were collected at the indicated time points (grey box). Cells were propagated in SC-URA media with 2 % glucose, repressing the expression of Sin3-TAP from the plasmid. **(B)** Schematic representation of the experimental setup. After growing the cells in glucose containing media for 24 h, the glucose was washed out and the cells were diluted to OD_{600} 0.1 in raffinose containing media. When the culture reached OD_{600} 0.4 Sin3 overexpression was induced by adding galactose (2%) to the media. Samples for Telo-3C and western blot were collected after 2 h of Sin3 overexpression. **(C)** Western blot for Sin3-TAP protein levels in pre-senescent and senescent cells upon 2 h of Sin3 overexpression. Sin3-TAP was detected using the PAP antibody. An anti-Actin western blot and Ponceau staining are shown as loading controls. **(D)** Telo-3C analysis in the indicated samples from pre-senescent and senescent time points (Figure 21A) using the primers P5 and P6. All interaction frequencies were

normalized to a control qPCR product. Relative interaction frequencies were calculated by setting the normalized interaction frequency of pre-senescent or senescent wt cells containing EV to 1 respectively (white bars). Mean +/- SD of 3 independent experiments. Adjusted p-values were obtained from two-way ANOVA with Sidak's multiple comparisons test (***p ≤ 0.001).

2.3.6 Telomeres unfold after prolonged MMS treatment

The transcriptional response of yeast cells during senescence shares many features with the transcriptional changes that cells experience upon treatment with methyl methanesulfonate (MMS) (Nautiyal et al. 2002). MMS is a DNA alkylator that induces replication fork stalling and as a result global DNA damage in the cell (Lundin et al. 2005). I tested whether the induction of DNA damage by MMS results in reduced telomere folding. To this end, an exponential culture of wt cells was exposed to 0.02 % MMS for one and two hours. This treatment resulted in the expected accumulation of cells in S phase (Figure 22A) and the activation of the DNA damage checkpoint as observed by Rad53 phosphorylation (Figure 22B). Interestingly, I observed that fold-back structures at telomere 1L were formed less frequently upon MMS treatment, and this effect became more pronounced over time (Figure 22C). During replicative senescence, the DDR at the telomere induces a cell cycle arrest. Similarly, exposing cells to MMS, a DNA damaging agent that acts genome wide, also results in an open telomere state. However, in contrast to telomerase negative cells during crisis, the protein levels of the telomere folding regulators Sir2, Sin3 and Set2 were not drastically altered upon prolonged MMS treatment (Figure 22D). For this reason, I hypothesize that telomere folding regulation upon MMS treatment might be different from replicative senescence.

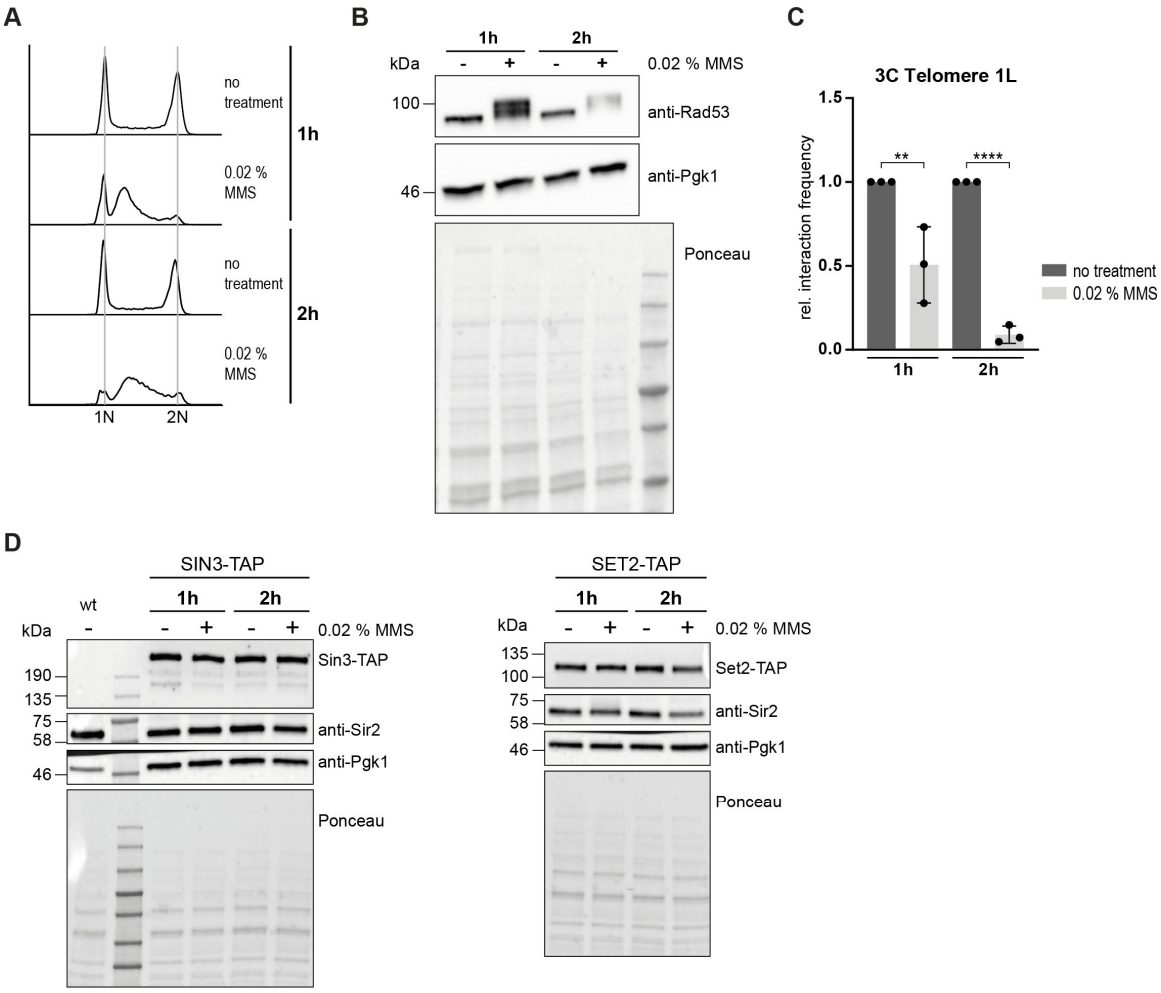

Figure 22. Telomeres unfold after prolonged MMS treatment. (A) Flow cytometry histograms for DNA content of wt cells either treated with 0.02 % MMS for 1 h or 2 h or left untreated. One representative sample per condition is shown. **(B)** Western blot to detect Rad53 phosphorylation using an anti-Rad53 antibody. The anti-Pgk1 antibody and Ponceau staining served as loading controls. **(C)** Telo-3C analysis of wt cells after 1 h or 2 h of MMS treatment (0.02 %). The interaction frequencies between the primers P5 and P6 are shown. All interaction frequencies were normalized to a control qPCR product. Relative interaction frequencies were calculated by setting the normalized interaction frequency of the untreated samples to 1. Mean +/- SD of 3 independent experiments. Adjusted p-values were obtained from two-way ANOVA with Sidak's multiple comparison test (**p ≤ 0.01, ****p ≤ 0.0001). **(D)** Western blot for endogenously tagged Sin3-TAP and Set2-TAP protein levels after cells were either treated with 0.02 % MMS for 1 h or 2 h or left untreated. Sin3-TAP or Set2-TAP were detected using the PAP antibody. Sir2 protein levels were detected using an anti-Sir2 antibody. Anti-Pgk1 western blot and Ponceau staining are shown as loading controls.

2.3.7 The absence of either Sin3, Set2 or Sir2 does not affect the protein levels of the respective other factors

Having identified Sir2, Sin3 and Set2 as regulators of telomere folding and players during replicative senescence, I aimed to gain insight into how these histone modifiers might influence each other. To this end, I analyzed their protein levels in the absence of the respective other factors. By western blotting I found that endogenously tagged Sin3-TAP protein levels were not drastically altered in *set2* or *sir2* mutants (**Figure 23A**) and endogenously tagged Set2-TAP levels were comparable to wt in *sin3* or *sir2* cells (**Figure 23B**). Similarly, endogenous Sir2 protein levels did not differ in cells

lacking *SIN3* or *SET2* (Figure 23C). These data suggest that the absence of either Sir2, Sin3 or Set2 does not affect the other factors' protein levels. Therefore, I propose the hypothesis that the downregulation of these factors during senescence might also be independent from each other. The lack of one of the factors is most likely not the cause for the decrease of the others. However, their behavior through the progression of senescence might be different from the situation in wt cells. Yet, with these western blot experiments subtle changes in protein levels might remain undetected. Additionally, I cannot draw any conclusion about the activity and localization of Sir2, Sin3 and Set2, since information about their ability to bind to telomeres in the respective knockout mutants is lacking.

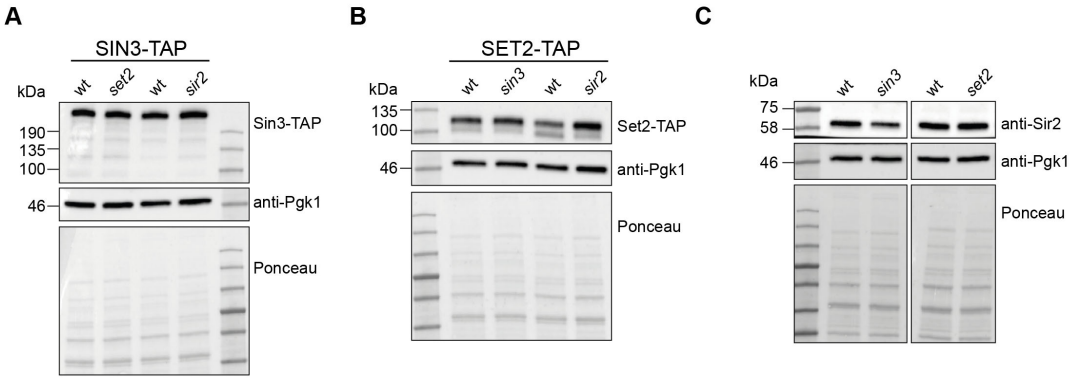

Figure 23. The absence of either Sin3, Set2 or Sir2 does not affect the protein levels of the respective other factors. (A) Western blot for Sin3 protein levels in *set2* and *sir2* mutants. Endogenously tagged Sin3-TAP was detected using the PAP antibody. The anti-Pgk1 antibody and Ponceau staining served as loading controls. **(B)** Western blot for Set2 protein levels in *sin3* and *sir2* mutants. Endogenously tagged Set2-TAP was detected using the PAP antibody. The anti-Pgk1 antibody and Ponceau staining served as loading controls. **(C)** Western blot for Sir2 protein levels in *sin3* and *set2* mutants. Sir2 was detected using an anti-Sir2 antibody. The anti-Pgk1 antibody and Ponceau staining served as loading controls.

2.4 Investigating the function of telomere folding

2.4.1 The opening of telomere folding does not result in more telomere-telomere fusions

I was interested in understanding the functional consequences of reduced telomere folding and if the opening of the folded telomere structure might lead to a higher incidence of non-homologous end joining (NHEJ) between telomeres. This analysis was performed by Marta Barrientos-Moreno in collaboration with the Prado lab (CABIMER, Seville, Spain). By quantitative PCR for telomere-telomere fusions (T-TFs) between chromosomes V and XV (**Figure 24A**) (Mieczkowski et al. 2003) we addressed how frequently T-TFs occur in *sir2, sin3* and *set2* mutants, where telomere folding is defective. The T-TF accumulating strain *mec1 tel1 sml1* served as a positive control (**Figure 24B**) (Craven et al. 2002; Chan & Blackburn 2003; Mieczkowski et al. 2003). In contrast, the telomeres of *sir2, sin3* or *set2* mutants did not undergo T-TFs more frequently than wt cells (**Figure 24B**). Also telomerase negative cells (*tlc1*) from liquid cultures of approximately PD 30 did not present more T-TFs and the double mutants of *sir2, sin3* and *set2* in combination with *TLC1* knockout showed similar T-TFs frequencies as wt cells (**Figure 24B**). Additionally, we aimed to analyze the impact of the absence of *SIN3* and *SET2* in a scenario when T-TFs drastically accumulate, in a *mec1 tel1 sml1* background. We found that the depletion of *SIN3* or *SET2* from these cells does not further increase the incidence of chromosome end fusions (**Figure 24C**), supporting a model where an unfolded telomere conformation does not render the telomere more accessible for NHEJ. Chromosome ends did also not present an increased incidence of T-TFs upon the depletion of the checkpoint kinase Rad53 (**Figure 24D**), where telomere folding was drastically decreased (**Figure 16D**). Similarly, when depleting Rad53 in a telomerase negative situation (*tlc1*), T-TF levels were not elevated (**Figure 24D**).

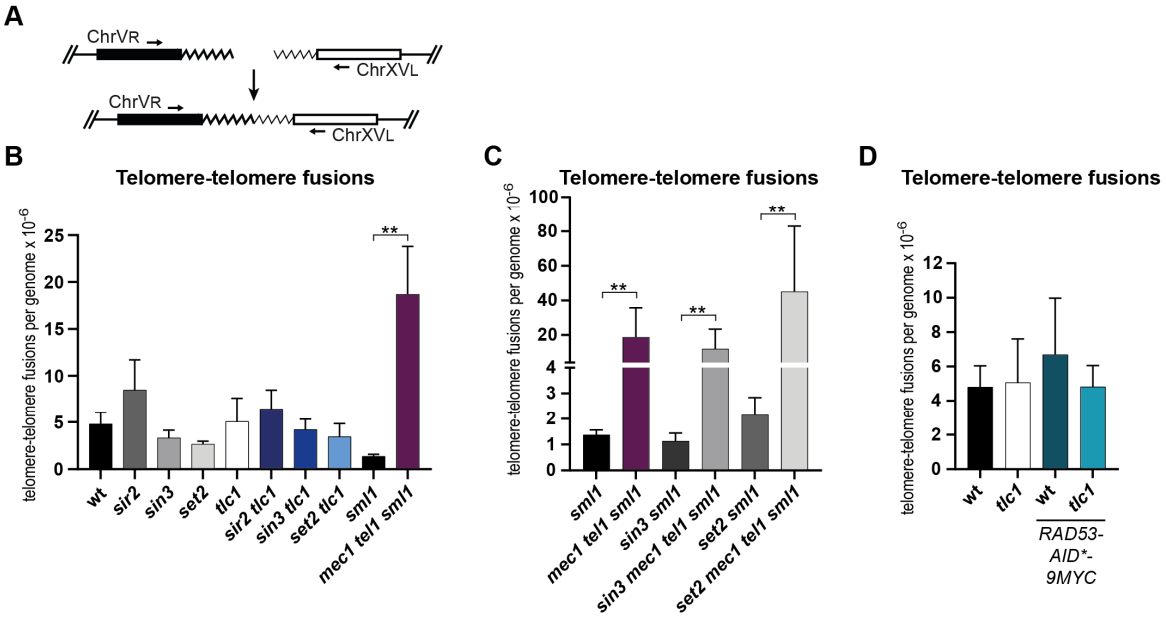

Figure 24. The opening of telomere folding does not result in more telomere-telomere fusions (T-TFs). (A) Scheme of the PCR assay to follow the accumulation of T-TFs between chromosome V and XV. Telomeres are depicted in a zig-zag pattern and primers are shown as arrows. **(B)** Quantitative T-TF frequency analysis of the indicated strains from liquid cultures of ~PD 30. Mean +/- SEM of 3-11 samples. P-value was obtained from Mann-Whitney test (**p ≤ 0.01). **(C)** Quantitative T-TF frequency analysis of the indicated strains from liquid cultures of ~PD 30. Mean +/- SEM of 3-11 samples. P-values were obtained from Mann-Whitney test (**p ≤ 0.01). **(D)** Quantitative T-TF frequency analysis after Rad53 was depleted for 2 h using 1 mM IAA in the strains bearing *RAD53-AID*-9MYC* (see **Figure 16B, C**). Mean +/- SEM of 4-5 samples. P-values were obtained from Mann-Whitney test (**p ≤ 0.01) and no significant differences were detected. These experiment were performed by Marta Barrientos-Moreno (Prado Lab, CABIMER, Seville, Spain).

In summary, we showed that decreased folding of yeast telomeres does not make them more susceptible to NHEJ. These data suggest that a folded telomere structure does not additionally protect chromosome ends from fusing, even in a scenario when telomeres are prone to fuse and cells accumulate large amounts of chromosome end fusions.

3 Appendix

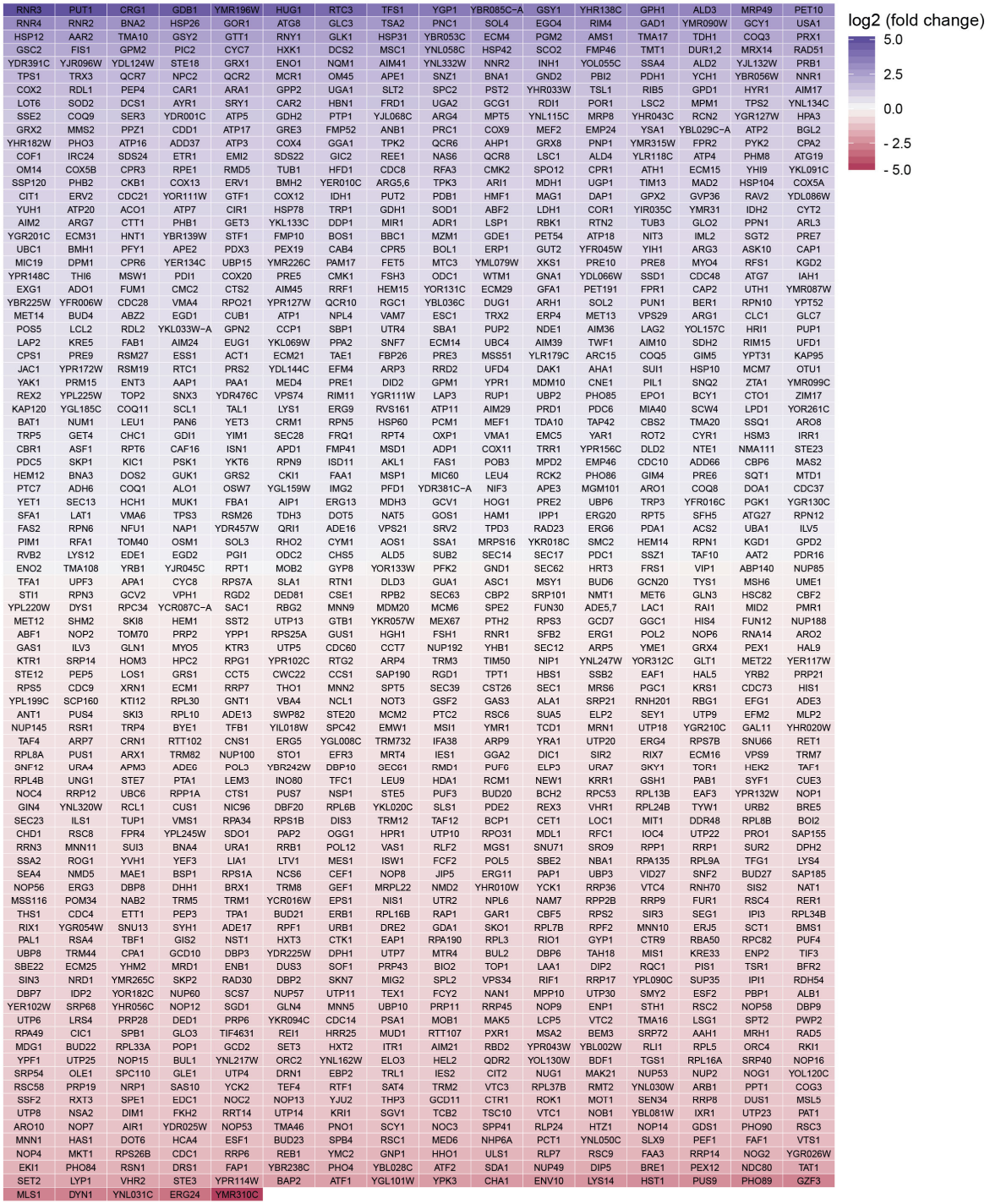

RNR3	PUT1	CRG1	GDB1	YMR196W	HUG1	RTC3	TFS1	YGP1	YBR085C-A	GSY1	YHR138C	GPH1	ALD3	MRP49	PET10
RNR4	RNR2	BNA2	HSP26	GOR1	ATG8	GLC3	TSA2	PNC1	SOL4	EGO4	RIM4	GAD1	YMR090W	GCY1	USA1
HSP12	AAR2	TMA10	GSY2	GTT1	RNY1	GLK1	HSP31	YBR053C	ECM4	PGM2	AMS1	TMA17	TDH1	COQ3	PRX1
GSC2	FIS1	GPM2	PIC2	CYC7	HXK1	DCS2	MSC1	YNL058C	HSP42	SCO2	FMP46	TMT1	DUR1,2	MRX14	RAD51
YDR391C	YJR096W	YDL124W	STE18	GRX1	ENO1	NQM1	AIM41	YNL332W	NNR2	INH1	YOL055C	SSA4	ALD2	YJL132W	PRB1
TPS1	TRX3	QCR7	NPC2	QCR2	MCR1	OM45	APE1	SNZ1	BNA1	GND2	PBI2	PDH1	YCH1	YBR056W	NNR1
COX2	RDL1	PEP4	CAR1	ARA1	GPP2	UGA1	SLT2	SPC2	PST2	YHR033W	TSL1	RIB5	GPD1	HYR1	AIM17
LOT6	SOD2	DCS1	AYR1	SRY1	CAR2	HBN1	FRD1	UGA2	GCG1	RDI1	POR1	LSC2	MPM1	TPS2	YNL134C
SSE2	COQ9	SER3	YDR001C	ATP5	GDH2	PTP1	YJL068C	ARG4	MPT5	YNL115C	MRP8	YHR043C	RCN2	YGR127W	HPA3
GRX2	MMS2	PPZ1	CDD1	ATP17	GRE3	FMP52	ANB1	PRC1	COX9	MEF2	EMP24	YSA1	YBL029C-A	ATP2	BGL2
YHR182W	PHO3	ATP16	ADD37	ATP3	COX4	GGA1	TPK2	QCR6	AHP1	GRX8	PNP1	YMR315W	FPR2	PYK2	CPA2
COF1	IRC24	SDS24	ETR1	EMI2	SDS22	GIC2	REE1	NAS6	QCR8	LSC1	ALD4	YLR118C	ATP4	PHM8	ATG19
OM14	COX5B	CPR3	RPE1	RMD5	TUB1	HFD1	CDC8	RFA3	CMK2	SPO12	CPR1	ATH1	ECM15	YHI9	YKL091C
SSP120	PHB2	CKB1	COX13	ERV1	BMH2	YER010C	ARG5,6	TPK3	ARI1	MDH1	UGP1	TIM13	MAD2	HSP104	COX5A
CIT1	ERV2	CDC21	YOR111W	GTF1	COX12	IDH1	PUT2	PDB1	HMF1	MAG1	DAP1	GPX2	GVP36	RAV2	YDL086W
YUH1	ATP20	ACO1	ATP7	CIR1	HSP78	TRP1	GDH1	SOD1	ABF2	LDH1	COR1	YIR035C	YMR31	IDH2	CYT2
AIM2	ARG7	CTT1	PHB1	GET3	YKL133C	DDP1	MIR1	ADR1	LSP1	RBK1	RTN2	TUB3	GLO2	PPN1	ARL3
YGR201C	ECM31	HNT1	YBR139W	STF1	FMP10	BOS1	BBC1	MZM1	GDE1	PET54	ATP18	NIT3	IML2	SGT2	PRE7
UBC1	BMH1	PFY1	APE2	PDX3	PEX19	CAB4	CPR5	BOL1	ERP1	GUT2	YFR045W	YIH1	ARG3	ASK10	CAP1
MIC19	DPM1	CPR6	YER134C	UBP15	YMR226C	PAM17	FET5	MTC3	YML079W	XKS1	PRE10	PRE8	MYO4	RFS1	KGD2
YPR148C	THI6	MSW1	PDI1	COX20	PRE5	CMK1	FSH3	ODC1	WTM1	GNA1	YDL066W	SSD1	CDC48	ATG7	IAH1
EXG1	ADO1	FUM1	CMC2	CTS2	AIM45	RRF1	HEM15	YOR131C	ECM29	GFA1	PET191	FPR1	CAP2	UTH1	YMR087W
YBR225W	YFR006W	CDC28	VMA4	RPO21	YPR127W	QCR10	RGC1	YBL036C	DUG1	ARH1	SOL2	PUN1	BER1	RPN10	YPT52
MET14	BUD4	ABZ2	EGD1	CUB1	ATP1	NPL4	VAM7	ESC1	TRX2	ERP4	MET13	VPS29	ARG1	CLC1	GLC7
POS5	LCL2	RDL2	YKL033W-A	GPN2	CCP1	SBP1	UTR4	SBA1	PUP2	NDE1	AIM36	LAG2	YOL157C	HRI1	PUP1
LAP2	KRE5	FAB1	AIM24	EUG1	YKL069W	PPA2	SNF7	ECM14	UBC4	AIM39	TWF1	AIM10	SDH2	RIM15	UFD1
CPS1	PRE9	RSM27	ESS1	ACT1	ECM21	TAE1	FBP26	PRE3	MSS51	YLR179C	ARC15	COQ5	GIM5	YPT31	KAP95
JAC1	YPR172W	RSM19	RTC1	PRS2	YDL144C	EFM4	ARP3	RRD2	UFD4	DAK1	AHA1	SUI1	HSP10	MCM7	OTU1
YAK1	PRM15	ENT3	AAP1	PAA1	MED4	PRE1	DID2	GPM1	YPR1	MDM10	CNE1	PIL1	SNQ2	ZTA1	YMR099C
REX2	YPL225W	TOP2	SNX3	YDR476C	VPS74	RIM11	YGR111W	LAP3	RUP1	UBP2	PHO85	EPO1	BCY1	CTO1	ZIM17
KAP120	YGL185C	COQ11	SCL1	TAL1	LYS1	ERG9	RVS161	ATP11	AIM29	PRD1	PDC6	MIA40	SCW4	LPD1	YOR261C
BAT1	NUM1	LEU1	PAN6	YET3	CRM1	RPN5	HSP60	PCM1	MEF1	TDA10	TAP42	CBS2	TMA20	SSQ1	ARO8
TRP5	GET4	CHC1	GDI1	YIM1	SEC28	FRQ1	RPT4	OXP1	VMA1	EMC5	YAR1	ROT2	CYR1	HSM3	IRR1
CBR1	ASF1	RPT6	CAF16	ISN1	APD1	FMP41	MSD1	ADP1	COX11	TRR1	YPR156C	DLD2	NTE1	NMA111	STE23
PDC5	SKP1	KIC1	PSK1	YKT6	RPN9	ISD11	AKL1	FAS1	POB3	MPD2	EMP46	CDC10	ADD66	CBP6	MAS2
HEM12	BNA3	DOS2	GUK1	GRS2	CKI1	FAA1	MSP1	MIC60	LEU4	RCK2	PHO86	GIM4	PRE6	SQT1	MTD1
PTC7	ADH6	COQ1	ALO1	OSW7	YGL159W	IMG2	PFD1	YDR381C-A	NIF3	APE3	MGM101	ARO1	COQ8	DOA1	CDC37
YET1	SEC13	HCH1	MUK1	FBA1	AIP1	ERG13	MDH3	GCV1	HOG1	PRE2	UBP6	TRP3	YFR016C	PGK1	YGR130C
SFA1	LAT1	VMA6	TPS3	RSM26	TDH3	DOT5	NAT5	GOS1	HAM1	IPP1	ERG20	RPT5	SFH5	ATG27	RPN12
FAS2	RPN6	NFU1	NAP1	YDR457W	QRI1	ADE16	VPS21	SRV2	TPD3	RAD23	ERG6	PDA1	ACS2	UBA1	ILV5
PIM1	RFA1	TOM40	OSM1	SOL3	RHO2	CYM1	AOS1	SSA1	MRPS16	YKR018C	SMC2	HEM14	RPN1	KGD1	GPD2
RVB2	LYS12	EDE1	EGD2	PGI1	ODC2	CHS5	ALD5	SUB2	SEC14	SEC17	PDC1	SSZ1	TAF10	AAT2	PDR16
ENO2	TMA108	YRB1	YJR045C	RPT1	MOB2	GYP8	YOR133W	PFK2	GND1	SEC62	HRT3	FRS1	VIP1	ABP140	NUP85
TFA1	UPF3	APA1	CYC8	RPS7A	SLA1	RTN1	DLD3	GUA1	ASC1	MSY1	BUD6	GCN20	TYS1	MSH6	UME1
STI1	RPN3	GCV2	VPH1	RGD2	DED81	CSE1	RPB2	SEC63	CBP2	SRP101	NMT1	MET6	GLN3	HSC82	CBF2
YPL220W	DYS1	RPC34	YCR087C-A	SAC1	RBG2	MNN9	MDM20	MCM6	SPE2	FUN30	ADE5,7	LAC1	RAI1	MID2	PMR1
MET12	SHM2	SKI8	HEM1	SST2	UTP13	GTB1	YKR057W	MEX67	PTH2	RPS3	GCD7	GGC1	HIS4	FUN12	NUP188
ABF1	NOP2	TOM70	PRP2	YPP1	RPS25A	GUS1	HGH1	FSH1	RNR1	SFB2	ERG1	POL2	NOP6	RNA14	ARO2
GAS1	ILV3	GLN1	MYO5	KTR3	UTP5	CDC60	CCT7	NUP192	YHB1	SEC12	ARP5	YME1	GRX4	PEX1	HAL9
KTR1	SRP14	HOM3	HPC2	RPG1	YPR102C	RTG2	ARP4	TRM3	TIM50	NIP1	YNL247W	YOR312C	GLT1	MET22	YER117W
STE12	PEP5	LOS1	GRS1	CCT5	CWC22	CCS1	SAP190	RGD1	TPT1	HBS1	SSB2	EAF1	HAL5	YRB2	PRP21
RPS5	CDC9	XRN1	ECM1	RRP7	THO1	MNN2	SPT5	SEC39	CST26	SEC1	MRS6	PGC1	KRS1	CDC73	HIS1
YPL199C	SCP160	KTI12	RPL30	GNT1	VBA4	NCL1	NOT3	GSF2	GAS3	ALA1	SRP21	RNH201	RBG1	EFG1	ADE3
ANT1	PUS4	SKI3	RPL10	ADE13	SWP82	STE20	MCM2	PTC2	RSC6	SUA5	ELP2	SEY1	UTP9	EFM2	MLP2
NUP145	RSR1	TRP4	BYE1	TFB1	YIL018W	SPC42	EMW1	MSI1	YMR1	TCD1	MRN1	UTP18	YGR210C	GAL11	YHR020W
TAF4	ARP7	CRN1	RTT102	CNS1	ERG5	YGL008C	TRM732	IFA38	ARP9	YRA1	UTP20	ERG4	RPS7B	SNU66	RET1
RPL8A	PUS1	ARX1	TRM82	NUP100	STO1	EFR3	MRT4	IES1	GGA2	DIC1	SIR2	RIX7	ECM16	VPS9	TRM7
SNF12	URA4	APM3	ADE6	POL3	YBR242W	DBP10	SEC61	RMD1	PUF6	ELP3	URA7	SKY1	TOR1	HEK2	TAF1
RPL4B	UNG1	STE7	PTA1	LEM3	INO80	TFC1	LEU9	HDA1	RCM1	NEW1	KRR1	GSH1	PAB1	SYF1	CUE3
NOC4	RRP12	UBC6	RPP1A	CTS1	PUS7	NSP1	STE5	PUF3	BUD20	BCH2	RPC53	RPL13B	EAF3	YPR132W	NOP1
GIN4	YNL320W	RCL1	CUS1	NIC96	DBF20	RPL6B	YKL020C	SLS1	PDE2	REX3	VHR1	RPL24B	TYW1	URB2	BRE5
SEC23	ILS1	TUP1	VMS1	RPA34	RPS1B	DIS3	TRM12	TAF12	BCP1	CET1	LOC1	MIT1	DDR48	RPL8B	BOI2
CHD1	RSC8	FPR4	YPL245W	SDO1	PAP2	OGG1	HPR1	UTP10	RPO31	MDL1	RFC1	IOC4	UTP22	PRO1	SAP155
RRN3	MNN11	SUI3	BNA4	URA1	RRB1	POL12	VAS1	RLF2	MGS1	SNU71	SRO9	RPP1	RRP1	SUR2	DPH2
SSA2	ROG1	YVH1	YEF3	LIA1	LTV1	MES1	ISW1	FCF2	POL5	SBE2	NBA1	RPA135	RPL9A	TFG1	LYS4
SEA4	NMD5	MAE1	BSP1	RPS1A	NCS6	CEF1	NOP8	JIP5	ERG11	PAP1	UBP3	VID27	SNF2	BUD27	SAP185
NOP56	ERG3	DBP8	DHH1	BRX1	TRM8	GEF1	MRPL22	NMD2	YHR010W	YCK1	RRP36	VTC4	RNH70	SIS2	NAT1
MSS116	POM34	NAB2	TRM5	TRM1	YCR016W	EPS1	NIS1	UTR2	NPL6	NAM7	RPP2B	RRP9	FUR1	RSC4	RER1
THS1	CDC4	ETT1	PEP3	TPA1	BUD21	ERB1	RPL16B	RAP1	GAR1	CBF5	RPS2	SIR3	SEG1	IPI3	RPL34B
RIX1	YGR054W	SNU13	SYH1	ADE17	RPF1	URB1	DRE2	GDA1	SKO1	RPL7B	RPF2	MNN10	ERJ5	SCT1	BMS1
PAL1	RSA4	TBF1	GIS2	NST1	HXT3	CTK1	EAP1	RPA190	RPL3	RIO1	GYP1	CTR9	RBA50	RPC82	PUF4
UBP8	TRM44	CPA1	GCD10	DBP3	YDR225W	DPH1	UTP7	MTR4	BUL2	DBP6	TAH18	MIS1	KRE33	ENP2	TIF3
SBE22	ECM25	YHM2	MRD1	ENB1	DUS3	SOF1	PRP43	BIO2	TOP1	LAA1	DIP2	RQC1	PIS1	TSR1	BFR2
SIN3	NRD1	YMR265C	SKP2	RAD30	DBP2	SKN7	MIG2	SPL2	VPS34	RIF1	RRP17	YPL090C	SUP35	IPI1	RDH54
DBP7	IDP2	YOR182C	NUP60	SCS7	NUP57	UTP11	TEX1	FCY2	NAN1	MPP10	UTP30	SMY2	ESF2	PBP1	ALB1
YER102W	SRP68	YHR056C	NOP12	SGD1	GLN4	MNN5	UBP10	PRP11	RRP45	NOP9	ENP1	STH1	RSC2	NOP58	DBP9
UTP6	LRS4	PRP28	DED1	PRP6	YKR094C	CDC14	PSA1	MOB1	MAK5	LCP5	VTC2	TMA16	LSG1	SPT2	PWP2
RPA49	CIC1	SPB1	GLO3	TIF4631	REI1	HRR25	MUD1	RTT107	PXR1	MSA2	BEM3	SRP72	AAH1	MRH1	RAD5
MDG1	BUD22	RPL33A	POP1	GCD2	SET3	HXT2	ITR1	AIM21	RBD2	YPR043W	YBL002W	RLI1	RPL5	ORC4	RKI1
YPF1	UTP25	NOP15	BUL1	YNL217W	ORC2	YNL162W	ELO3	HEL2	QDR2	YOL130W	BDF1	TGS1	RPL16A	SRP40	NOP16
SRP54	OLE1	SPC110	GLE1	UTP4	DRN1	EBP2	TRL1	IES2	CIT2	NUG1	MAK21	NUP53	NUP2	NOG1	YOL120C
RSC58	PRP19	NRP1	SAS10	YCK2	TEF4	RTF1	SAT4	TRM2	VTC3	RPL37B	RMT2	YNL030W	ARB1	PPT1	COG3
SSF2	RXT3	SPE1	EDC1	NOC2	NOP13	YJU2	THP3	GCD11	CTR1	ROK1	MOT1	SEN34	RRP8	DUS1	MSL5
UTP8	NSA2	DIM1	FKH2	RRT14	UTP14	KRI1	SGV1	TCB2	TSC10	VTC1	NOB1	YBL081W	IXR1	UTP23	PAT1
ARO10	NOP7	AIR1	YDR025W	NOP53	TMA46	PNO1	SCY1	NOC3	SPP41	RLP24	HTZ1	NOP14	GDS1	PHO90	RSC3
MNN1	HAS1	DOT6	HCA4	ESF1	BUD23	SPB4	RSC1	MED6	NHP6A	PCT1	YNL050C	SLX9	PEF1	FAF1	VTS1
NOP4	MKT1	RPS26B	CDC1	RRP6	REB1	YMC2	GNP1	HHO1	ULS1	RLP7	RSC9	FAA3	RRP14	NOG2	YGR026W
EKI1	PHO84	RSN1	DRS1	FAP1	YBR238C	PHO4	YBL028C	ATF2	SDA1	NUP49	DIP5	BRE1	PEX12	NDC80	TAT1
SET2	LYP1	VHR2	STE3	YPR114W	BAP2	ATF1	YGL101W	YPK3	CHA1	ENV10	LYS14	HST1	PUS9	PHO89	GZF3
MLS1	DYN1	YNL031C	ERG24	YMR310C											

Figure 25. List of all significantly up- or downregulated proteins in *tlc1* versus wt cells ($p \leq 0.05$) with log2 fold change (blue: upregulated; red: downregulated). Bioinformatics analysis was performed and figure was provided by Merve Öztürk (Butter lab, IMB Mainz).

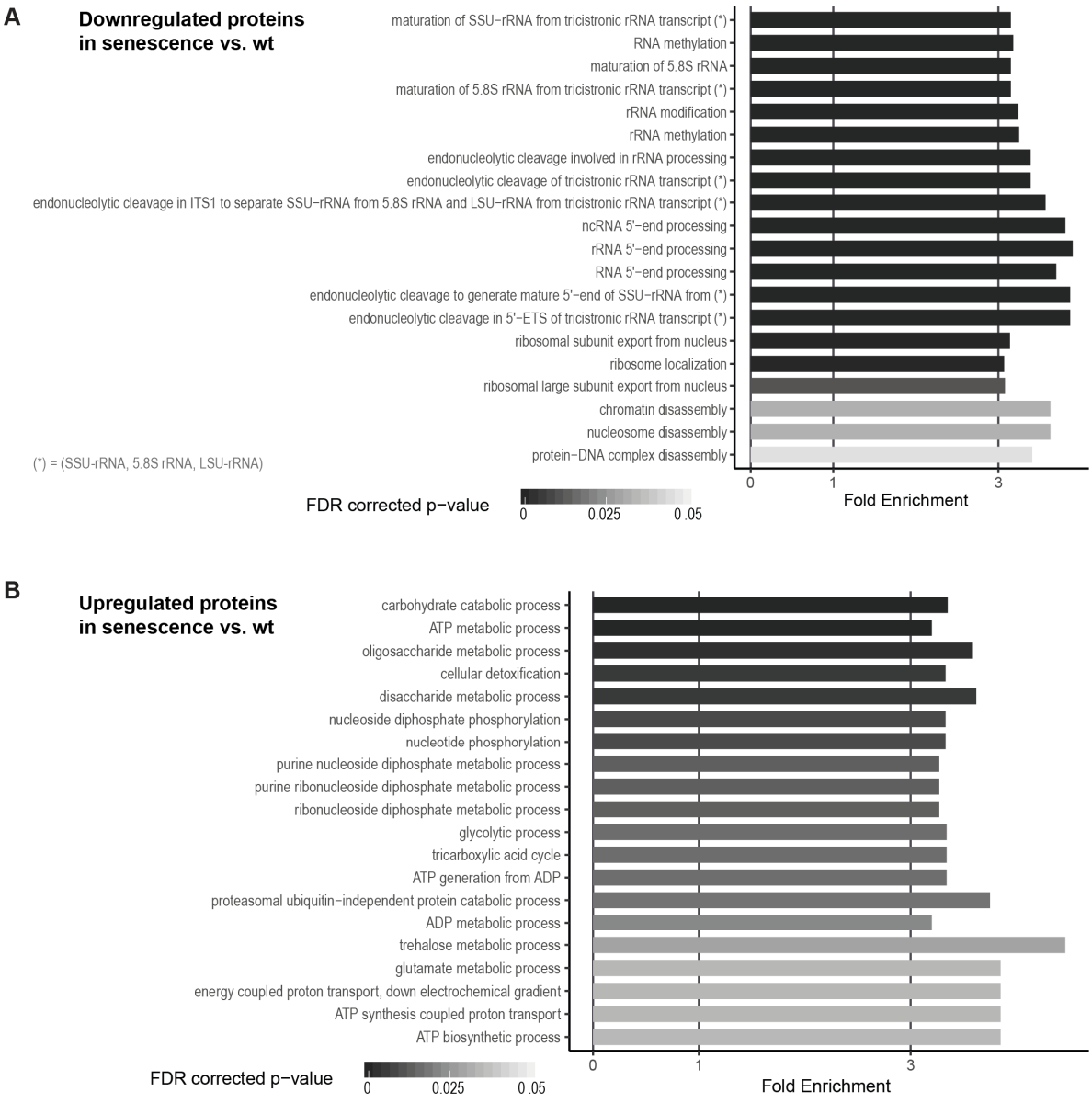

Figure 26. (A) Top 20 gene ontology (GO) terms for biological processes of 751 proteins downregulated in senescence compared to wt. **(B)** Top 20 GO terms for biological processes of 678 proteins upregulated in senescence compared to wt. Bioinformatics analysis was performed and figure was provided by Merve Öztürk (Butter lab, IMB Mainz).

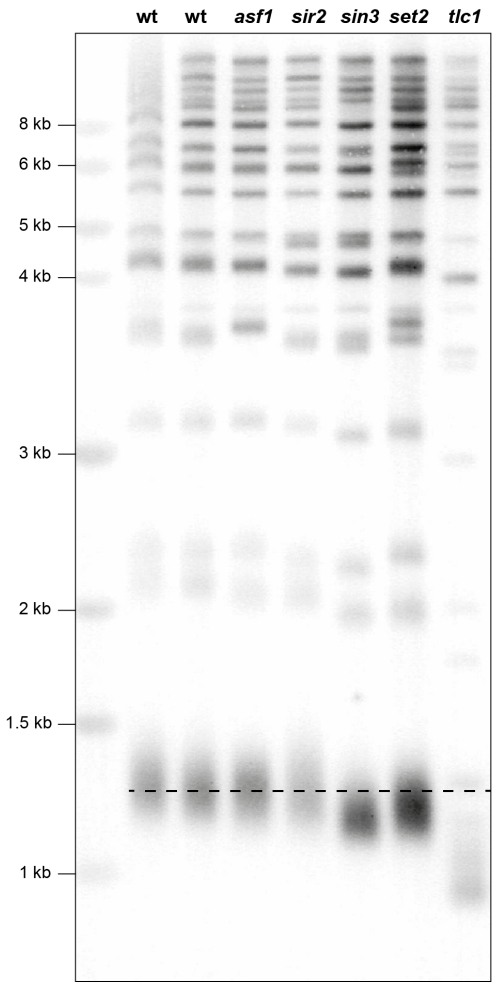

Figure 27. Uncropped Southern blot corresponding to **Figure 20D**.

4 Discussion

4.1 Telo-3C to study telomere folding in yeast

Until now, the analysis of telomere folding in budding yeast was based on a genetic reporter and ChIP experiments. Microscopy approaches have been challenging due to the smaller size of yeast telomeres compared to mammalian ones. In this doctoral dissertation, the chromosome conformation capture (3C) technique was adapted to directly detect and quantify the interaction of one telomere with its corresponding subtelomere. This Telo-3C methodology was initially established in the Luke lab by René Schellhaas (doctoral dissertation of René Schellhass 2016) and further optimized as part of this doctoral dissertation. Telo-3C allows us to investigate the regulation and possible functional implications of telomere-subtelomere contacts. Importantly, the data presented in this thesis solidifies the presence of a folded structure at budding yeast telomeres and furthermore suggests parallels with the t-loop in human cells.

Telo-3C was established and validated at telomere 1L in haploid yeast cells. The detection of Telo-3C ligation products supports the presence of a folded structure at this telomere (Figure 10). The sequences of the Telo-3C ligation junctions were confirmed by Sanger sequencing (data from the doctoral dissertation of René Schellhass 2016) and showed that Telo-3C exclusively detects intra-chromosomal telomere-subtelomere interactions at telomere 1L. As all of the Telo-3C primers (P5, P6 and P7) are specific for subtelomere 1L, we exclude that Telo-3C detects inter-chromosomal interactions between different telomeres, which is referred to as telomere clustering. Thus, we assume that the clustering of telomeres does not interfere with the Telo-3C analysis. This is supported by Hi-C studies that showed that intra-chromosomal interactions *in cis* generally occur more frequently than contacts between chromosomes *in trans* (Duan et al. 2010; Hsieh et al. 2015; McCord et al. 2020). In cells where telomeres were reported to lose clustering into 5-8 foci, such as in *yku* mutants or mutants of the SMC5/6 complex (Moradi-Fard et al. 2016; Hiraga et al. 2008), Telo-3C detected the same telomere folding frequency was as in wt cells (Figure 13, Figure 18). These observations suggest that telomere clustering does not bias the Telo-3C results. Thus, an impaired telomere clustering, which results in the distribution of single telomeres within the nuclear space, does not impede telomere folding. Interestingly, the hyper-clustering of yeast telomeres into one to three clusters can be induced by the overexpression of Sir3 (Ruault et al. 2011). Preliminary Telo-3C data showed that telomere-subtelomere interactions tend to increase upon hyper-clustering of telomeres (data not shown). In contrast to the observations that the loss of telomere clustering does not affect telomere folding, telomeres might fold back more frequently when forced into a hyper-clustered state.

Importantly, the Telo-3C analysis confirmed a decreased telomere folding in budding yeast mutants that were previously detected to be folding defective using other methods (Poschke et al. 2012; de Bruin et al. 2001). In the first study reporting the presence of a folded structure at budding yeast telomeres, the Sir2 histone deacetylase was implicated in its regulation (de Bruin et al. 2001). Telo-3C detected a decreased telomere folding in *sir2* mutants which is congruent with the report by de Bruin et al. (**Figure 20**). Telomere folding was also defective in cells lacking Sin3, which is consistent with Rap1- and Cdc13-Chip results, as well as with data obtained using a telomere folding reporter construct at a modified telomere (Poschke et al. 2012). Thus, Telo-3C offers a suitable methodology to investigate the folded structure at a natural, unmodified telomere in *S. cerevisiae.*

When characterizing the interactions of telomere 1L with its subtelomere, the Telo-3C interaction frequency diminishes with increasing distance from the telomeric tract (**Figure 10**). Nevertheless, the presence of ligation products between the telomeric anchor primer P5 and a primer with ~47 kb distance to the telomeric repeats (P9) argues that telomere 1L might also interact with loci of greater distance (**Figure 10**). These findings suggest, that telomeric repeats might touch down at multiple loci within the telomere-proximal region. Interestingly, in the study where the 3C technique was presented for the first time, the authors also analyzed the interaction of a telomere proximal locus to the rest of the chromosome (Dekker et al. 2002). In the work by Dekker et al., the anchor primer was designed at telomere 3L. However, the location of the anchor primer and its distance to the telomeric repeats as well as the location of the subtelomeric 3C primers were not described in detail (Dekker et al. 2002). The authors analyzed a region of approx. 40 kb from the chromosome end, which would roughly correspond to the region between the telomeric repeats and the P9 primer described in this thesis (**Figure 10**). Even though Dekker et al. detected a ligation product between the 40 kb region and the telomeric repeats of telomere 3L, the interaction frequency was drastically reduced, which is in accordance with the findings using Telo-3C (**Figure 10**) (Dekker et al. 2002).

Interestingly, interactions between telomere 1L and its subtelomeric regions occurred more frequently or stably than the selected internal non-telomeric interactions at a locus on the same chromosome (**Figure 11**). This internal locus on Chr. I was chosen due to the presence of NcoI restriction sites of comparable distances as they are present at telomere 1L. The locus is characterized by several genes and an origin of replication (ARS107) between primers P11 and P12. These genes encode for Lds1 (a protein involved in spore wall assembly), Psk1 (PAS domain-containing serine/threonine protein kinase), Tpd3 (the regulatory subunit A of the PP2A, a protein phosphatase), Ntg1 (DNA N-glycosylase and apurinic/apyrimidinic lyase) and Syn8 (an endosomal SNARE related to mammalian syntaxin 8). Except for *LDS1*, all genes are associated with active RNA

polymerase II (Rpb1-CTD-Ser2P and Rpb1-CTD-Ser5P) and characterized by H4K16 acetylation, an active chromatin mark (Mayer et al. 2010; Kirmizis et al. 2007). As expected, no substantial Sir2 binding was detected there, meaning that this internal region is euchromatic (Kirmizis et al. 2007). Since euchromatic regions are generally less condensed than heterochromatin, the euchromatin state of the internal region on Chr. I might contribute to the decreased contact frequencies observed by 3C (**Figure 11**). Consequently, the subtelomeric heterochromatin environment might encourage the formation or maintenance of a folded structure at the telomere (section 4.2.2). Alternatively, the more frequent telomere-subtelomere interactions compared to internal interactions might be explained by DNA ends generally having a greater mobility than internal loci which might be more constrained in their movement. As a result, the chromosome end might interact more frequently with nearby loci. It is challenging to test this hypothesis as the introduction of a break within the genome immediately triggers DNA repair activities. Indeed, it was shown that intra- and inter-chromosomal interactions around an induced DSB rather decrease or do not change (Oza et al. 2009).

When detecting and analyzing genomic interactions by any technique, there is always the question for the functionality of these interactions. If the respective interaction is meaningful, often gets discussed in the context of random collisions. Two loci can be considered in functional communication with each other when their interaction frequency is above the background of random collisions across the chromatin polymer (reviewed in McCord et al. 2020). However, the interactions that occur with a high level of confidence over background might not be the most relevant in terms of their functionality (reviewed in McCord et al. 2020). This is exemplified by enhancer-promoter interactions where a short and transient interaction can have the most meaningful outcome but might not be above background in a population of cells. By Telo-3C, telomere-subtelomere interactions at telomere 1L were shown to occur much more frequently than the analyzed internal interaction on Chr. I (**Figure 11**). This finding argues that the telomere folding interaction might be above background interactions across the yeast genome. Thus, the tight packing of chromosome ends into folded telomere structures likely contributes to telomere identity and perhaps to their functionality.

Chromosome interaction data obtained from 3C approaches generally provide average interaction frequencies over entire cell populations. The development of single-cell Hi-C gave further insight into the nature of chromosome contacts in individual cells (Nagano et al. 2013; Ramani et al. 2017; Stevens et al. 2017; Flyamer et al. 2017; Tan et al. 2018). These experiments showed that pairwise contacts are stochastic events in single cells. Thus, only by averaging stochastic contacts over many cells, interaction motifs such as TADs and their boundaries can be observed. Promoter-enhancer

interactions are also considered stochastic interactions. Nevertheless, their outcome for transcriptional regulation is meaningful. Although the Telo-3C analysis shows that telomere-subtelomere contacts are occurring, we cannot gain insight into how frequently the telomere folding occurs, how stable it is over time, or by which structural features it is characterized. Challenges for future studies will be to investigate the dynamics of telomere fold-back opening and closing, ideally on a single cell level. A previous study in mouse embryonic fibroblasts detected between 10-40 % of all telomeres in a t-loop conformation by employing microscopy techniques (Doksani et al. 2013). Due to the possible destabilization of t-loops during sample preparation, this percentage might likely be an underestimation of the t-loop occurrence *in vivo* (Doksani et al. 2013). The detected Telo-3C interaction frequency between telomere and subtelomere cannot be directly correlated to a proportion of folded telomeres at a given time point. However, the average telomere-subtelomere interaction frequency is altered under certain circumstances. This is for example the case during replicative senescence and in cells lacking known telomere folding regulators like Sir2 (Figure 17, Figure 20) (de Bruin et al. 2001). A decreased interaction frequency between telomere and subtelomere might refer to a weaker interaction within the folded telomere structure. It might also reflect a more dynamic folded structure which opens more frequently. A third possibility might be that telomeres in certain cells are unfolded over a longer period of time while telomeres in other cells are not affected at all. Since these interpretations are not mutually exclusive, these scenarios might happen all at once.

The subtelomeres adjacent to budding yeast telomeres are partially repetitive and contain elements that are shared between several chromosome ends. For this reason, the primer design and the choice of an appropriate restriction enzyme during the implementation of Telo-3C was challenging (doctoral dissertation of René Schellhass 2016). After establishing conditions that specifically detect intra-chromosomal contacts at telomere 1L in a reliable way (doctoral dissertation of René Schellhass 2016), we decided to focus the folding analysis on this telomere. The chromosome ends in budding yeast carry different combinations of X and Y' elements and it is evident that these elements impact telomeres in certain ways, for example in terms of SIR complex association and the telomere position effect (TPE) (Tham & Zakian 2002). Telomere structure might be regulated differently depending on the subtelomeric elements present or on the recruitment of telomere folding regulators. It is tempting to speculate that the presence of TG repeats between X and Y' elements or between two Y' elements might also affect telomere folding. A telomere "loop" structure could specifically form between the telomeric repeats and these internal telomeric sequences. This would go in line with the observation of interstitial t-loops in human cells (Wood et al. 2014). At telomere 1L, no internal stretches of TG repeats are annotated and therefore this

mechanism might be less likely to happen at this telomere. The Telo-3C analysis at telomere 1L, an X-only telomere, provides the basis towards understanding how telomere folding is regulated in budding yeast. In the future, it will interesting to adapt the Telo-3C methodology to other telomeres, including Y' telomeres. This might provide insight into differences and similarities of telomere folding between telomeres and could reveal new regulators for the folding of other telomeres.

4.2 Telomere folding in the context of chromosome architecture

Chromosome organization was proposed to be governed by two distinct mechanisms: active loop extrusion by the structural maintenance of chromosomes (SMC) complexes and compartmentalization driven by the self-attraction of heterochromatin (Mirny et al. 2019). In the following section, I will discuss which mechanism of chromosome organization might be underlying telomere folding based on the observations in this thesis.

4.2.1 Telomere folding and loop extrusion

In order to decipher if loop extrusion might be involved in the establishment of the folded telomere structure, I depleted the SMC complexes cohesin, condensin or SMC5/6 using auxin-inducible degrons on SMC1, SMC4 or SMC6 respectively. These experiments revealed that telomere folding is not reduced when any of the SMC complexes are depleted from yeast cells individually (**Figure 13**). This suggests that the process of how telomere folding is established and maintained might be independent from the mechanism of loop extrusion. Thus, I propose that neither the cohesin nor the condensin complex is involved in actively extruding telomeric and subtelomeric DNA to establish a folded structure. Consequently, I do not expect that the telomere fold-back has a defined boundary element, as it was described for TADs and CIDs (Rao et al. 2017; Wutz et al. 2017). Based on the assumption that loop extrusion might not be the mechanism underlying telomere folding, I suggest that the telomere fold-back does not have one specified touching point or loop anchor, as it was shown for chromatin loops mediated by cohesin (and additionally CTCF in mammalian cells) (Schwarzer et al. 2017; Wutz et al. 2017; Rao et al. 2017; Haarhuis et al. 2017). Nonetheless, based on the contact analysis over an average cell population I cannot rule out that the telomere fold-back resembles a loop or lariat-like structure of various lengths, which forms dynamically as it was suggested for enhancer-promoter interactions (K. Lee et al. 2015). Additionally, I conclude from these Telo-3C results that sister chromatid cohesion by cohesin is likely not involved in promoting a folded telomere structure.

Due to its described roles at telomeres, I considered the SMC5/6 complex as another potential regulator of telomere folding (Chavez et al. 2010; Noël & Wellinger 2011; Wan et al. 2013). Not only was it shown to associate with telomeres, but it is also important for telomere chromatin maintenance and telomere stability (Moradi-Fard et al. 2016; Torres-Rosell, Mahín, et al. 2005). Even though the SMC5/6 complex has DNA translocation and extrusion capacities, like the other SMC complexes, I showed that SMC5/6 is not involved in the formation of the telomere fold-back structure (Figure 13).

The depletion of the condensin member SMC4 resulted in a slight increase of telomere-subtelomere interactions at telomere 1L (Figure 13). This observation is consistent with my proposal that telomere folding is not established by loop extrusion, also not by the condensin complex. Based on this result, the condensin-dependent chromatin condensation before mitosis might rather counteract the formation of a folded telomere structure (Hirano & Mitchison 1994; Strunnikov et al. 1995; Gibcus et al. 2018). However, due to the analysis of telomere folding in an asynchronous culture, I cannot assign the slight increase of telomere folding after SMC4 depletion to a certain cell cycle phase. Therefore, it is difficult to draw conclusions about the effect of reduced chromosome condensation upon SMC4 depletion on telomere folding (Strunnikov et al. 1995; Strunnikov & Jessberger 1999).

The MRX (Mre11-Rad50-Xrs2) complex is characterized by a very similar architecture to the SMC complexes. The domain structure of Rad50 is complementary to the one of the SMC proteins and contains the typical coiled-coil regions forming a ring-like complex (Hopfner et al. 2000). During DSB repair, MRX was shown to associate with DNA ends and stabilize them by tethering them together (Gobbini et al. 2016). Telomere 1L was proficient in establishing a folded structure in cells lacking either Mre11 or Rad50 (Figure 18). Therefore, the stabilization of the telomere fold-back structure seems to be different from the end tethering mechanism at DSBs by the MRX complex. Telomere folding does not depend on the MRX ring complex for its establishment or maintenance. Also the Ku complex is a basket-like structure and binds to the free ends at DSBs as well as to telomeres and can slide along DNA (Blier et al. 1993). I show here, that the Ku complex is dispensable for the folding of telomere 1L (Figure 18). Thus, the Ku ring structure does not provide a scaffold for the stabilization of telomere folding.

4.2.2 Telomere folding as a heterochromatin domain at chromosome ends

Telomere folding was first discovered in budding yeast using a telomere folding reporter construct (see Figure 4) (de Bruin et al. 2001). Interestingly, only when the reporter gene and the downstream enhancer element (UAS*) were integrated close to the telomeric repeats, the transcription of the

reporter gene got activated via telomere folding. This was not the case when the same reporter construct was placed at an internal chromosomal locus, suggesting that folding interactions happen less frequently at this internal locus compared to telomeres (de Bruin et al. 2001). Consistent with these findings, I observed that the intra-chromosomal interactions between telomere and subtelomere occur much more frequently than interactions between internal loci on the same chromosome (**Figure 11**). This observation allows me to speculate about possible structural features of telomere folding in budding yeast. It may point towards the existence of a specific heterochromatin domain at the end of the chromosome which could favor the formation of a folded structure, or *vice versa*. This proposed heterochromatic telomere folding domain might exist in the shape of a condensed "knot", whereby interactions within the "knot" occur more frequently and more stably than outside this structure. Interestingly, the heterochromatin state of human telomeres was implicated in t-loop formation in a recent study (Zhang et al. 2019). Having observed a decondensation of telomeres after treating cells with the histone deacetylase inhibitor trichostatin A (TSA), the authors propose that this decondensation might disrupt t-loops or inhibit their formation (Zhang et al. 2019).

The presence of a heterochromatin telomere folding domain is supported by the finding that the chromatin modifiers Sir2, Sin3 and Set2 are required for its establishment and/or maintenance. Sir2, Sin3 and Set2 were demonstrated to promote histone deacetylation under certain conditions and hence might support a more heterochromatic environment. As part of the Rpd3L histone deacetylase complex, Sin3 is involved in the regulation of silencing on a genome-wide level (Rundlett et al. 1996; Sun & Hampsey 1999; Vannier et al. 1996). Additionally, H3K36 methylation mediated by Set2 correlates with histone deacetylation as this co-transcriptional histone methylation leads to the recruitment of the Rpd3S histone deacetylase complex (Keogh et al. 2005; Carrozza et al. 2005). Sir2, Sin3 and Set2 were all reported to be involved in telomere silencing or the regulation of the telomeric chromatin state. The integral role of the SIR complex at telomeres and for the maintenance of TPE is well characterized (Cockell et al. 1995; Aparicio 2013; Imai et al. 2000). However, the function of Set2 and Sin3 for TPE, telomere silencing and telomere folding might be more complex.

It is tempting to speculate which factors or chromatin landscapes might define the borders of the telomeric heterochromatin domain, possibly supported by telomere folding. Clearly, the histone acetyltransferase Sas2 is known to be an important factor for limiting the spreading of the SIR complex. By acetylating H4K16, Sas2 contributes to setting the boundary between the heterochromatic subtelomere and the more internal euchromatin (Kimura et al. 2002; Suka et al. 2002; Shia et al. 2006; Altaf et al. 2007; Xu et al. 2006). It was shown that the balance of Sas2 and

Sir2 activities at subtelomeres is indispensable for this boundary (Kimura et al. 2002; Suka et al. 2002). In the absence of Sas2, the SIR complex can spread way beyond the heterochromatin-euchromatin boundary which leads to its loss from subtelomeres (Kimura et al. 2002; Suka et al. 2002). Thus, subtelomeres become less heterochromatic and less silenced in *sas2* mutants. In this context, it would be interesting to test how the re-distribution of SIR complexes in *sas2* mutants affects the folding behavior of telomeres. Additionally, Set2-mediated H3K36 methylation and histone deacetylation by Sin3 were attributed a role in maintaining the heterochromatin boundary at telomeres. In the absence of either Set2 or Sin3, the SIR complex spreads from the telomeres towards internal euchromatin, beyond its natural borders (Tompa & Madhani 2007; Ryu et al. 2014; Zhou et al. 2009; Ehrentraut et al. 2010). In contrast to what happens in the absence of Sas2, subtelomeres become hyper-silenced when cells are lacking Set2 or Sin3, due to increased SIR complex association. As telomere folding is compromised in *sin3* and *set2* mutants, this suggests that the mechanism behind the unfolding of telomeres might be independent from TPE and subtelomeric silencing. Even though subtelomeres are hyper-silenced in *sin3* and *set2* mutants, as measured by the expression of reporter genes at subtelomeres, the absence of these chromatin modifiers leads to an opening of the folded telomere structure. Interestingly, the TERRA levels transcribed from telomere 1L in *sin3* and *set2* mutants were unchanged, in contrast to what is expected for hyper-silenced telomeres (Figure 20). One possible explanation for this finding is, that telomere 1L might behave differently from other telomeres where silencing was tested previously, and may not be hyper-silenced in the absence of Sin3 or Set2. Alternatively, TERRA degradation effects or the manipulation of the natural telomere by integrating the reporter might lead to different results. Since both Sin3 and Set2 have genome-wide roles in transcriptional regulation, I cannot rule out indirect effects of *SIN3* and *SET2* knockout on telomeric chromatin and transcription. However, their deletion did not drastically affect Sir2 protein levels which shows that Sir2 is not destabilized under these conditions (Figure 23).

It was previously suggested that silent chromatin might be needed for the formation of folded chromosome end structures (Pryde & Louis 1999). *Vice versa* it was hypothesized that telomere folding might be necessary for heterochromatin formation at telomeres (Grunstein 1997). Many of the fold-back defective mutants identified by the genetic telomere folding reporter are not characterized by decreased telomere silencing (Poschke et al. 2012). Therefore, Poschke et al. proposed that telomeric silencing can still be established even when the telomere fold-back is compromised (Poschke et al. 2012). This notion is supported by the Telo-3C results showing that the telomere folding defect in *sin3* and *set2* mutants is not necessarily coupled to a desilencing of telomeres (Figure 20). It is important to mention that most of the studies that addressed telomere

silencing employed reporter genes at different subtelomeric positions (Pryde & Louis 1999; Tham & Zakian 2002; Grunstein & Gasser 2013). Instead, measuring TERRA levels at unmodified telomeres might allow to elucidate the connection between telomere silencing and folding in more detail.

One tempting speculation is that the borders of a potential heterochromatin telomere folding domain are defined by a histone mark transition zone, as suggested for an extended silent domain (ESD) at subtelomeres (Hocher et al. 2018). Hocher et al. defined ESDs at subtelomeres of yeast chromosome ends by studying the spreading of Sir3 when overproduced. When Sir3 is overexpressed, none of the known boundary factors could block Sir3 spreading (Hocher et al. 2018). The authors identified H3K79 trimethylation (H3K79me3), mediated by the histone methyltransferase Dot1, as the most efficient barrier for heterochromatin spreading when Sir3 is present in excess (Hocher et al. 2018). They suggest that histone tail acetylation, e.g. by Sas2, might rather be a buffer for SIR spreading in contrast to H3K79me3 which blocks it and therefore protects euchromatin (Hocher et al. 2018). The borders of ESDs coincide with increased H3K36me3 and H3K79me3, among a few other histone marks. Thus, a distinct chromatin landscape at telomeres defines the characteristics of ESDs and its borders. A heterochromatin telomere folding domain might be defined by the same histone mark transition zone. It is tempting to speculate that a folded telomere structure might contribute to the establishment of extended silent domains at subtelomeres.

According to the arguments presented above (section 4.2.1), I propose that the folded telomere structure might rather not be formed by an active loop-extrusion process. I consider it more likely that the underlying mechanism is similar to compartmentalization, a process in which nuclear euchromatin and heterochromatin compartments are established supposedly by affinity-driven interactions within heterochromatin (Falk et al. 2019; Nuebler et al. 2018; Pereira et al. 2018). The formation of A and B compartments was shown to be independent of cohesin and CTCF in mammalian cells (Schwarzer et al. 2017). The interactions within compartments are even increased when cohesin or its loading complex is missing (Schwarzer et al. 2017). Since telomere folding was shown to be independent from the SMC complexes and depends on the presence of chromatin modifiers, I propose that attractive interactions between heterochromatin might be the basis for telomere folding, analogous to B compartments in mammalian cells. Interestingly, Micro-C results in mouse embryonic stem cells showed that boundaries in inactive B compartments were preferentially formed in repeat-rich regions (Hsieh et al. 2020). Since the mechanisms of chromosome organization by loop extrusion and compartmentalization seem to be highly conserved from yeast to man, this might point towards a similar boundary formation mechanism

at yeast telomeres. The authors also found that highly heterochromatic domains, Polycomb repressive regions, form nested sets of chromatin contacts rather than interacting through “loop” structures (Hsieh et al. 2020). These bundle interactions could be very similar at the highly heterochromatic telomere fold-back or “knot” structure at yeast chromosome ends.

The heterochromatin compartment formation in human and *Drosophila melanogaster* has been suggested to occur via liquid-liquid phase separation mechanisms (Altmeyer et al. 2015; Patel et al. 2015; Larson et al. 2017; Strom et al. 2017). Liquid-liquid phase separation describes the phenomenon when a solution of macromolecules such as proteins or nucleic acids condenses into a liquid droplet-like phase, separating from a more diluted phase (reviewed in Alberti et al. 2019). A described characteristic of liquid-liquid phase separation is the exclusion of certain factors according to their biochemical features. It was shown that post-translational modifications can regulate access or exclusion of factors from these domains (Banani et al. 2017). The liquid-liquid phase separation model is based on non-specific weak multivalent interactions, which are often attributed to intrinsically disordered protein domains that have a high chance of self-association. Interestingly, there is evidence that heterochromatin compartments exclude recombination factors in yeast supposedly to prevent the recombination between repetitive regions (Torres-Rosell et al. 2007). This segregation might be based on a liquid-liquid phase separation mechanism. Additionally, repetitive DNA elements themselves might contribute to liquid-liquid phase transition (Tang 2017). Therefore, this mechanism could play a role for the establishment of a heterochromatin telomere folding domain at chromosome ends in yeast. As specific RNAs have been shown to drive liquid-liquid phase separation, it is tempting to speculate that TERRA might contribute to the formation of this domain by potentially providing a scaffold for multivalent protein-RNA interactions (Alberti et al. 2019; Langdon & Gladfelter 2018; Langdon et al. 2018; C. H. Lee et al. 2015; Zhang et al. 2015).

As an alternative model to liquid-liquid phase separation, the heterochromatin domains at telomeres might be established by a phase separation within polymers mediated by bridging protein interactions (Erdel & Rippe 2018). Based on data from Sir3 overexpression studies, the polymer-polymer phase separation model might be more likely for yeast telomeres (Miné-Hattab & Taddei 2019). It is based on either specific or multivalent weak interactions between chromatin-binding proteins or chromatin components (Miné-Hattab & Taddei 2019). Interactions between Sir3 proteins were suggested to be involved in bridging telomeres for the formation of silencing foci (Meister & Taddei 2013; Ruault et al. 2011). Interestingly, it was shown by atomic force microscopy that the SIR complex has the ability to condense recombinant nucleosome arrays into compact chromatin fibers (Swygert et al. 2018).

It will be interesting to understand if one of these phase separation models might contribute to the formation of the proposed heterochromatic telomere folding domain. The deletion of intrinsically disordered domains in telomere binding proteins and telomere folding regulators might help to understand if liquid-liquid phase separation is involved in the establishment of this domain and in telomere folding itself.

4.3 The regulation of telomere folding

I was interested to address the interplay between telomere length and the establishment of a folded telomere structure. By analyzing telomere folding in several mutants with short telomeres, I found that telomere length might not be a major determinant of telomere folding. The Telo-3C analysis revealed that the loss of Upf1, yKu70, Mre11, Tel1 and Rad50 does not decrease telomere folding, even though these cells have extremely short telomeres, approx. 200 bp shorter than wt (Figure 18). This suggests, that the length of the TG repeats does not impose a physical constrain on telomere folding, as is has been proposed before for yeast telomeres (de Lange 2009). Short telomeres were proposed to bind less telomere-associated proteins because they bear less Rap1 binding sites and therefore might also recruit less SIR complexes (reviewed in Greider 2016). However, based on the finding that mutants with short telomeres are proficient for telomere folding, I propose that the decreased association of these proteins does not interfere with the formation of a fold-back structure.

The telomere folding analysis in the set of mutants with short telomeres allows to infer connections between telomere folding and several processes related to telomere stability, such as telomere silencing and chromosome end resection. Even though the telomeres of *upf1*, *yku70*, *mre11*, *tel1* and *rad50* were all similarly short, they do not share the same silencing status. When TPE was analyzed by the transcription of a *URA3* reporter at the subtelomere, *mre11*, *tel1* and *rad50* mutants behave similarly to wt cells (Runge & Zakian 1996; Boulton & Jackson 1998). TPE was shown to be nearly abolished in mutants of the yKu complex and modestly diminished in *upf1* mutants (Boulton & Jackson 1998; Laroche et al. 1998; Lew et al. 1998). Due to the integration of a reporter gene at the subtelomere and differences in TPE between telomeres, the desilencing of telomeres measured by a reporter construct does not always correlate with increased TERRA levels. I measured increased TERRA levels in *upf1* mutants, while TERRA levels were comparable to wt in *yku70*, *mre11*, *tel1* and *rad50* mutants (Figure 18). In cells lacking Upf1, an RNA helicase involved in non-sense mediated mRNA decay, the increased TERRA levels might indeed not arise from increased TERRA transcription. Instead, a described failure to release TERRA from telomeric chromatin might lead to its accumulation (Azzalin et al. 2007b; Chawla & Azzalin 2009). By analyzing

telomere folding and TERRA levels in a set of mutants with short telomeres, I conclude that increased TERRA levels from telomere 1L are not naturally accompanied by a telomere folding defect. Additionally, telomeres, where TPE is abolished as in *yku70* mutants, are not naturally unfolded. In *yku* mutants, telomeres are characterized by excessive 3' overhangs due to increased Exo1-dependent resection (Gravel et al. 1998; Bertuch & Lundblad 2004; Maringele & Lydall 2002). On the contrary, in *mre11* mutants the G-rich overhangs are shorter in comparison to wt telomeres (Larrivée et al. 2004). As both of these mutants are proficient for telomere folding, I assume that an exacerbated or diminished resection of telomeres might not impact their folding behavior. This is surprising as a strand invasion mechanism of the 3' overhang might be involved in the formation of the folded structure (section 4.5). However, the small overhang of *mre11* mutants retains its proper cell cycle regulation (Larrivée et al. 2004) and might therefore be enough to convey a strand invasion event.

After having confirmed the impact of the telomeric histone deacetylase Sir2 on telomere folding by Telo-3C, I addressed the role of the telomere binders Rif1 and Rif2. Both Rif1 and Rif2 have been implicated in telomere folding regulation from data using a genetic telomere folding reporter and chromatin immunoprecipitation (ChIP) (Poschke et al. 2012). The Rap1-ChIP signal in *rif1* and *rif2* mutants is specifically reduced at a distance of 0.5 kb and 1 kb from the telomeric repeats, pointing towards a decreased folding interaction at the tested telomere (Poschke et al. 2012). A mechanism was proposed where Rif2 contributes to the recruitment of the Rpd3L histone deacetylase complex to telomeres which is important for the establishment of a fold-back structure (Poschke et al. 2012). The Telo-3C revealed that the deletion of neither *RIF1* nor *RIF2* reduces the frequency of telomere folding, arguing that these two telomeric proteins might not contribute to the establishment of a folded structure at the unmodified telomere 1L (Figure 14). The discrepancy of data obtained with these two methods might arise from the different readouts of these approaches. When using the fold-back reporter construct, the telomere is not in its natural state but highly modified by introducing the reporter. This might lead to changes in the protein composition of the telomere and the subtelomere as well as in their chromatin environment. On the contrary, the Telo-3C methodology analyzes telomere-subtelomere interactions at the natural telomere 1L. Additionally, the absence of Rif1 or Rif2 from telomeres results in telomere elongation and alters their chromatin environment, possibly impacting on artificial and natural telomeres in different ways (Hardy et al. 1992; Wotton & Shore 1997). Even though the ChIP-based approach by Poschke et al. addressed the folding of an unmodified telomere, this method is indirect (Poschke et al. 2012). A major concern of the Rap1- or Cdc13-ChIP technique is that the signal might come from these telomeric proteins spreading into the subtelomeric region, instead of telomere folding. Therefore, ChIP

results might be biased by the chromatin environment affecting the spreading of telomere binders. Additionally, the over-elongated telomeres in *rif1* and *rif2* mutants might affect the binding or spreading of telomeric proteins. It is also important to mention that the fold-back reporter, the ChIP approaches and Telo-3C each address telomere folding at different telomeres. The fold-back reporter was introduced at telomere 7L, the Rap1- and Cdc13-ChIPs were analyzed at telomere 6R and Telo-3C examined the folding of telomere 1L. Despite all being X-only telomeres, they might still exhibit different telomere folding behaviors.

The over-elongated telomeres of *rif1* and *rif2* cells (Hardy et al. 1992; Wotton & Shore 1997) do not interfere with efficient telomere folding, according to the Telo-3C results (Figure 14). This finding supports the idea that telomere length *per se* is not a major determinant of telomere structure. The successful telomere folding in *rif1* mutants also suggests that telomere folding is likely different from chromatin architecture forming around a double strand break. It was recently described in human cells that 53BP1 and RIF1 form distinct nanodomains around a double strand break (Ochs et al. 2019). In this case, RIF1, together with cohesin, was proposed to localize to the boundaries of these domains and stabilize chromatin topology.

The behavior of t-loops and folded structures at telomeres during the cell cycle is of great interest in the field. Since the discovery of t-loops, a dynamic opening and closing has been expected circumventing the interference with other processes at chromosome ends. As the mammalian t-loop is based on a strand-invasion event, it has been speculated that unfolding is needed during S phase for the passage of the replication machinery and for c-strand fill-in (Zhao et al. 2009; Dai et al. 2010). Additionally, telomerase elongates the shortest telomeres in the cell and needs access to their 3' overhangs which might not be possible when it is tucked away in the t-loop (Doksani & de Lange 2014; Teixeira et al. 2004; Britt-Compton et al. 2009; Hemann et al. 2001). However, the t-loop opening during S phase has been difficult to prove experimentally with currently available methods (Mak et al. 2019; Zhang et al. 2019). Recent studies using 2D gel electrophoresis and a biochemical t-loop assay suggest that the t-loop might unfold twice during the cell cycle, for telomere replication during S phase and c-strand fill-in in late S/G2 phase (Mak et al. 2019; Zhang et al. 2019). However, these studies did not specifically detected a decreased proportion of t-loops at these time points but rather observed continued t-loop formation throughout the cell cycle (Mak et al. 2019; Zhang et al. 2019). Nevertheless, the consequences for telomere stability are detrimental when mechanisms for t-loop unwinding are lacking (Vannier et al. 2012; Sarek et al. 2015; Sarek et al. 2019). The S phase specific unfolding of t-loops was attributed to a phospho-switch in TRF2 which allows the specific association of RTEL1 to telomeres in a narrow window during telomere replication (Sarek et al. 2015; Sarek et al. 2019).

When analyzing the folding of telomere 1L in budding yeast, I did not observe significant changes during the cell cycle (Figure 12). Assuming that the telomere fold-back structure relies on a strand-invasion mechanism comparable to the t-loop (section 4.5), I would expect that telomere folding has to open in S phase. However, the Telo-3C results showed that the bulk of telomere fold-back structures does not drastically unfold when cells synchronously progress through the cell cycle. Again, the population analysis of telomere-subtelomere interaction frequencies might be a limitation for studying telomere folding during the progression through the cell cycle. As telomere unfolding, e.g. for replication, could be a transient event and individually timed in each cell, it might not be detectable by Telo-3C. Another explanation could be that telomeres open at a very specific time point during S phase which I might have missed in the analysis using 15 minute intervals. In order to achieve cell populations with improved levels of synchronization, elutriation could be applied (Futcher 1999; Amon 2002). With this method, synchronous cell populations can be obtained for each cell cycle phase by centrifugation, based on the separation of cells according to their size, mass and shape. Additionally, it would be interesting to test if the increased telomere-subtelomere interactions observed upon Sir3 overexpression (data not shown) might impede telomerase access to chromosome ends and possibly lead to telomere shortening.

4.4 Telomere folding during senescence

Replicative senescence was characterized as a potent tumor suppressor mechanism (reviewed in Campisi & D'Adda Di Fagagna 2007; Mieczkowski et al. 2003). Therefore, the underlying processes concerning telomere erosion and uncapping as well as chromosome architecture are of great interest. To gain insight into telomere structure during replicative senescence, I used telomerase negative yeast cells (*tlc1*) as a model for this process. Telomere folding decreases when cells enter replicative senescence and telomeres transition from a closed state to an unfolded state (Figure 17). By analyzing a set of mutants with very short telomeres, I showed that short telomeres *per* se do not lose the ability to form a folded structure (Figure 18). Thus, the amount of TG repeats at yeast telomeres do not affect the folded structure. According to this finding, I propose that the short telomere length during replicative senescence is not the main reason for the opening of the folded structure. Instead, this decreased telomere folding ability might rather be due to other aspects of the senescence program. This notion is also supported by the observation that telomere folding is decreased after MMS treatment (Figure 22), which was shown to result in a comparable gene expression response as observed during senescence in budding yeast (Nautiyal et al. 2002). In both cases, cells elicit a DNA damage response and a stress response in addition to an altered metabolic program (Nautiyal et al. 2002). To identify possible regulators of telomere folding during

senescence, we compared all down-regulated proteins during senescence as detected by our mass-spectrometry approach, to a published set of possible telomere folding regulators (**Figure 19**) (Poschke et al. 2012). This comparison rendered 21 overlapping candidates, five of which were histone modifiers: Set2, Sin3, Eaf3, Hda1 and Sir2 (**Figure 19**). Gene ontology analysis for molecular function showed that histone deacetylation was significantly enriched in the 21 overlapping candidates over all downregulated proteins during senescence (**Figure 19**). This suggests that telomere folding might require a specific heterochromatic environment of the subtelomere (section 4.2.2). Perturbations of histone modification may be the reason for the structural changes that occur at telomeres throughout senescence. The histone modifiers Sir2, Sin3 and Set2 are potential regulators of telomere folding during senescence (**Figure 20**). How they might affect the folding behavior of telomeres was discussed above (section 4.2.2). As their expression is decreased during senescence, their reduced availability could contribute to an unfolded telomere state during senescence (**Figure 20**). Both Sin3 and Set2 showed a drastic down-regulation at the peak of senescence when cells are in telomere crisis, which correlates with telomere unfolding (**Figure 17**, **Figure 20**). However, I cannot infer from this data if the absence of these histone modifiers is the cause for the opening of the folded structure. Alternatively, or in addition to the previous hypothesis, their absence in senescent cells might maintain an unfolded telomere structure, but additional factors might be required for the initial unfolding. By analyzing the protein levels of the Sin3, Set2 and Sir2 proteins in cells deleted for the respective other histone modifiers, I showed that the absence of either of them does not influence the availability of the others (**Figure 23**). Neither the lack of genome-wide histone deacetylation as a result of *SIN3* knockout, as part of the Rpd3 complex, nor the absence of H3K36me by deletion of *SET2* drastically affects the protein levels of Sir2, Sin3 or Set2 respectively (**Figure 23**). Even though this analysis was done in a telomerase positive background, the downregulation of the histone modifiers Sin3, Set2 and Sir2 during senescence might likely be independent from each other.

Sir2 levels did not drastically decrease during replicative senescence, however, I observed an uncharacterized modification on the protein by western blot (**Figure 20**). This suggests a specific regulation of Sir2's activity, localization or stability within the senescence program. Sir2 was previously shown to be SUMOylated during mother cell aging in yeast, which leads to its relocalization from telomeres to the nucleolus (Hannan et al. 2015). Therefore, during senescence Sir2 may also get redistributed from telomeres to the rDNA locus, contributing to the decreased telomere folding. Interestingly, with the progression of senescence, Sir2 was previously shown to lose its localization into five nuclear foci but instead appears as one or two bright foci in microscopy experiments (Straatman & Louis 2007). During senescence, Sir2 and Sir3 also lose their

colocalization which could reflect the relocalization of Sir2 to the nucleolus (Straatman & Louis 2007). In line with this hypothesis, subtelomeric H4K16 acetylation was shown to increase in senescent *tlc1* cells, as compared to pre-senescent cells (Kozak et al. 2010). The increased acetylation was observed more centromere-proximal, between 3 and 10 kb from the telomeric repeats, and depends on the histone acetyltransferase Sas2 (Kozak et al. 2010). Accordingly, SIR proteins were shown to relocalize from telomeres to genomic loci under various types of DNA damage (Martin et al. 1999), which could be the reason for my observation of telomere unfolding after exposure to MMS (**Figure 22**). Upon MMS treatment, the nuclear Sir3 signal was shown to transition from appearing as distinct foci to a diffuse nuclear signal due to the release of Sir3 from subtelomeric regions (Martin et al. 1999; Mills et al. 1999). As a result of SIR protein redistribution, also the TPE is impaired upon DNA damage (Martin et al. 1999). The response of telomeres to prolonged DNA damage, as for example induced by MMS treatment, might be similar to their behavior during senescence. Yet, the opening of telomere folding in both cases may be due to different mechanisms as Sin3, Set2 and Sir2 abundance was not affected by MMS treatment in the analyzed period of time (**Figure 22**). Nevertheless, both senescence and MMS exposure were connected to a subnuclear relocalization of the SIR proteins in previous studies. ChIP experiments, for the here identified telomere folding regulators Sin3 and Set2 in budding yeast, would give additional insight into the mechanisms underlying the unfolding of telomeres in these two scenarios.

Interestingly, the direct telomere binding protein Rap1 was shown to be redistributed during senescence (Platt et al. 2013). This is congruent with a previous microscopy study showing that senescent budding yeast cells lose the characteristic telomeric Rap1 foci (Straatman & Louis 2007). Instead, the Rap1 signal at crisis is diffuse throughout the nucleoplasm, similar to what was observed for Sir2 (Straatman & Louis 2007). The Rap1 redistribution might potentially contribute to decreased SIR binding at telomeres during senescence, since the targeting of the SIR proteins to telomeres depends on the presence of Rap1 (Moretti et al. 1994; Rusche et al. 2003). Additionally, it is evident that histone levels themselves drastically decrease during senescence in yeast and human cells (Platt et al. 2013; O'Sullivan et al. 2010) and that histone synthesis is sensitive to DNA damage signaling (O'Sullivan et al. 2010). This might also point towards a mechanism by which a reduced nucleosome occupancy at subtelomeres during senescence contributes to unfold the telomere structure.

Telomere unfolding during senescence could be connected to the permanent G2/M arrest that cells experience during this process. It is possible, that the cell cycle arrest alone, without a senescence or DNA damage response, might cause the opening of telomere folding. Even though I showed that

telomere folding is not affected by the cell cycle (Figure 12), a cell cycle arrest for a certain time might still affect telomere folding. To answer this question, telomere folding could be analyzed after arresting cells for several hours at the G2/M border, e.g. by depleting the activator of the anaphase-promoting complex Cdc20.

Interestingly, the yeast survivor cells obtained from the senescence assay are characterized by a telomere-subtelomere interaction frequency comparable to wt and pre-senescent cells (Figure 17). This suggests that their heterogeneous TG repeat length does not interfere with the telomere fold-back structure, which is in line with the finding that telomere length does not affect telomere folding (Figure 18). Genome-wide studies showed that the transcriptome and proteome of yeast survivors does not drastically differ from wt and pre-senescent telomerase negative cells (data not shown). Additionally, the telomeres of human ALT cells, the functional equivalents to yeast survivors, were shown to be proficient for engaging in a t-loop of heterogeneous sizes (Cesare & Griffith 2004). This observation indicates parallels between the yeast and human systems when telomeres are maintained by a telomerase-independent mechanism. In the senescence assay in liquid culture only type II survivors were obtained which are defined by the extension of the TG repeats (Lundblad & Blackburn 1993; Le et al. 1999; Teng & Zakian 1999). Therefore, the Telo-3C analysis does not provide any information about the telomere folding behavior of type I survivors, where Y' elements get amplified (Lundblad & Blackburn 1993; Le et al. 1999; Teng & Zakian 1999). It is possible that the amplification of Y' elements might influence telomere folding in a different way than the extension of TG repeats. However, from the Telo-3C analysis on a whole cell population, I cannot exclude that certain telomeres in survivors will unfold in specific situations, e.g. when they undergo telomere recombination events.

I wanted to test the direct involvement of the telomere folding regulator Sin3 in the unfolding of telomere 1L during senescence. I overexpressed Sin3 at the point during senescence when Sin3 protein levels dropped and telomere 1L was unfolded (Figure 17, Figure 20). The overexpression of Sin3 did not prevent the unfolding of telomere 1L and was also not sufficient to re-establish a telomere fold-back structure during senescence (Figure 21). Possibly, the supply of Sin3 protein for a short period of 2 hours might not have been enough to compensate for the drastic downregulation of Sin3 protein levels during crisis. Another explanation could be that the opening of the folded structure might only be prevented by an oversupply of Sin3 right before endogenous Sin3 levels drop. However, Sin3 overexpression might not be able to force the re-folding of telomeres once unfolded. Alternatively, I can imagine that the downregulation of Sin3 during senescence may contribute to the unfolding of telomeres in conjunction with a network of other factors within the senescence program. These other factors might include the histone modifiers

Sir2 and Set2 which were shown to be regulators of telomere folding in this thesis (Figure 20). Due to the genome-wide roles of Sin3 as part of the Rpd3 histone deacetylase complexes, the consequences of Sin3 overexpression might be complex and include indirect effects. Stoichiometric imbalances within large protein complexes, such as the Rpd3 complexes, or the mislocalization of Sin3 and other proteins might play a role as well (Moriya 2015).

In human cells, the cellular response to senescence has been heavily studied and there are some parallels to budding yeast. A striking feature of senescent human cells is the formation of senescence-associated heterochromatin foci (SAHF), specialized domains of facultative heterochromatin (Narita et al. 2003). Interestingly, constitutive heterochromatin domains such as telomeres are mostly excluded from SAHFs, even though SAHFs are highly compacted heterochromatin domains (Narita et al. 2003; R. Zhang et al. 2007; Ye et al. 2007; Funayama et al. 2006). On the contrary, there is evidence from telomerase negative mice and senescent human cells that telomeres become less heterochromatic upon telomere shortening or the onset of senescence (Benetti et al. 2007; Chandra et al. 2015). Upon telomere shortening in mice, telomeres and subtelomeres are covered with less heterochromatin histone marks (H3K9me3 and H4K20me3), less CBX3 (a heterochromatin protein 1 homolog), less DNA methylation and more histone acetylation (Benetti et al. 2007). Benetti et al. therefore suggest, that the loss of telomeric repeats changes telomeric and subtelomeric chromatin architecture towards a more “open” chromatin state (Benetti et al. 2007). Also in human cells a drastic loss of local interactions within heterochromatin regions was observed using Hi-C and FISH (Chandra et al. 2015). This was especially true for a subset of TADs featuring enrichment for the heterochromatin mark H3K9me3, late replication timing and lamina-associated domains (Chandra et al. 2015). Taken together, these findings from yeast and mammalian cells during senescence point towards a mechanism by which telomeres might serve as a reservoir for heterochromatin proteins that get redistributed under certain circumstances, such as cellular senescence.

4.5 Telomere folding, the DNA damage response and homology-directed repair proteins

The t-loop structure at human chromosome ends was proposed to stabilize via a strand invasion event of the 3’ overhang within the telomeric repeat tract (Griffith et al. 1999). Therefore, the basis of the t-loop is considered to be comparable to the d-loop intermediate arising during homology-directed repair (HDR) (Griffith et al. 1999). In accordance with this model, it was shown that several HDR factors transiently localize to telomeres after replication, including the key players RAD51 and RAD52, but also XRCC3, which binds and processes recombination intermediates (Verdun &

Karlseder 2006). In the yeast *K. lactis,* the formation of t-loops at over-elongated telomeres was shown to depend on the presence of Rad52 as well (Cesare et al. 2008). Using Telo-3C, I showed that in budding yeast the formation of telomere folding is also dependent on Rad51 and Rad52 (Figure 15). In analogy to the human system, the HDR machinery might assist the establishment of a fold-back structure at yeast telomeres. The heterogeneous telomeric repeat sequences and the relatively short 3' overhangs at budding yeast telomeres were proposed to be obstacles for the strand invasion (de Lange 2009). However, both Rad51 and Rad52 are indispensable for homology search and strand invasion during HDR (Figure 6). Therefore, a strand invasion mechanism into homologous sequences might be involved in the formation of the folded structure at budding yeast telomeres. This would further support the resemblance to mammalian t-loops but needs further experimental proof.

Interestingly, telomere folding decreased in cells depleted of the DNA damage checkpoint kinase Rad53 (Figure 16). However, the absence of neither Mec1 nor Tel1, both upstream kinases in DNA damage signaling, does not restrain the proper establishment of telomere folding (Figure 16, Figure 18). This suggests that these kinases might have redundant functions upstream of Rad53. Alternatively, Rad53 might promote telomere folding in another way, independently from Mec1 and Tel1. Analyzing telomere folding in *mec1 tel1* double mutants is complicated by the fact that they undergo replicative senescence (Ritchie et al. 1999; Chan et al. 2001). Additionally, the high incidence of telomere fusions in *mec1 tel1* mutants might interfere with the Telo-3C approach (Mieczkowski et al. 2003). The observation that a functional DNA damage checkpoint might be important for proper telomere structure goes in line with the finding that both ATM and ATR transiently localize to human telomeres during late S and G2 phases and are activated there (Verdun & Karlseder 2006; Verdun et al. 2005). This short-term checkpoint activation at telomeres might not only be required for completing replication of telomeres but also for processing telomeric overhangs. Additionally, Verdun and Karlseder showed that the checkpoint activation in turn transiently recruits the HDR machinery, which assists in t-loop formation (Verdun & Karlseder 2006). Accordingly, I found that in yeast cells lacking *RAD51* or *RAD52* the telomere-subtelomere interaction frequency was diminished (Figure 15). Importantly, BRCA2, the functional homolog of yeast Rad52 which is required for RAD51 loading in mammalian cells, was also described to bind telomeres in S phase (Badie et al. 2010). Furthermore, the loss of BRCA2 and RAD51 in mouse embryonic fibroblasts was connected to a telomere fragility phenotype and telomere dysfunction–induced foci (TIFs) accumulated in these cells (Badie et al. 2010). This study further underlines the importance of the HDR machinery at undamaged telomeres, possibly assisting in t-loop formation.

The action of HDR factors at telomeres needs to be tightly controlled. In case a Holliday junction is formed by branch migration at the d-loop, its resolution could result in the deletion of the t-loop or telomere fold-back and therefore big portions of the telomere might get lost (reviewed in De Lange 2004; Lustig 2003; Wright et al. 2018). In *S. cerevisiae* mutants carrying a truncated version of Rap1, the over-elongated telomeres of this mutant undergo rapid deletions and a structure similar to the t-loop was proposed as an intermediate during this process (Kyrion et al. 1992). Likely, the telomere binding protein complex fulfills the role of regulating and restricting the activity of HDR proteins at telomeres (De Lange 2004). Indeed, *in vitro* experiments revealed that TRF2 can inhibit telomeric d-loop formation by Rad51, while TRF1 can promote it, which supports a tight regulation of HDR factors at telomeres (Bower & Griffith 2014).

4.5.1 The three-state model for telomere protection

One aim of this thesis was to gain insight into the functional implications of telomere folding in budding yeast. Poschke et al. implicated the fold-back structure at yeast telomeres in end protection (Poschke et al. 2012). Telomere folding might protect telomeres from excessive resection, specifically when they are uncapped (Poschke et al. 2012). In mammalian cells, the t-loop was proposed to convey a protective function by restricting nucleases and DNA repair activities at telomeres (Griffith et al. 1999). There is evidence that supports a role of the t-loop in suppressing an ATM-mediated DNA damage response at telomeres (Van Ly et al. 2018; Cesare et al. 2013; Benarroch-Popivker et al. 2016). Despite the activation of the DNA damage response at telomeres lacking a t-loop structure, these telomeres are not subject to telomere fusions (Van Ly et al. 2018; Cesare et al. 2013; Benarroch-Popivker et al. 2016).

In order to dissect the interplay between telomere structure, telomere-telomere fusions (T-TFs) and the DNA damage checkpoint, T-TF levels were addressed in mutants defective for telomere folding in collaboration with the Prado lab (Marta Barrientos-Moreno, CABIMER, Seville, Spain) (**Figure 24**). We did not observe an increased incidence of T-TFs in cells lacking the described telomere folding regulators Sir2, Sin3 and Set2 (**Figure 24**). Moreover, when telomerase was deleted in addition to these histone modifiers, T-TFs did not increase. We observed the same behavior in cells depleted of the checkpoint kinase Rad53, where telomere folding occurs much less frequently (**Figure 24**). These data suggest that the NHEJ repair pathway cannot act on unfolded telomeres and they remain protected from fusions. Telomere folding also does not suppress the incidence of T-TFs under circumstances when telomeres are prone to fuse, such as in a *mec1 tel1* background (**Figure 24**). Therefore, we conclude that even when telomeres have lost their

protective capacities against fusions, telomere folding does not act as an additional layer of protection to prevent them.

These unfolded, but non-fusogenic yeast telomeres might have similarities with “intermediate” state telomeres, that have been outlined as part of a three-state model for human telomere protection (Cesare & Karlseder 2012; Cesare et al. 2009). In this model, telomeres exist in an either “closed”, “intermediate” or “uncapped” state. In the fully capped, “closed” state, the presence of a t-loop was suggested to prevent the activation of an ATM-dependent DNA damage response at telomeres. At “closed” state telomeres, t-loops and shelterin proteins collaborate to inhibit repair activities (as in Figure 28A top). In the “intermediate” state, a telomere activates a DNA damage response likely due to the loss of the protective t-loop structure at the chromosome end. This state, however, still retains the capacity to suppress fusions. At “intermediate” state telomeres, the presence of mammalian Rap1 was suggested to act as a backup mechanism when t-loop mediated protection is compromised (Benarroch-Popivker et al. 2016). This “intermediate” state might correspond to the observed yeast telomeres lacking a folded structure but being resistant to NHEJ (Figure 28B). In the “uncapped” state, telomeres are fully dysfunctional, telomere folding is not maintained and telomeres might be subject to repair activities including telomere fusions (Figure 28A bottom). In human cells, “uncapped” telomeres were associated with situations where telomeres are not covered by sufficient levels of shelterin or when telomeres erode in the absence of telomerase until telomeric crisis (Cesare & Karlseder 2012).

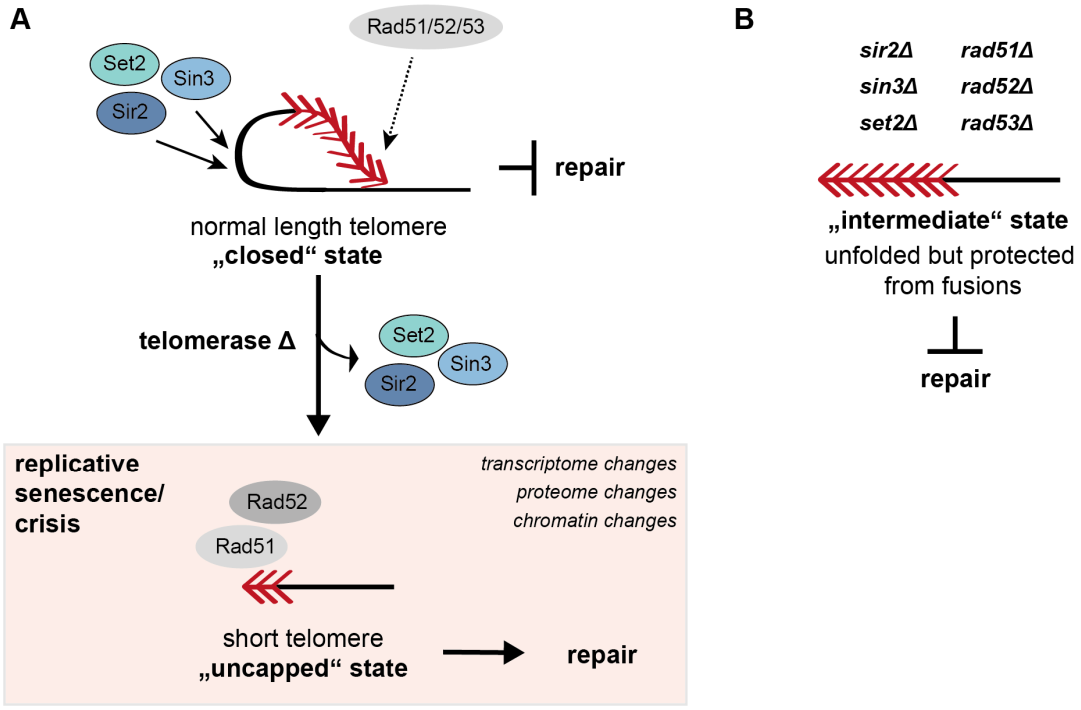

Figure 28. A three-state model for telomere protection in budding yeast. (A) Telomere folding is promoted by chromatin modifiers, the checkpoint kinase Rad53 and the recombinases, Rad51 and Rad52. Telomeres are refractory to DNA repair activities when they are in a "closed" state. Upon telomerase knockout and cells entering replicative senescence and crisis, the loss of the chromatin modifiers Sir2, Sin3 and Set2 might contribute to the maintenance of an open state. Short and "uncapped" telomeres are in an unfolded state, get processed and associate with recombination factors. Due to the absence of Sin3, Set2 and Sir2, a fold-back might not be established and hence the telomeres are channeled into homology-directed repair. The transition towards an "uncapped" telomere state is part of transcriptome, proteome and chromatin changes during senescence. **(B)** When certain telomere folding regulators are lacking, telomeres transition to an unfolded state in which they remain protected from telomere fusions. Sir2, Sin3, Set2, Rad51, Rad52 and Rad53 are among the tested telomere folding regulators. The unfolding of functional telomeres does not result in telomere repair and telomeres remain capped. This thereby resembles the "intermediate" state that has been described in human cells. Red arrowheads represent telomeric repeats.

My data support a model where specific histone modifiers establish a certain heterochromatin state at the telomere and collaborate with DDR and HDR factors to promote a folded telomere (**Figure 28A top**). The presence of the histone modifiers Sir2, Sin3 and Set2, as well as Rad51, Rad52 and Rad53, is required for a successful establishment of telomere folding (**Figure 28A top**). In wt yeast cells, DNA damage checkpoint factors, such as Rad53, and the HDR machinery (including Rad51 and Rad52) might only transiently associate with telomeres (**Figure 28A top**). There, they may assist in establishing a telomere fold-back structure including a potential strand invasion of the 3' overhang. In this scenario, telomere folding might prevent sister chromatid exchanges between telomeres and/or limit excessive resection, which corresponds to a "closed" telomere state (**Figure 28A top**). However, when either Sir2, Sin3 or Set2 are absent, telomeres do not fold-back efficiently and the telomeric chromatin is likely altered. I believe that this situation might represent "intermediate" state telomeres which have lost the folded structure but still suppress telomere fusions and other DNA repair activities (**Figure 28B**). Telomeres would also be in an "intermediate"

state when the checkpoint kinase Rad53 is depleted, and possibly also when Rad51 and Rad52 are missing (Figure 28B).

When telomerase negative cells enter replicative senescence and crisis, telomeres do not fold-back efficiently and this drastic reduction of telomere folding during crisis might be similar to the "uncapped" telomere state (Figure 28A bottom). Concomitantly, the levels of Sin3 and Set2 were reduced and Sir2 becomes modified. Therefore, the loss of these histone modifiers might contribute to the maintenance of an open telomere state during senescence (Figure 28A bottom). Thereby, the absence of the histone modifiers might either be the key event that provokes telomere unfolding or it may assist in maintaining an unfolded state and rather play a supportive role. The transition to "uncapped" state telomeres during replicative senescence and crisis comes along with global transcriptome, proteome and epigenetic changes, which I refer to as the senescence program (Figure 28A bottom). I hypothesize that due to the opening of telomere folding and additional telomere uncapping during senescence, these telomeres are subject to nuclease processing which allows for a more permanent accumulation of Rad51 and Rad52, as it was previously shown (Figure 28A bottom) (Fallet et al. 2014). In this scenario, when telomeres are in the "uncapped" state, the HDR factors Rad51 and Rad52 cannot promote telomere folding, possibly because the chromatin modifiers Sir2, Sin3 and Set2 are not present. The association of Rad51 and Rad52 with the "uncapped" telomeres then rather mediates homology search, strand invasion and homology directed repair for re-elongation via sister-chromatid exchanges and break-induced replication. The degree of telomere resection might be a major difference between "intermediate" and "uncapped" state telomeres. While the telomeres of the tested folding defective mutants are likely not subject to increased resection (shown for *sin3* in Poschke et al. 2012), the uncapped telomeres arising during senescence are characterized by more excessive resection (Fallet et al. 2014).

4.6 Possible functions of telomere folding in budding yeast

As proposed in the three-state model for telomere protection, the human t-loops contribute to safeguard the stability of chromosome ends. The folded structures at budding yeast telomeres might be regulated in a similar way (section 4.5.1). However, its function is less clear and several roles have been proposed for it. In the following, I will address two possible models for the function of telomere folding and discuss them with respect to the data obtained in this doctoral dissertation. These models concern telomere folding as a stress sensor and the telomere fold-back structure as a domain for replication timing control.

4.6.1 Telomere folding as a stress sensor regulating gene expression

The heterochromatic environment at telomeres regulates the silencing of subtelomeric genes which has been described as telomere position effect (TPE). This characteristic feature is a part of functional telomeres in many organisms (Baur et al. 2001; Levis et al. 1985; Russell & Nurse 1986). More recently, the idea that the telomeric repeats can regulate gene expression at more distant loci was put forward in studies using human cells (Robin et al. 2014). Via the physical interaction of a telomere with loci of several Mb distance, the proximity of the telomeric heterochromatin might impose transcriptional silencing at these regions, which was dubbed telomere position effect over long distances (TPE-OLD) (Robin et al. 2014). In budding yeast, telomere folding has been implicated in promoting a heterochromatin environment at telomeres, and might therefore regulate subtelomeric gene expression (Grunstein 1997). The previously observed discontinuous SIR protein association at yeast telomeres could indicate that the heterochromatin establishment at subtelomeres might not simply be based on a spreading mechanism (Ellahi et al. 2015). Instead, it is possible to imagine that the loci with increased SIR complex association result from the telomeric repeats coming into proximity, implying a folded structure (Figure 29). This idea is supported by the finding that only a small number of subtelomeric genes are silenced in a SIR-dependent manner and additional mechanisms might be in place to regulate their expression (Ellahi et al. 2015; Wyrick et al. 1999). The Telo-3C results revealed, that the relationship between heterochromatin at subtelomeres and telomere folding might be complex (section 4.3). In situations where TPE was shown to be drastically impaired, such as in mutants of the yKu complex, no telomere folding defect was observed (Figure 18). *Vice versa,* a reduced telomere-subtelomere interaction frequency does not necessarily lead to the desilencing of telomeres, as observed in *sin3* or *set2* mutants (Figure 20).

The senescence program in budding yeast appears to be similar to a the general response of cells to stress, as shown by genome-wide expression studies (Nautiyal et al. 2002). Accordingly, decreased telomere folding was observed during replicative senescence and upon MMS treatment, when a stress and a DNA damage response were induced (Figure 17, Figure 22). Thus, telomere structure might respond similarly to prolonged stress conditions (Figure 29). Both after MMS treatment and during senescence, the stress response is coupled to a cell cycle arrest. Remarkably, genes located within the subtelomere are among the most highly divergent genes and some subtelomeric gene clusters tend to be expressed specifically under stressful conditions (Ai et al. 2002; Harrison et al. 2002; Teytelman et al. 2008). This is consistent with the idea that certain subtelomeric genes are required for the response to stressful environments (Louis & Becker 2014). Thus, many situationally expressed genes are located within subtelomeric regions and were

reported to respond to stress, metabolic changes or non-standard growth conditions (Ai et al. 2002; Robyr et al. 2002; Smith et al. 2011).

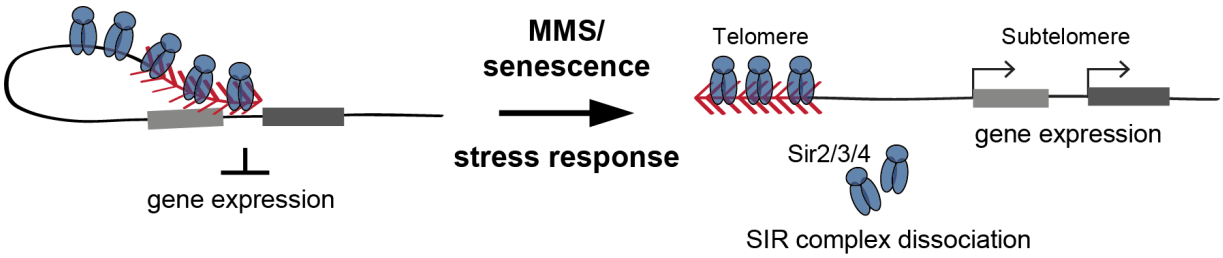

Figure 29: Telomere folding might act as a stress sensor to regulate subtelomeric gene expression. Telomere folding might contribute to the silencing of subtelomeric genes (grey boxes) by bringing these genes into close proximity to the telomeric repeats and the associated SIR complexes (left). The exposure to MMS or replicative senescence trigger a stress response and telomeres might serve as epigenetic stress sensors. The stress response correlates with the re-distribution of the SIR complexes within the nucleus and their dissociation from subtelomeres. Additionally telomere folding is compromised under these conditions and the transcription of subtelomeric stress-response genes gets promoted (right). Telomeric repeats are represented as red arrow heads.

Based on these observations, it is possible that the opening of telomere folding is part of a stress response and contributes to the desilencing of certain stress-related subtelomeric genes (**Figure 29**). I hypothesize that the telomere fold-back might affect gene expression of genes near "interaction points" of the folded structure, similar to what has been described as TPE-OLD in human cells (Robin et al. 2014). As mentioned above (section 4.4), a DNA damage response in budding yeast often comes along with the redistribution of telomeric proteins within the nucleus (Martin et al. 1999; Mills et al. 1999), which might also contribute to the proposed mechanism of desilencing stress-response genes at subtelomeres (**Figure 29**). Interestingly, human telomeres have been proposed to act as epigenetic stress sensors (Cesare & Karlseder 2012). This was described in the context of senescence, where shortening telomeres elicit a DNA damage response emitted by "intermediate" state telomeres. It was hypothesized that these stress signals cause a shift in chromatin structure, histone production and might induce the senescence program (Suram et al. 2012; Cesare & Karlseder 2012; O'Sullivan et al. 2010). Telomeres were also proposed to act as stress sensors upon prolonged mitotic arrest which was induced by different, telomere-unrelated means in human cells (Hayashi et al. 2012). In this scenario, telomeres were suggested to transition from the "closed" state to an "intermediate" state, losing the t-loop structure, and might contribute to ensure growth arrest and limit genome instability (Cesare & Karlseder 2012; Hayashi et al. 2012).

As discussed above, subtelomeric gene silencing mechanisms and telomere folding might be influencing each other (Pryde & Louis 1999; Grunstein 1997). However, it is very complicated to separate these two processes. Indeed, the question for the cause and consequence in the relationship of telomere folding and heterochromatin establishment still remains unresolved.

Nevertheless, the telomere fold-back might contribute to promoting a healthy telomere environment that can perform all of its necessary functions.

4.6.2 The telomere fold-back as a domain for replication timing control

The second potential model for the function of telomere folding concerns the timing of replication origin firing during S phase. Even though cells can tolerate perturbations in the replication timing program to a certain extent, the timing of origin firing is tightly regulated by highly conserved mechanisms. These mechanisms include chromatin environment and architecture, subnuclear positioning and the competition for limiting factors (reviewed in Yoshida et al. 2013). It is believed that the replication timing program coordinates transcription and replication and co-regulates replication and DNA repair activities. The misregulation of replication timing was proposed to contribute to replication stress and was shown to undergo drastic changes during development, underscoring the importance of proper control of early and late replication initiation (Aladjem et al. 2002; Kitsberg et al. 1993; Simon et al. 2001; Hiratani et al. 2008).

In budding yeast, replication origins cluster in replication foci within the nuclear space, similar to what has been described as early- and late-replicating domains in mammalian cells (Lengronne 2001; Pasero et al. 1997; Méchali 2010). Therefore, the higher-order organization of chromosomes might influence the late and early replication of origins. The replication clusters are not only regulated by the spatial organization of chromosomes but also by *cis* acting factors, such as the Forkhead box transcription factors Fkh1 and Fkh2 (Knott et al. 2012). Fkh1 and Fkh2 were shown to bind to early replication origins and might tether these together, forming early replication clusters which were also observed in Hi-C maps (Lõoke et al. 2013; Knott et al. 2012; Duan et al. 2010). Thereby, Fkh1 and Fkh2 advance origin firing and regulate early replication (Witten & Noble 2012; Tjong et al. 2012).

Interestingly, several of the telomere folding regulators identified in this thesis were implicated in the regulation of replication timing. The unfolding of the telomere fold-back structure seems to correlate with defects in replication timing control. Histone deacetylation was generally observed to delay replication initiation and especially the SIR and Rpd3 histone deacetylase complexes were implicated in replication timing control (Yoshida et al. 2014; Knott et al. 2009; Stevenson & Gottschling 1999; Vogelauer et al. 2002; Zappulla et al. 2002; Aparicio 2013). The SIR complex was shown to repress the early firing of telomere-proximal origins (Stevenson & Gottschling 1999). However, the deletion of *SIR2* also results in a general repression of all origins genome-wide, suggesting a different role of Sir2 at non-telomeric origins (Yoshida et al. 2014). In cells lacking several components of the Rpd3 complex, including Sin3, the genome-wide replication of late

origins is anticipated (Vogelauer et al. 2002; Aparicio et al. 2004; Knott et al. 2009; Yoshida et al. 2014). This might be different for telomere-proximal regions, as some of them were reported not to be affected by *RPD3* deletion (Aparicio et al. 2004). Also H3K36 methylation by Set2 was implicated in replication timing control (Pryde et al. 2009). Interestingly, Pryde at al. found that H3K36 mono-methylation (H3K36me1) and tri-methylation (H3K36me3), both placed by Set2, seem to have opposing effects on replication origin firing (Pryde et al. 2009). H3K36me1 increases at origins around the time of their firing, indicating that H3K36me1 might have a positive effect on replication initiation (Pryde et al. 2009). Conversely, early origins are depleted of H3K36me3 genome-wide compared to later firing origins (Pryde et al. 2009). Therefore, the authors suggest an inhibitory function of this modification on origin firing (Pryde et al. 2009).

Other scenarios where telomere folding is defective, such as telomere shortening during senescence or upon Rad53 depletion, correlate with the early firing of late replication origins. While yeast telomeres normally replicate late in S phase (Raghuraman 2001), short telomeres are characterized by early origin firing (Bianchi & Shore 2007a). Upon Rad53 inactivation, late origins fire earlier genome-wide, while the firing of early origins is not affected when Rad53 is not functional (Forey et al. 2020). Thus, the Mec1-Rad53 pathway delays the activation of later origins (Forey et al. 2020; Santocanale & Diffley 1998). Interestingly, a finding from the genome-wide screen for telomere folding regulators might also point towards a possible connection between telomere folding and replication timing control (Poschke et al. 2012). The transcription factor Fkh2 was identified as a potential regulator of telomere folding and is involved in clustering and activating early origins (Lõoke et al. 2013; Knott et al. 2012).

The interplay of the effects that all of the mentioned factors have on replication timing is complex and could also be indirect in some cases. However, it is interesting that the telomere folding defects in the addressed conditions, correlate with alterations in the replication timing program of these mutants. In order to find a possible explanation for this correlation, I want to address a model for the replication timing control via the telomeric protein Rif1. Even though Rif1 is not generally considered a telomere associated protein in mammalian cells, most of Rif1's non-telomeric functions are conserved from yeast to human, so is its role in DNA repair and DNA replication initiation (Yamazaki et al. 2012; Cornacchia et al. 2012; Hiraga et al. 2014; Davé et al. 2014; Mattarocci et al. 2014; Peace et al. 2014; Hiraga et al. 2017; Foti et al. 2016; Alver et al. 2017). Rif1 binds to the replication origins that it controls and inhibits their firing (Hafner et al. 2018; Lian et al. 2011). It is specifically involved in ensuring the late origin firing of telomere-proximal origins (within 50 kb from the repeats) (Hafner et al. 2018; Lian et al. 2011). Therefore, in *rif1* mutants the telomere-proximal origins that normally replicate late, fire earlier in S phase (Lian et al. 2011). Rif1

is sequestered at telomeres via its interaction with Rap1 (Mishra & Shore 1999). This sequestration limits the activity of Rif1 to the loci close to telomeres, where Rif1 is present in high concentrations, and prevents origin repression at other sites throughout the genome. Hafner et. al propose a model where the increased Rif1 concentration around telomeres creates a late-replicating "zone" for all telomere-proximal origins within that domain (Figure 30). Interestingly, this model is supported by Rif1-ChIP experiments in *S. cerevisiae*, where Rif1 binding was not only detected at the telomeric repeats themselves but also several kb into the subtelomere (Hiraga et al. 2018).

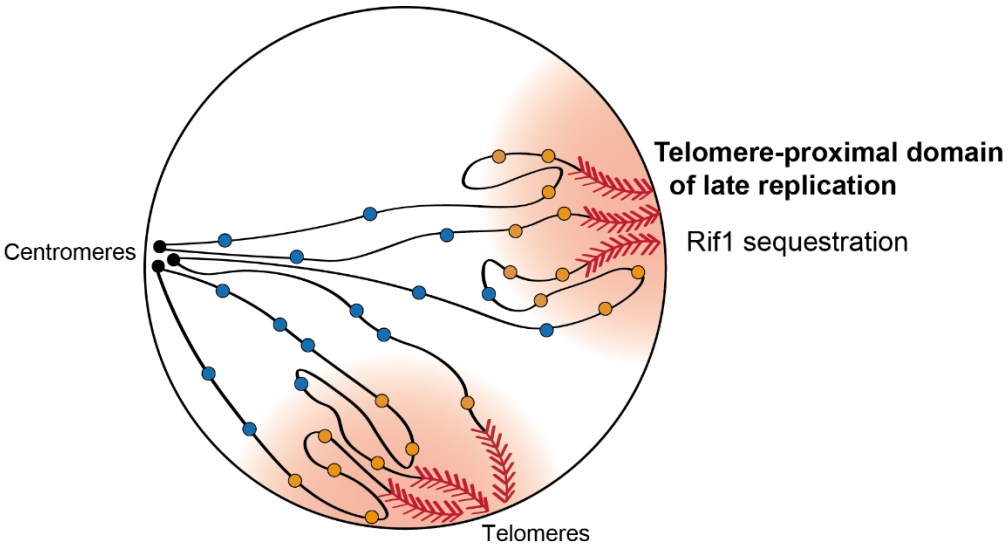

Figure 30: Telomere folding might contribute to the regulation of replication timing. Telomere folding might contribute to replication timing control by forming a replication timing domain for telomere-proximal origins. The late replication of telomere-proximal origins is mainly regulated by the binding of Rif1. Rif1 gets sequestered at telomeres via its interaction with the direct telomere binder Rap1. The telomere fold-back structure might additionally regulate the access of Rif1 to these telomere-proximal origins. Telomeric repeats are depicted as red arrow heads. Rif1-bound origins are shown in orange. Blue circles represent all other origins, not bound by Rif1. Figure and legend adapted from Hafner et al. 2018; Hafner et al. 2019.

It is not clear which mechanism brings Rif1 to the origins that it controls. It was proposed that Rif1 might diffuse away from the telomere and bind to telomere-proximal origins. Additionally, no enrichment motif for sequence-specific Rif1 binding was detected and no co-factor, except for Rap1, was identified that might recruit Rif1 to these origins (Hafner et al. 2019; Hafner et al. 2018). Chromatin or chromosome structures might support Rif1 binding to the origins that it regulates. I hypothesize that telomere folding might contribute to the establishment of this late-replicating domain at chromosome ends, by bringing Rif1-controlled origins into proximity of the telomeric repeats (Figure 30). Since telomeres of *rif1* mutants are proficient for folding (Figure 14), this model might not appear plausible as an explanation for how telomere folding contributes to a Rif1-dependent late-replicating zone around telomeres. However, even though Rif1 does not seem to be involved in the establishment of telomere folding, the telomere fold-back structure might contribute to the correct localization of Rif1 to the origins that it regulates. Telomere folding would

then support the positioning of Rif1 within the late-replicating zone in close proximity to the telomeric repeats.

Recently, an N-terminal DNA binding domain of Rif1 (Rif1-NTD) has been characterized as promoting DNA association independently from Rap1 (Mattarocci et al. 2017). This domain was shown to be important for Rif1's role in DNA repair but also for telomere homeostasis (Mattarocci et al. 2017). Rif1-NTD preferentially associates with ss-dsDNA junctions but has no sequence preference (Mattarocci et al. 2017). It has a hook-like, elongated structure, forming a head-to-tail dimer when crystallized together with DNA (Mattarocci et al. 2017). Interestingly, the dimer builds two channels accommodating two strands of DNA. Since Rif1 dimers can bind two DNA helices, it is tempting to speculate that this interaction might promote higher-order structures (Fontana et al. 2018). Even though the presence of Rif1 is not necessary for telomere folding to occur, Rif1 could still participate in the folded structures at telomeres encasing DNA strands.

4.7 Conclusions

In summary, my data indicate that the mechanism by which telomere folding is established might be different from canonical chromatin loops according to the loop extrusion model. Instead, folded telomere structures might rather be supported by a compartmentalization process driving the formation of heterochromatin domains at chromosome ends. The presence of these heterochromatin domains is supported by the finding that the chromatin modifiers Sir2, Sin3 and Set2 are required for telomere folding. Additionally, I have determined the checkpoint kinase Rad53 and the homologous recombination machinery, comprising the factors Rad51 and Rad52, as key folding regulators of budding yeast telomeres. The finding the HDR machinery may assist in the formation of the fold-back structure implies a potential strand invasion of the 3' overhang, resembling mammalian t-loops.

The results presented in this thesis are consistent with the three-state model for telomere protection where telomeres might exist in a "closed", an "intermediate" or an "uncapped" state. Yeast telomeres might transition from a folded, "closed" state to an unfolded, "intermediate" state when key telomere folding regulators are lacking. Importantly, "intermediate" state telomeres retain the ability to suppress telomere fusions. On the contrary, unfolded telomeres during replicative senescence and crisis might rather resemble an "uncapped" state where telomeres are deprotected and subject to processing.

I discussed two possible models for the function of telomere folding in *S. cerevisiae* that are in accordance with data presented in this thesis. On the one hand, the telomere fold-back structure

may serve as a stress sensor which unfolds upon a stress response and possibly contributes to the regulation of subtelomeric gene expression. One the other hand, it is tempting to speculate that the telomere fold-back structure might be a domain for replication timing control. In this role, telomere folding might contribute to the control of the late firing of telomere-proximal replication origins, potentially by mediating Rif1 binding.

5 Materials and Methods

5.1 Materials

5.1.1 Yeast strains

All yeast strains used in this work were derived from the *Saccharomyces cerevisiae* strain BY4741 (*MATa his3Δ1 leu2Δ0 met15Δ0 ura3Δ0*) (Winston et al. 1995). BY4741 is a derivative of the laboratory strain S288C (Mortimer & Johnston 1986). As indicated, many of the strains were taken or derived from the "*Saccharomyces* Genome Deletion Project" (Winzeler et al. 1999; Giaever et al. 2002; Wach et al. 1994). The "Yeast Mat a knockout collection" and the "Yeast Mat alpha knockout collection" were purchased from Dharmacon/ Horizon Discovery. Strains carrying endogenously TAP-tagged ORFs were derived from the "Yeast TAP-tagged ORFs collection" (Ghaemmaghami et al. 2003), purchased from Dharmacon/ Horizon Discovery. All deletions and the endogenous tagging of genes were confirmed by PCR.

Strain number	Name	Genotype	Figure	Source
yBL7	*wildtype*	*MATa; his3Δ1; leu2Δ0; ura3Δ0; met15Δ0*	Figure 10, Figure 11, Figure 14, Figure 15, Figure 18, Figure 20, Figure 22	Euroscarf
yMD1245	*tlc1* het. diploid	*MATa/MATalpha; his3Δ1/his3Δ1; leu2Δ0/leu2Δ0; ura3Δ0/ura3Δ0; MET15/met15Δ0; LYS2/lys2Δ0; TLC1/tlc1::HIS3*	Figure 17, Figure 19, Figure 21	Luke lab collection
yTW101	*upf1*	*MATa; his3Δ1; leu2Δ0; ura3Δ0; met15Δ0; upf1::KAN*	Figure 18	Dharmacon/ Horizon Discovery
yTW105	*ku70*	*MATa; his3Δ1; leu2Δ0; ura3Δ0; met15Δ0; ku70::KAN*	Figure 18	Dharmacon/ Horizon Discovery
yTW102	*mre11*	*MATa; his3Δ1; leu2Δ0; ura3Δ0; met15Δ0; mre11::KAN*	Figure 18	Dharmacon/ Horizon Discovery
yTW104	*tel1*	*MATa; his3Δ1; leu2Δ0; ura3Δ0; met15Δ0; tel1::KAN*	Figure 18	Dharmacon/ Horizon Discovery
yTW103	*rad50*	*MATa; his3Δ1; leu2Δ0; ura3Δ0; met15Δ0; rad50::KAN*	Figure 18	Dharmacon/ Horizon Discovery
yAL129	*tlc1*	*MATa; his3Δ1; leu2Δ0; ura3Δ0; met15Δ0; tlc1::NAT*	Figure 18	Luke lab collection

yTW50	*sir2*	*MATa; his3Δ1; leu2Δ0; ura3Δ0; met15Δ0; sir2::KAN*	Figure 20	Dharmacon/ Horizon Discovery
yTW409	*sin3* het. diploid	*MATa/MATalpha; his3Δ1/his3Δ1; leu2Δ0/leu2Δ0; ura3Δ0/ura3Δ0; MET15/met15Δ0; LYS2/lys2Δ0; SIN3/sin3::KAN*	Figure 20	This thesis
yTW385	*set2* het. diploid	*MATa/MATalpha; his3Δ1/his3Δ1; leu2Δ0/leu2Δ0; ura3Δ0/ura3Δ0; MET15/met15Δ0; LYS2/lys2Δ0; SET2/set2::KAN*	Figure 20	Dharmacon/ Horizon Discovery
yLP115	*SIN3-TAP tlc1* het. diploid	*MATa/MATalpha; his3Δ1/his3Δ1; leu2Δ0/leu2Δ0; ura3Δ0/ura3Δ0; MET15/met15Δ0; LYS2/lys2Δ0; SIN3/SIN3-TAP-HIS3; TLC1/tlc1::NAT*	Figure 20	Luke lab collection
yLP113	*SET2-TAP tlc1* het. diploid	*MATa/MATalpha; his3Δ1/his3Δ1; leu2Δ0/leu2Δ0; ura3Δ0/ura3Δ0; MET15/met15Δ0; LYS2/lys2Δ0; SET2/SET2-TAP-HIS3; TLC1/tlc1::NAT*	Figure 20	Luke lab collection
yTW51	*sin3*	*MATa; his3Δ1; leu2Δ0; ura3Δ0; met15Δ0; sin3::KAN*	Figure 20	Dharmacon/ Horizon Discovery
yTW75	*set2*	*MATa; his3Δ1; leu2Δ0; ura3Δ0; met15Δ0; set2::KAN*	Figure 20	Dharmacon/ Horizon Discovery
yTW209	*sir2 tlc1* het. diploid	*MATa/MATalpha; his3Δ1/his3Δ1; leu2Δ0/leu2Δ0; ura3Δ0/ura3Δ0; met15Δ0/met15Δ0; LYS2/lys2Δ; SIR2/sir2::KAN; TLC1/tlc1::NAT*	Figure 24	This thesis
yTW203	*sin3 tlc1* het. diploid	*MATa/MATalpha; his3Δ1/his3Δ1; leu2Δ0/leu2Δ0; ura3Δ0/ura3Δ0; met15Δ0/met15Δ0; LYS2/lys2Δ; SIN3/sin3::KAN; TLC1/tlc1::NAT*	Figure 24	This thesis
yTW201	*set2 tlc1* het. diploid	*MATa/MATalpha; his3Δ1/his3Δ1; leu2Δ0/leu2Δ0; ura3Δ0/ura3Δ0; met15Δ0/met15Δ0; LYS2/lys2Δ; SET2/set2::KAN; TLC1/tlc1::NAT*	Figure 24	This thesis
yKB244	wildtype	*MATa; his3Δ1; ura3Δ0; met15Δ0; leu2::pGPD-AFB2::LEU2*	Figure 13	Luke lab collection
yTW188	*SMC6-AID*-9MYC*	*MATa; his3Δ1; ura3Δ0; met15Δ0; leu2::pGPD-AFB2::LEU2; SMC6-AID*-9MYC::HYG*	Figure 13	This thesis
yTW190	*SMC1-AID*-9MYC*	*MATa; his3Δ1; ura3Δ0; met15Δ0; leu2::pGPD-AFB2::LEU2; SMC1-AID*-9MYC::HYG*	Figure 13	This thesis
yTW273	*SMC4-AID*-9MYC*	*MATa; his3Δ1; ura3Δ0; met15Δ0; leu2::pGPD-AFB2::LEU2; SMC4-AID*-9MYC::HYG*	Figure 13	This thesis
yTW57	*rif1*	*MATa; his3Δ1; leu2Δ0; ura3Δ0; met15Δ0; rif1::KAN*	Figure 14	Dharmacon/ Horizon Discovery

yTW58	*rif2*	*MATa; his3Δ1; leu2Δ0; ura3Δ0; met15Δ0; rif2::KAN*	Figure 14	Dharmacon/ Horizon Discovery
yBL301	*rad51*	*MATa; his3Δ1; leu2Δ0; ura3Δ0; met15Δ0; rad51::KAN*	Figure 15	Luke lab collection
yBL276	*rad52*	*MATa; his3Δ1; leu2Δ0; ura3Δ0; rad52::KAN*	Figure 15	Luke lab collection
yAM208	*wildtype*	*MATa; his3Δ1; leu2Δ0; ura3Δ0; met15Δ0; bar1::KAN*	Figure 16	Dharmacon/ Horizon Discovery
yDB212	*RAD53-AID*-9MYC*	*MATa; his3Δ1; ura3Δ0; met15Δ0; bar1::NAT; leu2::pGPD-AFB2::LEU2; RAD53-AID*-9MYC::HYG*	Figure 16	Luke lab collection
yTW389	*wildtype*	*MATa; his3Δ1; leu2Δ0; ura3Δ0; met15Δ0; lys2Δ0*	Figure 16	This thesis
yTW393	*sml1*	*MATa; his3Δ1; leu2Δ0; ura3Δ0; lys2Δ0; met15Δ0; sml1::KAN*	Figure 16	This thesis
yTW397	*sml1 mec1*	*MATa; his3Δ1; leu2Δ0; ura3Δ0; met15Δ0; sml1::KAN; mec1::HIS3*	Figure 16	This thesis
yTW256	*SIN3-TAP*	*MATa; his3Δ1; leu2Δ0; ura3Δ0; SIN3-TAP-HIS3*	Figure 20, Figure 22	This thesis
yTW259	*SIN3-TAP tel1*	*MATa; his3Δ1; leu2Δ0; ura3Δ0; met15Δ0; SIN3-TAP-HIS3; tel1::KAN*	Figure 20	This thesis
yTW267	*SET2-TAP*	*MATa; his3Δ1; leu2Δ0; ura3Δ0; met15Δ0; SET2-TAP-HIS3*	Figure 20, Figure 22	This thesis
yTW264	*SET2-TAP tel1*	*MATa; his3Δ1; leu2Δ0; ura3Δ0; met15Δ0; SET2-TAP-HIS3; tel1::KAN*	Figure 20	This thesis
yAM208	*bar1*	*MATa; his3Δ1; leu2Δ0; ura3Δ0; met15Δ0; bar1::KAN*	Figure 12	Dharmacon/ Horizon Discovery
yTW289	*SIN3-TAP set2* het. diploid	*MATa/MATalpha; his3Δ1/his3Δ1; leu2Δ0/leu2Δ0; ura3Δ0/ura3Δ0; met15Δ0/met15Δ0; LYS2/LYS2; SET2/set2::KAN; SIN3/SIN3-TAP-HIS*	Figure 23	This thesis
yTW330	*SIN3-TAP sir2* het. diploid	*MATa/MATalpha; his3Δ1/his3Δ1; leu2Δ0/leu2Δ0; ura3Δ0/ura3Δ0; met15Δ0/met15Δ0; LYS2/LYS2; SIR2/sir2::KAN; SIN3/SIN3-TAP-HIS*	Figure 23	This thesis
yTW292	*SET2-TAP sin3* het. diploid	*MATa/Mat alpha; his3Δ1/his3Δ1; leu2Δ0/leu2Δ0; ura3Δ0/ura3Δ0; met15Δ0/met15Δ0; LYS2/LYS2; SIN3/sin3::KAN; SET2/SET2-TAP-HIS*	Figure 23	This thesis
yTW328	*SET2-TAP sir2* het. diploid	*MATa/MATalpha; his3Δ1/his3Δ1; leu2Δ0/leu2Δ0; ura3Δ0/ura3Δ0; met15Δ0/met15Δ0; LYS2/LYS2; SIR2/sir2::KAN; SET2/SET2-TAP-HIS*	Figure 23	This thesis
D36	*mec1 tel1 sml1* het. diploid	*MATa/MATalpha; his3Δ1/his3Δ1; leu2Δ0/leu2Δ0; ura3Δ0/ura3Δ0; met15Δ0/met15Δ0; BAR1/bar1::HYG; SML1/sml1::HYG MEC1/mec1::NAT; TEL1/tel1::KAN*	Figure 24	Barrientos-Moreno et al. 2018

yTW207	*RAD53-AID*-9MYC tlc1* het. diploid	*MATa/Matalpha; his3Δ1/his3Δ1; ura3Δ0/ura3Δ0; met15Δ0/met15Δ0; LYS2/lys2Δ; RAD53/ RAD53-AID*-9MYC::HYG; leu2/leu2::pGPD-AFB2::LEU2 TLC1/tlc1::NAT*	Figure 24	This thesis
D37	*sin3 mec1 tel1 sml1* het. diploid	*MATa/Matalpha; his3Δ1/his3Δ1; leu2Δ0/leu2Δ0; ura3Δ0/ura3Δ0; MET15/met15Δ0; LYS2/lys2Δ0; sml1::HYG/sml1::HYG; MEC1/mec1::NAT; TEL11/tel1::KAN; SIN3/sin3::KAN*	Figure 24	Marta Barrientos-Moreno (Prado lab, CABIMER, Seville, Spain)
D39	*set2 mec1 tel1 sml1* het. diploid	*MATa/Matalpha; his3Δ1/his3Δ1; leu2Δ0/leu2Δ0; ura3Δ0/ura3Δ0; MET15/met15Δ0; LYS2/lys2Δ0; sml1::HYG/sml1::HYG; MEC1/mec1::NAT; TEL11/tel1::KAN; SET2/set2::KAN*	Figure 24	Marta Barrientos-Moreno (Prado lab, CABIMER, Seville, Spain)

5.1.2 Plasmids

The indicated overexpression plasmids were derived from the "Yeast ORF collection" (Gelperin et al. 2005), purchased from Dharmacon/ Horizon Discovery.

Plasmid number	Description	Source
pBL183	pGAL-TAP, 2µ (EV)	Dharmacon/ Horizon Discovery
pBL588	pGAL-Sin3-TAP, 2µ	Dharmacon/ Horizon Discovery
pBL455	pHyg-AID*-9myc	Morawska and Ulrich 2013
pBL488	pHis-AID*-9myc	Morawska and Ulrich 2013
pBL423	TG probe for Southern blot (pSP100)	Kind gift from M.P. Longhese

5.1.3 Oligonucleotides

Oligo number	Sequence (5' – 3')	Direction	Target	Application
oBL207	CACCACACCCACACACCACACCCACA	reverse	TERRA	reverse transcription
oBL292	CCCAGGTATTGCCGAAAGAATGC	forward	*ACT1*	qPCR
oBL293	TTTGTTGGAAGGTAGTCAAAGAAGCC	reverse	*ACT1*	reverse transcription, qPCR
oBL295	CGGTGGGTGAGTGGTAGTAAGTAGA	forward	TERRA from telomere 1L	qPCR
oBL296	ACCCTGTCCCATTCAACCATAC	reverse	TERRA from telomere 1L	qPCR

oBL358	GCGGTACCAGGGTTAGATTAGGGCTG	forward	Telomere 1L	Telomere PCR
oBL359	CGGGATCCGGGGGGGGGGGGGGGGG	reverse	All telomeres	Telomere PCR
oRS64	CCACCACCACATGCCATACT		P5 on telomere 1L	Telo-3C
oRS66	CCCGTTCGTAAAATTGGCGT		P6 on telomere 1L	Telo-3C
oRS68	AGGTACCCTGTTTGAACCAACT		P7 on telomere 1L	Telo-3C
oRS80	TCACATTGCGTCCAACTCCA		P9 on telomere 1L	Telo-3C
oRS39	GGCTGTCAGAATATGGGGCCGTAGTA	forward	Chr. V intergenic	Telo-3C normalization
oRS40	CACCCCGAAGCTGCTTTCACAATAC	reverse	Chr. V intergenic	Telo-3C normalization
oTW84	ATGATATTATTCCATGTGTC		P10, Chr. I	3C
oTW86	GCAATCTCCGCAATAGCAGT		P11, Chr. I	3C
oTW88	TCCTCCCAATAGACTGAGAC		P12, Chr. I	3C
oSM1	GAAGCGGATGGTAATGAGAC	forward	Telomere 1L	Southern blot probe
oSM2	AGATGTATGATGCTGGGGAG	reverse	Telomere 1L	Southern blot probe
ChrV-R-TTF	AAGAATTCGGTAAGAGACAACAGGGCTTGGAGG		Chr. V	T-TF analysis (Mieczkowski et al. 2003)
ChrXV-L-TTF	AAGAATTCTATGGTTAAATGGGGCAGGGTAACG		Chr. XV	T-TF analysis (Mieczkowski et al. 2003)
HIS4-UP	TCTGGCCTCATGGAATAGTAAGAAGGA	forward	*HIS4*	T-TF analysis (Mieczkowski et al. 2003)
HIS4-LO	ATAAACGCCACGACCCAAATCGATG	reverse	*HIS4*	T-TF analysis (Mieczkowski et al. 2003)
oTW78	AAGAAAACTCGTCGAAGATCATAACTTTGGACTTGAGCAATTACGCAGAACGTACGCTGCAGGTCGAC	forward	*SMC1*	Tagging with AID*-9MYC
oTW79	TAGATATTATTAGTTATTTGACGGGTTATAGCAGAGGTTGGTTTCATAGAATCGATGAATTCGAGCTCG	reverse	*SMC1*	Tagging with AID*-9MYC
oTW81	TCCACAGAATGAGAGACCCTGAGAGACAGAATAATTCCAATTTTTATAATCGTACGCTGCAGGTCGAC	forward	*SMC6*	Tagging with AID*-9MYC
oTW82	AATTCAAATAGACGATTACACAATATTTTGAATAATTACATGAAGAAACAATCGATGAATTCGAGCTCG	reverse	*SMC6*	Tagging with AID*-9MYC
oTW95	ATAGAACCAAAAGTACCACGATTAAAAACATAGATATCTTAAACAGAACTCGTACGCTGCAGGTCGAC	forward	*SMC4*	Tagging with AID*-9MYC

oTW96	TAGCATGATATTACAATCAGCAAGTGCTC TTGAATTGATTATTGTACTAGATCGATGA ATTCGAGCTCG	reverse	*SMC4*	Tagging with AID*-9MYC
oDB19	ACTAAACGACTTGGTAGAGTCAC	forward	*RAD53*	Tagging with AID*-9MYC
oDB20	AGCTTGTTGTACCACATCAAGCA	reverse	*RAD53*	Tagging with AID*-9MYC
oBL29	CTGCAGCGAGGAGCCGTAAT	reverse	TEF promoter	Tagging/KO confirmation
oBL30	GAATCGCAGACCGATACC	forward	KanR	Tagging/KO confirmation
oTW4	AACCCGGGGATCCGTCGACC	reverse	TAP-tag	confirmation
oTW10	AGTACGGGTAATGATATCGGATTTT	forward	*SIN3*	KO
oTW11	TAGGAAGTATAAAAGGAAGGGCAGT	forward	*RIF2*	KO confirmation
oTW13	CTTTTCCAAGCTACATCTAGCACTC	forward	*SIR2*	KO confirmation
oTW18	CAGGAAACAGCTATGAC	reverse	M13	Sanger sequencing
oTW19	GTAAAACGACGGCCAG	forward	M13	Sanger sequencing
oTW46	TTTAGTATCATCAGTTTCCCTTTGC	forward	*UPF1*	KO confirmation
oTW48	ATAACCATGCATCTTGCAATACTTT	forward	*RAD50*	KO confirmation
oTW49	TAGACGGACTCATAATTGAATGGTT	forward	*YKU70*	KO confirmation
oTW64	GAGAAGAAGCTGACTTCGACTATTG	forward	*SET2*	KO confirmation
oTW65	CACATGATATTATGAGCGTGATAGG	forward	*TEL1*	KO confirmation
oTW66	GTTCACAAGCAAGCCTGTAAATAAT	forward	*MRE11*	KO confirmation
oTW80	AACGTCCAGAGAATTGCTGC	forward	*SMC1*	Tagging confirmation
oTW83	TTGCGTTGGACGAATTCGAC	forward	*SMC6*	Tagging confirmation
oTW97	AGATGCCGCTCTGGATTTCA	forward	*SMC4*	Tagging confirmation
oTW116	TGTGCCAAAGCAGTGAACCT	forward	*SIN3*	KO confirmation
oTW117	ACCACATCCTTTCACTTCCC	reverse	*SIN3*	KO confirmation
oTW115	GTGAATCACTAGACGATTTTGGAGT	reverse	*SIN3*	KO

5.1.4 Media

5.1.4.1 Liquid media

Medium	Composition
Luria broth (LB) medium	10 g/l NaCl 10 g/l Bacto tryptone 5 g/l Bacto yeast extract
YPD medium	20 g/l peptone 10 g/l Bacto yeast extract 20 g/l glucose
Synthetic complete (SC) medium w/o amino acid	1.92 g/l Yeast synthetic dropout medium without amino acid 6.7 g/l Yeast nitrogen base without amino acids 20 g/l Glucose/ Galactose/ Raffinose

Sporulation (SPO) medium	5 mg/l zinc acetate 10 g/l potassium acetate

5.1.4.2 Agar plates

Medium	Composition
LB plates	10 g/l NaCl 10 g/l Bacto tryptone 5 g/l Bacto yeast extract 15 g/l Agar
SC plates w/o amino acid	1.92 g/l Yeast synthetic dropout medium w/o amino acid 6.7 g/l Yeast nitrogen base without amino acids 24 g/l Agar 20 g/l Glucose
YPD plates	65 g/l YPD agar
Presporulation (PRE-SPO) plates	30 g/l Standard nutrient broth 10 g/l Bacto yeast extract 20 g/l Agar 50 g/l Glucose
SC plates	6.7 g/l Yeast nitrogen base without amino acids 24 g/l Agar 20 g/ Glucose

5.1.5 Buffers and Solutions

Buffer/ Solution	Composition
Protein extraction solution 1	1.85 M NaOH 7.6 % β-mercaptoethanol
Protein extraction solution 2	50 % TCA
Urea buffer	120 mM Tris-HCl pH 6.8 5 % glycerol 8 M urea 143 mM β-mercaptoethanol 8 % SDS bromophenol blue
PEG mix	40 % (w/v) PEG 400 dissolved in LiAc mix, sterile filtered
10X SDS running buffer	25 mM Tris 192 mM glycine 0.1 % SDS adjusted to pH 8.3, autoclaved
5X PBS pH 7.4	685 mM Sodium chloride, 13.5 mM Potassium chloride 50 mM Disodium hydrogen phosphate 9 mM Potassium dihydrogen phosphate
1X PBST	1X PBS 0.1 % Tween-20

FA-lysis buffer	50 mM HEPES pH 7.5 140 mM NaCl 1 mM EDTA pH 8.0 1 % Triton X-100
FA-lysis buffer + SOD	50 mM HEPES pH 7.5 140 mM NaCl 1 mM EDTA pH 8.0 1 % Triton X-100 0.1 % sodium deoxycholate (SOD)
10X TBE	0.89 M Tris base 0.89 M boric acid 0.02 M EDTA pH 8.0
6X orange DNA loading dyer	15 % Ficoll 10 mM EDTA pH 8.0 Orange G
LiAc mix	0.1 M lithium acetate 1X TE
AE buffer	50 mM Na-Acetate pH 5.3 10 mM EDTA
10X TE	0.1 M Tris-HCl pH 7.5 10 mM EDTA pH 8.0
1 M Tris-HCl pH 7.5	1 M Tris base adjusted pH to 7.5 with HCl
20X SSC (Maniatis)	3 M NaCl 0.3 M Sodium citrate tribasic dihydrate adjusted to pH 7.0 with HCl
0.5 M EDTA pH 8.0	0.5 M disodium EDTA x 2 H_2O adjusted to pH 8.0 with NaOH

5.1.6 Antibiotics

Antibiotic	Supplier/Source	Identifier	Concentration
Carbenicillin disodium salt	Sigma Aldrich	C9231	100 µg/mL
G418 disulfate solution (Kanamycin)	AppliChem	A6798	250 µg/mL
Hygromycin B Gold	InvivoGen	ANT-HG-5	300 µg/mL
Nourseothricin-dihydrogen sulfate (ClonNaT)	Werner BioAgents	5000	100 µg/mL

5.1.7 Antibodies

Antibody	Supplier/Source	Identifier	Dilution
Immun-Star goat anti-mouse (GAM)-HRP conjugate	Bio-Rad	Cat#170-5047; RRID: AB_11125753	1:3000
Immun-Star goat anti-rabbit (GAR)-HRP conjugate	Bio-Rad	Cat#170-5046; RRID: AB_11125757	1:3000
IRDye 680RD goat anti-mouse IgG	LI-COR	Cat# 926-68070, RRID:AB_10956588	1:10,000

IRDye 800CW goat anti-rabbit IgG	LI-COR	Cat# 926-32211, RRID:AB_621843	1:10,000
Mouse monoclonal anti-Actin, clone C4	Millipore	Cat# MAB1501, RRID:AB_2223041	1:2000
Mouse monoclonal anti-MYC-tag (9B11)	Cell Signaling Technology/ NEB	Cat#2276S; RRID: AB_331783	1:1000
Mouse monoclonal anti-Phosphoglycerate Kinase (Pgk1) (22C5D8)	Invitrogen	Cat#459250; RRID: AB_2532235	1:20,0000
Mouse monoclonal anti-Rad53	Abcam	Cat# ab166859, RRID:AB_2801547	1:1000
Rabbit Peroxidase Anti-Peroxidase soluble complex (PAP)	Sigma Aldrich	Cat#P1291; RRID: AB_1079562	1:3000
Rabbit polyclonal anti-Sir2 (y-80)	Santa Cruz	Cat#sc-25753; RRID: AB_656457	1:1000

5.1.8 Reagents/Chemicals

Reagent/Chemical	Supplier/Source	Identifier
1 kb DNA ladder	NEB	N3232L
100 µCi SRP-203 [alpha-P32]Deoxyadenosine 5'triphosphate	Hartmann Analytic	SRP-203
100 bp DNA ladder	NEB	N3231L
2-Propanol	Sigma Aldrich	34959
Acetone	Sigma Aldrich	1.00014.1000
Agar	Sigma Aldrich	05040
Agarose	Sigma Aldrich	A9539
Ammonium Sulfate	Sigma Aldrich	31119
Bacto tryptone	BD Biosciences	211705
Bacto yeast extract	BD Biosciences	212750
Blue DNA loading dye (6X)	NEB	B7024S
Bradford solution	AppliChem	A6932,0500
Bromophenol Blue	Sigma Aldrich	B0126
cOmplete, Mini, EDTA-free Protease Inhibitor Cocktail	Sigma Aldrich	4693159001
Deoxynucleotide (dNTP) Solution Set	NEB	N0446S
DMSO	Sigma Aldrich	34943
Ethanol Absolute 99.8+%	Thermo Fisher Scientific	10437341
Formaldehyde Solution, 37 %	AppliChem	A0877
Galactose	AppliChem	A3609
Glucose	AppliChem	A1422
Glycerol	Thermo Fisher Scientific	17904
Glycine	Sigma Aldrich	15527
Glycogen, 20 mg/ml	Sigma Aldrich	10901393001
NEBuffer 4	NEB	B7004S
Peptone	AppliChem	A2210
PerfectHyb Plus Hybridization Buffer	Sigma Aldrich	H7033
Phenol	Sigma Aldrich	77608

Phenol:Chloroform:Isoamylalkohol 25:24:1	AppliChem	A2279
Potassium acetate	Sigma Aldrich	25059
Precision Blue™ Real-Time PCR Dye	Bio-Rad	1725555
Prestained Protein Marker, Broad Range (11 - 190 kDa)	NEB	P7706
Raffinose	AppliChem	A6882
SDS - 20 % solution	AppliChem	A0675
Skim milk powder	Sigma Aldrich	70166
Sodium acetate	Sigma Aldrich	S2889
Sodium chloride	Sigma Aldrich	31434
Sodium deoxycholate	Sigma Aldrich	D6750
Sodium hydroxide	Sigma Aldrich	30620
Standard nutrient broth	Sigma Aldrich	S4681
Super Signal West Dura Chemiluminescent Substrate	Thermo Fisher Scientific	10220294
Super Signal West Pico Chemiluminescent Substrate	Thermo Fisher Scientific	15669364
SYBR Safe DNA Gel Stain	Thermo Fisher Scientific	10328162
SYTOX Green Nucleic Acid Stain	Thermo Fisher Scientific	S7020
T4 DNA Ligase Reaction Buffer	NEB	B0202S
Trichloroacetic acid	Sigma Aldrich	27242
Triton X-100	Sigma Aldrich	X100
Trizma base	Sigma Aldrich	T1503
Tween-20	AppliChem	A4974
Urea	Sigma Aldrich	U5378
Yeast nitrogen base without amino acids	Sigma Aldrich	Y0626
Yeast synthetic dropout medium without uracil	Sigma Aldrich	Y1501
Yeastmarker carrier DNA	Takara	ST0029
YPD agar	Sigma Aldrich	Y1500
Zinc acetate	Sigma Aldrich	383317
α-factor mating pheromone	Zymo	Y1001
β-mercaptoethanol	Sigma Aldrich	M6250

5.1.9 Enzymes

Enzyme	Supplier/Source	Identifier
EcoRI	NEB	R0101S
Lyticase from Arthrobacter	Sigma Aldrich	L4025
NcoI-HF, 100,000 units/ml	NEB	R3193M
Phusion HF PCR Mastermix (2X)	NEB	M0531L
Proteinase K (20 mg/ml)	BioFroxx	1151ML010
Q5 Hot Start High-Fidelity DNA Polymerase	NEB	M0493S
RNase A, DNase and protease-free (10 mg/mL)	Thermo Fisher Scientific	EN0531
T4 DNA Ligase, ~2,000,000 units/ml	IMB core facility protein production	N/A
T4 DNA Ligase, 2,000,000 units/ml	NEB	M0202M
Taq PCR Mastermix (2X)	NEB	M0270L
Terminal Transferase	NEB	M0315S
XhoI	NEB	R0146S

5.1.10 Kits

Kit	Supplier/Source	Identifier
DECAprime Kit II	Thermo Fisher Scientific	10391555
Dynamo Flash SYBR GREEN qPCR Kit	Thermo Fisher Scientific	F415XL
Gentra Puregene Yeast/Bact. Kit	Qiagen	158567
QIAquick Gel Extraction Kit	Qiagen	28506
QIAquick PCR Purification Kit	Qiagen	28106
Qubit dsDNA HS Assay Kit	Thermo Fisher Scientific	10606433
RNase-Free DNase Set	Qiagen	79254
RNeasy MinElute Cleanup Kit	Qiagen	74204
Trans-Blot Turbo RTA Midi Nitrocellulose Transfer Kit	Bio-Rad	1704271

5.1.11 Additional materials

Material	Supplier/Source	Identifier
4–15 % Mini-PROTEAN TGX Precast Protein Gels, 15 well, 15 µl	Bio-Rad	4568086
4–15 % Mini-PROTEAN TGX Stain-Free Protein Gels, 10 well, 30 µl	Bio-Rad	4568083
7.5 % Mini-PROTEAN TGX Stain-Free Protein Gels, 10 well, 30 µl	Bio-Rad	4568023
Coverslip 22 x 22 mm	R. Langenbrinck	01-2222/x
GE Healthcare Amersham Protran Premium NC Nitrocellulose-Membrane, 0.45 µm	Thermo Fisher Scientific	15219804
Hard-Shell® 384-Well PCR Plates	Bio-Rad	HSP3805
Hybond-NX Nylon hybridization membrane	Sigma Aldrich	GERPN203T
Lysing Matrix C tubes	MP Biomedicals	11492410
Microscope slide	Neo Lab	1-6274
Microseal 'B' PCR Plate Sealing Film	Bio-Rad	MSB1001

5.1.12 Electronic devices

Device	Supplier/Source
BD FACSVerse Becton Dickinson	Becton Dickinson
ChemiDoc Touch Imaging System	Bio-Rad
Dissection Microscope MSM 400 Singer Instruments	Singer Instruments
FastPrep-25 MP Biomedicals	Biomedicals
Leica DM1000 LED Leica	Leica
Mini-PROTEAN Tetra Vertical Electrophoresis Cell	Bio-Rad
NanoDrop 2000 Thermo Scientific	Thermo Scientific
Odyssey CLx 9140	LI-COR
PowerPac Basic	Bio-Rad
Qubit 2.0 Fluorometer	Thermo Scientific
Real Time PCD Detection System CFX384 Touch	Bio-Rad

Sonifier 450	Branson
Spectrophotometer Ultrospec 2100 pro	Biochrom
Thermal Cycler C1000 Touch	Bio-Rad
Trans-Blot Turbo Transfer System	Bio-Rad
Typhoon FLA 9500	GE Healthcare
UV Stratalinker 2400	Stratagene

5.1.13 Software

Software	Supplier/Source
Adobe Illustrator 23.1	Adobe
BD FACSuite	Becton Dickinson
CFX Manager 3.1	Bio-Rad
Excel 2016	Microsoft
FileMaker Pro 10	File Maker Inc
FlowJo 10.6.1	Becton Dickinson
GraphPad Prism 8	GraphPad software
Image Lab 5.2.1	Bio-Rad
Image Studio 3.1	LI-COR
Mendeley Desktop 1.19.4	Elsevier
Word 2016	Microsoft

5.2 Methods

5.2.1 Yeast culture

If not stated otherwise, yeast strains were cultivated under standard conditions in YPD (yeast peptone dextrose) medium or SC (synthetic complete) medium without specific amino acids at 30 °C.

To obtain haploid cells from heterozygous diploid yeast strains, the diploids were prepared for sporulation by patching on pre-sporulation (PRE-SPO) plates. The cells were then grown overnight at 30 °C, added to 3 ml of sporulation (SPO) media and incubated at 23 °C. When the diploids have sporulated (after at least five days), 10 µl of yeast sporulation culture were treated with 10 µl of lyticase for 12 min at RT. The cells were distributed on the side of a YPD plate or SC plate without the respective amino acids in case the diploid contained a plasmid. The individual spores of tetrads were separated using micromanipulation and the plates were grown at 30 °C for 3 days until colonies were formed from single cells. Their genotypes were determined by replica plating on the respective selection or synthetic drop out media.

5.2.2 Yeast transformation

Approximately 15 OD_{600} units of exponentially growing yeast cells (1 OD_{600} unit corresponds to 1 ml of culture at OD_{600} 1) were collected by centrifuging at 300 rcf for 3 min at RT. The pellet was washed once with 5 ml of LiAc mix. Subsequently, the pellet was resuspended in 250 µl of LiAc mix containing 7 % DMSO and frozen at -80 °C in 100 µl aliquots.

For transformation, 0.2 – 0.5 µg of plasmid or 5 – 10 µl of a PCR reaction were added to 100 µl of competent yeast cells. Subsequently, 10 µl of yeastmarker carrier DNA and 700 µl of PEG mix were added and the cells were incubated at RT for 30 min rotating on a wheel. After a heat shock at 42 °C for 15 min the cells were centrifuged at 1000 rcf for 1 min and the pellet was resuspended in 300 µl YPD. The cells were incubated for 30 min (for plasmid transformations) or for 5 h (for integrations) at the appropriate growth temperature and afterwards plated on the respective selection plates.

5.2.3 Yeast strain generation

Standard yeast genetics methods were applied for strain generation (Guthrie & Fink 1991). Knockout strains of the respective genes were created according to Janke et al. 2004 and Longtine et al. 1998 or taken from the yeast knockout collection (Winzeler et al. 1999; Giaever et al. 2002; Wach et al. 1994).

Genes were tagged endogenously with auxin-inducible degrons (AID*) according to Morawska and Ulrich 2013. Briefly, the AID* cassette including a 9MYC tag and a selection marker (HYG or HIS) was amplified containing 50 bp homology arms to upstream and downstream of the STOP codon of the gene of interest. The PCR conditions are described in Janke et al. 2004, primers are listed in section 5.1.3 and the respective plasmids (pBL455 and pBL488) are listed in section 5.1.2. For C-terminal tagging of the protein of interest, 7.5 µl of PCR product was transformed into yeast cells (yKB244) containing the F-box protein Afb2 under the control of a GPD promoter (*leu2::pGPD-AFB2::LEU2)*. Correct integration was verified by PCR and western blotting.

5.2.4 Senescence curve

Liquid senescence assays were performed as described in Balk et al. 2013. Briefly, the OD_{600} of every culture was measured every 24 h using a spectrophotometer and the cultures were diluted back to an OD_{600} 0.01 in 25 ml YPD media. Population doublings (PDs) were counted starting from the spore colony, hence the start of the liquid culture was considered PD 0. The following PDs were determined as $\log_2(OD_{600}/0.01)$ and the relative viability was calculated respective to the OD_{600} on the first day of the senescence curve. All analyses during the senescence curve were performed on exponential cultures (~OD_{600} 0.6) diluted from the saturated culture after 24 h.

The experimental setup to overexpress Sin3 at different time points during senescence was performed as follows. Wt and *tlc1* cells carrying either an empty vector (EV) or a plasmid containing *SIN3-TAP* under the control of a galactose inducible promoter (pGAL-SIN3-TAP) were propagated for 10 days. To this end, the cells were diluted every 24 h to OD_{600} 0.02 in 10 ml SC-URA media containing 2 % glucose. The PDs of the cultures were calculated as $\log_2(OD_{600}/0.02)$. Western blot and Telo-3C analyses were executed on exponentially growing cells, as described in the following. Starting from saturated cultures after 24 h of growth, the cells were washed three times in 35 ml pre-warmed water and diluted to OD_{600} 0.1 in 80 ml SC-URA containing 2 % raffinose. When the culture reached OD_{600} 0.4, Sin3 overexpression was induced by adding 2 % galactose to the media. After growing the cells for 2 h in galactose containing media, samples for western blot were collected and cells were crosslinked for Telo-3C analysis.

5.2.5 Cell cycle arrest and release

To synchronize yeast cells in the cell cycle, *bar1* cells were diluted to OD_{600} 0.2 from a saturated overnight culture and grown at 25 °C until the culture reached OD_{600} 0.4. At this point, the exponential (exp.) samples for flow cytometry and western blot were collected and cells were crosslinked for Telo-3C analysis. To arrest cells in the G1 phase of the cell cycle, the culture was incubated with 1 µM α-factor for 2 h. Subsequently, the culture was washed three times with

200 ml pre-warmed water and resuspended in 25 °C warm YPD medium to OD_{600} 0.4 which was considered time point 0'. In the flowing time course, samples for flow cytometry and western blot were collected every 15 min and cells were crosslinked according to the Telo-3C protocol.

5.2.6 Bacteria transformation

For the transformation of a plasmid into DH5α *E. coli* cells, the chemically competent bacteria were thawed on ice, 5 ng of plasmid were added and the cells were gently mixed. After incubating for 30 min on ice, the bacteria were placed at 42 °C for 1 min and chilled on ice immediately after the heat shock. 300 µl of LB medium were added and the cells were incubated at 37 °C for 30 min. The cells were plated on LB plates containing the respective antibiotics and grown at 37 °C overnight.

5.2.7 Protein extraction

Protein extracts were prepared from 2 OD_{600} units of exponentially growing yeast cells. The respective amount of yeast culture was centrifuged at 17,000 rcf for 2 min and the pellet was resuspended in 150 µl of Protein extraction solution 1 and incubated on ice for 10 min. Subsequently, 150 µl of Protein extraction solution 2 were added, the mixture was vortexed briefly and incubated on ice for 10 min. After centrifugation for 2 min at 17,000 rcf and 4 °C, the pellet was washed with 1 ml cold acetone. Finally, the protein pellet was resuspended in 100 µl Urea buffer. In case the pH had to be adjusted, 1-5 µl of Tris/HCl pH 7.5 were added until the solution was blue. The protein extracts were incubated at 75 °C for 5 min and centrifuged at 17,000 rcf for 1 min. For the analysis of Rad53 phosphorylation, the protein extracts were incubated at 50 °C instead of 75 °C.

5.2.8 SDS-PAGE and western blot

3-10 µl of protein extracts were loaded on precast 4-15 % SDS-PAGE gels and run in SDS running buffer at 250 V until the blue loading front reached the bottom of the gel. For the analysis of Rad53 phosphorylation, the protein extracts were loaded on a 7.5 % SDS-PAGE gel and run at 100 V until the blue loading front reached the bottom of the gel. Proteins were blotted on a nitrocellulose membrane with the Trans-Blot Turbo Transfer System (Bio-Rad) using the High molecular weight program. Proteins were stained with Ponceau and imaged using the ChemiDoc Touch Imaging System (Bio-Rad). The membrane was blocked for 1 h with 5 % skim milk in PBST and subsequently incubated with primary antibodies at 4 °C overnight. The respective dilutions of all primary antibodies in 5 % skim milk in PBST are listed in section 5.1.7.

The membrane was washed four times for 10 min with PBST and subsequently incubated with the respective secondary antibody at RT (antibody dilutions see section 5.1.7). After additional three

washes with PBST the membrane was shortly incubated in PBS. Membranes with HRP-coupled secondary antibodies were developed using the Super Signal West Pico Chemiluminescent Substrate or the Super Signal West Dura Extended Duration Substrate on the ChemiDoc Touch Imaging System (Bio-Rad).

Membranes with secondary antibodies coupled to IRDyes were detected on the Odyssey CLx 9140 Imaging System (LI-COR) and processed via the Image studio software (LI-COR).

5.2.9 Flow cytometry analysis for DNA content

Yeast cells were collected (0.18 OD_{600} units) and the cell pellet was washed with 1 ml of water. Cells were fixed in 70 % ethanol overnight at 4°C. After fixation, cells were centrifuged at 17,000 rcf for 5 min and washed in 800 µl 50 mM Tris pH 7.5. RNA was digested in a 50 mM Tris solution containing 0.25 mg/ml RNase A for 2 h at 37 °C. Subsequently, 25 µl of 20 mg/ml proteinase K were added and incubated at 50 °C for 2 h. Samples were sonicated for 10 s in a BRANSON sonifier with a 3 mm sonication tip (“constant” mode and “level 1”). After sonication Sytox Green was added to a final concentration of 2 µM in 50 mM Tris and the cells were analyzed on a BD FACSVerse flow cytometer. 20,000 events were recorded per sample and the data was analyzed with the FACSuite software (BD).

5.2.10 Flow cytometry for cell viability

Yeast cells were collected (0.68 OD_{600} units) and pelleted at 4700 rcf for 1 min. The pellet was washed with 50 mM Tris pH 7.5 and resuspended in 1 ml 50 mM Tris pH 7.5 containing 0.5 µM Sytox Green. The stained cells were analyzed on BD FACSVerse flow cytometer. 20,000 events were recorded per sample and the data was analyzed with the FlowJo 10.6.1 software. As a control sample for dead cells, cells were incubated at 95 °C for 15 min and subjected to the described protocol.

5.2.11 Telomere chromosome conformation capture (Telo-3C)

25 ml of exponentially growing cells were crosslinked with 1.2 % formaldehyde at OD_{600} 0.4 for 20 min at room temperature. The reaction was quenched with 360 mM glycine for 5 min at RT and cells were placed on ice afterwards for at least 15 min. The cells were washed twice with cold PBS and the pellet was resuspended in 200 µl FA-lysis buffer containing cOmplete protease inhibitor cocktail. Cell lysis was performed in Lysing Matrix C tubes (MP Biomedicals) using a FastPrep device (MP Biomedicals; 2x 30 s with 1 min on ice in between runs; 6.5 M/s). Cell extracts were recovered in FA-lysis buffer containing 0.1 % sodium deoxycholate (FA-lysis buffer + SOD) and cOmplete protease inhibitor cocktail. The extracts were centrifuged for 15 min at 4 °C, 17,000 rcf. The pellet

was washed with FA-lysis buffer and resuspended in 200 ml of 20 mM Tris-HCl pH 7.5. The protein concentration of this 3C extract was determined by Bradford and a volume according to 60 µg of protein was digested with 100 units NcoI-HF overnight at 37 °C. The digestion reaction was stopped by incubating the samples at 65 °C for 20 min in the presence of 1 % SDS. The SDS was sequestered with 75 µl of 10 % Triton X-100 and 570 µl of 20 mM Tris-HCl pH 7.5 were added. The chromatin was pelleted for 15 min at 4 °C, 17,000 rcf, and resuspended in 750 µl ligation mixture containing 200 units T4 DNA ligase, 1X T4-Ligation buffer and Tris-HCl pH 7.5. After ligation at RT for 5 h, RNA was digested with 20 µg RNase A and crosslinks were reversed with 7.5 µl Proteinase K and 3.5 µl of 20 % SDS at 65 °C overnight. To isolate the DNA, the 3C reaction was mixed with 750 µl Phenol:Chloroform:Isoamylalcohol and the DNA was precipitated from the aqueous phase by adding 75 µl of 3 M KAc and 2 ml of 100 % Ethanol. The DNA pellet was washed with 70 % ethanol and resuspended in 40 µl ddH_2O. The DNA concentration was determined with Qubit HS DNA reagent. 1.5 ng of DNA were used per qPCR reaction, performed with the CFX384 Touch Real-Rime PCR Detection System (Bio-Rad) and Dynamo Flash SYBR GREEN. Primers for Telo-3C are listed in section 5.1.3 and were used in a final concentration of 0.5 µM in the qPCR reaction. The qPCR was performed with the following settings: 10 min at 95 °C; 40 cycles of 15 sec at 95 °C and 1 min at 60 °C; 5 min at 95 °C; 1 min at 65 °C. The melting curve of the amplicon was determined with a gradient from 65 °C to 97 °C with an increase of 0.5 °C/cycle in cycles of 5 sec.

The Telo-3C interaction frequency was normalized to an intergenic control PCR product (primers oRS39 and oRS40) as follows:

$$Ct(mean)intergenic = Average\ of\ Ct\ values\ for\ intergenic\ primers\ (oRS39 + oRS40)$$
$$Ct(mean)3C = Average\ of\ Ct\ values\ for\ 3C\ primers$$
$$dCt = Ct(mean)3C - Ct(mean)intergenic$$
$$ddCt = dCt - dCt(wt)$$
$$2^{(-ddCt)} \rightarrow 3C\ interaction\ frequency\ relative\ to\ wt$$

5.2.12 Southern blot

Genomic DNA (5 µg) was digested with XhoI for 5 h at 37 °C. The digested DNA was mixed with blue loading dye and loaded on a 0.8 % agarose gel along with 1 kB DNA ladder. The DNA was separated overnight at 50 V and afterwards denatured for 1 h (0.4 M NaOH, 0.6 M NaCl) and neutralized for 1 h (1 M Trizma Base, 1.5 M NaCl, pH 7.4). The DNA was transferred to a nylon membrane (Hybond NX) via capillary transfer in 10X SSC overnight and crosslinked to the membrane with UV light (auto X-link, UV Stratalinker). The membrane was pre-hybridized for 5 h at 55 °C in PerfectHyb Plus Hybridization Buffer. Hybridization of the respective radio-labeled probe was carried out overnight

at 55 °C. The membrane was washed twice in 2X SSC with 0.1 % SDS for 5 min and twice in 0.5X SSC with 0.1 % SDS for 20 min. All washing steps were performed at 55 °C. The signal was detected via the Typhoon FLA 9500 (GE Healthcare).

5.2.13 Probes for Southern blot

The telomere-specific probe was obtained by digestion of pBL423 with EcoRI followed by gel extraction using the QIAquick Gel Extraction Kit. Plasmid pBL423 was a kind gift from M.P. Longhese (pSP100). The probe for subtelomere 1L was generated by PCR with oligos oSM1 and oSM2 on genomic DNA from wt *S. cerevisiae*. The PCR product was separated on a 1 % agarose gel and purified using the QIAquick Gel Extraction Kit. 60 ng of each probe were labeled with dATP [α-32P] by random priming using the DECAprime kit II according to the manufacturer's instructions.

5.2.14 MS/MS

Mass spectrometry analysis was performed by Lara Perez Martinez (Butter lab, IMB Mainz). 1 OD_{600} unit of exponentially growing cells was resuspended in 1X LDS buffer supplemented with 100 mM DTT. Cells were boiled for 10 min at 95 °C and separated on a 4-12 % NuPAGE Bis–Tris precasted PAGE gel (Thermo Fisher Scientific). Samples were run at 180 V for 10 min and processed by in-gel digestion (Shevchenko et al. 2006). Briefly, samples were reduced in reduction buffer (10 mM DTT in 50 mM ammonium bicarbonate (ABC) buffer) for 1 h at 56 °C and alkylated in alkylation buffer (50 mM iodoacetamide (IAA) in 50 mM ABC buffer) for 45 min in the dark. Proteins were digested with 2 µg Protease LysC (Wako Chemicals) overnight at 37 °C in 50 mM ABC buffer. Digested peptides were desalted on a C18 StageTip as described (Rappsilber et al. 2007) and analyzed by nanoflow liquid chromatography on an EASY-nLC 1000 system (Thermo Fisher Scientific) coupled to a Q Exactive Plus mass spectrometer (Thermo Fisher Scientific). The peptides were separarated on a self-packed reverse phase capillary (75 µm diameter, 25 cm length packed with C18 beads of 1.9 µm (Dr Maisch GmbH)). The capillary was clamped on an electrospray ion source (Nanospray Flex™, Thermo Fisher Scientific). A 90 min gradient starting from 2 % - 60 % gradient acetonitrile in 0.1 % formic acid was used at a flow of 225 nl/min. Data was collected in data-dependent acquisition mode with one MS full scan followed by up to 10 MS/MS scan with HCD fragmentation.

5.2.15 MS data processing and bioinformatics analysis

MS data processing and bioinformatics analysis were performed by Merve Öztürk (Butter lab, IMB Mainz). MS raw files were processed using the MaxQuant software (version 1.5.2.8) and the ENSEMBL *S. cerevisiae* protein database (Saccharomyces_cerevisiae.R64-1-1.24). LFQ quantitation

and match between run options were activated. MaxQuant output files were analyzed using an in-house R script. Known contaminants, reverse hits and protein groups only identified by site modification were excluded. Identified protein groups (minimum 2 peptides, 1 of them unique) were further filtered to a minimum of 2 quantification events per experiment. Missing values were imputed using a downshifted and compressed beta distribution within the 0.001 and 0.015 percentile of the measured values for each replicate individually. The LFQ intensities were $\log_2$ transformed and a two sample Welch t-test was performed. Volcano plots were generated by plotting $-\log_{10}$(p-values) and fold changes. The threshold line for enriched proteins was defined with p-value = 0.05. Gene ontology analysis were performed with the PantherDB.org (Mi et al. 2019) overrepresentation Test (Release 20190711) with the annotation database released on 2019-07-03. Fisher's exact test followed by FDR correction was applied to calculate the p-values. Heatmap for enriched proteins were generated using the "pheatmap" (version 1.0.12) or "ggplot2" (version 3.2.1) package in R. Additionally the Venn diagram was generated using the "eulerr" (version 5.1.0) package in R (version 3.5.1).

5.2.16 Measurement of telomere length by PCR

Genomic DNA was extracted from 10 ml of exponentially growing cells with the Gentra Puregene Yeast/Bact. Kit according to the manufacturer's protocol. For the C-tailing reaction, 100 ng of genomic DNA were mixed with 0.9 µl of NEB buffer 4 in a final volume of 9 µl. To denature the DNA, the mixture was incubated at 96 °C for 10 min and cooled to 4 °C. 4 Units of terminal transferase were added together with dCTP in a final concentration of 0.1 mM. The C-tailing reaction was carried out as follows: 37 °C for 30 min; 65 °C for 10 min; 96 °C for 5 min; hold at 65 °C. Afterwards, 30 µl of pre-heated PCR mix were added to the DNA. The PCR mix contained 4 µl of 2 mM dNTPs, 4 µl of PCR buffer (670 mM Tris-HCl pH 8.8, 160 mM $(NH_4)_2SO_4$, 70 % glycerol, 0.1 % Tween-20), 0.4 µl Q5 hot start polymerase (2 U/µl) and the primers oBL358 and oBL359. The following cycling conditions were used for PCR: 95 °C for 3 min; 45 cycles of 95 °C for 30 s, 63 °C for 15 s and 72 °C for 20 sec; 72 °C for 5 min; hold at 4 °C. PCR products were mixed with orange loading dye and were separated on a 1.8 % agarose gel containing 1X SYBR Safe DNA gel stain.

5.2.17 RNA extraction and RT-qPCR to measure TERRA levels

For RNA extraction solid phenol was melted in a water bath and pre-equilibrated three times with an equal volume of AE buffer. 12 OD_{600} units of yeast cells were collected and the pellet was resuspended in 400 µl AE buffer. 40 µl 10 % SDS were added and the samples were vortexed. 500 ml of pre-equilibrated phenol were added and incubated at 65 °C for 5 min. After 5 min incubation on ice, the samples were centrifuged at 17,000 rcf for 3 min at 4 °C. The upper aqueous

phase was transferred to a new tube, mixed with 500 µl phenol:chloroform:isoamyl alcohol and incubated at RT for 5 min. After spinning the samples 17,000 rcf for 3 min the aqueous phase was again transferred to a new tube. Nucleic acids were precipitated by adding 40 µl sodium acetate (pH 5.3) and 1 ml ice cold 100 % ethanol and incubation for 20 min on ice. Nucleic acids were pelleted at 17,000 rcf for 3 min at 4 °C, the pellet was washed with 1 ml 80 % ethanol and air-dried. The pellet was resuspended in 87 µl RNase free water and DNA was digested for 30 min at 37 °C using 3 µl DNAse I and 10 µl RDD buffer. The RNA concentration was measured by Nanodrop and 50 µg of total RNA were cleaned up with the RNeasy MinElute Cleanup Kit eluting in 38 µl RNase free water. The DNase I treatment was repeated with 3 µl of enzyme and 10 µl of RDD buffer in a total volume of 100 µl and the RNA was purified using the RNeasy MinElute Cleanup Kit. Afterwards, the DNAse I treatment and RNA cleanup were repeated again like described before. In the final cleanup the RNA was eluted in 30 µl RNase free water and the concentration was determined by Nanodrop. The RNA was stored at -80 °C.

For reverse transcription 3 µg of RNA were mixed with 6 µl oligo mix containing 0.4 µl of 25 mM dNTPs, 1 µl of 10 µM CA oligo (oBL207), 0.4 µl of 10 µM actin oligo (oBL293) and 4.2 µl H_2O. The mixture was heated up to 90 °C for 1 min and then cooled down to 55 °C in a gradient of 0.8 °C/sec. The reverse transcription mix was added containing 1 µl of 0.1 M DTT, 2 µl H_2O, 4 µl 5X First Strand buffer and 1 µl SuperSkript III reverse transcriptase. As a control, the same reaction was also performed without the SuperSkript III enzyme. The mixture was incubated at 55 °C for 60 min followed by 15 min at 70 °C. The resulting cDNA was diluted by adding 80 µl H_2O to a final volume of 100 µl.

The qPCR was performed by the CFX384 Touch Real-Rime PCR Detection System (Bio-Rad) in a reaction volume of 10 µl using 5 µl DyNAmo Flash SYBR Green (Thermo Fisher Scientific), 2 µl cDNA and the respective primers in a final concentration of 0.5 µM (see section 5.1.3). The qPCR was performed with the following settings: 10 min at 95 °C; 40 cycles of 15 sec at 95 °C and 1 min at 60 °C; 5 min at 95 °C; 1 min at 65 °C. The melting curve of the amplicon was determined with a gradient from 65 °C to 97 °C with an increase of 0.5 °C/cycle in cycles of 5 sec.

The relative TERRA expression level was normalized to actin levels as follows:

$$Ct(mean)actin = Average\ of\ Ct\ values\ for\ actin$$
$$Ct(mean)TERRA = Average\ of\ Ct\ values\ for\ TERRA$$
$$dCt = Ct(mean)TERRA - Ct(mean)actin$$
$$ddCt = dCt - dCt(wt)$$
$$2^{(-ddCt)} \rightarrow\ TERRA\ expression\ relative\ to\ wt$$

5.2.18 Telomere-telomere fusions analysis

Telomere-telomere fusions (T-TFs) in the respective strains were analyzed by Marta Barrientos-Moreno (Prado Lab, CABIMER, Seville, Spain). The analysis was performed by quantitative PCR analyses as reported (Mieczkowski et al. 2003), with the modifications described in Barrientos-Moreno et al. 2018. Briefly, ~100 ng of *Sau3*A-treated genomic DNA extracted by standard protocols from asynchronous cultures was PCR-amplified for semi-quantitative analyses using a primer from the X element of chromosome XV-L and a primer from the Y' element of chromosome V-R (section 5.1.3). A DNA fragment from HIS4 was PCR-amplified as input control (section 5.1.3). T-TFs and HIS4 were PCR-amplified using 35-40 or 20 cycles, respectively, under the conditions previously reported, except for the annealing temperature (60 °C) and the extension time (30 sec). Quantitative analyses were performed by qPCR by using the same amount of *Sau3*A-treated genomic DNA, the oligonucleotides used for semi-quantitative analyses and the PCR conditions described previously (Mieczkowski et al. 2003). The frequency of T-TFs per genome was calculated with the formula:

$$\frac{T-TFs}{genome} = 2^{-N}$$

$$N = Ct(T-TFs) - Ct(HIS4)$$

Prior to applying this formula, the curves representing the increasing amounts of DNA for the two products as a function of the number of PCR cycles were confirmed to be parallel (i.e., the slope of the curve representing the log of the input amount versus ΔCt was < 0.1).

6 References

Abdallah, P. et al., 2009. A two-step model for senescence triggered by a single critically short telomere. *Nature Cell Biology*, 11(8), pp.988–993. Available at: http://www.nature.com/articles/ncb1911.

Aguilera, A. & García-Muse, T., 2012. R Loops: From Transcription Byproducts to Threats to Genome Stability. *Molecular Cell*, 46(2), pp.115–124. Available at: https://linkinghub.elsevier.com/retrieve/pii/S109727651200305X.

Ai, W. et al., 2002. Regulation of subtelomeric silencing during stress response. *Molecular Cell*, 10(6), pp.1295–1305.

Aladjem, M.I. et al., 2002. Replication Initiation Patterns in the β-Globin Loci of Totipotent and Differentiated Murine Cells: Evidence for Multiple Initiation Regions. *Molecular and Cellular Biology*, 22(2), pp.442–452.

Alberti, S., Gladfelter, A. & Mittag, T., 2019. Considerations and Challenges in Studying Liquid-Liquid Phase Separation and Biomolecular Condensates. *Cell*, 176(3), pp.419–434. Available at: https://doi.org/10.1016/j.cell.2018.12.035.

Alcasabas, A.A. et al., 2001. Mrc1 transduces signals of DNA replication stress to activate Rad53. *Nature Cell Biology*, 3(11), pp.958–965.

Alexander, J.M. et al., 2019. Live-cell imaging reveals enhancer-dependent sox2 transcription in the absence of enhancer proximity. *eLife*, 8.

Altaf, M. et al., 2007. Interplay of Chromatin Modifiers on a Short Basic Patch of Histone H4 Tail Defines the Boundary of Telomeric Heterochromatin. *Molecular Cell*, 28(6), pp.1002–1014.

Altmeyer, M. et al., 2015. Liquid demixing of intrinsically disordered proteins is seeded by poly(ADP-ribose). *Nature Communications*, 6(1), p.8088. Available at: http://www.nature.com/articles/ncomms9088.

Alver, R.C. et al., 2017. Reversal of DDK-Mediated MCM Phosphorylation by Rif1-PP1 Regulates Replication Initiation and Replisome Stability Independently of ATR/Chk1. *Cell Reports*, 18(10), pp.2508–2520.

Amiard, S. et al., 2007. A topological mechanism for TRF2-enhanced strand invasion. *Nature Structural & Molecular Biology*, 14(2), pp.147–154. Available at: http://www.nature.com/articles/nsmb1192.

Amon, A., 2002. Synchronization procedures. *Methods in Enzymology*, 351, pp.457–467.

Anbalagan, S. et al., 2011. Rif1 supports the function of the CST complex in yeast telomere capping. *PLoS Genetics*, 7(3).

Anderson, M.Z. et al., 2014. Silencing Is Noisy: Population and Cell Level Noise in Telomere-Adjacent Genes Is Dependent on Telomere Position and Sir2. *PLoS Genetics*, 10(7).

Andrey, G. et al., 2017. Characterization of hundreds of regulatory landscapes in developing limbs reveals two regimes of chromatin folding. *Genome Research*, 27(2), pp.223–233.

Andrulis, E.D. et al., 2002. Esc1, a Nuclear Periphery Protein Required for Sir4-Based Plasmid Anchoring and Partitioning. *Molecular and Cellular Biology*, 22(23), pp.8292–8301.

Ang, J.S. et al., 2016. Dosage mutator genes in saccharomyces cerevisiae: A novel mutator mode-of-action of the Mph1 DNA helicase. *Genetics*, 204(3), pp.975–986.

Ansari, A. & Hampsey, M., 2005. A role for the CPF 3′ -end processing machinery in RNAP II-dependent gene looping. *Genes and Development*, 19(24), pp.2969–2978.

Aparicio, J.G. et al., 2004. The Rpd3-Sin3 Histone Deacetylase Regulates Replication Timing and Enables Intra-S Origin Control in Saccharomyces cerevisiae. *Molecular and Cellular Biology*, 24(11), pp.4769–4780.

Aparicio, O.M., 2013. Location, location, location: it's all in the timing for replication origins. *Genes & Development*, 27(2), pp.117–128.

Arnerić, M. & Lingner, J., 2007. Tel1 kinase and subtelomere-bound Tbf1 mediate preferential elongation of short telomeres by telomerase in yeast. *EMBO Reports*, 8(11), pp.1080–1085.

Arnoult, N. et al., 2010. Replication timing of human telomeres is chromosome arm-specific, influenced by subtelomeric structures and connected to nuclear localization. J. E. Haber, ed. *PLoS genetics*, 6(4), p.e1000920. Available at: https://dx.plos.org/10.1371/journal.pgen.1000920.

Arnoult, N., Van Beneden, A. & Decottignies, A., 2012. Telomere length regulates TERRA levels through increased trimethylation of telomeric H3K9 and HP1α. *Nature Structural & Molecular Biology*, 19(9), pp.948–956. Available at: http://www.nature.com/articles/nsmb.2364.

Arora, R. et al., 2014. RNaseH1 regulates TERRA-telomeric DNA hybrids and telomere maintenance in ALT tumour cells. *Nature communications*, 5(1), p.5220. Available at: http://www.nature.com/articles/ncomms6220.

Arora, R. & Azzalin, C.M., 2015. Telomere elongation chooses TERRA ALTernatives. *RNA Biology*, 12(9), pp.938–941.

Artandi, S.E. & DePinho, R.A., 2009. Telomeres and telomerase in cancer. *Carcinogenesis*, 31(1), pp.9–18.

Artandl, S.E. et al., 2000. Telomere dysfunction promotes non-reciprocal translocations and epithelial cancers in mice. *Nature*, 406(6796), pp.641–645.

Arudchandran, A. et al., 2000. The absence of ribonuclease H1 or H2 alters the sensitivity of Saccharomyces cerevisiae to hydroxyurea, caffeine and ethyl methanesulphonate: implications for roles of RNases H in DNA replication and repair. *Genes to Cells*, 5(10), pp.789–802. Available at: http://doi.wiley.com/10.1046/j.1365-2443.2000.00373.x.

Audebert, M., Salles, B. & Calsou, P., 2008. Effect of double-strand break DNA sequence on the PARP-1 NHEJ pathway. *Biochemical and Biophysical Research Communications*, 369(3), pp.982–988.

Audebert, M., Salles, B. & Calsou, P., 2004. Involvement of poly(ADP-ribose) polymerase-1 and XRCC1/DNA ligase III in an alternative route for DNA double-strand breaks rejoining. *Journal of Biological Chemistry*, 279(53), pp.55117–55126.

Azzalin, C.M. et al., 1997. Fluorescence in situ hybridization with a synthetic (T2AG3)n polynucleotide detects several intrachromosomal telomere-like repeats on human chromosomes. *Cytogenetic and Genome Research*, 78(2), pp.112–115.

Azzalin, C.M. et al., 2007a. Telomeric Repeat–Containing RNA and RNA Surveillance Factors at Mammalian Chromosome Ends. *Science*, 318(November), pp.798–801.

Azzalin, C.M. et al., 2007b. Telomeric Repeat Containing RNA and RNA Surveillance Factors at Mammalian Chromosome Ends. *Science*, 318(5851), pp.798–801. Available at: http://www.sciencemag.org/cgi/doi/10.1126/science.1147182.

Badie, S. et al., 2010. BRCA2 acts as a RAD51 loader to facilitate telomere replication and capping. *Nature Structural and Molecular Biology*, 17(12), pp.1461–1469.

Badrinarayanan, A. et al., 2012. In Vivo Architecture and Action of Bacterial Structural Maintenance of Chromosome Proteins. *Science*, 338(6106), pp.528–531. Available at: https://www.sciencemag.org/lookup/doi/10.1126/science.1227126.

Balk, B. et al., 2013. Telomeric RNA-DNA hybrids affect telomere-length dynamics and senescence. *Nature Structural and Molecular Biology*, 20(10), pp.1199–1206.

Ballenstefen, W. & Schmitt, H.D., 1997. Periplasmic Bar1 protease of Saccharomyces cerevisiae is active before reaching its extracellular destination. *Eur. J. Biochem*, 147, pp.142–147.

Banani, S.F. et al., 2017. Biomolecular condensates: Organizers of cellular biochemistry. *Nature Reviews Molecular Cell Biology*, 18(5), pp.285–298.

Bannister, A.J. & Kouzarides, T., 2011. Regulation of chromatin by histone modifications. *Cell Research*, 21(3), pp.381–395. Available at: http://www.nature.com/articles/cr201122.

Barrientos-Moreno, M. et al., 2018. Histone depletion prevents telomere fusions in pre-senescent cells. *PLoS Genetics*, 14(6), pp.1–22.

Barthel, F.P. et al., 2017. Systematic analysis of telomere length and somatic alterations in 31 cancer types. *Nature Genetics*, 49(3), pp.349–357.

Baumann, P., 2001. Pot1, the Putative Telomere End-Binding Protein in Fission Yeast and Humans. *Science*, 292(5519), pp.1171–1175. Available at: https://www.sciencemag.org/lookup/doi/10.1126/science.1060036.

Baur, J.A. et al., 2001. Telomere position effect in human cells. *Science*, 292(5524), pp.2075–2077.

Beagrie, R.A. et al., 2017. Complex multi-enhancer contacts captured by genome architecture mapping. *Nature*, 543(7646), pp.519–524.

Belmont, A.S., 2014. Large-scale chromatin organization: The good, the surprising, and the still perplexing. *Current Opinion in Cell Biology*, 26(1), pp.69–78.

Benarroch-Popivker, D. et al., 2016. TRF2-Mediated Control of Telomere DNA Topology as a Mechanism for Chromosome-End Protection. *Molecular Cell*, 61(2), pp.274–286.

Benetti, R., García-Cao, M. & Blasco, M.A., 2007. Telomere length regulates the epigenetic status of mammalian telomeres and subtelomeres. *Nature Genetics*, 39(2), pp.243–250.

Bennardo, N. et al., 2008. Alternative-NHEJ is a mechanistically distinct pathway of mammalian chromosome break repair J. E. Haber, ed. *PLoS Genetics*, 4(6), p.e1000110. Available at: https://dx.plos.org/10.1371/journal.pgen.1000110.

Berger, A.B. et al., 2008. High-resolution statistical mapping reveals gene territories in live yeast. *Nature Methods*, 5(12), pp.1031–1037.

Bermudez-Lopez, M. et al., 2010. The Smc5/6 complex is required for dissolution of DNA-mediated sister chromatid linkages. *Nucleic Acids Research*, 38(19), pp.6502–6512.

Bermúdez-López, M. et al., 2015. ATPase-dependent control of the Mms21 SUMO ligase during DNA repair. S. Jentsch, ed. *PLoS biology*, 13(3), p.e1002089. Available at: http://dx.plos.org/10.1371/journal.pbio.1002089.

Bernstein, B.E., Tong, J.K. & Schreiber, S.L., 2000. Genomewide studies of histone deacetylase function in yeast. *Proceedings of the National Academy of Sciences of the United States of*

America, 97(25), pp.13708–13713.

Bertuch, A.A. & Lundblad, V., 2004. EXO1 Contributes to Telomere Maintenance in Both Telomerase-Proficient and Telomerase-Deficient Saccharomyces cerevisiae. *Genetics*, 166(4), pp.1651–1659.

Betts Lindroos, H. et al., 2006. Chromosomal Association of the Smc5/6 Complex Reveals that It Functions in Differently Regulated Pathways. *Molecular Cell*, 22(6), pp.755–767. Available at: https://linkinghub.elsevier.com/retrieve/pii/S1097276506003297.

Bianchi, A., 1997. TRF1 is a dimer and bends telomeric DNA. *The EMBO Journal*, 16(7), pp.1785–1794. Available at: http://emboj.embopress.org/cgi/doi/10.1093/emboj/16.7.1785.

Bianchi, A., Negrini, S. & Shore, D., 2004. Delivery of yeast telomerase to a DNA break depends on the recruitment functions of Cdc13 and Est1. *Molecular Cell*, 16(1), pp.139–146.

Bianchi, A. & Shore, D., 2007a. Early Replication of Short Telomeres in Budding Yeast. *Cell*, 128(6), pp.1051–1062.

Bianchi, A. & Shore, D., 2007b. Increased association of telomerase with short telomeres in yeast. *Genes and Development*, 21(14), pp.1726–1730.

Bintu, B. et al., 2018. Super-resolution chromatin tracing reveals domains and cooperative interactions in single cells. *Science (New York, N.Y.)*, 362(6413), p.eaau1783. Available at: https://www.sciencemag.org/lookup/doi/10.1126/science.aau1783.

Bitterman, K.J., Medvedik, O. & Sinclair, D.A., 2003. Longevity Regulation in Saccharomyces cerevisiae: Linking Metabolism, Genome Stability, and Heterochromatin. *Microbiology and Molecular Biology Reviews*, 67(3), pp.376–399.

Blackburn, E.H. & Gall, J.G., 1978. A tandemly repeated sequence at the termini of the extrachromosomal ribosomal RNA genes in Tetrahymena. *Journal of Molecular Biology*, 120(1), pp.33–53. Available at: https://linkinghub.elsevier.com/retrieve/pii/0022283678902942.

Blier, P.R. et al., 1993. Binding of Ku protein to DNA. Measurement of affinity for ends and demonstration of binding to nicks. *The Journal of biological chemistry*, 268(10), pp.7594–601. Available at: http://www.ncbi.nlm.nih.gov/pubmed/8463290.

Bolzer, A. et al., 2005. Three-dimensional maps of all chromosomes in human male fibroblast nuclei and prometaphase rosettes T. Misteli, ed. *PLoS Biology*, 3(5), pp.0826–0842. Available at: https://dx.plos.org/10.1371/journal.pbio.0030157.

Bonetti, D. et al., 2009. Multiple Pathways Regulate 3′ Overhang Generation at S. cerevisiae Telomeres. *Molecular Cell*, 35(1), pp.70–81. Available at: http://dx.doi.org/10.1016/j.molcel.2009.05.015.

Bonetti, D. et al., 2010. Shelterin-like proteins and Yku inhibit nucleolytic processing of Saccharomyces cerevisiae telomeres. J. E. Haber, ed. *PLoS genetics*, 6(5), p.e1000966. Available at: http://www.ncbi.nlm.nih.gov/pubmed/20523746.

Boos, D. & Ferreira, P., 2019. Origin firing regulations to control genome replication timing. *Genes*, 10(3), pp.1–21.

Boulton, S. & Jackson, S.P., 1996. Identification of a Saccharomyces cerevisiae Ku80 homologue: roles in DNA double strand break rejoining and in telomeric maintenance. *Nucleic Acids Research*, 24(23), pp.4639–4648. Available at: https://academic.oup.com/nar/article-lookup/doi/10.1093/nar/24.23.4639.

Boulton, S.J. & Jackson, S.P., 1998. Components of the Ku-dependent non-homologous end-joining pathway are involved in telomeric length maintenance and telomeric silencing. *EMBO Journal*, 17(6), pp.1819–1828. Available at: http://emboj.embopress.org/cgi/doi/10.1093/emboj/17.6.1819.

Bower, B.D. & Griffith, J.D., 2014. TRF1 and TRF2 differentially modulate Rad51-mediated telomeric and nontelomeric displacement loop formation in vitro. *Biochemistry*, 53(34), pp.5485–5495.

Branzei, D. et al., 2006. Ubc9- and Mms21-Mediated Sumoylation Counteracts Recombinogenic Events at Damaged Replication Forks. *Cell*, 127(3), pp.509–522. Available at: https://linkinghub.elsevier.com/retrieve/pii/S0092867406012785.

Brigati, C. et al., 1993. An essential yeast gene encoding a TTAGGG repeat-binding protein. *Molecular and Cellular Biology*, 13(2), pp.1306–1314. Available at: http://mcb.asm.org/lookup/doi/10.1128/MCB.13.2.1306.

Britt-Compton, B. et al., 2009. Short telomeres are preferentially elongated by telomerase in human cells. *FEBS Letters*, 583(18), pp.3076–3080.

Britton, R.A., Lin, D.C.-H. & Grossman, A.D., 1998. Characterization of a prokaryotic SMC protein involved in chromosome partitioning. *Genes & Development*, 12(9), pp.1254–1259. Available at: http://www.genesdev.org/cgi/doi/10.1101/gad.12.9.1254.

Broccoli, D. et al., 1997. Human telomeres contain two distinct Myb–related proteins, TRF1 and TRF2. *Nature Genetics*, 17(2), pp.231–235. Available at: http://www.nature.com/articles/ng1097-231.

Brosh, R.M. et al., 1999. Functional and physical interaction between WRN helicase and human replication protein A. *Journal of Biological Chemistry*, 274(26), pp.18341–18350.

de Bruin, D. et al., 2000. Telomere Folding Is Required for the Stable Maintenance of Telomere Position Effects in Yeast. *Molecular and Cellular Biology*, 20(21), pp.7991–8000.

de Bruin, D. et al., 2001. Telomere looping permits gene activation by a downstream UAS in yeast. *Nature*, 409(6816), pp.109–113.

Brunet, A. & Berger, S.L., 2014. Epigenetics of Aging and Aging-related Disease. *The Journals of Gerontology Series A: Biological Sciences and Medical Sciences*, 69(Suppl 1), pp.S17–S20. Available at: https://academic.oup.com/biomedgerontology/article-lookup/doi/10.1093/gerona/glu042.

Bryan, T.M. et al., 1997. Evidence for an alternative mechanism for maintaining telomere length in human tumors and tumor-derived cell lines. *Nature Medicine*, 3(11), pp.1271–1274.

Bryan, T.M. et al., 1995. Telomere elongation in immortal human cells without detectable telomerase activity. *The EMBO Journal*, 14(17), pp.4240–4248.

Bupp, J.M. et al., 2007. Telomere anchoring at the nuclear periphery requires the budding yeast Sad1-UNC-84 domain protein Mps3. *Journal of Cell Biology*, 179(5), pp.845–854.

Bustard, D.E. et al., 2012. During Replication Stress, Non-Smc Element 5 (Nse5) Is Required for Smc5/6 Protein Complex Functionality at Stalled Forks. *Journal of Biological Chemistry*, 287(14), pp.11374–11383. Available at: http://www.jbc.org/lookup/doi/10.1074/jbc.M111.336263.

Bystricky, K. et al., 2005. Chromosome looping in yeast: Telomere pairing and coordinated movement reflect anchoring efficiency and territorial organization. *Journal of Cell Biology*, 168(3), pp.375–387.

Cajal, S.R., 1903. Un sencillo metodo de coloracion selectiva del reticulo protoplasmico y sus efectos en los diversos organos nerviosos de vertebrados e invertebrados. *Trab Lab Investig Biol Univ Madr*, 2, pp.129–221.

Campisi, J. & D'Adda Di Fagagna, F., 2007. Cellular senescence: When bad things happen to good cells. *Nature Reviews Molecular Cell Biology*, 8(9), pp.729–740.

Cannavo, E. & Cejka, P., 2014. Sae2 promotes dsDNA endonuclease activity within Mre11-Rad50-Xrs2 to resect DNA breaks. *Nature*, 514(7520), pp.122–125.

Carmen, A.A., Milne, L. & Grunstein, M., 2002. Acetylation of the yeast histone H4 N terminus regulates its binding to heterochromatin protein SIR3. *Journal of Biological Chemistry*, 277(7), pp.4778–4781.

Carr, A.M., Paek, A.L. & Weinert, T., 2011. DNA replication: Failures and inverted fusions. *Seminars in Cell & Developmental Biology*, 22(8), pp.866–874. Available at: https://linkinghub.elsevier.com/retrieve/pii/S108495211100187X.

Carrozza, M.J. et al., 2005. Histone H3 methylation by Set2 directs deacetylation of coding regions by Rpd3S to suppress spurious intragenic transcription. *Cell*, 123(4), pp.581–592.

Celli, G.B., Denchi, E.L. & de Lange, T., 2006. Ku70 stimulates fusion of dysfunctional telomeres yet protects chromosome ends from homologous recombination. *Nature Cell Biology*, 8(8), pp.885–890.

Celli, G.B. & de Lange, T., 2005. DNA processing is not required for ATM-mediated telomere damage response after TRF2 deletion. *Nature Cell Biology*, 7(7), pp.712–718.

Cesare, A.J. et al., 2009. Spontaneous occurrence of telomeric DNA damage response in the absence of chromosome fusions. *Nature Structural and Molecular Biology*, 16(12), pp.1244–1251.

Cesare, A.J. et al., 2003. Telomere looping in P. sativum (common garden pea). *Plant Journal*, 36(2), pp.271–279.

Cesare, A.J. et al., 2008. Telomere Loops and Homologous Recombination-Dependent Telomeric Circles in a Kluyveromyces lactis Telomere Mutant Strain. *Molecular and Cellular Biology*, 28(1), pp.20–29.

Cesare, A.J. et al., 2013. The Telomere deprotection response is functionally distinct from the Genomic DNA damage response. *Molecular Cell*, 51(2), pp.141–155.

Cesare, A.J. & Griffith, J.D., 2004. Telomeric DNA in ALT Cells Is Characterized by Free Telomeric Circles and Heterogeneous t-Loops. *Molecular and Cellular Biology*, 24(22), pp.9948–9957. Available at: http://mcb.asm.org/cgi/doi/10.1128/MCB.24.22.9948-9957.2004.

Cesare, A.J. & Karlseder, J., 2012. A three-state model of telomere control over human proliferative boundaries. *Current Opinion in Cell Biology*, 24(6), pp.731–738.

Chai, W. et al., 2002. Human Ku70/80 associates physically with telomerase through interaction with hTERT. *Journal of Biological Chemistry*, 277(49), pp.47242–47247.

Chan, A., Boulé, J.B. & Zakian, V.A., 2008. Two pathways recruit telomerase to Saccharomyces cerevisiae telomeres S. Biggins, ed. *PLoS Genetics*, 4(10), p.e1000236. Available at: https://dx.plos.org/10.1371/journal.pgen.1000236.

Chan, R.K. & Otte, C.A., 1982. Physiological Characterization of Saccharomyces cerevisiae Mutants Supersensitive to Gl Arrest by a Factor and ac Factor Pheromones. *Molecular and Cellular*

Biology, 2(1), pp.21–29.

Chan, S.W. & Blackburn, E.H., 2003. Telomerase and ATM/Tel1p Protect Telomeres from Nonhomologous End Joining Short. *Molecular Cell*, 11, pp.1379–1387.

Chan, S.W.L. et al., 2001. Altering telomere structure allows telomerase to act in yeast lacking ATM kinases. *Current Biology*, 11(16), pp.1240–1250.

Chandra, T. et al., 2015. Global reorganization of the nuclear landscape in senescent cells. *Cell Reports*, 10(4), pp.471–483. Available at: http://dx.doi.org/10.1016/j.celrep.2014.12.055.

Chanut, P. et al., 2016. Coordinated nuclease activities counteract Ku at single-ended DNA double-strand breaks. *Nature Communications*, 7(1), p.12889. Available at: http://www.nature.com/articles/ncomms12889.

Chavez, A. et al., 2010. Sumoylation and the Structural Maintenance of Chromosomes (Smc) 5/6 Complex Slow Senescence through Recombination Intermediate Resolution. *Journal of Biological Chemistry*, 285(16), pp.11922–11930. Available at: http://www.jbc.org/lookup/doi/10.1074/jbc.M109.041277.

Chawla, R. & Azzalin, C.M., 2009. The telomeric transcriptome and SMG proteins at the crossroads. *Cytogenetic and Genome Research*, 122(3–4), pp.194–201.

Chen, B. et al., 2013. Dynamic imaging of genomic loci in living human cells by an optimized CRISPR/Cas system. *Cell*, 155(7), pp.1479–1491.

Chen, Q., Ijpma, A. & Greider, C.W., 2001. Two survivor pathways that allow growth in the absence of telomerase are generated by distinct telomere recombination events. *Molecular and cellular biology*, 21(5), pp.1819–27. Available at: http://www.ncbi.nlm.nih.gov/pubmed/11238918.

Chiruvella, K.K., Liang, Z. & Wilson, T.E., 2013. Repair of Double-Strand Breaks by End Joining. *Cold Spring Harbor Perspectives in Biology*, 5(5), pp.a012757–a012757. Available at: http://cshperspectives.cshlp.org/lookup/doi/10.1101/cshperspect.a012757.

Cho, K.S., 2016. Polymer physics. *Springer Series in Materials Science*, 241, pp.231–281.

Chubb, J.R. et al., 2002. Chromatin motion is constrained by association with nuclear compartments in human cells. *Current Biology*, 12(6), pp.439–445.

Churikov, D. et al., 2016. SUMO-Dependent Relocalization of Eroded Telomeres to Nuclear Pore Complexes Controls Telomere Recombination. *Cell Reports*, 15(6), pp.1242–1253.

Clerici, M. et al., 2008. The Yku70-Yku80 complex contributes to regulate double-strand break processing and checkpoint activation during the cell cycle. *EMBO Reports*, 9(8), pp.810–818.

Cockell, M. et al., 1995. The carboxy termini of Sir4 and RAP1 affect Sir3 localization: Evidence for a multicomponent complex required for yeast telomeric silencing. *Journal of Cell Biology*, 129(4), pp.909–924.

Cornacchia, D. et al., 2012. Mouse Rif1 is a key regulator of the replication-timing programme in mammalian cells. *EMBO Journal*, 31(18), pp.3678–3690.

Cosgrove, A.J., Nieduszynski, C.A. & Donaldson, A.D., 2002. Ku complex controls the replication time of DNA in telomere regions. *Genes and Development*, 16(19), pp.2485–2490.

Craven, R.J. et al., 2002. Regulation of Genome Stability by TEL1 and MEC1, Yeast Homologs of the Mammalian ATM and ATR Genes. *Genetics*, 507(June), p.16.

Cremer, T. et al., 1982. Analysis of chromosome positions in the interphase nucleus of Chinese hamster cells by laser-UV-microirradiation experiments. *Human Genetics*, 62(3), pp.201–209.

Cremer, T. & Cremer, C., 2001. Chromosome territories, nuclear architecture and gene regulation in mammalian cells. *Nature Reviews Genetics*, 2(4), pp.292–301.

Cremer, T. & Cremer, M., 2010. Chromosome Territories. *Cold Spring Harbor Perspectives in Biology*, 2(3), pp.a003889–a003889. Available at: http://cshperspectives.cshlp.org/lookup/doi/10.1101/cshperspect.a003889.

Croft, J.A. et al., 1999. Differences in the Localization and Morphology of Chromosomes in the Human Nucleus. *Journal of Cell Biology*, 145(6), pp.1119–1131. Available at: https://rupress.org/jcb/article/145/6/1119/29348/Differences-in-the-Localization-and-Morphology-of.

Cubiles, M.D. et al., 2018. Epigenetic features of human telomeres. *Nucleic Acids Research*, 46(5), pp.2347–2355.

Cusanelli, E., Romero, C.A.P. & Chartrand, P., 2013. Telomeric Noncoding RNA TERRA Is Induced by Telomere Shortening to Nucleate Telomerase Molecules at Short Telomeres. *Molecular Cell*, 51, pp.780–791.

Cuylen, S., Metz, J. & Haering, C.H., 2011. Condensin structures chromosomal DNA through topological links. *Nature Structural & Molecular Biology*, 18(8), pp.894–901. Available at: http://www.nature.com/articles/nsmb.2087.

D'Ambrosio, C. et al., 2008. Identification of cis-acting sites for condensin loading onto budding yeast chromosomes. *Genes & Development*, 22(16), pp.2215–2227. Available at: http://genesdev.cshlp.org/cgi/doi/10.1101/gad.1675708.

Dai, X. et al., 2010. Molecular steps of G-overhang generation at human telomeres and its function in chromosome end protection. *EMBO Journal*, 29(16), pp.2788–2801.

Daley, J.M. et al., 2005. Nonhomologous End Joining in Yeast. *Annual Review of Genetics*, 39(1), pp.431–451.

Davé, A. et al., 2014. Protein Phosphatase 1 Recruitment by Rif1 Regulates DNA Replication Origin Firing by Counteracting DDK Activity. *Cell Reports*, 7(1), pp.53–61.

David, K. & Kevin, S., 1997. Repression by Ume6 involves recruitment of a complex containing Sin3 corepressor and Rpd3 histone deacetylase to target promoters. *Cell*, 89(3), pp.365–371.

Dekker, J. et al., 2002. Capturing Chromosome Conformation. *Science*, 295(5558), pp.1306–1311. Available at: https://www.sciencemag.org/lookup/doi/10.1126/science.1067799.

Dekker, J., 2006. The three "C" s of chromosome conformation capture: Controls, controls, controls. *Nature Methods*, 3(1), pp.17–21.

Dekker, J. & Mirny, L., 2016. The 3D Genome as Moderator of Chromosomal Communication. *Cell*, 164(6), pp.1110–1121. Available at: http://dx.doi.org/10.1016/j.cell.2016.02.007.

Denchi, E.L. & De Lange, T., 2007. Protection of telomeres through independent control of ATM and ATR by TRF2 and POT1. *Nature*, 448(7157), pp.1068–1071.

Deng, Z. et al., 2012. A role for CTCF and cohesin in subtelomere chromatin organization, TERRA transcription, and telomere end protection. *EMBO Journal*, 31(21), pp.4165–4178.

Deng, Z. et al., 2009. TERRA RNA Binding to TRF2 Facilitates Heterochromatin Formation and ORC

Recruitment at Telomeres. *Molecular Cell*, 35(4), pp.403–413.

Denker, A. & De Laat, W., 2016. The second decade of 3C technologies: Detailed insights into nuclear organization. *Genes and Development*, 30(12), pp.1357–1382.

Diede, S.J. & Gottschling, D.E., 1999. Telomerase-Mediated Telomere Addition In Vivo Requires DNA Primase and DNA Polymerases. *Cell*, 99, pp.723–733.

Dimitrova, N. et al., 2008. 53BP1 promotes non-homologous end joining of telomeres by increasing chromatin mobility. *Nature*, 456(7221), pp.524–528.

Ding, H. et al., 2004. Regulation of Murine Telomere Length by Rtel. *Cell*, 117(7), pp.873–886. Available at: https://linkinghub.elsevier.com/retrieve/pii/S0092867404005409.

Dionne, I. & Wellinger, R.J., 1996. Cell cycle-regulated generation of single-stranded G-rich DNA in the absence of telomerase. *Proceedings of the National Academy of Sciences of the United States of America*, 93(24), pp.13902–13907.

Dionne, I. & Wellinger, R.J., 1998. Processing of telomeric DNA ends requires the passage of a replication fork. *Nucleic Acids Research*, 26(23), pp.5365–5371.

Dixon, J.R. et al., 2012. Topological domains in mammalian genomes identified by analysis of chromatin interactions. *Nature*, 485(7398), pp.376–380.

Doksani, Y. et al., 2013. Super-resolution fluorescence imaging of telomeres reveals TRF2-dependent T-loop formation. *Cell*, 155(2), pp.345–356.

Doksani, Y. & de Lange, T., 2014. The role of double-strand break repair pathways at functional and dysfunctional telomeres. *Cold Spring Harbor Perspectives in Biology*, 6(12), pp.1–15.

Dostie, J. et al., 2006. Chromosome Conformation Capture Carbon Copy (5C): A massively parallel solution for mapping interactions between genomic elements. *Genome Research*, 16(10), pp.1299–1309.

Downs, J.A., Lowndes, N.F. & Jackson, S.P., 2000. A role for Saccharomyces cerevisiae histone H2A in DNA repair. *Nature*, 408(6815), pp.1001–1004.

Drissen, R. et al., 2004. The active spatial organization of the β-globin locus requires the transcription factor EKLF. *Genes and Development*, 18(20), pp.2485–2490.

Duan, X. et al., 2009. Structural and Functional Insights into the Roles of the Mms21 Subunit of the Smc5/6 Complex. *Molecular Cell*, 35(5), pp.657–668. Available at: https://linkinghub.elsevier.com/retrieve/pii/S1097276509004730.

Duan, Z. et al., 2010. A three-dimensional model of the yeast genome. *Nature*, 465(7296), pp.363–367. Available at: http://www.nature.com/articles/nature08973.

Dynek, J.N. & Smith, S., 2004. Resolution of Sister Telomere Association Is Required for Progression Through Mitosis. *Science*, 304(5667), pp.97–100.

Eeftens, J. & Dekker, C., 2017. Catching DNA with hoops-biophysical approaches to clarify the mechanism of SMC proteins. *Nature Structural and Molecular Biology*, 24(12), pp.1012–1020.

Ehrentraut, S. et al., 2010. Rpd3-dependent boundary formation at telomeres by removal of Sir2 substrate. *Proceedings of the National Academy of Sciences*, 107(12), pp.5522–5527. Available at: http://www.pnas.org/cgi/doi/10.1073/pnas.0909169107.

Ellahi, A., Thurtle, D.M. & Rine, J., 2015. The chromatin and transcriptional landscape of native saccharomyces cerevisiae telomeres and subtelomeric domains. *Genetics*, 200(2), pp.505–

521.

Enomoto, S., Glowczewski, L. & Berman, J., 2002. MEC3, MEC1, and DDC2 Are Essential Components of a Telomere Checkpoint Pathway Required for Cell Cycle Arrest during Senescence in Saccharomyces cerevisiae. *Molecular biology of the cell*, 13(6), pp.2001–2015.

Episkopou, H. et al., 2014. Alternative Lengthening of Telomeres is characterized by reduced compaction of telomeric chromatin. *Nucleic Acids Research*, 42(7), pp.4391–4405.

Erdel, F. & Rippe, K., 2018. Formation of Chromatin Subcompartments by Phase Separation. *Biophysical Journal*, 114(10), pp.2262–2270. Available at: https://doi.org/10.1016/j.bpj.2018.03.011.

Falk, M. et al., 2019. Heterochromatin drives compartmentalization of inverted and conventional nuclei. *Nature*, 570(7761), pp.395–399. Available at: http://dx.doi.org/10.1038/s41586-019-1275-3.

Fallet, E. et al., 2014. Length-dependent processing of telomeres in the absence of telomerase. *Nucleic Acids Research*, 42(6), pp.3648–3665.

Feeser, E.A. & Wolberger, C., 2008. Structural and Functional Studies of the Rap1 C-Terminus Reveal Novel Separation-of-Function Mutants. *Journal of Molecular Biology*, 380(3), pp.520–531.

Feng, Z. et al., 2011. Rad52 inactivation is synthetically lethal with BRCA2 deficiency. *Proceedings of the National Academy of Sciences of the United States of America*, 108(2), pp.686–691.

Ferguson, B.M. & Fangman, W.L., 1992. A position effect on the time of replication origin activation in yeast. *Cell*, 68(2), pp.333–339.

Ferraiuolo, M.A. et al., 2012. From cells to chromatin: Capturing snapshots of genome organization with 5C technology. *Methods*, 58(3), pp.255–267.

Ferreira, H.C. et al., 2011. The PIAS homologue Siz2 regulates perinuclear telomere position and telomerase activity in budding yeast. *Nature Cell Biology*, 13(7), pp.867–874. Available at: http://dx.doi.org/10.1038/ncb2263.

Flavahan, W.A. et al., 2016. Insulator dysfunction and oncogene activation in IDH mutant gliomas. *Nature*, 529(7584), pp.110–114.

Flyamer, I.M. et al., 2017. Single-nucleus Hi-C reveals unique chromatin reorganization at oocyte-to-zygote transition. *Nature*, 544(7648), pp.110–114.

Fontana, G.A. et al., 2018. Shepherding DNA ends: Rif1 protects telomeres and chromosome breaks. *Microbial Cell*, 5(7), pp.327–343.

Forey, R. et al., 2020. Mec1 Is Activated at the Onset of Normal S Phase by Low-dNTP Pools Impeding DNA Replication. *Molecular Cell*, 78(3), p.396–410.e4. Available at: https://doi.org/10.1016/j.molcel.2020.02.021.

Foti, R. et al., 2016. Nuclear Architecture Organized by Rif1 Underpins the Replication-Timing Program. *Molecular Cell*, 61(2), pp.260–273.

Fouché, N. et al., 2006. The Basic Domain of TRF2 Directs Binding to DNA Junctions Irrespective of the Presence of TTAGGG Repeats. *Journal of Biological Chemistry*, 281(49), pp.37486–37495. Available at: http://www.jbc.org/lookup/doi/10.1074/jbc.M608778200.

Fourel, G. et al., 1999. Cohabitation of insulators and silencing elements in yeast subtelomeric regions. *EMBO Journal*, 18(9), pp.2522–2537.

Fousteri, M.I. & Lehmann, A.R., 2000. A novel SMC protein complex in Schizosaccharomyces pombe contains the Rad18 DNA repair protein. *EMBO Journal*, 19(7), pp.1691–1702.

Franke, M. et al., 2016. Formation of new chromatin domains determines pathogenicity of genomic duplications. *Nature*, 538(7624), pp.265–269.

Friedman, K.L. et al., 1997. Replication profile of Saccharomyces cerevisiae chromosome VI. *Genes to Cells*, 2(11), pp.667–678.

Fudenberg, G. et al., 2016. Formation of Chromosomal Domains by Loop Extrusion. *Cell Reports*, 15(9), pp.2038–2049. Available at: http://dx.doi.org/10.1016/j.celrep.2016.04.085.

Fullwood, M.J. et al., 2009. An oestrogen-receptor-α-bound human chromatin interactome. *Nature*, 462(7269), pp.58–64.

Funayama, R. et al., 2006. Loss of linker histone H1 in cellular senescence. *Journal of Cell Biology*, 175(6), pp.869–880.

Futcher, B., 1999. Cell cycle synchronization. *Methods in Cell Science*, 21(2–3), pp.79–86.

Gall, J.G. & Pardue, M.L., 1969. Formation and detection of RNA-DNA hybrid molecules in cytological preparations. *Proceedings of the National Academy of Sciences of the United States of America*, 63(2), pp.378–383.

Gan, W. et al., 2011. R-loop-mediated genomic instability is caused by impairment of replication fork progression. *Genes and Development*, 25(19), pp.2041–2056.

Ganji, M. et al., 2018. Real-time imaging of DNA loop extrusion by condensin. *Science*, 360(6384), pp.102–105. Available at: http://www.ncbi.nlm.nih.gov/pubmed/29472443.

Gao, H. et al., 2007. RPA-like proteins mediate yeast telomere function. *Nature Structural & Molecular Biology*, 14(3), pp.208–214. Available at: http://www.nature.com/articles/nsmb1205.

García-Cao, M. et al., 2004. Epigenetic regulation of telomere length in mammalian cells by the Suv39h1 and Suv39h2 histone methyltransferases. *Nature Genetics*, 36(1), pp.94–99.

Garcia, V. et al., 2011. Bidirectional resection of DNA double-strand breaks by Mre11 and Exo1. *Nature*, 479(7372), pp.241–244.

Garvik, B., Carson, M. & Hartwell, L., 1995. Single-stranded DNA arising at telomeres in cdc13 mutants may constitute a specific signal for the RAD9 checkpoint. *Molecular and Cellular Biology*, 15(11), pp.6128–6138. Available at: http://mcb.asm.org/lookup/doi/10.1128/MCB.15.11.6128.

Gassler, J. et al., 2017. A mechanism of cohesin-dependent loop extrusion organizes zygotic genome architecture. *The EMBO journal*, 36(24), pp.3600–3618. Available at: http://www.ncbi.nlm.nih.gov/pubmed/29217590.

Gelinas, A.D. et al., 2009. Telomere capping proteins are structurally related to RPA with an additional telomere-specific domain. *Proceedings of the National Academy of Sciences of the United States of America*, 106(46), pp.19298–19303.

Gelperin, D.M. et al., 2005. Biochemical and genetic analysis of the yeast proteome with a movable ORF collection. *Genes and Development*, 19(23), pp.2816–2826.

Gerlich, D. et al., 2006. Condensin I Stabilizes Chromosomes Mechanically through a Dynamic Interaction in Live Cells. *Current Biology*, 16(4), pp.333–344. Available at:

https://linkinghub.elsevier.com/retrieve/pii/S0960982206010220.

Germier, T. et al., 2017. Real-Time Imaging of a Single Gene Reveals Transcription-Initiated Local Confinement. *Biophysical Journal*, 113(7), pp.1383–1394.

Geronimo, C.L. & Zakian, V.A., 2016. Getting it done at the ends: Pif1 family DNA helicases and telomeres. *DNA Repair*, 44, pp.151–158. Available at: http://dx.doi.org/10.1016/j.dnarep.2016.05.021.

Ghaemmaghami, S. et al., 2003. Global analysis of protein expression in yeast. *Nature*, 425(6959), pp.737–741.

Gheldof, N., Tabuchi, T.M. & Dekker, J., 2006. The active FMR1 promoter is associated with a large domain of altered chromatin conformation with embedded local histone modifications. *Proceedings of the National Academy of Sciences of the United States of America*, 103(33), pp.12463–12468.

Ghosh, A.K. et al., 2012. RECQL4, the protein mutated in Rothmund-Thomson syndrome, functions in telomere maintenance. *Journal of Biological Chemistry*, 287(1), pp.196–209.

Giaever, G. et al., 2002. Functional profiling of the Saccharomyces cerevisiae genome. *Nature*, 418(6896), pp.387–391. Available at: http://doi.wiley.com/10.1002/yea.320101310.

Gibcus, J.H. et al., 2018. A pathway for mitotic chromosome formation. *Science*, 359(6376), p.eaao6135. Available at: http://www.ncbi.nlm.nih.gov/pubmed/29348367.

Gilbert, C.S., Green, C.M. & Lowndes, N.F., 2001. Budding yeast Rad9 is an ATP-dependent Rad53 activating machine. *Molecular Cell*, 8(1), pp.129–136.

Giraud-Panis, M.J. et al., 2010. CST Meets Shelterin to Keep Telomeres in Check. *Molecular Cell*, 39(5), pp.665–676.

Gobbini, E. et al., 2016. Functions and regulation of the MRX complex at DNA double-strand breaks. *Microbial Cell*, 3(8), pp.329–337.

Goel, S., Krishnamurthy, S. & Hampsey, M., 2012. Mechanism of Start Site Selection by RNA Polymerase II. *Journal of Biological Chemistry*, 287(1), pp.557–567. Available at: http://www.jbc.org/lookup/doi/10.1074/jbc.M111.281576.

Gonzalo, S. et al., 2006. DNA methyltransferases control telomere length and telomere recombination in mammalian cells. *Nature Cell Biology*, 8(4), pp.416–424.

Gotta, M. et al., 1996. The clustering of telomeres and colocalization with Rap1, Sir3, and Sir4 proteins in wild-type Saccharomyces cerevisiae. *The Journal of Cell Biology*, 134(6), pp.1349–1363. Available at: http://www.jcb.org/cgi/doi/10.1083/jcb.134.6.1349.

Gottschling, D.E. et al., 1990. Position effect at S. cerevisiae telomeres: Reversible repression of Pol II transcription. *Cell*, 63(4), pp.751–762.

Goudsouzian, L.K., Tuzon, C.T. & Zakian, V.A., 2006. S. cerevisiae Tel1p and Mre11p are required for normal levels of Est1p and Est2p telomere association. *Molecular Cell*, 24(4), pp.603–610.

Graf, M. et al., 2017. Telomere Length Determines TERRA and R-Loop Regulation through the Cell Cycle. *Cell*, 170(1), p.72–85.e14.

Grandin, N., 2001. Ten1 functions in telomere end protection and length regulation in association with Stn1 and Cdc13. *The EMBO Journal*, 20(5), pp.1173–1183.

Grandin, N., Bailly, A. & Charbonneau, M., 2005. Activation of Mrc1, a mediator of the replication

checkpoint, by telomere erosion. *Biology of the Cell*, 97(10), pp.799–814.

Gravel, S. et al., 1998. Yeast Ku as a regulator of chromosomal DNA end structure. *Science*, 280(5364), pp.741–744.

Gravel, S. & Wellinger, R.J., 2002. Maintenance of Double-Stranded Telomeric Repeats as the Critical Determinant for Cell Viability in Yeast Cells Lacking Ku. *Molecular and Cellular Biology*, 22(7), pp.2182–2193.

Greenwell, P.W. et al., 1995. TEL1, a gene involved in controlling telomere length in S. cerevisiae, is homologous to the human ataxia telangiectasia gene. *Cell*, 82(5), pp.823–829. Available at: https://linkinghub.elsevier.com/retrieve/pii/0092867495904794.

Greider, C.W., 2016. Regulating telomere length from the inside out: The replication fork model. *Genes and Development*, 30(13), pp.1483–1491.

Greider, C.W. & Blackburn, E.H., 1989. A telomeric sequence in the RNA of Tetrahymena telomerase required for telomere repeat synthesis. *Nature*, 337(6205), pp.331–337.

Greider, C.W. & Blackburn, E.H., 1985. Identification of a specific telomere terminal transferase activity in tetrahymena extracts. *Cell*, 43(2), pp.405–413. Available at: https://linkinghub.elsevier.com/retrieve/pii/0092867485901709.

Greider, C.W. & Blackburn, E.H., 1987. The telomere terminal transferase of tetrahymena is a ribonucleoprotein enzyme with two kinds of primer specificity. *Cell*, 51(6), pp.887–898. Available at: https://linkinghub.elsevier.com/retrieve/pii/0092867487905769.

Griffith, J.D. et al., 1999. Mammalian telomeres end in a large duplex loop. *Cell*, 97(4), pp.503–514.

Grunstein, M., 1997. Molecular model for telomeric heterochromatin in yeast. *Current Opinion in Cell Biology*, 9(3), pp.383–387.

Grunstein, M. & Gasser, S.M., 2013. Epigenetics in Saccharomyces cerevisiae. *Cold Spring Harbor Perspectives in Biology*, 5(7), pp.a017491–a017491. Available at: http://cshperspectives.cshlp.org/lookup/doi/10.1101/cshperspect.a017491.

Grzenda, A. et al., 2009. Sin3: Master scaffold and transcriptional corepressor. *Biochimica et Biophysica Acta - Gene Regulatory Mechanisms*, 1789(6–8), pp.443–450. Available at: http://dx.doi.org/10.1016/j.bbagrm.2009.05.007.

Gu, B. et al., 2018. Transcription-coupled changes in nuclear mobility of mammalian cis-regulatory elements. *Science*, 359(6379), pp.1050–1055.

Guacci, V., Koshland, D. & Strunnikov, A., 1997. A Direct Link between Sister Chromatid Cohesion and Chromosome Condensation Revealed through the Analysis of MCD1 in S. cerevisiae. *Cell*, 91(1), pp.47–57. Available at: https://linkinghub.elsevier.com/retrieve/pii/S0092867401800088.

Guthrie, C. & Fink, G., 1991. Guide to yeast genetics and molecular biology. *Methods in Enzymology*, 194, pp.389–398.

Haaf, T. & Schmid, M., 1991. Chromosome topology in mammalian interphase nuclei. *Experimental Cell Research*, 192(2), pp.325–332.

Haarhuis, J.H.I. et al., 2017. The Cohesin Release Factor WAPL Restricts Chromatin Loop Extension. *Cell*, 169(4), p.693–707.e14. Available at: https://linkinghub.elsevier.com/retrieve/pii/S0092867417304269.

Haering, C.H. et al., 2002. Molecular Architecture of SMC Proteins and the Yeast Cohesin Complex. *Molecular Cell*, 9(4), pp.773–788. Available at: https://linkinghub.elsevier.com/retrieve/pii/S1097276502005154.

Hafner, L. et al., 2018. Rif1 binding and control of chromosome-internal DNA replication origins is limited by telomere sequestration. *CellReports*, 23(4), pp.983–992. Available at: https://doi.org/10.1016/j.celrep.2018.03.113.

Hafner, L., Shore, D. & Mattarocci, S., 2019. ChECing out Rif1 action in freely cycling cells. *Current genetics*, 65(2), pp.429–434. Available at: http://link.springer.com/10.1007/s00294-018-0902-0.

Hanahan, D. & Weinberg, R.A., 2011. Hallmarks of cancer: the next generation. *Cell*, 144(5), pp.646–74. Available at: http://www.ncbi.nlm.nih.gov/pubmed/21376230.

Hand, R., 1975. Regulation of DNA replication on subchromosomal units of mammalian cells. *Journal of Cell Biology*, 64(1), pp.89–97.

Handoko, L. et al., 2011. CTCF-mediated functional chromatin interactome in pluripotent cells. *Nature Genetics*, 43(7), pp.630–638. Available at: http://www.nature.com/articles/ng.857.

Hang, L.E. et al., 2011. SUMOylation regulates telomere length homeostasis by targeting Cdc13. *Nature Structural & Molecular Biology*, 18(8), pp.920–926. Available at: http://www.nature.com/articles/nsmb.2100.

Hannan, A. et al., 2015. Sumoylation of Sir2 differentially regulates transcriptional silencing in yeast. *Nucleic Acids Research*, 43(21), pp.10213–10226.

Hansen, A.S. et al., 2017. CTCF and cohesin regulate chromatin loop stability with distinct dynamics. *eLife*, 6. Available at: https://elifesciences.org/articles/25776.

Hardy, C.F.J., Sussel, L. & Shore, D., 1992. A RAP1-interacting protein involved in transcriptional silencing and telomere length regulation. *Genes and Development*, 6(5), pp.801–814.

Harrison, P. et al., 2002. A small reservoir of disabled ORFs in the yeast genome and its implications for the dynamics of proteome evolution. *Journal of Molecular Biology*, 316(3), pp.409–419.

Hayashi, M.T. et al., 2012. A telomere-dependent DNA damage checkpoint induced by prolonged mitotic arrest. *Nat Struct Mol Biol*, 19(4), pp.387–394.

Hayflick, L. & Moorhead, P.S., 1961. The serial cultivation of human diploid cell strains. *Experimental Cell Research*, pp.585–621.

Hecht, A. et al., 1995. Histone H3 and H4 N-termini interact with SIR3 and SIR4 proteins: a molecular model for the formation of heterochromatin in yeast. *Cell*, 80(4), pp.583–92. Available at: papers2://publication/uuid/5979295E-ECD2-47F8-A252-554BD1D22417.

Hector, R.E. et al., 2012. Mec1p associates with functionally compromised telomeres. *Chromosoma*, 121(3), pp.277–290.

Hector, R.E. et al., 2007. Tel1p Preferentially Associates with Short Telomeres to Stimulate Their Elongation. *Molecular Cell*, 27(5), pp.851–858.

Heitz, E., 1928. Das heterochromatin der moose. *Jahrb wiss Bot*, 69, pp.762–818.

Hemann, M.T. et al., 2001. The shortest telomere, not average telomere length, is critical for cell viability and chromosome stability. *Cell*, 107(1), pp.67–77.

Henriques, T. et al., 2012. Transcription termination between polo and snap, two closely spaced

tandem genes of D. melanogaster. *Transcription*, 3(4), pp.198–212. Available at: http://www.tandfonline.com/doi/abs/10.4161/trns.21967.

Henson, J.D. et al., 2002. Alternative lengthening of telomeres in mammalian cells. *Oncogene*, 21(4), pp.598–610. Available at: http://www.nature.com/articles/1205058.

Herrmann, G., Lindahl, T. & Schär, P., 1998. Saccharomyces cerevisiae LIF1: A function involved in DNA double-strand break repair related to mammalian XRCC4. *EMBO Journal*, 17(14), pp.4188–4198.

Heun, P. et al., 2001. The positioning and dynamics of origins of replication in the budding yeast nucleus. *Journal of Cell Biology*, 152(2), pp.385–400.

Hiraga, S. et al., 2017. Human RIF 1 and protein phosphatase 1 stimulate DNA replication origin licensing but suppress origin activation . *EMBO reports*, 18(3), pp.403–419.

Hiraga, S. et al., 2018. Budding yeast Rif1 binds to replication origins and protects DNA at blocked replication forks. *EMBO reports*, 19(9). Available at: https://onlinelibrary.wiley.com/doi/abs/10.15252/embr.201846222.

Hiraga, S.I. et al., 2014. Rif1 controls DNA replication by directing Protein Phosphatase 1 to reverse Cdc7- mediated phosphorylation of the MCM complex. *Genes and Development*, 28(4), pp.372–383.

Hiraga, S.I., Botsios, S. & Donaldson, A.D., 2008. Histone H3 lysine 56 acetylation by Rtt109 is crucial for chromosome positioning. *Journal of Cell Biology*, 183(4), pp.641–651.

Hirano, T., 2006. At the heart of the chromosome: SMC proteins in action. *Nature Reviews Molecular Cell Biology*, 7(5), pp.311–322. Available at: http://www.nature.com/articles/nrm1909.

Hirano, T., Kobayashi, R. & Hirano, M., 1997. Condensins, Chromosome Condensation Protein Complexes Containing XCAP-C, XCAP-E and a Xenopus Homolog of the Drosophila Barren Protein. *Cell*, 89(4), pp.511–521.

Hirano, T. & Mitchison, T.J., 1994. A heterodimeric coiled-coil protein required for mitotic chromosome condensation in vitro. *Cell*, 79(3), pp.449–458.

Hiratani, I. et al., 2008. Global reorganization of replication domains during embryonic stem cell differentiation. *PLoS Biology*, 6(10), pp.2220–2236.

Hocher, A. et al., 2018. Expanding heterochromatin reveals discrete subtelomeric domains delimited by chromatin landscape transitions. *Genome Research*, 28(12), pp.1867–1881.

Hopfner, K.P. et al., 2000. Structural biology of Rad50 ATPase: ATP-driven conformational control in DNA double-strand break repair and the ABC-ATPase superfamily. *Cell*, 101(7), pp.789–800.

Hoppe, G.J. et al., 2002. Steps in Assembly of Silent Chromatin in Yeast: Sir3-Independent Binding of a Sir2/Sir4 Complex to Silencers and Role for Sir2-Dependent Deacetylation. *Molecular and Cellular Biology*, 22(12), pp.4167–4180.

Horowitz, H., Thorburn, P. & Haber, J.E., 1984. Rearrangements of highly polymorphic regions near telomeres of Saccharomyces cerevisiae. *Molecular and Cellular Biology*, 4(11), pp.2509–2517. Available at: http://mcb.asm.org/lookup/doi/10.1128/MCB.4.11.2509.

Hsieh, T.-H.S. et al., 2020. Resolving the 3D Landscape of Transcription-Linked Mammalian Chromatin Folding. *Molecular Cell*, 78(3), p.539–553.e8. Available at: https://linkinghub.elsevier.com/retrieve/pii/S1097276520301507.

Hsieh, T.H.S. et al., 2015. Mapping Nucleosome Resolution Chromosome Folding in Yeast by Micro-C. *Cell*, 162(1), pp.108–119. Available at: http://dx.doi.org/10.1016/j.cell.2015.05.048.

Hsieh, T.H.S. et al., 2016. Micro-C XL: Assaying chromosome conformation from the nucleosome to the entire genome. *Nature Methods*, 13(12), pp.1009–1011.

Hsu, H.-L., 2000. Ku acts in a unique way at the mammalian telomere to prevent end joining. *Genes & Development*, 14(22), pp.2807–2812. Available at: http://www.genesdev.org/cgi/doi/10.1101/gad.844000.

Hsu, H.-L. et al., 1999. Ku is associated with the telomere in mammals. *Proceedings of the National Academy of Sciences*, 96(22), pp.12454–12458. Available at: http://www.pnas.org/cgi/doi/10.1073/pnas.96.22.12454.

Hu, B. et al., 2011. ATP Hydrolysis Is Required for Relocating Cohesin from Sites Occupied by Its Scc2/4 Loading Complex. *Current Biology*, 21(1), pp.12–24. Available at: https://linkinghub.elsevier.com/retrieve/pii/S0960982210015903.

Huang, C. & Zhu, B., 2018. Roles of H3K36-specific histone methyltransferases in transcription: antagonizing silencing and safeguarding transcription fidelity. *Biophysics Reports*, 4(4), pp.170–177. Available at: http://link.springer.com/10.1007/s41048-018-0063-1.

Huber, M.D., 2002. G4 DNA unwinding by BLM and Sgs1p: substrate specificity and substrate-specific inhibition. *Nucleic Acids Research*, 30(18), pp.3954–3961.

Hudson, D.F. et al., 2003. Condensin Is Required for Nonhistone Protein Assembly and Structural Integrity of Vertebrate Mitotic Chromosomes. *Developmental Cell*, 5(2), pp.323–336. Available at: https://linkinghub.elsevier.com/retrieve/pii/S1534580703001990.

Hug, N. & Lingner, J., 2006. Telomere length homeostasis. *Chromosoma*, 115(6), pp.413–425.

Hughes, J.R. et al., 2014. Analysis of hundreds of cis-regulatory landscapes at high resolution in a single, high-throughput experiment. *Nature Genetics*, 46(2), pp.205–212.

Hwang, J.Y. et al., 2008. Smc5-Smc6 complex suppresses gross chromosomal rearrangements mediated by break-induced replications. *DNA Repair*, 7(9), pp.1426–1436.

Ichikawa, Y. et al., 2015. Nucleosome organization and chromatin dynamics in telomeres. *Biomolecular Concepts*, 6(1), pp.67–75. Available at: https://www.degruyter.com/view/journals/bmc/6/1/article-p67.xml.

Iglesias, N. et al., 2011. Subtelomeric repetitive elements determine TERRA regulation by Rap1/Rif and Rap1/Sir complexes in yeast. *EMBO Reports*, 12(6), pp.587–593.

IJpma, A.S. & Greider, C.W., 2003. Short Telomeres Induce a DNA Damage Response in Saccharomyces cerevisiae. *Molecular biology of the cell*, 13(6), pp.2001–2015.

Imai, S.I. et al., 2000. Transcriptional silencing and longevity protein Sir2 is an NAD-dependent histone deacetylase. *Nature*, 403(6771), pp.795–800.

Ivessa, A.S. et al., 2002. Saccharomyces Rrm3p, a 5′ to 3′ DNA helicase that promotes replication fork progression through telomeric and subtelomeric DNA. *Genes and Development*, 16(11), pp.1383–1396.

Jacobs, J.J.L. & De Lange, T., 2004. Significant role for p16INK4a in p53-independent telomere-directed senescence. *Current Biology*, 14(24), pp.2302–2308.

Janicki, S.M. et al., 2004. From silencing to gene expression: Real-time analysis in single cells. *Cell*,

116(5), pp.683–698.

Janke, C. et al., 2004. A versatile toolbox for PCR-based tagging of yeast genes: New fluorescent proteins, more markers and promoter substitution cassettes. *Yeast*, 21(11), pp.947–962.

Jensen, R.B., Carreira, A. & Kowalczykowski, S.C., 2010. Purified human BRCA2 stimulates RAD51-mediated recombination. *Nature*, 467(7316), pp.678–683.

Jeppsson, K. et al., 2014. The Chromosomal Association of the Smc5/6 Complex Depends on Cohesion and Predicts the Level of Sister Chromatid Entanglement M. Lichten, ed. *PLoS Genetics*, 10(10), p.e1004680. Available at: https://dx.plos.org/10.1371/journal.pgen.1004680.

Johnson, F.B. et al., 2001. The Saccharomyces cerevisiae WRN homolog Sgs1p participates in telomere maintenance in cells lacking telomerase. *EMBO Journal*, 20(4), pp.905–913.

Joshi, A.A. & Struhl, K., 2005. Eaf3 chromodomain interaction with methylated H3-K36 links histone deacetylation to pol II elongation. *Molecular Cell*, 20(6), pp.971–978.

Kadauke, S. & Blobel, G.A., 2009. Chromatin loops in gene regulation. *Biochimica et Biophysica Acta - Gene Regulatory Mechanisms*, 1789(1), pp.17–25. Available at: http://www.ncbi.nlm.nih.gov/pubmed/18675948.

Kadosh, D. & Struhl, K., 1998a. Histone deacetylase activity of Rpd3 is important for transcriptional repression in vivo. *Genes and Development*, 12(6), pp.797–805.

Kadosh, D. & Struhl, K., 1998b. Targeted Recruitment of the Sin3-Rpd3 Histone Deacetylase Complex Generates a Highly Localized Domain of Repressed Chromatin In Vivo. *Molecular and Cellular Biology*, 18(9), pp.5121–5127. Available at: https://portlandpress.com/biochemj/article/475/24/3921/49835/Corepressor-coactivator-and-general-transcription.

Kakui, Y. et al., 2017. Condensin-mediated remodeling of the mitotic chromatin landscape in fission yeast. *Nature Genetics*, 49(10), pp.1553–1557. Available at: http://www.nature.com/articles/ng.3938.

Kaminker, P.G. et al., 2009. A novel form of the telomere-associated protein TIN2 localizes to the nuclear matrix. *Cell Cycle*, 8(6), pp.931–939.

Kegel, A. et al., 2011. Chromosome length influences replication-induced topological stress. *Nature*, 471(7338), pp.392–396. Available at: http://www.nature.com/articles/nature09791.

Kempfer, R. & Pombo, A., 2020. Methods for mapping 3D chromosome architecture. *Nature Reviews Genetics*, 21(4), pp.207–226. Available at: http://www.nature.com/articles/s41576-019-0195-2.

Keogh, M. et al., 2005. Cotranscriptional Set2 Methylation of Histone H3 Lysine 36 Recruits a Repressive Rpd3 Complex. *Cell*, 123(4), pp.593–605. Available at: https://linkinghub.elsevier.com/retrieve/pii/S0092867405011591.

Khadaroo, B. et al., 2009. The DNA damage response at eroded telomeres and tethering to the nuclear pore complex. *Nature Cell Biology*, 11(8), pp.980–987.

Kim, W. et al., 2016. Regulation of the Human Telomerase Gene TERT by Telomere Position Effect—Over Long Distances (TPE-OLD): Implications for Aging and Cancer. *PLoS Biology*, 14(12), pp.1–25.

Kimura, A., Umehara, T. & Horikoshi, M., 2002. Chromosomal gradient of histone acetylation

established by Sas2p and Sir2p functions as a shield against gene silencing. *Nature Genetics*, 32(3), pp.370–377.

Kirmizis, A. et al., 2007. Arginine methylation at histone H3R2 controls deposition of H3K4 trimethylation. *Nature*, 449(7164), pp.928–932.

Kitsberg, D. et al., 1993. Replication structure of the human & beta;-globin gene domain. *Nature*, 366(6455), pp.588–590.

Knott, S.R. V et al., 2009. Genome-wide replication profiles indicate an expansive role for Rpd3L in regulating replication initiation timing or efficiency, and reveal genomic loci of Rpd3 function in Saccharomyces cerevisiae. *Genes and Development*, 23(9), pp.1077–1090.

Knott, S.R.V. et al., 2012. Forkhead transcription factors establish origin timing and long-range clustering in S. cerevisiae. *Cell*, 148(1–2), pp.99–111.

Koc, K.N. et al., 2016. Pif1 removes a Rap1-dependent barrier to the strand displacement activity of DNA polymerase δ. *Nucleic Acids Research*, 44(8), pp.3811–3819.

Koering, C.E. et al., 2002. Human telomeric position effect is determined by chromosomal context and telomeric chromatin integrity. *EMBO Reports*, 3(11), pp.1055–1061.

König, P. et al., 1996. The Crystal Structure of the DNA-Binding Domain of Yeast RAP1 in Complex with Telomeric DNA. *Cell*, 85(1), pp.125–136. Available at: https://linkinghub.elsevier.com/retrieve/pii/S0092867400810880.

Kozak, M.L. et al., 2010. Inactivation of the Sas2 histone acetyltransferase delays senescence driven by telomere dysfunction. *EMBO Journal*, 29(1), pp.158–170. Available at: http://dx.doi.org/10.1038/emboj.2009.314.

Krogan, N.J. et al., 2003. Methylation of Histone H3 by Set2 in Saccharomyces cerevisiae Is Linked to Transcriptional Elongation by RNA Polymerase II. *Molecular and Cellular Biology*, 23(12), pp.4207–4218.

Kurdistani, S.K. & Grunstein, M., 2003. Histone acetylation and deacetylation in yeast. *Nature Reviews Molecular Cell Biology*, 4(4), pp.276–284.

Kyrion, G., Boakye, K.A. & Lustig, A.J., 1992. C-terminal truncation of RAP1 results in the deregulation of telomere size, stability, and function in Saccharomyces cerevisiae. *Molecular and Cellular Biology*, 12(11), pp.5159–5173.

Lafuente-Barquero, J. et al., 2017. The Smc5/6 complex regulates the yeast Mph1 helicase at RNA-DNA hybrid-mediated DNA damage F. Storici, ed. *PLOS Genetics*, 13(12), p.e1007136. Available at: https://dx.plos.org/10.1371/journal.pgen.1007136.

Lainé, J.-P. et al., 2009. A physiological role for gene loops in yeast. *Genes & Development*, 23(22), pp.2604–2609. Available at: http://genesdev.cshlp.org/lookup/doi/10.1101/gad.1823609.

Lakadamyali, M. & Cosma, M.P., 2015. Advanced microscopy methods for visualizing chromatin structure. *FEBS Letters*, 589(20), pp.3023–3030.

Lallemand-Breitenbach, V. & de The, H., 2010. PML Nuclear Bodies. *Cold Spring Harbor Perspectives in Biology*, 2(5), pp.a000661–a000661. Available at: http://cshperspectives.cshlp.org/lookup/doi/10.1101/cshperspect.a000661.

Lammens, A., Schele, A. & Hopfner, K.-P., 2004. Structural Biochemistry of ATP-Driven Dimerization and DNA-Stimulated Activation of SMC ATPases. *Current Biology*, 14(19), pp.1778–1782. Available at: https://linkinghub.elsevier.com/retrieve/pii/S0960982204007109.

Langdon, E.M. et al., 2018. mRNA structure determines specificity of a polyQ-driven phase separation. *Science*, 360(6391), pp.922–927.

Langdon, E.M. & Gladfelter, A.S., 2018. A New Lens for RNA Localization: Liquid-Liquid Phase Separation. *Annual Review of Microbiology*, 72(1), pp.255–271.

de Lange, T., 2009. How Telomeres Solve the End-Protection Problem. *Science*, 326(5955), pp.948–952.

de Lange, T., 2018. Shelterin-Mediated Telomere Protection. *Annual Review of Genetics*, 52(1), pp.223–247.

de Lange, T. et al., 1990. Structure and variability of human chromosome ends. *Molecular and Cellular Biology*, 10(2), pp.518–527. Available at: http://mcb.asm.org/lookup/doi/10.1128/MCB.10.2.518.

De Lange, T., 2004. T-loops and the origin of telomeres. *Nature Reviews Molecular Cell Biology*, 5(4), pp.323–329.

Lansdorp, P.M., 2008. Telomeres, stem cells, and hematology. *Blood*, 111(4), pp.1759–1765.

Lanz, M.C., Dibitetto, D. & Smolka, M.B., 2019. DNA damage kinase signaling: checkpoint and repair at 30 years. *The EMBO journal*, 38(18), p.e101801. Available at: https://onlinelibrary.wiley.com/doi/abs/10.15252/embj.2019101801.

Laroche, T. et al., 1998. Mutation of yeast Ku genes disrupts the subnuclear organization of telomeres. *Current Biology*, 8(11), pp.653–657. Available at: https://linkinghub.elsevier.com/retrieve/pii/S0960982298702520.

Larrivée, M., LeBel, C. & Wellinger, R.J., 2004. The generation of proper constitutive G-tails on yeast telomeres is dependent on the MRX complex. *Genes and Development*, 18(12), pp.1391–1396.

Larrivée, M. & Wellinger, R.J., 2006. Telomerase- and capping-independent yeast survivors with alternate telomere states. *Nature cell biology*, 8(7), pp.741–7. Available at: http://www.nature.com/articles/ncb1429.

Larson, A.G. et al., 2017. Liquid droplet formation by HP1α suggests a role for phase separation in heterochromatin. *Nature*, 547(7662), pp.236–240.

Le, S. et al., 1999. RAD50 and RAD51 define two pathways that collaborate to maintain telomeres in the absence of telomerase. *Genetics*, 152(1), pp.143–52. Available at: http://www.ncbi.nlm.nih.gov/pubmed/10224249.

Le, T.B.K. et al., 2013. High-Resolution Mapping of the Spatial Organization of a Bacterial Chromosome. *Science*, 342(6159), pp.731–734. Available at: https://www.sciencemag.org/lookup/doi/10.1126/science.1242059.

Lee, C.H., Occhipinti, P. & Gladfelter, A.S., 2015. PolyQ-dependent RNA-protein assemblies control symmetry breaking. *Journal of Cell Biology*, 208(5), pp.533–544.

Lee, J.S. & Shilatifard, A., 2007. A site to remember: H3K36 methylation a mark for histone deacetylation. *Mutation Research - Fundamental and Molecular Mechanisms of Mutagenesis*, 618(1–2), pp.130–134.

Lee, K. et al., 2015. Dynamic enhancer–gene body contacts during transcription elongation. *Genes and Development*, 29(19), pp.1992–1997.

Lee, K. & Sang, E.L., 2007. Saccharomyces cerevisiae Sae2- and Tel1-dependent single-strand DNA formation at DNA break promotes microhomology-mediated end joining. *Genetics*, 176(4), pp.2003–2014. Available at: http://www.genetics.org/lookup/doi/10.1534/genetics.107.076539.

Lei, M., Podell, E.R. & Cech, T.R., 2004. Structure of human POT1 bound to telomeric single-stranded DNA provides a model for chromosome end-protection. *Nature Structural & Molecular Biology*, 11(12), pp.1223–1229. Available at: http://www.nature.com/articles/nsmb867.

Lenain, C. et al., 2006. The Apollo 5′ Exonuclease Functions Together with TRF2 to Protect Telomeres from DNA Repair. *Current Biology*, 16(13), pp.1303–1310.

Lendvay, T.S. et al., 1996. Senescence mutants of Saccharomyces cerevisiae with a defect in telomere replication identify three additional EST genes. *Genetics*, 144(4), pp.1399–1412.

Lengronne, A., 2001. Monitoring S phase progression globally and locally using BrdU incorporation in TK+ yeast strains. *Nucleic Acids Research*, 29(7), pp.1433–1442.

Levis, R., Hazelrigg, T. & Rubin, G.M., 1985. Effects of genomic position on the expression of transduced copies of the white gene of Drosophila. *Science*, 229(4713), pp.558–561.

Lew, J.E., Enomoto, S. & Berman, J., 1998. Telomere Length Regulation and Telomeric Chromatin Require the Nonsense-Mediated mRNA Decay Pathway. *Molecular and Cellular Biology*, 18(10), pp.6121–6130.

Li, B. et al., 2003. The Set2 histone methyltransferase functions through the phosphorylated carboxyl-terminal domain of RNA polymerase II. *Journal of Biological Chemistry*, 278(11), pp.8897–8903.

Li, G. et al., 2012. Extensive promoter-centered chromatin interactions provide a topological basis for transcription regulation. *Cell*, 148(1–2), pp.84–98.

Lian, H.Y. et al., 2011. The effect of Ku on telomere replication time is mediated by telomere length but is independent of histone tail acetylation. *Molecular Biology of the Cell*, 22(10), pp.1753–1765.

Liaw, H. & Lustig, A.J., 2006. Sir3 C-Terminal Domain Involvement in the Initiation and Spreading of Heterochromatin. *Molecular and Cellular Biology*, 26(20), pp.7616–7631.

Lieberman-Aiden, E. et al., 2009. Comprehensive Mapping of Long-Range Interactions Reveals Folding Principles of the Human Genome. *Science*, 326(5950), pp.289–293. Available at: http://www.sciencemag.org/cgi/doi/10.1126/science.1181369.

Lillard-Wetherell, K. et al., 2004. Association and regulation of the BLM helicase by the telomere proteins TRF1 and TRF2. *Human Molecular Genetics*, 13(17), pp.1919–1932.

Linger, B.R. & Price, C.M., 2009. Conservation of telomere protein complexes: shuffling through evolution. *Critical Reviews in Biochemistry and Molecular Biology*, 44(6), pp.434–446. Available at: http://www.tandfonline.com/doi/full/10.3109/10409230903307329.

Lingner, J., Cooper, J.P. & Cech, T.R., 1995. Telomerase and DNA end replication: No longer a lagging strand problem? *Science*, 269(5230), pp.1533–1534.

Liou, G.G. et al., 2005. Assembly of the SIR complex and its regulation by O-acetyl-ADP-ribose, a product of NAD-dependent histone deacetylation. *Cell*, 121(4), pp.515–527. Available at: https://linkinghub.elsevier.com/retrieve/pii/S0092867405003545.

Liu, X. et al., 2017. In Situ Capture of Chromatin Interactions by Biotinylated dCas9. *Cell*, 170(5), p.1028–1043.e19. Available at: https://linkinghub.elsevier.com/retrieve/pii/S0092867417308917.

Lok, B.H. et al., 2013. RAD52 inactivation is synthetically lethal with deficiencies in BRCA1 and PALB2 in addition to BRCA2 through RAD51-mediated homologous recombination. *Oncogene*, 32(30), pp.3552–3558.

Lok, B.H. & Powell, S.N., 2012. Molecular pathways: Understanding the role of Rad52 in homologous recombination for therapeutic advancement. *Clinical Cancer Research*, 18(23), pp.6400–6406.

Lombard, D.B. et al., 2008. SIRT6 in DNA repair, metabolism and ageing. *Journal of Internal Medicine*, 263(2), pp.128–141. Available at: http://www.ncbi.nlm.nih.gov/pubmed/18226091.

Longhese, M.P. et al., 2000. Checkpoint proteins influence telomeric silencing and length maintenance in budding yeast. *Genetics*, 155(4), pp.1577–1591.

Longtine, M.S. et al., 1998. Additional modules for versatile and economical PCR-based gene deletion and modification in Saccharomyces cerevisiae. *Yeast*, 14(10), pp.953–961.

Lõoke, M. et al., 2013. Chromatin-dependent and-independent regulation of DNA replication origin activation in budding yeast. *EMBO Reports*, 14(2), pp.191–198.

Lopez-Serra, L. et al., 2013. Budding Yeast Wapl Controls Sister Chromatid Cohesion Maintenance and Chromosome Condensation. *Current Biology*, 23(1), pp.64–69. Available at: https://linkinghub.elsevier.com/retrieve/pii/S0960982212013747.

Losada, A., 2005. Dynamic molecular linkers of the genome: the first decade of SMC proteins. *Genes & Development*, 19(11), pp.1269–1287. Available at: http://www.genesdev.org/cgi/doi/10.1101/gad.1320505.

Louis, E.J., 1995. The chromosome ends ofSaccharomyces cerevisiae. *Yeast*, 11(16), pp.1553–1573. Available at: http://doi.wiley.com/10.1002/yea.320111604.

Louis, E.J. & Becker, M.M., 2014. Subtelomeres. *Springer*, ISBN 978-3.

Ludérus, M.E.E. et al., 1996. Structure, subnuclear distribution, and nuclear matrix association of the mammalian telomeric complex. *Journal of Cell Biology*, 135(4), pp.867–881.

Luger, K. et al., 1997. Crystal structure of the nucleosome core particle at 2.8 Å resolution. *Nature*, 389(6648), pp.251–260.

Luke, B. et al., 2008. The Rat1p 5′ to 3′ Exonuclease Degrades Telomeric Repeat-Containing RNA and Promotes Telomere Elongation in Saccharomyces cerevisiae. *Molecular Cell*, 32(4), pp.465–477. Available at: http://dx.doi.org/10.1016/j.molcel.2008.10.019.

Lundblad, V. & Blackburn, E.H., 1993. An alternative pathway for yeast telomere maintenance rescues est1- senescence. *Cell*, 73(2), pp.347–360.

Lundblad, V. & Szostak, J.W., 1989. A mutant with a defect in telomere elongation leads to senescence in yeast. *Cell*, 57(4), pp.633–643.

Lundin, C. et al., 2005. Methyl methanesulfonate (MMS) produces heat-labile DNA damage but no detectable in vivo DNA double-strand breaks. *Nucleic Acids Research*, 33(12), pp.3799–3811.

Luo, K., Vega-Palas, M.A. & Grunstein, M., 2002. Rap1-Sir4 binding independent of other Sir, yKu,

or histone interactions initiates the assembly of telomeric heterochromatin in yeast. *Genes and Development*, 16(12), pp.1528–1539. Available at: http://www.genesdev.org/cgi/doi/10.1101/gad.988802.

Lupiáñez, D.G. et al., 2015. Disruptions of topological chromatin domains cause pathogenic rewiring of gene-enhancer interactions. *Cell*, 161(5), pp.1012–1025.

Lustig, A.J., 2003. Clues to catastrophic telomere loss in mammals from yeast telomere rapid deletion. *Nature Reviews Genetics*, 4(11), pp.916–923.

Lustig, A.J. & Petes, T.D., 1986. Identification of yeast mutants with altered telomere structure. *Proceedings of the National Academy of Sciences of the United States of America*, 83(5), pp.1398–1402.

Van Ly, D. et al., 2018. Telomere Loop Dynamics in Chromosome End Protection. *Molecular Cell*, 71(4), p.510–525.e6.

Lydall, D. & Weinert, T., 1995. Yeast checkpoint genes in DNA damage processing: Implications for repair and arrest. *Science*, 270(5241), pp.1488–1491.

Ma, J.-L. et al., 2003. Yeast Mre11 and Rad1 Proteins Define a Ku-Independent Mechanism To Repair Double-Strand Breaks Lacking Overlapping End Sequences. *Molecular and Cellular Biology*, 23(23), pp.8820–8828.

Maciejowski, J. & De Lange, T., 2017. Telomeres in cancer: Tumour suppression and genome instability. *Nature Reviews Molecular Cell Biology*, 18(3), pp.175–186.

Maestroni, L., Matmati, S. & Coulon, S., 2017. Solving the telomere replication problem. *Genes*, 8(2), pp.1–16.

Mak, S.S.M. et al., 2019. T-loops Refold after Telomerase Extension and Unfold Again at Late S/G2 for C-strand Fill-in. *bioRxiv*, p.869982.

Makarov, V.L., Hirose, Y. & Langmore, J.P., 1997. Long G Tails at Both Ends of Human Chromosomes Suggest a C Strand Degradation Mechanism for Telomere Shortening. *Cell*, 88(5), pp.657–666. Available at: https://linkinghub.elsevier.com/retrieve/pii/S009286740081908X.

Makovets, S., Herskowitz, I. & Blackburn, E.H., 2004. Anatomy and Dynamics of DNA Replication Fork Movement in Yeast Telomeric Regions. *Molecular and Cellular Biology*, 24(9), pp.4019–4031.

Mansour, W.Y., Rhein, T. & Dahm-Daphi, J., 2010. The alternative end-joining pathway for repair of DNA double-strand breaks requires PARP1 but is not dependent upon microhomologies. *Nucleic Acids Research*, 38(18), pp.6065–6077.

Marcand, S. et al., 2000. Cell cycle restriction of telomere elongation. *Current Biology*, 10(8), pp.487–490.

Marcand, S. et al., 2008. Multiple pathways inhibit NHEJ at telomeres. *Genes and Development*, 22(9), pp.1153–1158.

Maringele, L. & Lydall, D., 2002. EXO1-dependent single-stranded DNA at telomeres activates subsets of DNA damage and spindle checkpoint pathways in budding yeast yku70Δ mutants. *Genes and Development*, 16(15), pp.1919–1933.

Marshall, O.J. et al., 2016. Cell-type-specific profiling of protein-DNA interactions without cell isolation using targeted DamID with next-generation sequencing. *Nature Protocols*, 11(9), pp.1586–1598.

Marshall, W.F. et al., 1997. Interphase chromosomes undergo constrained diffusional motion in living cells. *Current Biology*, 7(12), pp.930–939.

Martin, S.G. et al., 1999. Relocalization of telomeric Ku and SIR proteins in response to DNA strand breaks in yeast. *Cell*, 97(5), pp.621–633.

Martínez, P. et al., 2009. Increased telomere fragility and fusions resulting from TRF1 deficiency lead to degenerative pathologies and increased cancer in mice. *Genes and Development*, 23(17), pp.2060–2075.

Masuda-Sasa, T. et al., 2008. Processing of G4 DNA by Dna2 helicase/nuclease and replication protein A (RPA) provides insights into the mechanism of Dna2/RPA substrate recognition. *Journal of Biological Chemistry*, 283(36), pp.24359–24373.

Masui, O. et al., 2011. Live-cell chromosome dynamics and outcome of X chromosome pairing events during ES cell differentiation. *Cell*, 145(3), pp.447–458.

Mattarocci, S. et al., 2016. Rif1: A conserved regulator of DNA replication and repair hijacked by telomeres in yeasts. *Frontiers in Genetics*, 7(MAR), pp.1–7.

Mattarocci, S. et al., 2014. Rif1 Controls DNA replication timing in yeast through the PP1 Phosphatase Glc7. *Cell Reports*, 7(1), pp.62–69.

Mattarocci, S. et al., 2017. Rif1 maintains telomeres and mediates DNA repair by encasing DNA ends. *Nature Structural and Molecular Biology*, 24(7), pp.588–595.

Mayer, A. et al., 2010. Uniform transitions of the general RNA polymerase II transcription complex. *Nature Structural and Molecular Biology*, 17(10), pp.1272–1278.

McClintock, B., 1939. The behavior in successive nuclear divisions of a chromosome broken at meiosis. *Proceedings of the National Academy of Sciences of the United States of America*, 25, pp.405–416.

McClintock, B., 1941. The Stability of Broken Ends of Chromosomes in Zea Mays. *Genetics*, 26(2), pp.234–282.

McCord, R.P., Kaplan, N. & Giorgetti, L., 2020. Chromosome Conformation Capture and Beyond: Toward an Integrative View of Chromosome Structure and Function. *Molecular Cell*, 77(4), pp.688–708. Available at: https://doi.org/10.1016/j.molcel.2019.12.021.

McDonald, M.J. et al., 2016. Mutation at a distance caused by homopolymeric guanine repeats in Saccharomyces cerevisiae. *Science Advances*, 2(5), p.e1501033. Available at: https://advances.sciencemag.org/lookup/doi/10.1126/sciadv.1501033.

McElligott, R., 1997. The terminal DNA structure of mammalian chromosomes. *The EMBO Journal*, 16(12), pp.3705–3714. Available at: http://emboj.embopress.org/cgi/doi/10.1093/emboj/16.12.3705.

McGee, J.S. et al., 2010. Reduced Rif2 and lack of Mec1 target short telomeres for elongation rather than double-strand break repair. *Nature Structural & Molecular Biology*, 17(12), pp.1438–1445. Available at: http://www.nature.com/articles/nsmb.1947.

McGinty, R.K. & Tan, S., 2015. Nucleosome structure and function. *Chemical Reviews*, 115(6), pp.2255–2273.

Méchali, M., 2010. Eukaryotic DNA replication origins: Many choices for appropriate answers. *Nature Reviews Molecular Cell Biology*, 11(10), pp.728–738. Available at: http://www.nature.com/articles/nrm2976.

Meister, P. & Taddei, A., 2013. Building silent compartments at the nuclear periphery: A recurrent theme. *Current Opinion in Genetics and Development*, 23(2), pp.96–103.

Menolfi, D. et al., 2015. Essential Roles of the Smc5/6 Complex in Replication through Natural Pausing Sites and Endogenous DNA Damage Tolerance. *Molecular Cell*, 60(6), pp.835–846. Available at: http://dx.doi.org/10.1016/j.molcel.2015.10.023.

Metcalfe, J.A. et al., 1996. Accelerated telomere shortening in ataxia telangiectasia. *Nature Genetics*, 13(3), pp.350–353.

Meyne, J. et al., 1990. Distribution of non-telomeric sites of the (TTAGGG)n telomeric sequence in vertebrate chromosomes. *Chromosoma*, 99(1), pp.3–10.

Mi, H. et al., 2019. PANTHER version 14: more genomes, a new PANTHER GO-slim and improvements in enrichment analysis tools. *Nucleic Acids Research*, 47(D1), pp.D419–D426. Available at: https://academic.oup.com/nar/article/47/D1/D419/5165346.

Michaelis, C., Ciosk, R. & Nasmyth, K., 1997. Cohesins: Chromosomal Proteins that Prevent Premature Separation of Sister Chromatids. *Cell*, 91(1), pp.35–45. Available at: https://linkinghub.elsevier.com/retrieve/pii/S0092867401800076.

Michishita, E. et al., 2008. SIRT6 is a histone H3 lysine 9 deacetylase that modulates telomeric chromatin. *Nature*, 452(7186), pp.492–496.

Mieczkowski, P.A. et al., 2003. Genetic regulation of telomere-telomere fusions in the yeast Saccharomyces cerevisae. *Proceedings of the National Academy of Sciences*, 100(19), pp.10854–10859. Available at: http://www.pnas.org/cgi/doi/10.1073/pnas.1934561100.

Mifsud, B. et al., 2015. Mapping long-range promoter contacts in human cells with high-resolution capture Hi-C. *Nature Genetics*, 47(6), pp.598–606.

Miller, K.M., Rog, O. & Cooper, J.P., 2006. Semi-conservative DNA replication through telomeres requires Taz1. *Nature*, 440(7085), pp.824–828.

Mills, K.D., Sinclair, D.A. & Guarente, L., 1999. MEC1-dependent redistribution of the Sir3 silencing protein from telomeres to DNA double-strand breaks. *Cell*, 97(5), pp.609–620.

Mimitou, E.P. & Symington, L.S., 2008. Sae2, Exo1 and Sgs1 collaborate in DNA double-strand break processing. *Nature*, 455(7214), pp.770–774.

Miné-Hattab, J. & Taddei, A., 2019. Physical principles and functional consequences of nuclear compartmentalization in budding yeast. *Current Opinion in Cell Biology*, 58, pp.105–113. Available at: https://linkinghub.elsevier.com/retrieve/pii/S0955067418301649.

Mirny, L.A., Imakaev, M. & Abdennur, N., 2019. Two major mechanisms of chromosome organization. *Current Opinion in Cell Biology*, 58(June), pp.142–152. Available at: https://doi.org/10.1016/j.ceb.2019.05.001.

Mishra, K. & Shore, D., 1999. Yeast Ku protein plays a direct role in telomeric silencing and counteracts inhibition by Rif proteins. *Current Biology*, 9(19), pp.1123–1126.

Misino, S. et al., 2018. Increased TERRA levels and RNase H sensitivity are conserved hallmarks of post-senescent survivors in budding yeast. *Differentiation*, 100, pp.37–45. Available at: https://linkinghub.elsevier.com/retrieve/pii/S0301468117301494.

Mizuguchi, T. et al., 2014. Cohesin-dependent globules and heterochromatin shape 3D genome architecture in S. pombe. *Nature*, 516(7531), pp.432–435.

Mohaghegh, P., 2001. The Bloom's and Werner's syndrome proteins are DNA structure-specific helicases. *Nucleic Acids Research*, 29(13), pp.2843–2849.

Mondoux, M.A. & Zakian, V.A., 2007. Subtelomeric elements influence but do not determine silencing levels at Saccharomyces cerevisiae telomeres. *Genetics*, 177(4), pp.2541–2546.

Monneron, A. & Bernhard, W., 1969. Fine structural organization of the interphase nucleus in some mammalian cells. *Journal of Ultrasructure Research*, 27(3–4), pp.266–288.

Montero, J.J. et al., 2018. TERRA recruitment of polycomb to telomeres is essential for histone trymethylation marks at telomeric heterochromatin. *Nature Communications*, 9(1), p.1548. Available at: http://www.nature.com/articles/s41467-018-03916-3.

Moradi-Fard, S. et al., 2016. Smc5/6 Is a Telomere-Associated Complex that Regulates Sir4 Binding and TPE. *PLoS Genetics*, 12(8), pp.1–22.

Moravec, M. et al., 2016. TERRA promotes telomerase-mediated telomere elongation in Schizosaccharomyces pombe . *EMBO reports*, 17(7), pp.999–1012.

Morawska, M. & Ulrich, H.D., 2013. An expanded tool kit for the auxin-inducible degron system in budding yeast. *Yeast*, 30(9), pp.341–351.

Moretti, P. et al., 1994. Evidence that a complex of SIR proteins interacts with the silencer and telomere-binding protein RAP1. *Genes and Development*, 8(19), pp.2257–2269.

Moretti, P. & Shore, D., 2001. Multiple Interactions in Sir Protein Recruitment by Rap1p at Silencers and Telomeres in Yeast. *Molecular and Cellular Biology*, 21(23), pp.8082–8094.

Moriya, H., 2015. Quantitative nature of overexpression experiments. *Molecular Biology of the Cell*, 26(22), pp.3932–3939.

Morrow, D.M. et al., 1995. TEL1, an S. cerevisiae homolog of the human gene mutated in ataxia telangiectasia, is functionally related to the yeast checkpoint gene MEC1. *Cell*, 82(5), pp.831–840.

Mortimer, R.K. & Johnston, J.R., 1986. Genealogy of principal strains of the yeast genetic stock center. *Genetics*, 113(1), pp.35–43.

Mostoslavsky, R. et al., 2006. Genomic instability and aging-like phenotype in the absence of mammalian SIRT6. *Cell*, 124(2), pp.315–329.

Moyzis, R.K. et al., 1988. A highly conserved repetitive DNA sequence, (TTAGGG)n, present at the telomeres of human chromosomes. *Proceedings of the National Academy of Sciences*, 85(18), pp.6622–6626. Available at: http://www.pnas.org/cgi/doi/10.1073/pnas.85.18.6622.

Müller, H.J., 1938. The remaking of chromosomes. *Collect.Net*, 8, pp.182–195.

Muñoz-Jordán, J.L. et al., 2001. T-Loops At Trypanosome Telomeres. *EMBO Journal*, 20(3), pp.579–588.

Murnane, J.P. et al., 1994. Telomere dynamics in an immortal human cell line. *The EMBO Journal*, 13(20), pp.4953–4962.

Murnane, J.P., 2012. Telomere dysfunction and chromosome instability. *Mutation Research - Fundamental and Molecular Mechanisms of Mutagenesis*, 730(1–2), pp.28–36.

Murti, K.G. & Prescott, D.M., 1999. Telomeres of polytene chromosomes in a ciliated protozoan terminate in duplex DNA loops. *Proceedings of the National Academy of Sciences*, 96(25), pp.14436–14439. Available at: http://www.pnas.org/cgi/doi/10.1073/pnas.96.25.14436.

Myung, K., Datta, A. & Kolodner, R.D., 2001. Suppression of spontaneous chromosomal rearrangements by S phase checkpoint functions in Saccharomyces cerevisiae. *Cell*, 104(3), pp.397–408.

Nagai, S., Heun, P. & Gasser, S.M., 2010. Roles for nuclear organization in the maintenance of genome stability. *Epigenomics*, 2(2), pp.289–305. Available at: https://www.futuremedicine.com/doi/10.2217/epi.09.49.

Nagano, T. et al., 2017. Cell-cycle dynamics of chromosomal organization at single-cell resolution. *Nature*, 547(7661), pp.61–67.

Nagano, T. et al., 2015. Single-cell Hi-C for genome-wide detection of chromatin interactions that occur simultaneously in a single cell. *Nature Protocols*, 10(12), pp.1986–2003.

Nagano, T. et al., 2013. Single-cell Hi-C reveals cell-to-cell variability in chromosome structure. *Nature*, 502(7469), pp.59–64.

Naito, T., Matsuura, A. & Ishikawa, F., 1998. Circular chromosome formation in a fission yeast mutant defective in two ATM homologues. *Nature Genetics*, 20(2), pp.203–206.

Nakada, D., Matsumoto, K. & Sugimoto, K., 2003. ATM-related Tel1 associates with double-strand breaks through an Xrs2-dependent mechanism. *Genes and Development*, 17(16), pp.1957–1962.

Nanavaty, V. et al., 2017. Trypanosoma brucei RAP1 maintains telomere and subtelomere integrity by suppressing TERRA and telomeric RNA: DNA hybrids. *Nucleic Acids Research*, 45(10), pp.5785–5796.

Narita, M. et al., 2003. Rb-mediated heterochromatin formation and silencing of E2F target genes during cellular senescence. *Cell*, 113(6), pp.703–716.

Nasmyth, K. & Haering, C.H., 2005. THE STRUCTURE AND FUNCTION OF SMC AND KLEISIN COMPLEXES. *Annual Review of Biochemistry*, 74(1), pp.595–648. Available at: http://www.annualreviews.org/doi/10.1146/annurev.biochem.74.082803.133219.

Nasmyth, K., Stillman, D. & Kipling, D., 1987. Both positive and negative regulators of HO transcription are required for mother-cell-specific mating-type switching in yeast. *Cell*, 48(4), pp.579–587.

Nautiyal, S., DeRisi, J.L. & Blackburn, E.H., 2002. The genome-wide expression response to telomerase deletion in Saccharomyces cerevisiae. *Proceedings of the National Academy of Sciences*, 99(14), pp.9316–9321. Available at: http://www.pnas.org/cgi/doi/10.1073/pnas.142162499.

Nergadze, S.G. et al., 2009. CpG-island promoters drive transcription of human telomeres. *Rna*, 15(12), pp.2186–2194.

New, J.H. et al., 1998. Rad52 protein stimulates DNA strand exchange by Rad51 and replication protein A. *Nature*, 391(6665), pp.407–410.

Newlon, C.S. & Theis, J.F., 1993. The structure and function of yeast ARS elements. *Current Opinion in Genetics and Development*, 3(5), pp.752–758.

Ng, L.J. et al., 2009. Telomerase activity is associated with an increase in DNA methylation at the proximal subtelomere and a reduction in telomeric transcription. *Nucleic Acids Research*, 37(4), pp.1152–1159.

Nguyen, D.T. et al., 2017. The chromatin remodelling factor ATRX suppresses R-loops in transcribed

telomeric repeats . *EMBO reports*, 18(6), pp.914–928.

Nikitina, T. & Woodcock, C.L., 2004. Closed chromatin loops at the ends of chromosomes. *Journal of Cell Biology*, 166(2), pp.161–165.

Nishikawa, T. et al., 2001. Solution Structure of a Telomeric DNA Complex of Human TRF1. *Structure*, 9(12), pp.1237–1251. Available at: https://linkinghub.elsevier.com/retrieve/pii/S0969212601006888.

Nizami, Z., Deryusheva, S. & Gall, J.G., 2010. The Cajal Body and Histone Locus Body. *Cold Spring Harbor Perspectives in Biology*, 2(7), pp.a000653–a000653. Available at: http://cshperspectives.cshlp.org/lookup/doi/10.1101/cshperspect.a000653.

Noël, J.-F. & Wellinger, R.J., 2011. Abrupt telomere losses and reduced end-resection can explain accelerated senescence of Smc5/6 mutants lacking telomerase. *DNA Repair*, 10(3), pp.271–282. Available at: https://linkinghub.elsevier.com/retrieve/pii/S1568786410003873.

Nora, E.P. et al., 2012. Spatial partitioning of the regulatory landscape of the X-inactivation centre. *Nature*, 485(7398), pp.381–385. Available at: http://www.nature.com/articles/nature11049.

Nora, E.P. et al., 2017. Targeted Degradation of CTCF Decouples Local Insulation of Chromosome Domains from Genomic Compartmentalization. *Cell*, 169(5), p.930–944.e22.

Nuebler, J. et al., 2018. Chromatin organization by an interplay of loop extrusion and compartmental segregation. *Proceedings of the National Academy of Sciences of the United States of America*, 115(29), pp.E6697–E6706.

Nugent, C.I. et al., 1996. Cdc13p: A single-strand telomeric DNA-binding protein with a dual role in yeast telomere maintenance. *Science*, 274(5285), pp.249–252.

O'Sullivan, J.M. et al., 2004. Gene loops juxtapose promoters and terminators in yeast. *Nature Genetics*, 36(9), pp.1014–1018.

O'Sullivan, R.J. et al., 2010. Reduced histone biosynthesis and chromatin changes arising from a damage signal at telomeres. *Nature Structural and Molecular Biology*, 17(10), pp.1218–1225.

Ochs, F. et al., 2019. Stabilization of chromatin topology safeguards genome integrity. *Nature*, 574(7779), pp.571–574. Available at: http://www.nature.com/articles/s41586-019-1659-4.

Ogino, H. et al., 1998. Release of telomeric DNA from chromosomes in immortal human cells lacking telomerase activity. *Biochemical and Biophysical Research Communications*, 248(2), pp.223–227.

Oliveira, R.A. et al., 2010. Cohesin cleavage and Cdk inhibition trigger formation of daughter nuclei. *Nature Cell Biology*, 12(2), pp.185–192. Available at: http://www.nature.com/articles/ncb2018.

Olovnikov, A.M., 1973. A theory of marginotomy. *Journal of Theoretical Biology*, 41(1), pp.181–190. Available at: https://linkinghub.elsevier.com/retrieve/pii/0022519373901987.

Olovnikov, A.M., 1971. Principle of marginotomy in template synthesis of polynucleotides. *Doklady Akademii nauk SSSR*.

Onishi, M. et al., 2007. Role of the Conserved Sir3-BAH Domain in Nucleosome Binding and Silent Chromatin Assembly. *Molecular Cell*, 28(6), pp.1015–1028.

Opresko, P.L. et al., 2002. Telomere-binding protein TRF2 binds to and stimulates the Werner and Bloom syndrome helicases. *Journal of Biological Chemistry*, 277(43), pp.41110–41119.

Opresko, P.L. et al., 2004. The werner syndrome helicase and exonuclease cooperate to resolve telomeric D loops in a manner regulated by TRF1 and TRF2. *Molecular Cell*, 14(6), pp.763–774.

Osborn, A.J. & Elledge, S.J., 2003. Mrc1 is a replication fork component whose phosphorylation in response to DNA replication stress activates Rad53. *Genes and Development*, 17(14), pp.1755–1767.

Ou, H.D. et al., 2017. ChromEMT: Visualizing 3D chromatin structure and compaction in interphase and mitotic cells. *Science*, 357(6349).

van Overbeek, M. & de Lange, T., 2006. Apollo, an Artemis-Related Nuclease, Interacts with TRF2 and Protects Human Telomeres in S Phase. *Current Biology*, 16(13), pp.1295–1302. Available at: https://linkinghub.elsevier.com/retrieve/pii/S0960982206015661.

Oza, P. et al., 2009. Mechanisms that regulate localization of a DNA double-strand break to the nuclear periphery. *Genes and Development*, 23(8), pp.912–927.

Paeschke, K., Capra, J.A. & Zakian, V.A., 2011. DNA Replication through G-Quadruplex Motifs Is Promoted by the Saccharomyces cerevisiae Pif1 DNA Helicase. *Cell*, 145(5), pp.678–691.

Palladino, F. et al., 1993. SIR3 and SIR4 proteins are required for the positioning and integrity of yeast telomeres. *Cell*, 75(3), pp.543–555.

Palm, W. & de Lange, T., 2008. How Shelterin Protects Mammalian Telomeres. *Annual Review of Genetics*, 42(1), pp.301–334.

Palstra, R.J. et al., 2003. The β-globin nuclear compartment in development and erythroid differentiation. *Nature Genetics*, 35(2), pp.190–194.

Pan, X. et al., 2017. FANCM, BRCA1, and BLM cooperatively resolve the replication stress at the ALT telomeres. *Proceedings of the National Academy of Sciences of the United States of America*, 114(29), pp.E5940–E5949.

Pandita, T.K., Pathak, S. & Geard, C.R., 1995. Chromosome end associations, telomeres and telomerase activity in ataxia telangiectasia cells. *Cytogenetic and Genome Research*, 71(1), pp.86–93.

Pâques, F. & Haber, J.E., 1999. Multiple Pathways of Recombination Induced by Double-Strand Breaks in Saccharomyces cerevisiae. *Microbiology and Molecular Biology Reviews*, 63(2), pp.349–404. Available at: http://microbialcell.com/researcharticles/shepherding-dna-ends-rif1-protects-telomeres-and-chromosome-breaks/.

Pardo, B. & Marcand, S., 2005. Rap1 prevents telomere fusions by nonhomologous end joining. *EMBO Journal*, 24(17), pp.3117–3127.

Pasero, P., Braguglia, D. & Gasser, S.M., 1997. ORC-dependent and origin-specific initiation of DNA replication at defined foci in isolated yeast nuclei. *Genes and Development*, 11(12), pp.1504–1518.

Patel, A. et al., 2015. A Liquid-to-Solid Phase Transition of the ALS Protein FUS Accelerated by Disease Mutation. *Cell*, 162(5), pp.1066–1077.

Paull, T.T. & Gellert, M., 2000. A mechanistic basis for Mre11-directed DNA joining at microhomologies. *Proceedings of the National Academy of Sciences of the United States of America*, 97(12), pp.6409–6414.

Peace, J.M., Ter-Zakarian, A. & Aparicio, O.M., 2014. Rif1 Regulates Initiation Timing of Late

Replication Origins throughout the S. cerevisiae Genome M. Muzi-Falconi, ed. *PLoS ONE*, 9(5), p.e98501. Available at: https://dx.plos.org/10.1371/journal.pone.0098501.

Pebernard, S. et al., 2008. Localization of Smc5/6 to centromeres and telomeres requires heterochromatin and SUMO, respectively. *EMBO Journal*, 27(22), pp.3011–3023.

Pederson, T., 2011. The nucleolus. *Cold Spring Harbor Perspectives in Biology*, 3(3), pp.1–15.

Pedram, M. et al., 2006. Telomere Position Effect and Silencing of Transgenes near Telomeres in the Mouse. *Molecular and Cellular Biology*, 26(5), pp.1865–1878.

Pereira, M.C.F. et al., 2018. Complementary chromosome folding by transcription factors and cohesin. *bioRxiv*.

Pethrick, R.A., 1988. The theory of polymer dynamics M. Doi and S. F. Edwards, Oxford University Press, Oxford, 1986. pp. xiii + 391, price £40.00. ISBN 0-19-85 1976-1. *British Polymer Journal*, 20(3), pp.299–299. Available at: http://doi.wiley.com/10.1002/pi.4980200324.

Pfeiffer, V. & Lingner, J., 2012. TERRA promotes telomere shortening through exonuclease 1-mediated resection of chromosome ends. *PLoS Genetics*, 8(6).

De Piccoli, G. et al., 2006. Smc5-Smc6 mediate DNA double-strand-break repair by promoting sister-chromatid recombination. *Nature Cell Biology*, 8(9), pp.1032–1034.

Pickersgill, H. et al., 2006. Characterization of the Drosophila melanogaster genome at the nuclear lamina. *Nature Genetics*, 38(9), pp.1005–1014. Available at: http://www.nature.com/articles/ng1852.

Platt, J.M. et al., 2013. Rap1 relocalization contributes to the chromatin-mediated gene expression profile and pace of cell senescence. *Genes and Development*, 27(12), pp.1406–1420.

Polotnianka, R.M., Li, J. & Lustig, A.J., 1998. The yeast Ku heterodimer is essential for protection of the telomere against nucleolytic and recombinational activities. *Current Biology*, 8(14), pp.831–835. Available at: https://linkinghub.elsevier.com/retrieve/pii/S0960982298703252.

Poloumienko, A. et al., 2001. Completion of replication map of Saccharomyces cerevisiae chromosome III. *Molecular Biology of the Cell*, 12(11), pp.3317–3327.

Pope, B.D. et al., 2014. Topologically associating domains are stable units of replication-timing regulation. *Nature*, 515(7527), pp.402–405.

Porter, S.E. et al., 1996. The DNA-binding protein Hdf1p (a putative Ku homologue) is required for maintaining normal telomere length in Saccharomyces cerevisiae. *Nucleic Acids Research*, 24(4), pp.582–585. Available at: https://academic.oup.com/nar/article-lookup/doi/10.1093/nar/24.4.582.

Poschke, H. et al., 2012. Rif2 promotes a telomere fold-back structure through Rpd3L recruitment in budding yeast. J. D. Griffith, ed. *PLoS genetics*, 8(9), p.e1002960. Available at: https://dx.plos.org/10.1371/journal.pgen.1002960.

Potts, P.R. & Yu, H., 2007. The SMC5/6 complex maintains telomere length in ALT cancer cells through SUMOylation of telomere-binding proteins. *Nature Structural and Molecular Biology*, 14(7), pp.581–590.

Poulet, A. et al., 2009. TRF2 promotes, remodels and protects telomeric Holliday junctions. *The EMBO Journal*, 28(6), pp.641–651. Available at: http://emboj.embopress.org/cgi/doi/10.1038/emboj.2009.11.

Power, P. et al., 2011. Sub-Telomeric core X and Y' Elements in S.cerevisiae Suppress Extreme Variations in Gene Silencing M. Bryk, ed. *PLoS ONE*, 6(3), p.e17523. Available at: https://dx.plos.org/10.1371/journal.pone.0017523.

Pryde, F. et al., 2009. H3 K36 methylation helps determine the timing of Cdc45 association with replication origins. *PLoS ONE*, 4(6).

Pryde, F.E. & Louis, E.J., 1999. Limitations of silencing at native yeast telomeres. *EMBO Journal*, 18(9), pp.2538–2550.

Qi, H. & Zakian, V.A., 2000. The Saccharomyces telomere-binding protein Cdc13p interacts with both the catalytic subunit of DNA polymerase α and the telomerase-associated Est1 protein. *Genes and Development*, 14(14), pp.1777–1788.

Quinodoz, S.A. et al., 2018. Higher-Order Inter-chromosomal Hubs Shape 3D Genome Organization in the Nucleus. *Cell*, 174(3), p.744–757.e24.

Rabl, C., 1885. Über Zellteilung. *Morphol-Jahrbuch*, 10, pp.214–330.

Raghuraman, M.K., 2001. Replication Dynamics of the Yeast Genome. *Science*, 294(5540), pp.115–121. Available at: http://www.sciencemag.org/cgi/doi/10.1126/science.294.5540.115.

Ramani, V. et al., 2017. Massively multiplex single-cell Hi-C. *Nature Methods*, 14(3), pp.263–266.

Rao, S.S.P. et al., 2014. A 3D map of the human genome at kilobase resolution reveals principles of chromatin looping. *Cell*, 159(7), pp.1665–1680.

Rao, S.S.P. et al., 2017. Cohesin Loss Eliminates All Loop Domains. *Cell*, 171(2), p.305–320.e24.

Rappsilber, J., Mann, M. & Ishihama, Y., 2007. Protocol for micro-purification, enrichment, pre-fractionation and storage of peptides for proteomics using StageTips. *Nature protocols*, 2(8), pp.1896–906. Available at: http://www.ncbi.nlm.nih.gov/pubmed/17703201.

Reid, J.L., Moqtaderi, Z. & Struhl, K., 2004. Eaf3 Regulates the Global Pattern of Histone Acetylation in Saccharomyces cerevisiae. *Molecular and Cellular Biology*, 24(2), pp.757–764.

Renauld, H. et al., 1993. Silent domains are assembled continuously from the telomere and are defined by promoter distance and strength, and by SIR3 dosage. *Genes and Development*, 7(7 A), pp.1133–1145.

Ricci, M.A. et al., 2015. Chromatin Fibers Are Formed by Heterogeneous Groups of Nucleosomes In Vivo. *Cell*, 160(6), pp.1145–1158. Available at: https://linkinghub.elsevier.com/retrieve/pii/S0092867415001324.

Rippe, K. & Luke, B., 2015. TERRA and the state of the telomere. *Nature Structural and Molecular Biology*, 22(11), pp.853–858. Available at: http://www.nature.com/doifinder/10.1038/nsmb.3078.

Ritchie, K.B., Mallory, J.C. & Petes, T.D., 1999. Interactions of TLC1 (Which Encodes the RNA Subunit of Telomerase), TEL1 , and MEC1 in Regulating Telomere Length in the Yeast Saccharomyces cerevisiae . *Molecular and Cellular Biology*, 19(9), pp.6065–6075.

Ritchie, K.B. & Petes, T.D., 2000. The Mre11p / Rad50p / Xrs2p Complex and the Tel1p Function in a Single Pathway for Telomere Maintenance in Yeast. *Genetics*, 155, pp.475–479.

Robert, I., Dantzer, F. & Reina-San-Martin, B., 2009. Parp1 facilitates alternative NHEJ, whereas Parp2 suppresses IgH/c-myc translocations during immunoglobulin class switch recombination. *Journal of Experimental Medicine*, 206(5), pp.1047–1056.

Robin, J.D. et al., 2015. SORBS2 transcription is activated by telomere position effect-over long distance upon telomere shortening in muscle cells from patients with facioscapulohumeral dystrophy. *Genome Research*, 25(12), pp.1781–1790.

Robin, J.D. et al., 2014. Telomere position effect: Regulation of gene expression with progressive telomere shortening over long distances. *Genes and Development*, 28(22), pp.2464–2476.

Robinett, C.C. et al., 1996. In vivo localization of DNA sequences and visualization of large-scale chromatin organization using lac operator/repressor recognition. *Journal of Cell Biology*, 135(6 II), pp.1685–1700.

Robyr, D. et al., 2002. Microarray deacetylation maps determine genome-wide functions for yeast histone deacetylases. *Cell*, 109(4), pp.437–446.

Robyr, D., Kurdistani, S.K. & Grunstein, M., 2003. Analysis of Genome-Wide Histone Acetylation State and Enzyme Binding Using DNA Microarrays. *Methods in Enzymology*, 376, pp.289–304.

Ruan, C. et al., 2015. Nucleosome contact triggers conformational changes of Rpd3S driving high-affinity H3K36me nucleosome engagement. *Cell Reports*, 10(2), pp.204–215.

Ruault, M. et al., 2011. Clustering heterochromatin: Sir3 promotes telomere clustering independently of silencing in yeast. *Journal of Cell Biology*, 192(3), pp.417–431.

Rubertis, F. De et al., 1996. The histone deacetylase RPD3 counteracts genomic silencing in Drosophila and yeast. *Nature*, (384), pp.589–591.

Rundlett, S.E. et al., 1996. HDA1 and RPD3 are members of distinct yeast histone deacetylase complexes that regulate silencing and transcription. *Proceedings of the National Academy of Sciences of the United States of America*, 93(25), pp.14503–14508.

Runge, K.W. & Zakian, V.A., 1996. TEL2, an essential gene required for telomere length regulation and telomere position effect in Saccharomyces cerevisiae. *Molecular and Cellular Biology*, 16(6), pp.3094–3105.

Rusche, L.N., Kirchmaier, A.L. & Rine, J., 2003. The Establishment, Inheritance, and Function of Silenced Chromatin in Saccharomyces cerevisiae. *Annual Review of Biochemistry*, 72(1), pp.481–516. Available at: http://www.annualreviews.org/doi/10.1146/annurev.biochem.72.121801.161547.

Russell, P. & Nurse, P., 1986. Schizosaccharomyces pombe and saccharomyces cerevisiae: A look at yeasts divided. *Cell*, 45(6), pp.781–782.

Ryba, T. et al., 2010. Evolutionarily conserved replication timing profiles predict long-range chromatin interactions and distinguish closely related cell types. *Genome Research*, 20(6), pp.761–770.

Ryu, H.Y., Rhie, B.H. & Ahn, S.H., 2014. Loss of the Set2 histone methyltransferase increases cellular lifespan in yeast cells. *Biochemical and Biophysical Research Communications*, 446(1), pp.113–118.

Saad, H. et al., 2014. DNA Dynamics during Early Double-Strand Break Processing Revealed by Non-Intrusive Imaging of Living Cells B. van Steensel, ed. *PLoS Genetics*, 10(3), p.e1004187. Available at: https://dx.plos.org/10.1371/journal.pgen.1004187.

Sabourin, M., Tuzon, C.T. & Zakian, V.A., 2007. Telomerase and Tel1p Preferentially Associate with Short Telomeres in S. cerevisiae. *Molecular Cell*, 27(4), pp.550–561.

Sabourin, M. & Zakian, V.A., 2008. ATM-like kinases and regulation of telomerase : lessons from

yeast and mammals. *Trends in Cell Biology*, 18(May), pp.337–346.

Sallmyr, A., Tomkinson, A.E. & Rassool, F. V., 2008. Up-regulation of WRN and DNA ligase lllά in chronic myeloid leukemia: Consequences for the repair of DNA double-strand breaks. *Blood*, 112(4), pp.1413–1423.

Sanborn, A.L. et al., 2015. Chromatin extrusion explains key features of loop and domain formation in wild-type and engineered genomes. *Proceedings of the National Academy of Sciences*, 112(47), pp.E6456–E6465. Available at: http://www.pnas.org/lookup/doi/10.1073/pnas.1518552112.

Sanchez, Y. et al., 1999. Control of the DNA damage checkpoint by Chk1 and Rad53 protein kinases through distinct mechanisms. *Science*, 286(5442), pp.1166–1171.

Sanchez, Y. et al., 1996. Regulation of RAD53 by the ATM-like kinases MEC1 and TEL1 in yeast cell cycle checkpoint pathways. *Science*, 271(5247), pp.357–360.

Santocanale, C. & Diffley, J.F.X., 1998. A Mec1-and Rad53-dependent checkpoint controls late-firing origins of DNA replication. *Nature*, 395(6702), pp.615–618.

Sanyal, A. et al., 2012. The long-range interaction landscape of gene promoters. *Nature*, 489(7414), pp.109–113. Available at: http://www.nature.com/articles/nature11279.

Sarek, G. et al., 2019. CDK phosphorylation of TRF2 controls t-loop dynamics during the cell cycle. *Nature*, 575(7783), pp.523–527.

Sarek, G. et al., 2015. TRF2 recruits RTEL1 to telomeres in s phase to promote t-loop unwinding. *Molecular Cell*, 57(4), pp.622–635.

Sarkar, J. et al., 2015. SLX4 contributes to telomere preservation and regulated processing of telomeric joint molecule intermediates. *Nucleic Acids Research*, 43(12), pp.5912–5923.

Schellhass, R., 2016. Towards a mechanistic understanding of telomere loop structures in S. cerevisiae.

Schmidt, J.C. & Cech, T.R., 2015. Human telomerase: Biogenesis, trafficking, recruitment, and activation. *Genes and Development*, 29(11), pp.1095–1105.

Schober, H. et al., 2008. Controlled exchange of chromosomal arms reveals principles driving telomere interactions in yeast. *Genome Research*, 18(2), pp.261–271.

Schoeftner, S. & Blasco, M.A., 2008. Developmentally regulated transcription of mammalian telomeres by DNA-dependent RNA polymerase II. *Nature Cell Biology*, 10(2), pp.228–236. Available at: http://www.nature.com/articles/ncb1685.

Schoenfelder, S. et al., 2018. Promoter Capture Hi-C: High-resolution, Genome-wide Profiling of Promoter Interactions. *Journal of Visualized Experiments*, 2018(136). Available at: https://www.jove.com/video/57320/promoter-capture-hi-c-high-resolution-genome-wide-profiling-promoter.

Schwartz, M.F. et al., 2002. Rad9 phosphorylation sites couple Rad53 to the Saccharomyces cerevisiae DNA damage checkpoint. *Molecular Cell*, 9(5), pp.1055–1065.

Schwarzer, W. et al., 2017. Two independent modes of chromatin organization revealed by cohesin removal. *Nature*, 551(7678), pp.51–56. Available at: http://www.nature.com/articles/nature24281.

Sen, D. & Gilbert, W., 1988. Formation of parallel four-stranded complexes by guanine-rich motifs

in DNA and its implications for meiosis. *Nature*, 334(6180), pp.364–366. Available at: http://www.nature.com/articles/334364a0.

Sexton, T. et al., 2012. Three-Dimensional Folding and Functional Organization Principles of the Drosophila Genome. *Cell*, 148(3), pp.458–472. Available at: https://linkinghub.elsevier.com/retrieve/pii/S0092867412000165.

Sfeir, A. et al., 2009. Mammalian Telomeres Resemble Fragile Sites and Require TRF1 for Efficient Replication. *Cell*, 138(1), pp.90–103. Available at: http://dx.doi.org/10.1016/j.cell.2009.06.021.

Sfeir, A. & De Lange, T., 2012. Removal of shelterin reveals the telomere end-protection problem. *Science*, 336(6081), pp.593–597.

Sharma, V.M. et al., 2007. Histone Deacetylases RPD3 and HOS2 Regulate the Transcriptional Activation of DNA Damage-Inducible Genes. *Molecular and Cellular Biology*, 27(8), pp.3199–3210.

Shevchenko, A. et al., 2006. In-gel digestion for mass spectrometric characterization of proteins and proteomes. *Nature Protocols*, 1(6), pp.2856–2860. Available at: http://www.nature.com/articles/nprot.2006.468.

Shia, W.J., Li, B. & Workman, J.L., 2006. SAS-mediated acetylation of histone H4 Lys 16 is required for H2A.Z incorporation at subtelomeric regions in Saccharomyces cerevisiae. *Genes and Development*, 20(18), pp.2507–2512.

Shima, H., Suzuki, M. & Shinohara, M., 2005. Isolation and characterization of novel xrs2 mutations in Saccharomyces cerevisiae. *Genetics*, 170(1), pp.71–85.

Shinohara, A. & Ogawa, T., 1998. Stimulation by Rad52 of yeast Rad51-mediated recombination. *Nature*, 391(6665), pp.404–407.

Shroff, R. et al., 2004. Distribution and dynamics of chromatin modification induced by a defined DNA double-strand break. *Current Biology*, 14(19), pp.1703–1711.

De Silanes, I.L. et al., 2014. Identification of TERRA locus unveils a telomere protection role through association to nearly all chromosomes. *Nature Communications*, 5, p.4723.

De Silanes, I.L., D'Alcontres, M.S. & Blasco, M.A., 2010. TERRA transcripts are bound by a complex array of RNA-binding proteins. *Nature Communications*, 1(3), p.33. Available at: http://www.nature.com/articles/ncomms1032.

Silva, B. et al., 2019. FANCM limits ALT activity by restricting telomeric replication stress induced by deregulated BLM and R-loops. *Nature Communications*, 10(1), p.2253. Available at: http://www.nature.com/articles/s41467-019-10179-z.

Simon, I. et al., 2001. Developmental regulation of DNA replication timing at the human β globin locus. *EMBO Journal*, 20(21), pp.6150–6157.

Simsek, D. et al., 2011. DNA Ligase III Promotes Alternative Nonhomologous End-Joining during Chromosomal Translocation Formation J. E. Haber, ed. *PLoS Genetics*, 7(6), p.e1002080. Available at: https://dx.plos.org/10.1371/journal.pgen.1002080.

Singer, M.S. & Gottschling, D.E., 1994. TLC1: Template RNA component of Saccharomyces cerevisiae telomerase. *Science*, 266(5184), pp.404–409.

Smith, J.J. et al., 2011. Environment-responsive transcription factors bind subtelomeric elements and regulate gene silencing. *Molecular Systems Biology*, 7(1), p.455. Available at:

https://onlinelibrary.wiley.com/doi/abs/10.1038/msb.2010.110.

Smith, S. et al., 1998. Tankyrase, a poly(ADP-ribose) polymerase at human telomeres. *Science*, 282(5393), pp.1484–1487.

Smith, S. & De Lange, T., 2000. Tankyrase promotes telomere elongation in human cells. *Current Biology*, 10(20), pp.1299–1302.

Smogorzewska, A. et al., 2002. DNA ligase IV-dependent NHEJ of deprotected mammalian telomeres in G1 and G2. *Current Biology*, 12(19), pp.1635–1644.

Solovei, I., Thanisch, K. & Feodorova, Y., 2016. How to rule the nucleus: divide et impera. *Current Opinion in Cell Biology*, 40, pp.47–59. Available at: http://dx.doi.org/10.1016/j.ceb.2016.02.014.

Song, K. et al., 2000. Interaction of human Ku70 with TRF2. In *FEBS Letters*. pp. 81–85.

Soudet, J., Jolivet, P. & Teixeira, M.T., 2014. Elucidation of the DNA end-replication problem in saccharomyces cerevisiae. *Molecular Cell*, 53(6), pp.954–964.

Speicher, M.R., Ballard, S.G. & Ward, D.C., 1996. Karyotyping human chromosomes by combinatorial multi-fluor FISH. *Nature Genetics*, 12(4), pp.368–375.

Splinter, E. et al., 2006. CTCF mediates long-range chromatin looping and local histone modification in the β-globin locus. *Genes and Development*, 20(17), pp.2349–2354.

Sridhar, A., Kedziora, S. & Donaldson, A.D., 2014. At Short Telomeres Tel1 Directs Early Replication and Phosphorylates Rif1 C. S. Newlon, ed. *PLoS Genetics*, 10(10), p.e1004691. Available at: https://dx.plos.org/10.1371/journal.pgen.1004691.

Stack, S.M., Brown d., B. & Dewey, W.C., 1977. Visualization of interphase chromosomes. *Journal of Cell Science*, Vol. 26, pp.281–299.

Stansel, R.M., De Lange, T. & Griffith, J.D., 2001. T-loop assembly in vitro involves binding of TRF2 near the 3′ telomeric overhang. *EMBO Journal*, 20(19), pp.5532–5540.

van Steensel, B. & Belmont, A.S., 2017. Lamina-Associated Domains: Links with Chromosome Architecture, Heterochromatin, and Gene Repression. *Cell*, 169(5), pp.780–791.

Van Steensel, B. & Henikoff, S., 2000. Identification of in vivo DNA targets of chromatin proteins using tethered Dam methyltransferase. *Nature Biotechnology*, 18(4), pp.424–428.

Sternberg, P.W. et al., 1987. Activation of the yeast HO gene by release from multiple negative controls. *Cell*, 48(4), pp.567–577.

Stevens, T.J. et al., 2017. 3D structures of individual mammalian genomes studied by single-cell Hi-C. *Nature*, 544(7648), pp.59–64.

Stevenson, J.B. & Gottschling, D.E., 1999. Telomeric chromatin modulates replication timing near chromosome ends. *Genes and Development*, 13(2), pp.146–151.

Straatman, K.R. & Louis, E.J., 2007. Localization of telomeres and telomere-associated proteins in telomerase-negative Saccharomyces cerevisiae. *Chromosome Research*, 15(8), pp.1033–1050.

Strahl-Bolsinger, S. et al., 1997. SIR2 and SIR4 interactions differ in core and extended telomeric heterochromatin in yeast. *Genes and Development*, 11(1), pp.83–93.

Strahl, B.D. et al., 2002. Set2 Is a Nucleosomal Histone H3-Selective Methyltransferase That

Mediates Transcriptional Repression. *Molecular and Cellular Biology*, 22(5), pp.1298–1306.

Strom, A.R. et al., 2017. Phase separation drives heterochromatin domain formation. *Nature*, 547(7662), pp.241–245.

Ström, L. et al., 2004. Postreplicative Recruitment of Cohesin to Double-Strand Breaks Is Required for DNA Repair. *Molecular Cell*, 16(6), pp.1003–1015. Available at: https://linkinghub.elsevier.com/retrieve/pii/S1097276504007178.

Strunnikov, A. V., Hogan, E. & Koshland, D., 1995. SMC2, a Saccharomyces cerevisiae gene essential for chromosome segregation and condensation, defines a subgroup within the SMC family. *Genes and Development*, 9(5), pp.587–599.

Strunnikov, A. V. & Jessberger, R., 1999. Structural maintenance of chromosomes (SMC) proteins: Conserved molecular properties for multiple biological functions. *European Journal of Biochemistry*, 263(1), pp.6–13.

Suka, N., Luo, K. & Grunstein, M., 2002. Sir2p and Sas2p opposingly regulate acetylation of yeast histone H4 lysine16 and spreading of heterochromatin. *Nature Genetics*, 32(3), pp.378–383.

Sun, H. et al., 1998. The Bloom's syndrome helicase unwinds G4 DNA. *Journal of Biological Chemistry*, 273(42), pp.27587–27592.

Sun, Z. et al., 1998. Rad53 FHA domain associated with phosphorylated Rad9 in the DNA damage checkpoint. *Science*, 281(5374), pp.272–274.

Sun, Z.W. & Hampsey, M., 1999. A general requirement for the Sin3-Rpd3 histone deacetylase complex in regulating silencing in Saccharomyces cerevisiae. *Genetics*, 152(3), pp.921–932.

Sung, P., 1997. Function of yeast Rad52 protein as a mediator between replication protein A and the Rad51 recombinase. *Journal of Biological Chemistry*, 272(45), pp.28194–28197.

Suram, A. et al., 2012. Oncogene-induced telomere dysfunction enforces cellular senescence in human cancer precursor lesions. *EMBO Journal*, 31(13), pp.2839–2851.

Swygert, S.G. et al., 2018. SIR proteins create compact heterochromatin fibers. *Proceedings of the National Academy of Sciences of the United States of America*, 115(49), pp.12447–12452.

Szostak, J.W. & Blackburn, E.H., 1982. Cloning yeast telomeres on linear plasmid vectors. *Cell*, 29(1), pp.245–255. Available at: https://linkinghub.elsevier.com/retrieve/pii/009286748290109X.

Taddei, A. & Gasser, S.M., 2012. Structure and function in the budding yeast nucleus. *Genetics*, 192(1), pp.107–129.

Takahashi, Y.H. et al., 2011. Dot1 and Histone H3K79 Methylation in Natural Telomeric and HM Silencing. *Molecular Cell*, 42(1), pp.118–126.

Takai, H., Smogorzewska, A. & De Lange, T., 2003. DNA damage foci at dysfunctional telomeres. *Current Biology*, 13(17), pp.1549–1556.

Tan-Wong, S.M. et al., 2008. Dynamic interactions between the promoter and terminator regions of the mammalian BRCA1 gene. *Proceedings of the National Academy of Sciences*, 105(13), pp.5160–5165. Available at: http://www.pnas.org/lookup/doi/10.1073/pnas.0801048105.

Tan-Wong, S.M. et al., 2012. Gene Loops Enhance Transcriptional Directionality. *Science*, 338(6107), pp.671–675. Available at: https://www.sciencemag.org/lookup/doi/10.1126/science.1224350.

Tan-Wong, S.M., Wijayatilake, H.D. & Proudfoot, N.J., 2009. Gene loops function to maintain

transcriptional memory through interaction with the nuclear pore complex. *Genes & Development*, 23(22), pp.2610–2624. Available at: http://genesdev.cshlp.org/lookup/doi/10.1101/gad.1823209.

Tan, L. et al., 2018. Three-dimensional genome structures of single diploid human cells. *Science*, 361(6405), pp.924–928.

Tang, S.-J., 2017. Potential Role of Phase Separation of Repetitive DNA in Chromosomal Organization. *Genes*, 8(10), p.279. Available at: http://www.mdpi.com/2073-4425/8/10/279.

Tardat, M. & Déjardin, J., 2018. Telomere chromatin establishment and its maintenance during mammalian development. *Chromosoma*, 127(1), pp.3–18.

Tarsounas, M. et al., 2004. Telomere maintenance requires the RAD51D recombination/repair protein. *Cell*, 117(3), pp.337–347.

Tasselli, L. et al., 2016. SIRT6 deacetylates H3K18ac at pericentric chromatin to prevent mitotic errors and cellular senescence. *Nature Structural and Molecular Biology*, 23(5), pp.434–440.

Teixeira, M.T., 2013. Saccharomyces cerevisiae as a Model to Study Replicative Senescence Triggered by Telomere Shortening. *Frontiers in Oncology*, 3(April), pp.1–16. Available at: http://journal.frontiersin.org/article/10.3389/fonc.2013.00101/abstract.

Teixeira, M.T. et al., 2004. Telomere length homeostasis is achieved via a switch between telomerase-extendible and-nonextendible states. *Cell*, 117(3), pp.323–335.

Teng, S.-C. & Zakian, V.A., 1999. Telomere-Telomere Recombination Is an Efficient Bypass Pathway for Telomere Maintenance in Saccharomyces cerevisiae . *Molecular and Cellular Biology*, 19(12), pp.8083–8093.

Teng, S. et al., 2000. Telomerase-Independent Lengthening of Yeast Telomeres Occurs by an Abrupt Rad50p-Dependent, Rif-Inhibited Recombinational Process. *Molecular Cell*, 6(4), pp.947–952. Available at: https://linkinghub.elsevier.com/retrieve/pii/S1097276505000948.

Tennen, R.I. et al., 2011. SIRT6 is required for maintenance of telomere position effect in human cells. *Nature Communications*, 2(1), p.433. Available at: http://www.nature.com/articles/ncomms1443.

Teytelman, L., Eisen, M.B. & Rine, J., 2008. Silent but Not Static: Accelerated Base-Pair Substitution in Silenced Chromatin of Budding Yeasts G. S. Barsh, ed. *PLoS Genetics*, 4(11), p.e1000247. Available at: https://dx.plos.org/10.1371/journal.pgen.1000247.

Tham, W.-H. & Zakian, V.A., 2002. Transcriptional silencing at Saccharomyces telomeres: implications for other organisms. *Oncogene*, 21(4), pp.512–521. Available at: http://www.nature.com/articles/1205078.

Tham, W.H. et al., 2001. Localization of Yeast Telomeres to the Nuclear Periphery Is Separable from Transcriptional Repression and Telomere Stability Functions. *Molecular Cell*, 8(1), pp.189–199.

The, G.D., Riviere, M. & Bernhard, W., 1960. Examen au microscope electronique de la tumeur VX2 du lapin domestique derivee du papillome de Shope. *Bull. du Cancer*, 47, pp.570–584.

Therizols, P. et al., 2010. Chromosome arm length and nuclear constraints determine the dynamic relationship of yeast subtelomeres. *Proceedings of the National Academy of Sciences*, 107(5), pp.2025–2030. Available at: http://www.pnas.org/lookup/doi/10.1073/pnas.0914187107.

Thurtle, D.M. & Rine, J., 2014. The molecular topography of silenced chromatin in Saccharomyces

cerevisiae. *Genes and Development*, 28(3), pp.245–258.

Tjong, H. et al., 2012. Physical tethering and volume exclusion determine higher-order genome organization in budding yeast. *Genome Research*, 22(7), pp.1295–1305.

Tokutake, Y. et al., 1998. Extra-chromosomal telomere repeat DNA in telomerase-negative immortalized cell lines. *Biochemical and Biophysical Research Communications*, 247(3), pp.765–772.

Tolhuis, B. et al., 2002. Looping and interaction between hypersensitive sites in the active β-globin locus. *Molecular Cell*, 10(6), pp.1453–1465.

Tomaska, L. et al., 2002. T-Loops in Yeast Mitochondria. *Mitochondrion*, 1(5), pp.455–459.

Tompa, R. & Madhani, H.D., 2007. Histone H3 lysine 36 methylation antagonizes silencing in Saccharomyces cerevisiae independently of the Rpd3S histone deacetylase complex. *Genetics*, 175(2), pp.585–593.

Torres-Rosell, J., Machín, F., et al., 2005. SMC5 and SMC6 genes are required for the segregation of repetitive chromosome regions. *Nature Cell Biology*, 7(4), pp.412–419. Available at: http://www.nature.com/articles/ncb1239.

Torres-Rosell, J., Mahín, F., et al., 2005. SMC5 and SMC6 genes are required for the segregation of repetitive chromosome regions. *Nature Cell Biology*, 7(4), pp.412–419.

Torres-Rosell, J. et al., 2007. The Smc5-Smc6 complex and SUMO modification of Rad52 regulates recombinational repair at the ribosomal gene locus. *Nature Cell Biology*, 9(8), pp.923–931.

Tsukamoto, Y., Kato, J.I. & Ikeda, H., 1997. Silencing factors participate in DNA repair and rscombination in Saccharomyces cersvisiae. *Nature*, 388(6645), pp.900–903.

Tsukamoto, Y., Taggart, A.K.P. & Zakian, V.A., 2001. The role of the Mre11-Rad50-Xrs2 complex in telomerase- mediated lengthening of Saccharomyces cerevisiae telomeres. *Current Biology*, 11, pp.1328–1335.

Uhlmann, F. et al., 2000. Cleavage of Cohesin by the CD Clan Protease Separin Triggers Anaphase in Yeast. *Cell*, 103(3), pp.375–386. Available at: https://linkinghub.elsevier.com/retrieve/pii/S0092867400001306.

Uhlmann, F., 2016. SMC complexes: From DNA to chromosomes. *Nature Reviews Molecular Cell Biology*, 17(7), pp.399–412.

Uhlmann, F. & Nasmyth, K., 1998. Cohesion between sister chromatids must be established during DNA replication. *Current Biology*, 8, pp.1095–1102.

Ünal, E. et al., 2004. DNA Damage Response Pathway Uses Histone Modification to Assemble a Double-Strand Break-Specific Cohesin Domain. *Molecular Cell*, 16(6), pp.991–1002. Available at: https://linkinghub.elsevier.com/retrieve/pii/S1097276504007191.

Uringa, E.J. et al., 2012. RTEL1 contributes to DNA replication and repair and telomere maintenance. *Molecular Biology of the Cell*, 23(14), pp.2782–2792.

Vakoc, C.R. et al., 2005. Proximity among distant regulatory elements at the β-globin locus requires GATA-1 and FOG-1. *Molecular Cell*, 17(3), pp.453–462.

Valentin, G., 1836. Repertorium Für Anatomie Und Physiologie. *Verlag von Veit Und Comp, Berlin1*, pp.1–293.

Vannier, D., Balderes, D. & Shore, D., 1996. Evidence That the Transcriptional Regulators SIN3 and

RPD3, and a Novel Gene (SDS3) with Similar Functions, Are Involved in Transcriptional Silencing in S. cerevisiae. *Genetics*, (144), pp.1343–1353.

Vannier, J.B. et al., 2012. RTEL1 dismantles T loops and counteracts telomeric G4-DNA to maintain telomere integrity. *Cell*, 149(4), pp.795–806. Available at: http://dx.doi.org/10.1016/j.cell.2012.03.030.

Vannier, J.B. et al., 2013. RTEL1 is a replisome-associated helicase that promotes telomere and genome-wide replication. *Science*, 342(6155), pp.239–242.

Venkatesh, S. et al., 2012. Set2 methylation of histone H3 lysine 36 suppresses histone exchange on transcribed genes. *Nature*, 489(7416), pp.452–455.

Verdun, R.E. et al., 2005. Functional human telomeres are recognized as DNA damage in G2 of the cell cycle. *Molecular Cell*, 20(4), pp.551–561.

Verdun, R.E. & Karlseder, J., 2006. The DNA Damage Machinery and Homologous Recombination Pathway Act Consecutively to Protect Human Telomeres. *Cell*, 127(4), pp.709–720.

Verzijlbergen, K.F. et al., 2009. Multiple histone modifications in euchromatin promote heterochromatin formation by redundant mechanisms in Saccharomyces cerevisiae. *BMC Molecular Biology*, 10, pp.1–16.

Vian, L. et al., 2018. The Energetics and Physiological Impact of Cohesin Extrusion. *Cell*, 173(5), p.1165–1178.e20.

Vogel, M.J., Peric-Hupkes, D. & van Steensel, B., 2007. Detection of in vivo protein - DNA interactions using DamID in mammalian cells. *Nature Protocols*, 2(6), pp.1467–1478.

Vogelauer, M. et al., 2000. Global histone acetylation and deacetylation in yeast. *Nature*, 408(6811), pp.495–498.

Vogelauer, M. et al., 2002. Histone Acetylation Regulates the Time of Replication Origin Firing. *Molecular Cell*, 10(5), pp.1223–1233. Available at: http://www.ncbi.nlm.nih.gov/pubmed/12453428.

Wach, A. et al., 1994. New heterologous modules for classical or PCR-based gene disruptions in Saccharomyces cerevisiae. *Yeast*, 10(13), pp.1793–1808.

Wagner, R., 1835. Einige Bemerkungen und Fragen uber das Keimblaschen (vesicula germinativa). *Muller's Archiv. Anat. Physiol. Wissenschaft. Med.*, pp.373–377.

Walker, J.R., Corpina, R.A. & Goldberg, J., 2001. Structure of the Ku heterodimer bound to dna and its implications for double-strand break repair. *Nature*, 412(6847), pp.607–614.

Walmsley, R.W. et al., 1984. Unusual DNA sequences associated with the ends of yeast chromosomes. *Nature*, 310(5973), pp.157–160. Available at: http://www.nature.com/articles/310157a0.

Wan, Y. et al., 2013. The functional role of SUMO E3 ligase Mms21p in the maintenance of subtelomeric silencing in budding yeast. *Biochemical and Biophysical Research Communications*, 438(4), pp.746–752. Available at: https://linkinghub.elsevier.com/retrieve/pii/S0006291X13012709.

Wang, H. et al., 2005. DNA ligase III as a candidate component of backup pathways of nonhomologous end joining. *Cancer Research*, 65(10), pp.4020–4030.

Wang, H. et al., 2011. Single molecule studies of physiologically relevant telomeric tails reveal POT1

mechanism for promoting G-quadruplex unfolding. *Journal of Biological Chemistry*, 286(9), pp.7479–7489.

Wang, R.C., Smogorzewska, A. & De Lange, T., 2004. Homologous recombination generates t-loop-sized deletions at human telomeres. *Cell*, 119(3), pp.355–368.

Wang, Y., Fairley, J.A. & Roberts, S.G.E., 2010. Phosphorylation of TFIIB Links Transcription Initiation and Termination. *Current Biology*, 20(6), pp.548–553. Available at: https://linkinghub.elsevier.com/retrieve/pii/S0960982210001417.

Wang, Y., Ghosh, G. & Hendrickson, E.A., 2009. Ku86 represses lethal telomere deletion events in human somatic cells. *Proceedings of the National Academy of Sciences of the United States of America*, 106(30), pp.12430–12435.

Watson, J., 1972. Origin of Concatemeric T7DNA. *Nature*, 239(94), pp.197–201.

Weber, B. et al., 1990. Characterization and organization of DNA sequences adjacent to the human telomere associated repeat (TTAGGG)n. *Nucleic Acids Research*, 18(11), pp.3353–3361.

Wellinger, R.J., Wolf, A.J. & Zakian, V.A., 1993. Saccharomyces telomeres acquire single-strand TG1-3 tails late in S phase. *Cell*, 72(1), pp.51–60.

Wellinger, R.J. & Zakian, V.A., 2012. Everything you ever wanted to know about Saccharomyces cerevisiae telomeres: Beginning to end. *Genetics*, 191(4), pp.1073–1105.

Van De Werken, H.J.G. et al., 2012. Robust 4C-seq data analysis to screen for regulatory DNA interactions. *Nature Methods*, 9(10), pp.969–972.

Winston, F., Dollard, C. & Ricupero-Hovasse, S.L., 1995. Construction of a set of convenient saccharomyces cerevisiae strains that are isogenic to S288C. *Yeast*, 11(1), pp.53–55.

Winzeler, E.A. et al., 1999. Functional characterization of the S. cerevisiae genome by gene deletion and parallel analysis. *Science*, 285(5429), pp.901–906.

Witten, D.M. & Noble, W.S., 2012. On the assessment of statistical significance of three-dimensional colocalization of sets of genomic elements. *Nucleic Acids Research*, 40(9), pp.3849–3855.

Wood, A., Schneider, J. & Shilatifard, A., 2005. Cross-talking histones: implications for the regulation of gene expression and DNA repair. *Biochemistry and Cell Biology*, 83(4), pp.460–467. Available at: http://www.nrcresearchpress.com/doi/10.1139/o05-116.

Wood, A.M. et al., 2015. A beginning of the end: New insights into the functional organization of telomeres. *Nucleus*, 6(3), pp.172–178.

Wood, A.M. et al., 2014. TRF2 and lamin A/C interact to facilitate the functional organization of chromosome ends. *Nature Communications*, 5(1), p.5467. Available at: http://www.nature.com/articles/ncomms6467.

Wotton, D. & Shore, D., 1997. A novel Rap1p-interacting factor, Rif2p, cooperates with Rif1p to regulate telomere length in Saccharomyces cerevisiae. *Genes and Development*, 11(6), pp.748–760.

Wright, J.H., Gottschling, D.E. & Zakian, V.A., 1992. Saccharomyces telomeres assume a non-nucleosomal chromatin structure. *Genes and Development*, 6(2), pp.197–210.

Wright, W.D., Shah, S.S. & Heyer, W.D., 2018. Homologous recombination and the repair of DNA double-strand breaks. *Journal of Biological Chemistry*, 293(27), pp.10524–10535.

Wu, D., Topper, L.M. & Wilson, T.E., 2008. Recruitment and dissociation of nonhomologous end joining proteins at a DNA double-strand break in Saccharomyces cerevisiae. *Genetics*, 178(3), pp.1237–1249.

Wu, N. & Yu, H., 2012. The Smc complexes in DNA damage response. *Cell & Bioscience*, 2(1), p.5. Available at: http://cellandbioscience.biomedcentral.com/articles/10.1186/2045-3701-2-5.

Wutz, G. et al., 2017. Topologically associating domains and chromatin loops depend on cohesin and are regulated by CTCF, WAPL, and PDS5 proteins. *The EMBO Journal*, 36(24), pp.3573–3599.

Wyrick, J.J. et al., 1999. Chromosomal landscape of nucleosome-dependent gene expression and silencing in yeast. *Nature*, 402(6760), pp.418–421.

Xiao, T. et al., 2003. Phosphorylation of RNA polymerase II CTD regulates H3 methylation in yeast. *Genes and Development*, 17(5), pp.654–663.

Xu, E.Y., Zawadzki, K.A. & Broach, J.R., 2006. Single-Cell Observations Reveal Intermediate Transcriptional Silencing States. *Molecular Cell*, 23(2), pp.219–229.

Yabuki, N., Terashima, H. & Kitada, K., 2002. Mapping of early firing origins on a replication profile of budding yeast. *Genes to Cells*, 7(8), pp.781–789.

Yamashita, M. et al., 1997. The efficiency and timing of initiation of replication of multiple replicons of Saccharomyces cerevisiae chromosome VI. *Genes to Cells*, 2(11), pp.655–665.

Yamazaki, S. et al., 2012. Rif1 regulates the replication timing domains on the human genome. *EMBO Journal*, 31(18), pp.3667–3677.

Ye, J. et al., 2010. TRF2 and Apollo Cooperate with Topoisomerase 2α to Protect Human Telomeres from Replicative Damage. *Cell*, 142(2), pp.230–242.

Ye, X. et al., 2007. Definition of pRB- and p53-Dependent and -Independent Steps in HIRA/ASF1a-Mediated Formation of Senescence-Associated Heterochromatin Foci. *Molecular and Cellular Biology*, 27(7), pp.2452–2465.

Yeager, T.R. et al., 1999. Telomerase-negative immortalized human cells contain a novel type of promyelocytic leukemia (PML) body. *Cancer Research*, 59(17), pp.4175–4179.

Yi, D.G. et al., 2016. Yap1 and Skn7 genetically interact with Rad51 in response to oxidative stress and DNA double-strand break in Saccharomyces cerevisiae. *Free Radical Biology and Medicine*, 101, pp.424–433.

Yoshida, K. et al., 2014. The Histone Deacetylases Sir2 and Rpd3 Act on Ribosomal DNA to Control the Replication Program in Budding Yeast. *Molecular Cell*, 54(4), pp.691–697.

Yoshida, K., Poveda, A. & Pasero, P., 2013. Time to be versatile: Regulation of the replication timing program in budding yeast. *Journal of Molecular Biology*, 425(23), pp.4696–4705. Available at: http://dx.doi.org/10.1016/j.jmb.2013.09.020.

Zakian, V.A., Blanton, H.M. & Wetzel, L., 1986. Distribution of Telomere-Associated Sequences in Yeast. In *Extrachromosomal Elements in Lower Eukaryotes*. Boston, MA: Springer US, pp. 493–498. Available at: http://link.springer.com/10.1007/978-1-4684-5251-8_37.

Zaman, Z., Heid, C. & Ptashne, M., 2002. Telomere looping permits repression “at a distance” in yeast. *Current Biology*, 12(11), pp.930–933.

Zappulla, D.C., Sternglanz, R. & Leatherwood, J., 2002. Control of replication timing by a

transcriptional silencer. *Current Biology*, 12(11), pp.869–875.

Zeman, M.K. & Cimprich, K.A., 2014. Causes and consequences of replication stress. *Nature Cell Biology*, 16(1), pp.2–9. Available at: http://www.nature.com/articles/ncb2897.

Zhan, Y. et al., 2017. Reciprocal insulation analysis of Hi-C data shows that TADs represent a functionally but not structurally privileged scale in the hierarchical folding of chromosomes. *Genome Research*, 27(3), pp.479–490.

Zhang, H. et al., 2015. RNA Controls PolyQ Protein Phase Transitions. *Molecular Cell*, 60(2), pp.220–230.

Zhang, R., Chen, W. & Adams, P.D., 2007. Molecular Dissection of Formation of Senescence-Associated Heterochromatin Foci. *Molecular and Cellular Biology*, 27(6), pp.2343–2358. Available at: https://mcb.asm.org/content/27/6/2343.

Zhang, Y. et al., 2007. Role of Dnl4-Lif1 in nonhomologous end-joining repair complex assembly and suppression of homologous recombination. *Nature Structural and Molecular Biology*, 14(7), pp.639–646.

Zhang, Z. et al., 2019. 2D gel electrophoresis reveals dynamics of t-loop formation during the cell cycle and t-loop in maintenance regulated by heterochromatin state. *Journal of Biological Chemistry*, 294(16), pp.6645–6656. Available at: http://www.jbc.org/lookup/doi/10.1074/jbc.RA119.007677.

Zhang, Z. et al., 2011. A packing mechanism for nucleosome organization reconstituted across a eukaryotic genome. *Science*, 332(6032), pp.977–980.

Zhao, X. & Blobel, G., 2005. A SUMO ligase is part of a nuclear multiprotein complex that affects DNA repair and chromosomal organization. *Proceedings of the National Academy of Sciences of the United States of America*, 102(13), pp.4777–4782.

Zhao, X., Muller, E.G.D. & Rothstein, R., 1998. A suppressor of two essential checkpoint genes identifies a novel protein that negatively affects dNTP pools. *Molecular Cell*, 2(3), pp.329–340.

Zhao, Y. et al., 2009. Telomere Extension Occurs at Most Chromosome Ends and Is Uncoupled from Fill-In in Human Cancer Cells. *Cell*, 138(3), pp.463–475.

Zhao, Z. et al., 2006. Circular chromosome conformation capture (4C) uncovers extensive networks of epigenetically regulated intra- and interchromosomal interactions. *Nature Genetics*, 38(11), pp.1341–1347.

Zheng, M. et al., 2019. Multiplex chromatin interactions with single-molecule precision. *Nature*, 566(7745), pp.558–562.

Zhou, J. et al., 2009. Histone deacetylase Rpd3 antagonizes Sir2-dependent silent chromatin propagation. *Nucleic Acids Research*, 37(11), pp.3699–3713.

Zhou, Y.B. et al., 1998. Position and orientation of the globular domain of linker histone H5 on the nucleosome. *Nature*, 395(6700), pp.402–405.

Zhu, X.D. et al., 2000. Cell-cycle-regulated association of RAD50/MRE11/NBS1 with TRF2 and human telomeres. *Nature Genetics*, 25(3), pp.347–352.

Zhu, Z. et al., 2008. Sgs1 Helicase and Two Nucleases Dna2 and Exo1 Resect DNA Double-Strand Break Ends. *Cell*, 134(6), pp.981–994.

Zill, O.A. et al., 2010. Co-Evolution of Transcriptional Silencing Proteins and the DNA Elements

Specifying Their Assembly E. J. Louis, ed. *PLoS Biology*, 8(11), p.e1000550. Available at: https://dx.plos.org/10.1371/journal.pbio.1000550.

Zou, L. & Elledge, S.J., 2003. Sensing DNA damage through ATRIP recognition of RPA-ssDNA complexes. *Science*, 300(5625), pp.1542–1548.

Acknowledgements

Curriculum Vitae